# Application of Radiotracer Techniques for Interwell Studies

IAEA

**International Atomic Energy Agency**

# IAEA RADIATION TECHNOLOGY SERIES PUBLICATIONS

One of the main objectives of the IAEA Radioisotope Production and Radiation Technology programme is to enhance the expertise and capability of IAEA Member States in utilizing the methodologies for radiation processing, compositional analysis and industrial applications of radioisotope techniques in order to meet national needs as well as to assimilate new developments for improving industrial process efficiency and safety, development and characterization of value-added products, and treatment of pollutants/hazardous materials.

Publications in the IAEA Radiation Technology Series provide information in the areas of: radiation processing and characterization of materials using ionizing radiation, and industrial applications of radiotracers, sealed sources and non-destructive testing. The publications have a broad readership and are aimed at meeting the needs of scientists, engineers, researchers, teachers and students, laboratory professionals, and instructors. International experts assist the IAEA Secretariat in drafting and reviewing these publications. Some of the publications in this series may also be endorsed or co-sponsored by international organizations and professional societies active in the relevant fields.

There are two categories of publications: the **IAEA Radiation Technology Series and the IAEA Radiation Technology Reports**.

## IAEA RADIATION TECHNOLOGY SERIES

Publications in this category present guidance information or methodologies and analyses of long term validity, for example protocols, guidelines, codes, standards, quality assurance manuals, best practices and high level technological and educational material.

## IAEA RADIATION TECHNOLOGY REPORTS

In this category, publications complement information published in the IAEA Radiation Technology Series in the areas of: radiation processing of materials using ionizing radiation, and industrial applications of radiotracers, sealed sources and NDT. These publications include reports on current issues and activities such as technical meetings, the results of IAEA coordinated research projects, interim reports on IAEA projects, and educational material compiled for IAEA training courses dealing with radioisotope and radiopharmaceutical related subjects. In some cases, these reports may provide supporting material relating to publications issued in the IAEA Radiation Technology Series.

All of these publications can be downloaded cost free from the IAEA web site:

http://www.iaea.org/Publications/index.html

Further information is available from:

Marketing and Sales Unit
International Atomic Energy Agency
Vienna International Centre
PO Box 100
1400 Vienna, Austria

Readers are invited to provide feedback to the IAEA on these publications. Information may be provided through the IAEA web site, by mail at the address given above, or by email to:

Official.Mail@iaea.org

# APPLICATION OF
# RADIOTRACER TECHNIQUES FOR
# INTERWELL STUDIES

The following States are Members of the International Atomic Energy Agency:

AFGHANISTAN
ALBANIA
ALGERIA
ANGOLA
ARGENTINA
ARMENIA
AUSTRALIA
AUSTRIA
AZERBAIJAN
BAHRAIN
BANGLADESH
BELARUS
BELGIUM
BELIZE
BENIN
BOLIVIA
BOSNIA AND HERZEGOVINA
BOTSWANA
BRAZIL
BULGARIA
BURKINA FASO
BURUNDI
CAMBODIA
CAMEROON
CANADA
CENTRAL AFRICAN
  REPUBLIC
CHAD
CHILE
CHINA
COLOMBIA
CONGO
COSTA RICA
CÔTE D'IVOIRE
CROATIA
CUBA
CYPRUS
CZECH REPUBLIC
DEMOCRATIC REPUBLIC
  OF THE CONGO
DENMARK
DOMINICA
DOMINICAN REPUBLIC
ECUADOR
EGYPT
EL SALVADOR
ERITREA
ESTONIA
ETHIOPIA
FINLAND
FRANCE
GABON
GEORGIA
GERMANY

GHANA
GREECE
GUATEMALA
HAITI
HOLY SEE
HONDURAS
HUNGARY
ICELAND
INDIA
INDONESIA
IRAN, ISLAMIC REPUBLIC OF
IRAQ
IRELAND
ISRAEL
ITALY
JAMAICA
JAPAN
JORDAN
KAZAKHSTAN
KENYA
KOREA, REPUBLIC OF
KUWAIT
KYRGYZSTAN
LAO PEOPLE'S DEMOCRATIC
  REPUBLIC
LATVIA
LEBANON
LESOTHO
LIBERIA
LIBYA
LIECHTENSTEIN
LITHUANIA
LUXEMBOURG
MADAGASCAR
MALAWI
MALAYSIA
MALI
MALTA
MARSHALL ISLANDS
MAURITANIA
MAURITIUS
MEXICO
MONACO
MONGOLIA
MONTENEGRO
MOROCCO
MOZAMBIQUE
MYANMAR
NAMIBIA
NEPAL
NETHERLANDS
NEW ZEALAND
NICARAGUA
NIGER

NIGERIA
NORWAY
OMAN
PAKISTAN
PALAU
PANAMA
PAPUA NEW GUINEA
PARAGUAY
PERU
PHILIPPINES
POLAND
PORTUGAL
QATAR
REPUBLIC OF MOLDOVA
ROMANIA
RUSSIAN FEDERATION
SAUDI ARABIA
SENEGAL
SERBIA
SEYCHELLES
SIERRA LEONE
SINGAPORE
SLOVAKIA
SLOVENIA
SOUTH AFRICA
SPAIN
SRI LANKA
SUDAN
SWEDEN
SWITZERLAND
SYRIAN ARAB REPUBLIC
TAJIKISTAN
THAILAND
THE FORMER YUGOSLAV
  REPUBLIC OF MACEDONIA
TUNISIA
TURKEY
UGANDA
UKRAINE
UNITED ARAB EMIRATES
UNITED KINGDOM OF
  GREAT BRITAIN AND
  NORTHERN IRELAND
UNITED REPUBLIC
  OF TANZANIA
UNITED STATES OF AMERICA
URUGUAY
UZBEKISTAN
VENEZUELA
VIETNAM
YEMEN
ZAMBIA
ZIMBABWE

The Agency's Statute was approved on 23 October 1956 by the Conference on the Statute of the IAEA held at United Nations Headquarters, New York; it entered into force on 29 July 1957. The Headquarters of the Agency are situated in Vienna. Its principal objective is "to accelerate and enlarge the contribution of atomic energy to peace, health and prosperity throughout the world".

# APPLICATION OF RADIOTRACER TECHNIQUES FOR INTERWELL STUDIES

# COPYRIGHT NOTICE

# FOREWORD

Tracer technology plays an important role in oilfield development and operation. Interwell tracer testing is an important reservoir engineering tool for the secondary and tertiary recovery of oil. Most of the oilfields in many developing countries are in the stage of secondary recovery. Moreover, the oil industry remains a priority in these countries. Interwell tracer testing is also used in geothermal reservoirs to gain better understanding of reservoir geology and to optimize production and re-injection programmes. Today, the use of tracers for interwell communication studies is an established technique.

The IAEA facilitates the transfer of technology, and an important part of this process is the provision of relevant literature that may be used for reference purposes or as an aid to teaching. This publication aims to provide not only an extensive description of what can be achieved by the application of radiotracer techniques in interwell investigations in onshore and offshore fields, but also sound and experience based guidance on all aspects of the design and implementation of experiments and the interpretation of results. It describes the principles and the state of the art of radiotracer techniques for interwell investigations.

The publication contains guidance on the technical steps of interwell tracer testing, as well as input from participants of the coordinated research project (CRP) on Validation of Tracers and Software for Interwell Investigations. The major achievements of the CRP and novel developments in tracer methodologies and technologies as applied to interwell investigations are also included. The unedited reports of the CRP participants, as presented at the final research coordination meeting, and software for interwell data interpretation are included as support materials on the accompanying CD–ROM. The publication has been prepared with contributions from all CRP participants. The IAEA gratefully acknowledges all contributors to this publication, especially T. Bjornstad for compiling and reviewing it.

The IAEA officer responsible for this publication was Joon-Ha Jin of the Division of Physical and Chemical Sciences.

# CONTENTS

# 1. INTRODUCTION

## 1.1. BACKGROUND

Tracer applications can be found in almost any phase of oil field development. Interwell tracer technology is an important reservoir engineering tool for the secondary and tertiary recovery of oil. Interwell tracer testing is also used in geothermal reservoirs to gain a better understanding of reservoir geology and to optimize production and reinjection programmes. The main purpose of conducting interwell tracer tests in oil and geothermal reservoirs is to monitor, qualitatively and quantitatively, the injected fluid connections between injection and production wells and to map the flow field, reservoir heterogeneities and volumetric sweep (contacted volumes) between wells. Tracer is added into injection fluid via an injection well and observed in the surrounding production wells (Fig. 1). Tracer response is then used to describe the flow pattern and thereby gain a better understanding of the reservoir. This knowledge is important in optimizing oil recovery. Most of the information given by the tracer response curves cannot be obtained by means of other techniques.

Fluid flow in most reservoirs is anisotropic. The reservoir structures are usually layered and frequently contain significant heterogeneities leading to
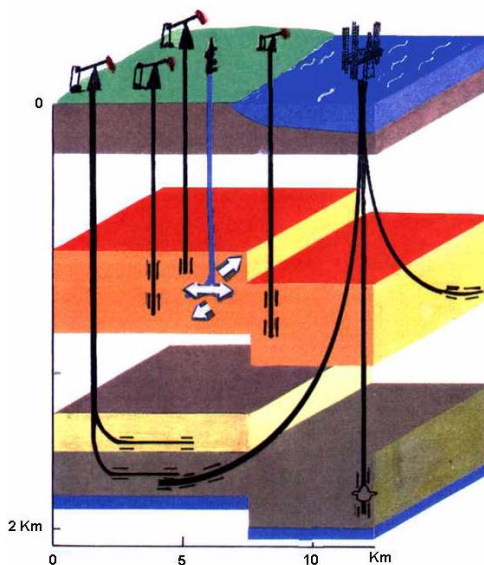


*FIG. 1.  Principle of tracer injection method for interwell communications.*

directional variations in the extent of flow. Hence, the effective fluid movement can be difficult to predict. This is where tracer technology plays an important role, assuming that the movement of the tracer reflects the movement of the injected fluid. Obviously, it is most important to assure that the properties of the tracer meet this requirement as closely as possible; there should be a minimum quantity of undesired loss or delay. The physical and geochemical conditions of the reservoir define the constraints. As a result, tracers found to work properly in one reservoir, may not work satisfactorily in another.

Apart from radioactive and chemical tracers, stable isotopes of the water molecule ($^2$H and $^{18}$O) can be employed as effective tracing tools to identify the source (origin) of produced water, both in geothermal as well as oilfield applications. On the basis of stable isotope indices, the relative contribution of different sources of water towards produced water may be estimated. However, in the cases of geothermal reservoirs and high temperature oil reservoirs, the $^{18}$O content of injected water is likely to be modified due to $^{18}$O exchange between water and host rock. However, $^2$H is considered as conservative and can safely be used to estimate relative contributions.

A field radiotracer investigation consists, in brief, of the following main steps:

(1)  Design of tracer strategy, involving consultation with reservoir engineers
(2)  Selection of applicable tracers
(3)  Application to the relevant authorities based on a safety report
(4)  Tracer mixture preparation, calibration and quality assurance
(5)  Selection/design of tracer injection and sampling procedures
(6)  Tracer transportation to injection site
(7)  Implementation of radiation safety procedures at the injection site
(8)  Tracer injection
(9)  Radioactivity contamination survey
(10) Injection equipment decontamination and handling of radioactive waste
(11) Tracer sampling and sample transportation to analytical laboratory
(12) Tracer analysis
(13) Data evaluation and simulation
(14) Reporting of results

The IAEA Coordinated Research Project (CRP) on Validation of Tracers and Software for Interwell Investigations has developed, prepared, tested and validated several tracers, techniques and software packages. The main group activities of the CRP were:

- Laboratory intercomparison on analysis of the tritiated water (HTO) in field samples (brines);
- Intercomparison on evaluation of field data with a simple software package (Anduril);
- Laboratory intercomparison on analysis of mixtures of the two water tracers HTO and $^{14}CH_3OH$;
- Application of the PORO streamline simulator on field data provided by different companies.

A short summary of the main achievements of the CRP is given below:

*Tracer preparation, quality assurance and analysis*: Synthesis, preparation, analysis and quality control of several tracers both individually and in mixtures: HTO, $SCN^-$ ($^{14}C$ or $^{35}S$ labelled), radiolabelled alcohols, $[Co(CN)_6]^{3-}$ (radiolabelled), $^{125}I^-$ ($^{131}I^-$) and gold nanoparticles have been established or validated. Criteria for selecting the more adapted tracers have been investigated. Laboratory intercomparison analysis of mixtures of HTO and $^{14}CH_3OH$ was successfully done. Ions and stable isotopes in produced water have been used as indicators to support the interwell tracer test.

*Experimental procedure for tracer tests*: Intercomparison of the injection and sampling strategies has been done and rules have been proposed to carry out the tracer experiments. Tracer injection techniques, both bypassing and direct pumping into the well head, have been compared. Well head samplers and procedures for collecting water sample have been developed and tested in the field. Safety procedures have been established and implemented.

*Interpretation and modelling*: Several models for interwell tracer data interpretation have been tested and compared. Rules and advice have been established to select the more suitable model and/or software packages, depending on the field structure and configuration. The following models (software packages) have been studied: Brigham (home-made code), dispersion (Anduril), streamlines (PORO), chemical engineering (Disproof) and computational fluid dynamics (CFD)(Caste and CONSOL). New possible approaches of compartmental modelling have been suggested for fractured oil or geothermal reservoirs.

The publication represents a form of monograph dedicated to tracer methods as applied to interwell investigations in oil and geothermal reservoirs. It consists of three sections and four appendices.

The first section gives the background and arguments for the use of tracers and presents the general view on tracers and tracer techniques as applied in interwell investigations in oil and geothermal fields. The status of tracer technology worldwide is given as well.

Section two deals with technical steps in the practical application of interwell tracer technology, including planning of field tests (tracer selection, injection and sampling), field related operation and implementation, tracer measurement and data interpretation.

Section three covers new tracer development, including tracer quality control, behaviour of tracers in various environments, and analytical methods for tracer measurement. Finally, the CRP achievements are summarized in a short section.

The four appendices provide the following information:

- Appendix I is allocated to field case studies performed by the various institutions involved.
- Appendix II deals with laboratory intercomparison tests on analysis of HTO and HTO + $^{14}CH_3OH$ in mixtures as well as operation of the tracer interpretation software Anduril on practical cases common for all laboratories.
- Appendix III provides procedures and protocols for measuring tracers in produced water.
- Appendix IV describes two software packages produced and tested during the CRP period: Anduril software for simple data treatment and PORO software for more advanced streamline simulation.

## 1.2.   INTERWELL TRACER TECHNOLOGY USE IN OILFIELDS

The efficiency of the water flooding process is highly dependent on the rock and fluid characteristics. In general, it will be less efficient if heterogeneities are present in the reservoir, such as permeability barriers or high permeability channels that impede an efficient volumetric sweep and thereby a good oil displacement by the injected water.

Natural production mechanisms, or primary production, contribute to extraction from the reservoir of about 25% of the original oil in place. This means that 75% of the existing oil remains in the pores and fissures of the rocks. The production flow rate depends on the differential pressure between the permeable layer and the bottom of the well, the average permeability, the layer thickness and the oil viscosity. The main natural production mechanisms are the expansion of the oil, water and gas and, in certain cases, the water influx from aquifers connected to the reservoir.

When primary oil production decreases in a field because of a reduction in the original pressure, water is usually injected to increase the oil production. Injected water in special wells (injection wells) forces the oil remaining in certain

layers to emerge from other wells (production wells) surrounding the injector. This technique, commonly termed secondary recovery, contributes to the extraction of up to 50% of the original oil in place. Although this technique was firstly used in old reservoirs in which oil production had decreased, it is nowadays a common practice to begin the exploitation of new wells with fluid injection as a way to optimize oil recovery. For this reason, the name secondary recovery is being replaced by the more general term enhanced oil recovery.

For oil reservoirs, interwell tracer data are important in order to optimize the production strategy (injection balance) in the reservoir and thereby maximize the oil recovery. In geothermal reservoirs, interwell tracer tests are used to improve the understanding of reservoir geology and to optimize production and re-injection programmes and thereby enthalpy production from the reservoir. During the last 10–15 years there has been substantial progress on tracer technology development. This has resulted in improved basic knowledge and new technology.

Detailed analysis of the response curves obtained from interwell studies allows the following:

— Detection of high permeability channels, barriers and fractures;
— Detection of communications between layers;
— Evaluation of the fraction of the injection water reaching each production well;
— Determination of residence time distributions;
— Indication of different stratifications in the same layer;
— Determination of preferential flow directions in the reservoir;
— Determination of swept volume of the reservoir.

All this information can be used to make operational water flooding decisions in order to increase oil production.

Tracer technology is a powerful tool for tracing the movement of the injected fluid through the oil reservoir, monitoring reservoir performance, investigating unexpected anomalies in flow and verifying suspected geological barriers or flow channels. Generally, the injected fluid is labelled with tracer (radioactive or non-radioactive) and the produced fluid from the well(s) of interest is sampled and analysed to determine the tracer response curve. The analysis of tracer response curves can provide important information about the character of the reservoir and makes it possible to optimize the injection regime and improve production strategy.

Such information can be used to evaluate flood performance, optimize the balance between injection and production rates, help make decisions on infill

drilling and enhanced oil recovery programmes and improve the accuracy of the reservoir model.

In industrialized countries, tracers have been used to measure fluid flow in reservoirs for several decades [1–4]. A summary of theIR earlier use (before 1990) from the perspective of tracer behavior is provided by Bjornstad [5]. There are some success stories and some reports on experiments, which have largely failed. The reason for failures is mainly due to insufficient knowledge of tracer behaviour under changing reservoir conditions.

Knowledge of tracer behaviour is gained through dedicated laboratory investigations, through the above-mentioned oil field experience, groundwater movement investigations, atmospheric tracing experiments and also, to a significant degree, through the work carried out on the migration of radioactive species in soil for the purpose of evaluating radioactive waste repository sites.

Although the integrated knowledge from these areas is substantial, the information obtained is not always consistent. Results from one area of investigation cannot readily be transferred to new fields because of both scaling problems and changing experimental conditions. During the last 20 years there have been substantial programmes on tracer technology development in a few R&D laboratories in Europe and North America. This has resulted in new basic knowledge and new technology.

During the past few years, a number of 'traditional' radioactive and non-radioactive water tracers have been re-examined along the lines described above, and the search for new possible tracer compounds is ongoing. Ultra-low detection limits are required. Among the non-radioactive compounds, the fluorinated aromatic acids have attracted special attention because of their success in tracing groundwater flow. A comprehensive quantity of information has been generated with respect to their thermal stability and reservoir flow behaviour in dynamic laboratory experiments under simulated reservoir conditions. Some of the compounds passed through the quality checks in good shape. Others show instability or other unwanted properties which excludes them from use in reservoirs, at least under certain specific reservoir conditions. The compounds with sufficiently 'good marks' from laboratory experiments were extensively tested in full field experiments in the early 1990s.

A selection of the non-radioactive polyfluorinated benzoic acids were established as industry standards for tracing water flow in oil reservoirs more than 10 years ago and details have been published in open literature [6]. Currently, the continued development has resulted in new families of non-radioactive tracers qualified for oil reservoir water tracing. However, the identity of these compounds is not revealed in the open literature. Individual compounds have certain limitations on their use and are not generally applicable. It is important to know these limitations in detail in order to apply them correctly.

Some information can be found in Refs [7] and [8], but most of the data remain unpublished as private confidential research reports.

## 1.3. INTERWELL TRACER TECHNOLOGY USE IN GEOTHERMAL FIELDS

The energy production potential, or capacity, of geothermal systems is highly variable. It is primarily determined by the pressure decline caused by mass extraction, but also by heat content. Pressure declines continuously with time in systems that are closed or with limited recharge. The production potential of geothermal systems is, therefore, often limited by lack of water rather than lack of heat. Geothermal resource management involves controlling energy extraction from geothermal systems underground so as to maximize the resulting benefits, without overexploiting the resource.

When geothermal systems are overexploited, production from the systems has to be reduced, often drastically, resulting in an insufficient steam supply to power plants or in loss of wells. Overexploitation mostly occurs for two reasons. Firstly, inadequate monitoring and data collection contribute to poor understanding of the system and lack of reliable modeling and, therefore, the systems respond unexpectedly to long term production. Secondly, overexploitation occurs when many users utilize the same resource/system without common management or control.

The main purpose of tracer testing in geothermal reservoir management is to predict possible cooling of production wells resulting from the long term injection of colder fluid and/or the invasion of natural groundwater. In a geothermal field, the primary resource is water, both as liquid and as steam. A direct measure of its behaviour is thus of obvious importance to field management. Water tracing is the only technique that gives a direct indication of underground flow patterns and velocities.

Information gained from tracer testing of geothermal reservoirs is similar to that obtained from oilfields and includes:

(a)  Proper diagnostics of the reservoir comprising evidence of direct connections between the tracer injection point (either within or outside the field) and monitoring wells in the field;
(b)  Measurement of direction, speed and mean residence time of water movement;
(c)  Determination of the extent to which groundwater downflows intrude into production wells;

(d)   Identification of breakthrough (arrival time or first appearance of tracer in the production well);

(e)   Quantification of the tracer quantity collected in each production well;

(f)   Information needed for calibration or verification of physical models of the geothermal reservoir.

All of this information will aid in gaining an understanding of the nature of a geothermal system, but the measurements, which bear upon injection and groundwater intrusion or cooling potential, have the greatest impact on field management.

# 2.  TECHNICAL STEPS IN THE APPLICATION OF INTERWELL TRACER TECHNOLOGY

## 2.1.  PLANNING AN INTERWELL TRACER TEST

### 2.1.1.   Wells to trace

The purpose of interwell tests and the kind of technical information that can be derived from them are described above both for oil fields and geothermal fields.

For both reservoir types the interwell tracer tests give quantitative information on the fluid dynamics in a reservoir. Dynamic information from a reservoir may, in addition, be obtained by three other methods: (i) logging of production rates (profiles) of reservoir fluids, (ii) pressure testing and (iii) time-lapse seismic examinations (4-D seismic). However, these methods and tracer testing are complementary and cannot directly replace one another.

Selection of wells to trace must be based on the best available information on the reservoir and the additional knowledge needed in order to optimize reservoir performance. The technical personnel with the most intimate knowledge of the reservoir lithology, stratigraphy and structure are the reservoir engineers together with reservoir geologists. Therefore, an optimum selection of wells should be performed in teamwork with these specialists and the tracer specialist.

## 2.1.2. Quantity of tracer to inject

### 2.1.2.1. Maximum dilution method

If the reservoir is well known and a reliable model exists, the best estimate of the quantity of tracer required for an interwell study is obtained by numerical simulation of the various flow patterns involved. Then the quantity of tracer (mass or activity) needed for a specific experiment is calculated from the theoretical response and the detection limit. However, if the reservoir is well known, there is not much reason to perform a tracer test for reservoir evaluation purposes.

Most reservoirs, however, are poorly known, at least when it comes to the flow dynamics of reservoir fluids. Experience has shown that in this case some simple calculations may be equally trustworthy.

Owing to lack of better information, the quantity of tracer to be used can be based upon a purely geometrical consideration. Suppose that the reservoir is a homogeneous cylindrical volume around the injection well as shown in Fig. 2. Let the active pore volume be $V_p$, which may be calculated by Eq. (1):

$$V_p = \pi\, r^2\, h\, \Phi\, S_w \tag{1}$$

where

$h$      is the thickness of the tagged layer (m);
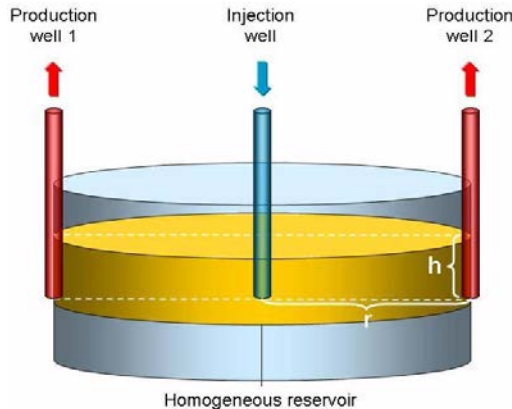$r$      is the distance between injection well and production well (m);



FIG. 2.  Injection and production wells in a homogeneous circular reservoir.

$\Phi$    is the porosity of the tagged layer (fraction, non-dimensional);
$S_w$    is the water saturation (fraction, non-dimensional).

Assuming tracer dispersal is uniform in the available reservoir volume, then the expected output mean concentration is established by the detection limit ($L_D$) of the tracer. In the case of a radiotracer, $L_D$ depends on the background, the counting geometry, internal counting efficiency, decay scheme characteristics and the measurement time. The activity ($A_0$) to be injected to obtain a mean concentration equal to the detection limit is calculated by Eq. (2):

$$A_0 = L_D V_p \tag{2}$$

For a tracer pulse injection, which of course will not distribute tracer evenly throughout the whole reservoir section, tracer concentration in the response pulse at production wells will be considerably higher than the detection limit. However, this cannot always be guaranteed because of the possible existence of high permeability streaks, so-called 'thief' zones and adjacent water contacts where most of the injected tracer may disappear and never show up in production wells. Therefore, a safety factor $F_1$ is normally introduced to Eq. (2). This factor may differ for various reservoir types and known reservoir heterogeneities, but $F_1 \sim 2\text{–}10$ is common. Additionally, if the reservoir is known to be anisotropic and the flow known to have directional tendencies, a second factor, $F_2$, may be introduced to account for this anisotropy. This factor, $F_2$, may take values both below and above 1, i.e. wells along the prevailing flow direction have $F_2 > 1$ while those lying in the flow shadow have $F_2 < 1$.

Thus, the final simplified equation for the quantity of tracer to be injected is:

$$A_0 = F_1 F_2 L_D \pi r^2 h \Phi S_w \tag{3}$$

The required activity calculated by Eq. (3) only represents an approximation, but it is good enough as a reference value. The experience gained after having carried out a number of operations in different reservoirs is valuable in modifying the estimate values in order to determine the real quantity of tracer to use.

### 2.1.2.2. Reservoir and well information to consider during planning

In order to perform a proper planning process, a variety of detailed reservoir and well information should be considered. These are listed below.

Parameters to be provided by the oil company:

- Well pattern (e.g. inverted five-spot, line drive, irregular pattern, etc., map of the lateral distribution is preferable);
- Well types (vertical, horizontal, undulating, complex, etc.);
- Distance from injector well(s) $i$ to producer well(s) $p$ ($r_{ip}$ (m));
- Whether it is possible to inject different tracer in each perforated zone or producing layer ($j$) and height of each layer ($h_j$ (m));
- Height of the combined pay zones ($\Sigma h_j$ (m));
- Permeability (or water relative permeability) in each layer, $j$ ($k_j$);
- Average porosity of reservoir rock ($\Phi$);
- Reservoir pressure (for gas tracers) ($p$ (bar));
- Reservoir temperature ($T$ (K));
- Estimated water saturation ($S_w$);
- Estimated oil saturation ($S_o$);
- Salinity (main salt components and their concentration (g/mL));
- Reservoir water pH;
- Special gas composition (e.g. $H_2S$) (to plan analytical strategy/method);
- Special oil composition (API);
- Estimated or calculated water cut (for planning sampling strategy);
- Injection water rate ($m^3$/d).

Parameter to be provided by the analytical laboratory:

- Lower limit of detection for each type of tracer $t$ ($L_{Dt}$) and associated required sample volume.

### 2.1.3.   Selection of tracers

*2.1.3.1. Tracer classification*

Reservoir tracers can be divided into two categories:

(1)   *Passive or conservative (or also, less precisely, termed ideal) tracers*: The requirement is that the tracer shall passively follow the fluid phase or phase fraction into which it is injected without exhibiting any chemical or physical behaviour different from that of the traced component itself. In addition, the tracer must not perturb the behaviour of the traced phase in any way and neither must the fluid phase or its components perturb tracer behaviour. In petroleum reservoirs, passive (or in practice near-passive) tracers are used in studies of water flooding.

(2)   *Active (also, less precisely, termed non-ideal or reacting) tracers*: The tracer behaves in a qualitatively predictable way and is used to measure a property of the system into which it is injected. The degree of active take-up is a quantitative measure of the property being determined.

Examples of active tracers include:

- Phase partition (with the potential to measure oil saturation in the water contact reservoir zone);
- Sorbtion onto rock, either reversibly or irreversibly (with the potential to measure ion exchange capacity of formation rock);
- Hydrolyzation (e.g. for measurement of water saturation, or temperature if the water saturation is known);
- Thermal degradation (to measure reservoir temperature away from wells);
- Microbial degradation (to measure microbial activity).

It is practical to divide the available interwell reservoir tracers into three types based on their different production mode, treatment and analytical methods:

 (i)   Stable isotope ratios;
 (ii)  Non-radioactive chemical species;
(iii)  Radioactive atoms or molecules.

Zemel, in his book on Tracers in the Oil Field [9], argues that radioactive and non-radioactive chemical tracers are not necessarily different kinds of tracers, but that radioactive tracers are only radioactively tagged chemical tracers. He might as well have included tracers based on stable isotopic ratios in this argument by stating that isotopic ratio tracers are only chemical tracers labelled with a different stable isotope ratio. It is correct that the flooding properties and survivability in reservoirs are determined by the chemical properties of the tracer compound. It is not, however, generally valid that the same materials without a radioactive tag are also useful tracers. This all depends on the degree of their natural occurrence in reservoir fluids and on their detectability by non-radiochemical methods.

Tracers may also be classified as intrinsic or extrinsic:

Intrinsic tracers are molecules containing an isotope (radioactive or stable) of one of the molecules' natural elements, which makes the labelled molecule particularly detectable by nuclear or mass spectrometric methods in systems where the dynamic characteristics and general behaviour of the non-labelled

molecule are followed in a given medium. For example, in the case of water, there are three such labels: oxygen-18 ($^1H_2{}^{18}O$) and deuterium ($^1H^2H^{16}O$) measured as isotopic ratios ($^{18}O/^{16}O$ by $\delta^{18}O$ and $^2H/^1H$ by $\delta D$) by mass spectrometric techniques and tritium ($^1H\,^3H^{16}O$) measured by nuclear techniques (in practice, liquid scintillation counting). In this case, the water molecule is traced from the inside, in the confines of its nucleus. In this case, the water tracer will (in practice) follow all movements and reactions of the water itself.

Extrinsic tracers are made up of atoms or molecules supposedly to sharing the same dynamic characteristics and, in general, the same mass flow behaviour as the investigated medium. Falling into this category are all the substances that allow for tracing outside the molecular or ionic structure. For example, in case of water, $^{131}I^-$, $S^{14}CN^-$ and $[^{60}Co(CN)_6]^{3-}$ are examples of extrinsic tracers. They will not follow water in all its movements because of their charge and because they are basically a salt which will not, for instance, evaporate with the water.

Tracers may further be classified as artificial or natural:

Artificial tracers are generally defined as those tracers which are produced artificially and are deliberately introduced (injected) into the system under study. Most of the tracers employed in industrial applications, including geospherical tracing, are artificial tracers. They are further classified as radioactive and non-radioactive artificial tracers.

Natural tracers are those tracers that exist in nature, generated by nature itself. Such tracers are, for instance, the noble gas $^{222}Rn$ that may be used to follow mass flow in extended open systems, isotopic ratios of hydrogen atoms ($\delta D$) to study, for instance, the movement of injected sea water in an oil reservoir, provided its $\delta D$ value is sufficiently different from that of formation water, etc. Such tracers are mainly used to trace processes in environmental, geospherical, biological and agricultural studies and are not especially relevant for study of industrial processes in general.

The last class that will be mentioned here are activable tracers:

Activable tracers differ from other tracers only by the fact that they contain a chemical element with a special capacity (high activation cross-section) to be analysed in minute quantities by instrumental neutron activation analysis. As such, they are of special interest to the radiotracer specialists. These compounds are either organometallic covalently bound compounds or simply electrostatically bound chelate complexes. Their main advantage is that they do not pose any radiological hazards during operation and they have a practically infinite shelf

life in comparison to radiotracers. On the other hand, there is always a danger of contamination of the collected sample before activation.

In order to hinder sample contamination, all chemicals and mechanical components in contact with the liquid sample must be virtually free of activable element. These samples are activated with thermal or epithermal neutrons and sample measurements are carried out in a laboratory equipped with high resolution gamma spectrometers.

Metallo-organic compounds may also be analysed in trace quantities with other trace analytical techniques, for instance by inductively coupled plasma mass spectrometry. Such compounds may include other metals than those which are optimal for instrumental neutron activation analysis.

### 2.1.3.2. Characteristics of a water tracer

In order to qualify a water tracer on the basis of dynamic behaviour as passive ('very good') or near-passive ('good'), the type of job the tracer is expected to fulfil needs to be carefully defined. If the job is to measure fluid communication exclusively, a near-passive tracer may work as well as a true passive tracer.

*Non-charged tracer species*: A true passive water tracer is one that mimics all movements and interactions that the water molecules undergo in the traced water volume. In practice, the only radioactive compound that fulfils this requirement is radioactive water (HTO). Movements can, for instance, be the free movement in and out of dead-end pores insensitive to columbic forces set up by negatively charged rock surfaces. Interactions can include exchange with connate water in the rock pores or exchange with crystal water molecules. Thus, it can sometimes be observed that HTO seems to lag behind the injection water breakthrough as measured, for instance, by salt balance (ionic logging) or that the HTO production profile is somewhat more skewed. In the literature this has been incorrectly interpreted to HTO instablility under reservoir conditions, and that it may be subject to isotope exchange reactions of tritium with hydrogen in neighbouring hydrogen-containing compounds, some of which are stationary.

Other non-charged radiotracers include, for instance, tritiated methanol ($CH_2TOH$) and the other radiolabelled light alcohols. These will behave qualitatively similar to HTO with respect to the diffusive and convective parts, but differ as regards interactions.

*Anionic tracers*: Of electrically charged tracers, anions represent the more applicable ones. In laboratory experiments, however, ion exclusion is observed, i.e. negatively charged species tend to be repelled from the negatively charged rock surfaces. As a result, the tracers tend to flow in the middle of the fluid-conducting pores. They will not easily enter into dead-end pores or through

narrow pore throats. This results in a somewhat smaller available pore volume for anions than for non-charged species. In laboratory experiments, the production profile differs in reproducible ways from that of HTO, but in full-sized field experiments this difference is not that obvious.

Anionic tracers are represented by $S^{14}CN^-$. A typical production profile is given in Fig. 3. This profile is compared with the production profile of the simultaneously injected HTO. The difference in shape is enhanced by subtracting the normalized HTO profile from the normalized $S^{14}CN^-$ profile. The result is given in Fig. 4. It is evident from the curve that the breakthrough of HTO precedes that of $S^{14}CN^-$ and that the tail of the HTO profile is more pronounced. This profile difference is qualitatively reproduced for all near-passive anionic water tracers and illustrates the phenomenon which has become known as anionic exclusion. The flow rate is increased, for instance, by a factor of 10 (i.e. to 200 cm/d), the first down-dip in the normalized difference curve disappears and the breakthrough of the anionic tracer precedes that of the reference tracer, HTO.

On the basis of such curves, retention factors may be derived from Eq. (4) and the production profiles found by such experiments.

$$1 + \beta = V_T/V_S \tag{4}$$



NORMALIZED TRACER DISPERSION PROFILES

$S^{14}CN^-$ AND HTO IN BEREA SANDSTONE

HTO
$S^{14}CN^-$
Temperature = 90 °C
Pressure = 200 bar
200 cm crushed BEREA core
Mobil phase: Seawater
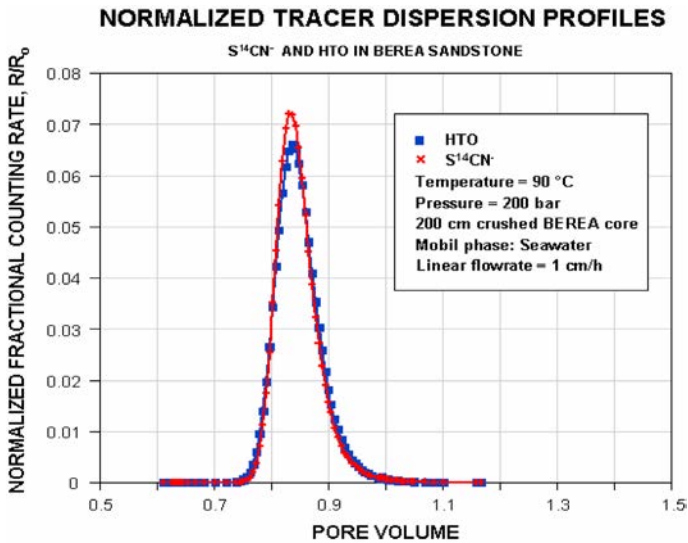Linear flowrate = 1 cm/h

*FIG. 3. Normalized production curves of HTO and $S^{14}CN^-$ from laboratory flooding experiments on sandstone in a flow rig.*
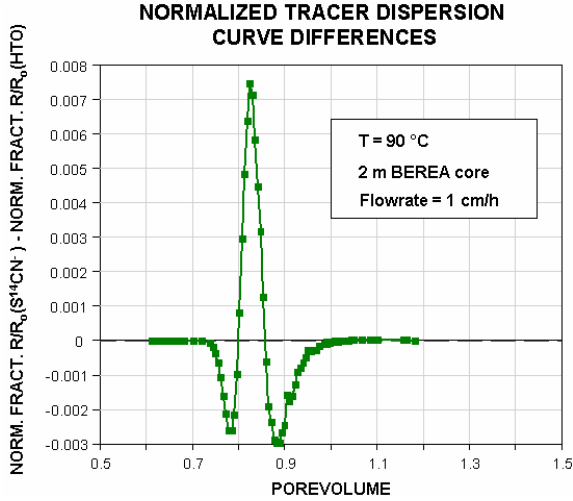
FIG. 4. *Difference between the normalized production curves of HTO and S$^{14}$CN$^-$.*

where

β     is the retention factor;
$V_T$   is the retention volume for the tracer candidate;
$V_S$   is the retention volume for the standard reference tracer.

The retention volume may be represented by the peak maximum value or the mass mid-point (first moment ($\mu_1$)) for non-symmetric profiles. These values are best found by fitting the profile with an analytical function consisting of polynomials.

For monovalent anions, the retention factors are in the range 0.0 to –0.03, indicating that such tracers pass faster through the reservoir rock than the water itself (represented by HTO).

Some anionic tracers may show complex behaviour. Radioactive iodine ($^{125}$I$^-$ and $^{131}$I$^-$) breaks through before water but has a substantially longer tail than HTO. Both reversible sorption and ion exclusion seem to play a role here.

*Cationic tracers*: These are in general not applicable. However, experiments have qualified $^{22}$Na$^+$ as an applicable water tracer in saline (greater than sea water salinity) waters. In such waters, the non-radioactive $^{23}$Na$^+$ will operate as a molecular carrier for the tracer molecule. The retention factor has been measured in the range of β ≈ 0.07 at reservoir conditions in carbonate rock (chalk) [10]. Accordingly, the tracer is somewhat delayed by sorption on, and ion exchange with, the reservoir rock, but in a reversible fashion.

16

In the literature there is also a report on the successful use of $^{134}Cs^+$ and $^{137}Cs^+$ in a carbonate reservoir [11]. This tracer cannot, however, be generally used as it will adsorb strongly (and irreversibly under ordinary reservoir conditions) on clay-containing rocks. There is also the reported use of other cationic species such as $^{60}Co^{3+}$ and other cobalt isotopes, but these compounds have never been produced back.

*2.1.3.3. Selection of conditionally qualified tracers*

For unambiguous, single phase tracing of water in secondary or tertiary recovery schemes, the following practical tracer selection criteria apply to passive tracers:

- Insignificant degradation, reservoir and production conditions (i.e. high stability against thermal, chemical, physical and microbial degradation and a suitable half-life for radiotracers);
- Insignificant phase partitioning;
- Insignificant sorption on reservoir minerals;
- Insignificant natural occurrence in involved fluids (low background);
- Detectable in very low concentrations in reservoir fluid samples;
- Toxicity and radiotoxicity at acceptable levels;
- Non-problematic preparations, handling and logistics;
- Adequate commercial availability of components for preparation of tracer mixture;
- Acceptable cost.

For geothermal tracers, all of the above criteria apply except for the second item. For the tracing of $H_2O$ movement, in many reservoirs it will be advantageous to apply simultaneously selective tracers for the condensed water phase, selective tracers for the vapour phase and tracers for both phases.

Tables 1 and 2 list some water radiotracers which have been conditionally qualified for water tracing in oilfield operations and in geothermal operations, respectively, conditionally because each one has certain limitations to be observed.

Tables 3 and 4 list examples of corresponding non-radioactive tracers used in oilfields and geothermal fields, respectively.

TABLE 1. COMMON RADIOLABELLED WATER TRACERS FOR OILFIELDS

| Water tracer compound | Half-life | Main radiation characteristics | Comments |
|---|---|---|---|
| HTO | 12.32 y | $\beta^-$ (18 keV) | Generally applicable |
| $CH_2TOH$ [a] | 12.32 y | $\beta^-$ (18 keV) | Caution at temperatures >100°C (partition into gas phase) |
| $CH_3CHTOH$ [b] | 12.32 y | $\beta^-$ (18 keV) | Caution at temperatures >100°C (partition into gas phase), some biodegradation below 70–80°C |
| $CH_3CTOHCH_3$ | 12.32 y | $\beta^-$ (18 keV) | Reasonably general application |
| $S^{14}CN^-$ | 5730 y | $\beta^-$ (156 keV) | For $T < 90$–100°C, long term experiments |
| $^{35}SCN^-$ | 87 d | $\beta^-$ (167 keV) | For $T < 90$–100°C, medium term experiments |
| $^{36}Cl^-$ | $3 \times 10^5$ y | $\beta^-$ (709 keV) | High temperature reservoirs, long term, EMS analysis |
| $^{125}I^-$ | 60 d | $\gamma$ (35.5 keV) | Reducing chemical conditions, medium term |
| $^{131}I^-$ | 8 d | $\beta^-$ (606 keV), $\gamma$ (364.5 keV) | Reducing chemical conditions, short term (fracture detection) |
| $[^{56}Co(CN)_6]^{3-}$ | 77.7 d | $\beta^+$ (1459 keV), $\gamma$ (846.8 keV, 1238.3 keV) | Use with caution at $T < 90$°C, medium term |
| $[^{57}Co(CN)_6]^{3-}$ | 271.8 d | $\gamma$ (122.1 keV, 136.5 keV) | Use with caution at $T < 90$°C, medium to long term |
| $[^{58}Co(CN)_6]^{3-}$ | 70.9 d | $\beta^+$ (470 keV), $\gamma$ (810.8 keV) | Use with caution at $T < 90$°C, medium term |

TABLE 1. COMMON RADIOLABELLED WATER TRACERS FOR OILFIELDS (cont.)

| Water tracer compound | Half-life | Main radiation characteristics | Comments |
|---|---|---|---|
| $[^{60}Co(CN)_6]^{3-}$ | 5.27 y | $\beta^-$ (317.9 keV), $\gamma$ (1173.2 keV, 1332.4 keV) | Use with caution at $T < 90°C$, long term |
| $[Co(^{14}CN)(CN)_5]^{3-}$ | 5730 y | $\beta^-$ (156 keV) | Use with caution at $T < 90°C$, long term |
| $^{22}Na^+$ | 2.6 y | $\beta^+$ (545 keV), $\gamma$ (1274.5 keV) | High temperature tracer in saline reservoirs, long term, slight reversible sorption |

a   The alcohol tracers may also be labelled with $^{14}C$.
b   Position of the tritium in the alcohol compounds heavier than methanol may vary.

TABLE 2. COMMON RADIOLABELLED WATER TRACERS FOR GEOTHERMAL RESERVOIRS

| Water tracer compound | Half-life | Main radiation characteristics | Comments |
|---|---|---|---|
| HTO | 12.32 y | $\beta^-$ (18 keV) | Generally applicable, tracer for condensed and vapour phases |
| $CH_2TOH$[a] | 12.32 y | $\beta^-$ (18 keV) | Tracer for condensed and vapour phases |
| $CH_3CHTOH$[b] | 12.32 y | $\beta^-$ (18 keV) | Some biodegradation below 70–80°C, tracer for condensed and vapour phases |
| $CH_3CTOHCH_3$ | 12.32 y | $\beta^-$ (18 keV) | Reasonably general application, tracer for condensed and vapour phases |
| $^{125}I^-$ | 60 d | $\gamma$ (35.5 keV) | Reducing chemical conditions, medium term, tracer for condensed phase |
| $^{131}I^-$ | 8 d | $\beta^-$ (606 keV), $\gamma$ (364.5 keV) | Reducing chemical conditions, short term (fracture detection), tracer for condensed phase |

a  The alcohol tracers may also be labelled with $^{14}C$.
b  Position of the tritium in the alcohol compounds heavier than methanol may vary.

TABLE 3. COMMON NON-RADIOACTIVE TRACERS FOR OILFIELDS

| Tracer | Temperature limitations | Remarks |
|---|---|---|
| *Inorganic molecules* | | |
| $D_2O$ | None | Limit in use: Natural content of deuterium in waters |
| $SCN^-$ | <90°C | If oxygen scavenger is absent: ~100°C |
| $[Co(CN)_6]^{3-}$ | <90°C | Limit in use: 'Natural' cobalt in waters and equipment for handling samples |
| *Organic molecules* | | |
| Three monofluoro benzoic acids: 2-FBA, 3-FBA, 4-FBA | <130°C | Some of the monofluorinated benzoic acids may experience some biodegradation at $T < \sim 70°C$ |
| Six difluoro benzoic acids: 2,3-DFBA, 2,4-DFBA, 2,5-DFBA, 2,6-DFBA, 3,4-DFBA, 3,5-DFBA | <120°C | |
| Six trifluoro benzoic acids: 2,3,4-TriFBA, 2,3,5-TriFBA, 2,3,6-TriFBA, 2,4,6-TriFBA, 3,4,5-TriFBA, 3,4,6-TriFBA | <120°C | Stable against biodegradation |
| Two tetrafluoro benzoic acids: 2,3,4,5-TFBA, 2,3,5,6-TFBA | <100°C | Stable against biodegradation |

TABLE 4.  COMMON NON-RADIOACTIVE WATER AND VAPOUR TRACERS FOR GEOTHERMAL RESERVOIRS

| Tracer | Temperature limitations | Remarks |
|---|---|---|
| Sodium benzoate | | Generally applicable to water dominated reservoirs |
| | | *Dyes* |
| Rhodamine WT | <160°C[a] | Ref. [12] |
| Fluorescine | <200°C[a] | Ref. [12] |
| | | *Naphtalene sulphonates* |
| 1-NS | <320°C[a] | Ref. [13], tracer for condensed phase |
| 2-NS | <320°C[a] | Ref. [13], tracer for condensed phase |
| 1,5-NDS | <280°C[a] | Ref. [12], tracer for condensed phase |
| 2,6-NDS | <320°C[a] | Ref. [13], tracer for condensed phase |
| 2,7-NDS | <320°C[a] | Ref. [13], tracer for condensed phase |
| 1,3,6-NTS | <290°C[a] | Ref. [12], some biodegradation below 70–80°C, tracer for condensed phase |
| 1,3,6,8-PTSA[b] | <260°C[a] | Ref. [12], tracer for condensed phase |

TABLE 4.  COMMON NON-RADIOACTIVE WATER AND VAPOUR TRACERS FOR GEOTHERMAL RESERVOIRS (cont.)

| Tracer | Temperature limitations | Remarks |
| --- | --- | --- |
| *Hydrofluorocarbons + SF$_6$* | | |
| Freon R-134a, (CF$_3$CH$_2$F) | <5% degraded in 50 d at 225°C | Ref. [14], tracer for vapour phase |
| Freon R-23, CHF$_3$ | Thermally stable | Ref. [14], tracer for vapour phase |
| SF$_6$ | No degradation in 14 d at 300°C | Ref. [15], tracer for vapour phase, 10% degraded in 14 d at 330°C |
| *Cyclic perfluorinated hydrocarbons* | | |
| PFC family | $T > 300°C$ | Tracers for the gas (vapour) phase |
| *Alcohols* | | |
| Methanol (CH$_3$OH) | No degradation in 14 d at 320°C | Refs [15–17], tracer for both condensed and vapour phases |
| Ethanol (CH$_3$CH$_2$OH) | 8% degradation in 7 d at 300°C | Refs [15–17], tracer for both condensed and vapour phases |
| n-propanol (CH$_3$CH$_3$CH$_2$OH) | 19% degradation in 14 d at 280°C | Refs [15–17], tracer for both condensed and vapour phases |

[a] $T_{1/2}$ (>400 d) here defined as the time needed at the indicated temperature to reduce the concentration by thermal breakdown to half of its original value.
[b] Pyrene tetrasulphonate.

### 2.1.4. Injection strategy

There are principally two different injection strategies:

(i) *Pulse injection:* The full tracer volume is injected within a time period which is short in relation to its movements between injector and producer. In practice, injection times of up to several tens of hours may be considered a pulse injection. Most oilfield reservoir tests utilize pulse injection. There are various pulse injection procedures.

(ii) *Continuous injection:* A diluted tracer volume is injected by pumping continuously over time. The pumping speed is preferably adjusted to the varying injection water flow rate in order to keep a constant tracer concentration in the injected water. Injection times may be as long as one year or more. By knowing the injected tracer concentration and by logging the tracer concentration in each production well, the fraction of injection waters in the produced water from each well can be derived directly. Only a small fraction of injections are performed in this way.

There is also another point to consider in the injection strategy, whether to emply topside or downhole injection. If the well construction and completion allows for downhole injection, it must be considered whether it is feasible (technically and economically) or desirable to inject separately in each reservoir section (for stratified reservoirs). This latter method requires that each reservoir section can be isolated during the injection.

Most tracer injections are carried out as integral topside injections; the water (and the tracer) injected at the well head will enter the formation through perforations in the various strata in an quantity which is approximately proportional to the water-relative permeability of the various zones.

### 2.1.5. Sampling strategy

The sampling frequency and procedure should be well planned. An inadequately planned and prepared sampling programme may ruin the whole tracer project. Important aspects to consider are the following:

- *Is each individual production well accessible for sampling?* In most land based reservoirs this is the case. In offshore wells where the wellhead is 'dry', i.e. placed on a platform above sea level, this may also be the case. However, for subsea completion where the well heads are placed on the sea bed, each individual well may not normally and easily be accessible for frequent sampling. In this situation, the well flows from several wells come

together and are co-mingled in one transportation pipeline from the bottom hub to the receiver installation either on an offshore platform or onshore. Individual well sampling may not be possible in this case. However, in order to enable production testing of individual wells, the bottom hub is normally equipped with valves on the production line from each individual well. Thus, by closing these valves according to a certain procedure, the production from one well may be increased at the expense of the others. In this way, the production of a certain tracer may be associated with a specific well (or a limited selection of wells) each time a production logging operation is carried out.

- *Cross-contamination*: When each individual well is accessible for sampling and the sampling is performed directly in the flow line, there is a very limited possibility for cross-contamination of the collected samples, i.e. that waters from various wells mix in the same sample. However, human error and erroneous labelling of the collected sample may happen and lead to confusion in the results. Most often, the collection of water samples, even from individual wells on a platform, is performed on a test separator which is common for several wells. In this case, cross-contamination can more easily happen. The remedy is to ensure that all water from testing of the previous well is swept out before sampling the next well.

- *Sampling procedure*: Regarding concrete sampling procedures some questions must be considered, Will it be discontinuous sampling involving personnel for each individual operation? In which case, who is going to do the job? Are there special requirements for sampling containers or stabilization additives to the sampled fluids (e.g. for preventing microbial degradation of the tracer during transportation and sampling)? Is it possible to adapt some form of automatic batch sampling so that personnel are not so involved at each operation? These are all questions that must be clarified upfront.

- *Sampling frequency*: How often should samples be collected? This question should be answered on the basis of a best estimate of expected tracer breakthrough. As a general rule, the sampling frequency should be relatively high in the beginning, starting shortly (a few days) after injection. All samples are stored safely. As an example, each fifth sample is sent for tracer analysis. After the first tracer detection, the previous four samples are analysed with priority reversed in order to determine more precisely the tracer breakthrough time. After tracer breakthrough, the high sampling frequency should be maintained and each sample analysed until the tracer production peak lies on a decaying slope. On the tail of the curve, the sampling can be less frequent.

The sampling frequency (samples/d) depends on the geometrical size of the tested field section and on the flow rates involved. In an average sized reservoir with well distances in the range of 500–1000 m, a sampling frequency in the beginning can be one sample each 2–4 d, followed by the same frequency after tracer breakthrough. After having passed the peak maximum, the frequency can be reduced to one sample per week or per two weeks and later even to one sample per month. It is, however, recommended that sampling and analysis be continued as long as possible, since much information from a tracer test lies in the tail of the curve. The $L_D$ value for the particular tracer sets a practical limit to the sampling period.

## 2.2. IMPLEMENTATION OF FIELD RELATED OPERATIONS

### 2.2.1. Preparation of a technical safety report

Before implementing a tracer operation in the field, an application for the radiotracer experiment has to be submitted to the national radiological protection authority for evaluation and acceptance. To ensure that persons are protected from harmful effects of radiation, such application must comply with the International Basic Safety Standards [18] or equivalent national regulations. No practical action is taken before permission is granted by the relevant authority.

The safety evaluation report is the basis for this application. Such a report may contain an introductory description of experiments, descriptions of radiotracers, transportation and storage of radiotracers and injection methods, as well as radiation safety measures for all radiotracer related works.

The authorized person or organization will have the prime responsibility to ensure that radioactive material is used safely and in compliance with relevant regulations and standards. Guidance on occupational radiation protection, development of safety assessment plans and safe transport of radioactive material has been published by the IAEA [18–21].

### 2.2.2. Preparation and transportation of radiotracer

Radiotracers for interwell purposes are often purchased from a commercial company as an aqueous solution, sometimes as a dry salt. Whenever the radiotracer can be purchased in dry form this is preferred because it enhances the shelf life of the tracer due to reduced autoradiolysis.

The radiotracers are provided in suitable transport containers which depend on characteristics of the radioisotopes. In most of cases, the supplied radiotracers

*FIG. 5. Container for transportion and flow through injection of beta emitting tracers.*

are ready for injection, and transported to injection sites according to transportation regulations [21].

In the case of exclusively beta emitting tracers, for instance HTO and $S^{14}CN^-$, it is advantageous to add a small quantity of a short lived gamma emitter in the form of a water tracer, for instance $^{131}I^-$, for easy monitoring of the injection process during field operation.

Figure 5 shows an example of container for transportation and flow through injection of beta emitting tracers. It has a volume of 100 mL and is rated to a pressure of 350 bar.

The container in its plastic and lead support is mounted inside a transportation drum lined with shock absorbant material, as shown in Fig. 6. The transportation drum is labelled with the correct radioactivity transportation index and information about the type and quantity of the radionuclide according to the national regulations.

## 2.2.3. Injection methods

### 2.2.3.1. Pulse injection

There are two main procedures for tracer pulse injection:

(i)  Integral (topside) injection at the well head where the tracer enters all available perforated zones and is injected into the reservoir according to the injectivity in the various zones.

(ii) Downhole injection where different tracers may be injected in different isolated zones.

*FIG. 6. Drum lined with shock absorbant material for transportation of the container.*

*Topside radiotracer bypass injection*: This is the simplest, cheapest and most frequently used injection method. The practical implementation procedure depends on the tracer to be injected, i.e. the procedure is simplest for beta emitters and somewhat more cumbersome for strong, high energy gamma emitters. The techniques range from mechanical crushing of tracer-containing glass vials in the injection stream to controlled pump operated injection and soluble solid state tracer slug injection.

Below, a well-proven technique for water radiotracer injection is described. The tracer mixture is prepared in a 100 mL flow through high pressure (rated to 500 bar) steel cylinder fitted with high pressure valves at both ends (total liquid volume ≈ 70 mL). For beta tracers, a small quantity of a short lived gamm emitter (often $^{131}I^-$) is added for monitoring purposes.

Figure 7 illustrates typical small-sized injection equipment fitted into a suitcase shaped transportation container which may be carried by hand. The equipment is coupled to the main injection line as a bypass at two positions across a throttle valve. The function of the throttle valve is to set up a pressure difference between the two positions. The tracer container is connected to the equipment as shown. There are possibilities for pump operation of preparative fluids (inlet for chemicals) before tracer injection. The tracer is injected by by passed injection water driven by the pressure difference, and without any use of pumps. The injection efficiency is monitored by external gamma detectors in cases where a small quantity of a gamma emitting tracer is added to the tracer container. A typical injection time is <10 s for >99% of the tracer. However, rinsing continues
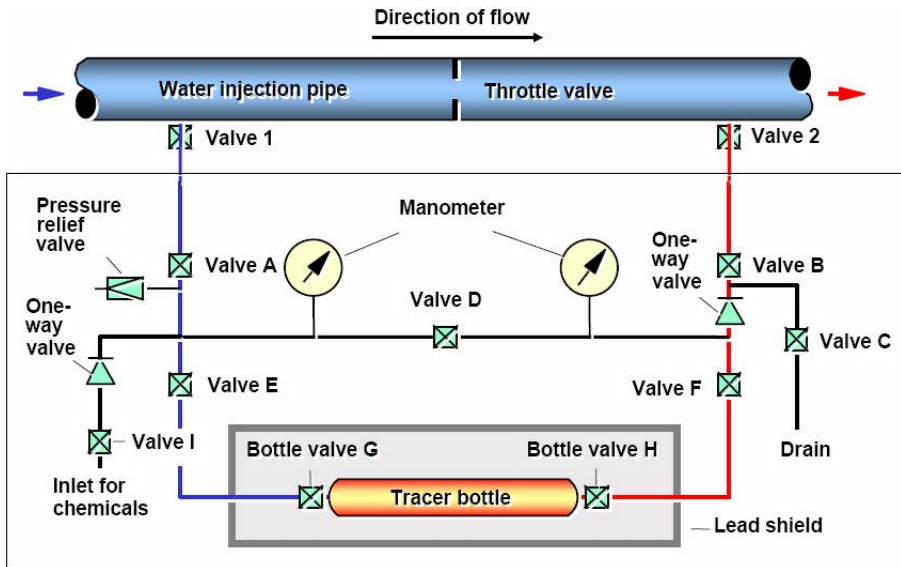
*FIG. 7. Small-sized injection apparatus for topside pulse injection of radiotracers.*

for 60 min to clean out any remaining traces of activity from the injection apparatus.

For some tracers, it is advantageous to apply an extra non-radioactive molecular carrier in the injection phase (e.g. for $^{125}I^-$ and radiolabelled $[Co(CN)_6]^{3-}$). These tracers are injected using the same injection apparatus but now connected only to the main flow line at the outlet connection point. The injection is performed by pump operation where injection water containing carrier and other tracer preserving chemicals is pumped from an injection water reservoir.

*Topside radiotracer 'crushing' injection*: Figure 8 shows equipment for crushing injection of tracer. A 20 mL tracer glass vial containing a beta emitting tracer is loaded into the holder of the injector.

The equipment is then installed at the well head of the injector (Fig. 9). By operation of the hand wheels (A and B), the tracer vial will be crushed by the central bar and the tracer thereby released into the well. As with the bypass injection described above, a small quantity (a few megabecquerels) of a gamma emitting tracer, for instance $^{131}I^-$, is utilized as a second tracer to monitor the injection process and confirm successful injection.

*Pump operated radiotracer topside pulse injection*: Pulse injection may also be carried out by means of pumping. When a gamma emitting tracer is used,
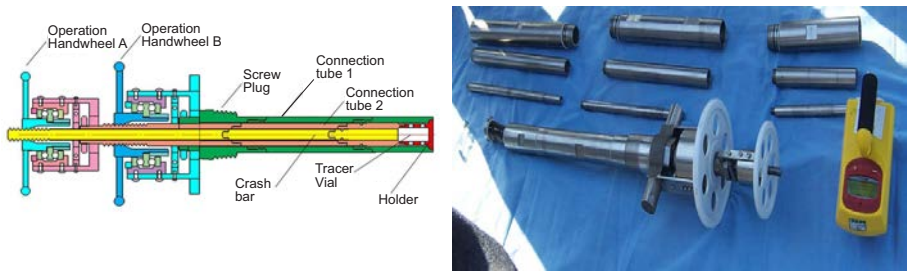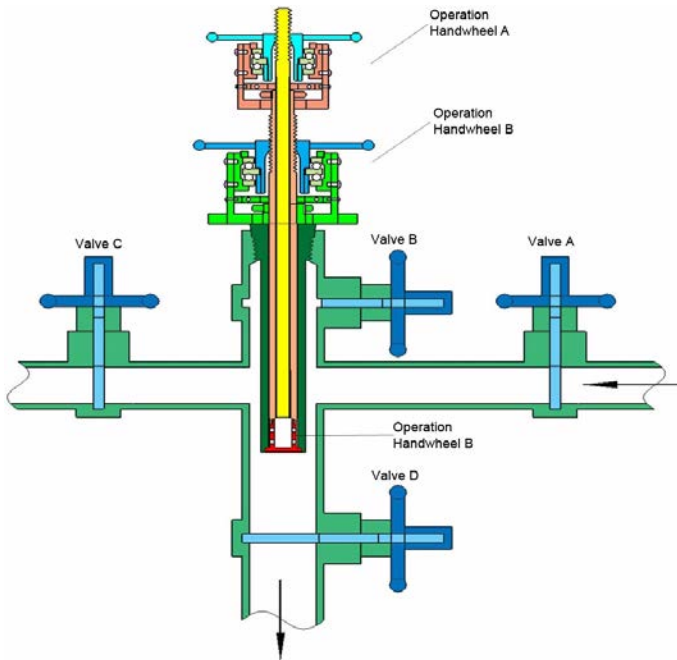
FIG. 8.  Crushing injection equipment.



FIG. 9.  Installation of the crushing injection equipment at the well head of an injector.

the radiation load to the operators has to be monitored in order to minimize any dose.

In this case, the transportation cage with the original lead shield may also be used during injection by leaving the radioactive liquid inside, connecting a slim flow line to the bottle and injecting the tracer by means of a high pressure suction pump. Useful equipment for this purpose is illustrated in Fig. 10.
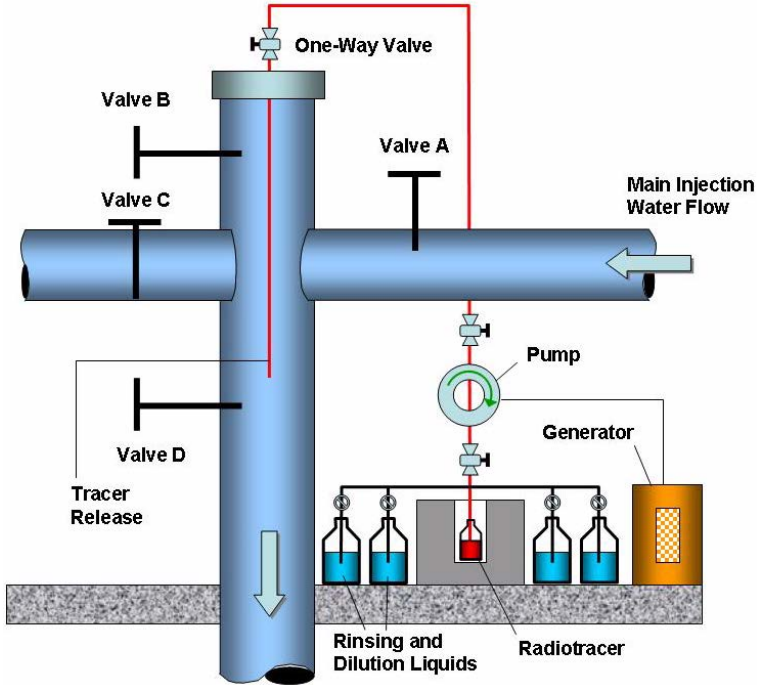
*FIG. 10. Piston pump system for injection of gamma emitting tracers such as $[^{60}Co(CN)_6]^{3-}$. It can also be used for beta emitters such as HTO and $S^{14}CN^-$.*

*Pump operated topside pulse injection of non-radioactive tracers*: As mentioned previously, non-radioactive tracers are mainly liquid (aqueous) solutions of weak acids or salts. Over long distances, it is most convenient to transport the tracer compound in dry form (Fig. 11) and perform, whenever possible, the dissolution operation at the well site.

Some of the tracer compounds have limited water solubility. Weak acids may need addition of a base such as NaOH or KOH in order to promote dissolution. Finally, several hundred litres may be required for injection, even for an ordinary-sized reservoir section. Hence, injection requires higher capacity pumps than previously described. Figure 12 gives an example of both the tracer solution container and the pneumatically operated pumps used for injection.

This type of tracer injection may take a few hours depending on the volume of the tracer solution. In principle, this represents a square injection pulse but it may be regarded as an instantaneous pulse injection when compared with the transit time through the reservoir.

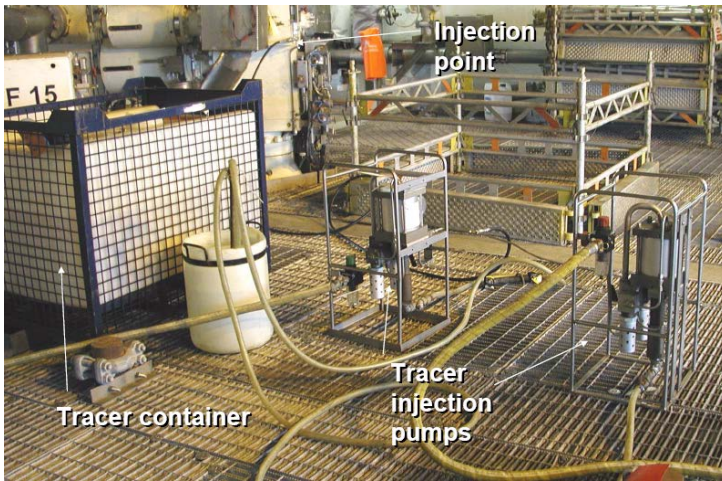FIG. 11. Example of tracer chemicals in dry form in transportation containers.



FIG. 12. Injection equipment for non-radioactive tracer solutions, here shown on the deck of an offshore production platform in the North Sea.

*Downhole pulse injection*: Downhole injection offers several advantages over topside injection:

- Removal of the danger for contamination of topside equipment. This may be especially important for radiolabelled $[Co(CN)_6]^{3-}$ and possibly other complexes which may react chemically in the injection tubing.
- For stratified reservoirs, each zone may be uniquely labelled with a special tracer. This makes it possibile to examine vertical permeability in reservoirs and detect any extensive sealing.
- For horizontal wells which cover an extensive lateral reservoir section, zone injection is absolutely desirable for optimal information.
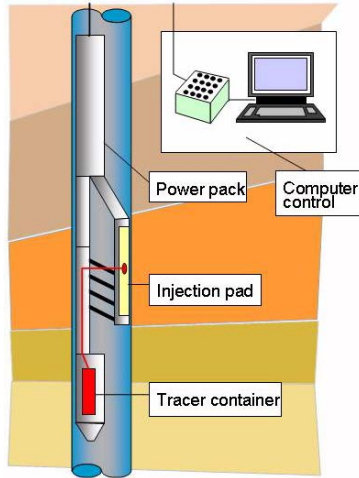
*FIG. 13. Downhole tracer injection tool.*

Downhole injection is not yet in general use although field tests have been successfully carried out [11]. A few attempts have been made to construct tools for general application, one of which is illustrated in Fig. 13 [10]. It is mainly constructed for vertical and deviated wells. It can be lowered into the well by a wireline which makes signal transfer possible. The tool is remotely operated from topside by PC control. It is based on the principle of a moving arm sealing onto the perforated section of the well through which the tracer solution is pumped at low speed during somewhat reduced rate of ordinary water injection. The tool is not yet in operation due to high cost of operation.

Lately, it has become technically possible to position downhole injection tools in horizontal wells by means of a well tractor. Combined with inflatable packers on the same line, sections may be isolated for specific tracer injection. Such injection equipment is composed of general and readily available components. It is therefore technically possible to conduct zone injection, but the first large scale field experiment has yet to be carried out. Some well completions are constructed to allow water injection into selected isolated zones. These completions can be used for selective zone tracer injection although the addition of tracer itself is carried out topside.

### 2.2.3.2. Continuous radiotracer injection

This method has been applied mainly for injected water. It is useful, especially where unsaturated water–wet rock may absorb short tracer pulses by water imbibition from the injected water front edge. Ideally, the method requires
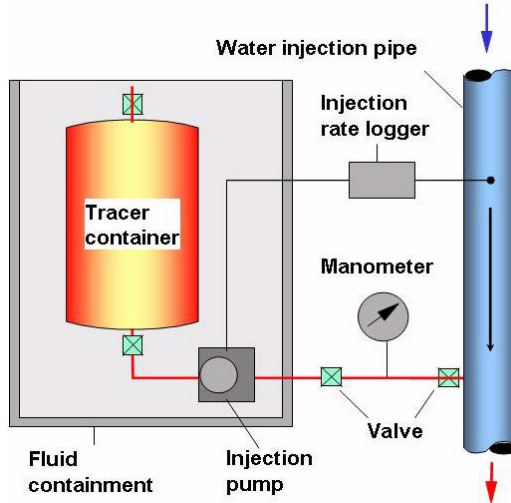
33

*FIG. 14. Tracer injection arrangement for continuously constant concentration injection of beta emitting water tracers.*

continuous logging of the water injection rate and corresponding adjustment of the tracer dosage rate in order to maintain a constant concentration of tracer in the injected fluid. A simpler arrangement can be implemented if a constant water injection rate can be assured. An example of a tracer injection arrangement is shown in Fig. 14.

Typically, the tracer used is HTO and the concentration in the tracer container is 370 MBq/L. The tracer concentration in the injection water, and the corresponding rate of tracer dosage, depends on the detection limit in the analytical laboratory and on the expected fraction of traced injected water in the produced water. The design should be a tracer concentration at the top of the production curve (at 'equilibrium') corresponding to some 100–1000 Bq/L in the produced water.

There is an example of a field experiment with continuous injection of HTO tracer and a subsequent tracer pulse injection ($^{125}$I$^-$). Such operations may be laborious and cumbersome, especially for offshore operations. They require access to tracer engineers on a semi-continuous basis; regular controls with the equipment and tracer solutions will have to be performed. In addition, long term storage and use of radioactive solutions give rise to some scepticism among petroleum rig personnel. This method should only be used if there are clear advantages over the pulse injection method.

In principle, this method may be used also for non-radioactive tracers, but the tracer reservoir volume has to be larger and the pump somewhat different

from both that described in Fig. 12 (smaller than this) and that used in Fig. 14 (somewhat larger than this).

### 2.2.4. Actions for radiation safety at the injection site

Detailed procedures for operations before, during and after injection should be described in the technical safety report. Some of the important points to be considered for radiation safety at an injection site involve:

- Informing well site personnel about the nature of the work to be done. In the case of radiotracers, explanations should be given in some detail, especially with regard to contamination/decontamination, radiation risks, doses etc.
- Preparing the injection site, setting up the equipment and connecting to the injection pipeline. In the case of injection against high pressure (several hundred bars), all connection points have to be leak tested before starting to pump the radiotracer solution. The injection area has to be cordoned off and signs displayed in order to deter unauthorized persons from entering.
- Ensuring that all operational personnel wear suitable protective clothing and personal dosimeters.
- Preparing monitoring and decontamination equipment to handle potential spills and leakages according to the written procedures.
- Flushing pure injection water through the injection apparatus and connected equipment for an extended period (~1 h) to clean out any traces of the radiotracer before disconnecting injection equipment.
- In the case of any leakages, performing the planned and prepared-for decontamination operation and enclosing any contaminated parts in suitable plastic bags for transportation back to radiotracer company's premises for further decontamination.
- As a final check of the injection site before leaving, carrying out sweep tests for on-site analysis with relevant nuclear detection equipment.
- Finally, collecting urine samples from all personnel present during injection for subsequent laboratory analysis for any ingested or inhaled activity.

## 2.3. TRACER ANALYSIS STEPS

### 2.3.1. Fluid sampling in production wells

Sampling must be carried out according to the planned schedule and in most cases should start immediately after injection.

Sampling frequency will depend on the basic understanding of reservoir production dynamics. The decision to stop sampling is made jointly by the end-user and tracer team based upon the development of the tracer production curve and cannot be planned a priori. Generally, sample volumes of 0.5–1.0 L are preferred. This enables repeated analysis of the same sample if desirable. This possibility may be important for quality assurance of the analysis. In the case of water cut, preferably less than ~10% of the water sample is collected at the separator equipment point where the majority of the oil is removed.

In the case of too much oil, the water has to be recovered from a complex oil–water emulsion, and the quantity of water recovered may still be too little to obtain a high quality analysis with the best detection limit. For sampling in geothermal wells this problem does not exist.

A typical sampling schedule is introduced below. Tools for well head sampling include:

- Personal protective equipment (safety glasses, gloves, personal $H_2S$ monitor and respirator (if required by local rules), etc.);
- Crescent wrenches;
- 20 L bucket for oil and water spills;
- 1 roll of electrical tape for sealing up the bottle cap;
- 1 L plastic wide mouth sample bottles;
- Absorbent pads (for oil spills);
- Rags (for water spill);
- Felt tipped permanent marker for writing on bottles;
- Sampling record book.

The sample is marked and identified by the well number, date of collection and, preferably, by the initials of the sampling engineer. The actual schedule of sampling and the method used is field dependent. Different methods may be considered:

- Manual sampling carried out by the operator;
- Automatic sampling at the well head;
- Continuous sampling;
- Downhole sampling.

### 2.3.1.1. Sampling of geothermal fluids

Geothermal fluid sampling for tracer analysis of isotopes such as tritium and $^{125}I^-$ ($^{131}I^-$) in both vapour and liquid systems is done through a condensation process of the fluid, as shown in Fig. 15.
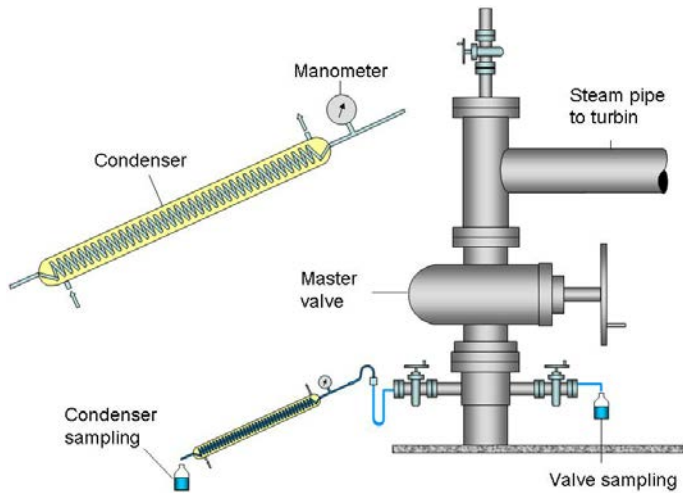
*FIG. 15. Schematic diagram of a condenser used for sampling in geothermal wells in Indonesia.*

The sampling procedure is as follows:

• The condensation of the geothermal fluid is achieved using the condenser apparatus shown in Fig. 15.
• The condenser is connected to the well head. Cool water flows into the condenser countercurrent to the geothermal fluid which is transported in the spiral tube.
• The valve at the well head is opened to allow hot fluid to flow into the condenser.
• Water from the vapour or hot liquid is condensed to ambient temperature. This water is collected in a plastic bottle of 1 L or 2 L capacity.

Sampling in the Philippines (at the Energy Development Corporation) makes use of a Weber separator, where steam and water are separated during sampling. In the Philippine geothermal fields, the Weber separator is connected along two phase lines (shown in Fig. 16) and samples are collected separately for water and steam condensate.

*FIG. 16. Sampling of HTO in a geothermal well in the Philippines using a Weber separator.*

### 2.3.1.2. Oilfield sampling

Manual sampling

(i)     Direct method

In the oilfield, the simplest form of manual sampling is performed by using a plastic bottle. The bottle is connected to a bleed valve which is mounted on the production line. Further, the bottle should be connected to a gas treatment system (flaring, venting) that takes care of any associated gas. A schematic of the system is shown in Fig. 17. By careful opening of the valve, the liquids are bled off from the production pipeline into the bottle. A mixture of oil and water is normally collected by this method (Fig. 18).

(ii)    Well head sampling method

Another somewhat more sophisticated manual sampling method involves the use of a phase separator that is connected to the well head (Fig. 19). The sampling procedure is as follows:

• The separator equipment is connected to the well head.
• The valve at the well head is opened and a mixture of oil and water flows through the main pipeline. A bypass is led into the separator.
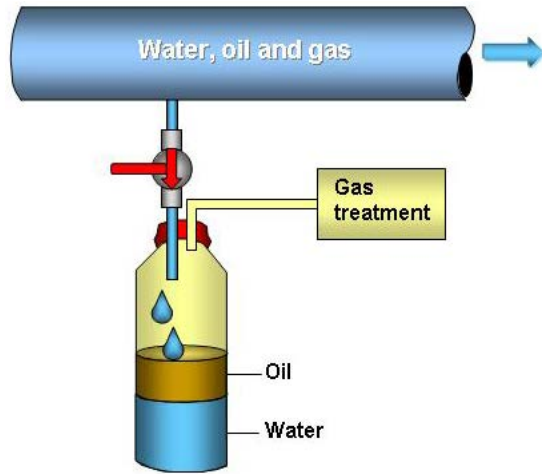
*FIG. 17. Schematic of the manually operated sampling of water from the production pipeline.*



*FIG. 18. Manual sampling at the well head of an oil well.*

*FIG. 19. Separator sampler used for water sampling in oil wells.*

- The oil phase is located in the upper part of the separator and is from there continuously transported back to the main pipeline.
- The water phase accumulates in the bottom of the separator.
- Water samples can be collected continuously from this equipment by opening the valve at the bottom of the separator.

Automatic sampling

Sampling is always a vital procedure for conducting interwell tracer tests and timely sampling is most important in ensuring that a test is successful. The automatic sampler shown in Fig. 20 is designed to be installed at the well head. It can automatically collect seven samples within a planned period, e.g. over one day, one week or two weeks. The automatic sampler consists of a separator (A), a control unit (B), a mini-pump (C), seven water sample containers (D1–D7) and electromagnetic valves (V1–V12) (see Fig. 20). In many cases, the electromagnetic valves should be substituted with pneumatic valves due to the probability of gas leakage and the danger of an explosion caused by the electronic circuits.

The functioning of the automatic sampler is as follows:

(1)    The multiphase flow enters through valve V1 into the separator.
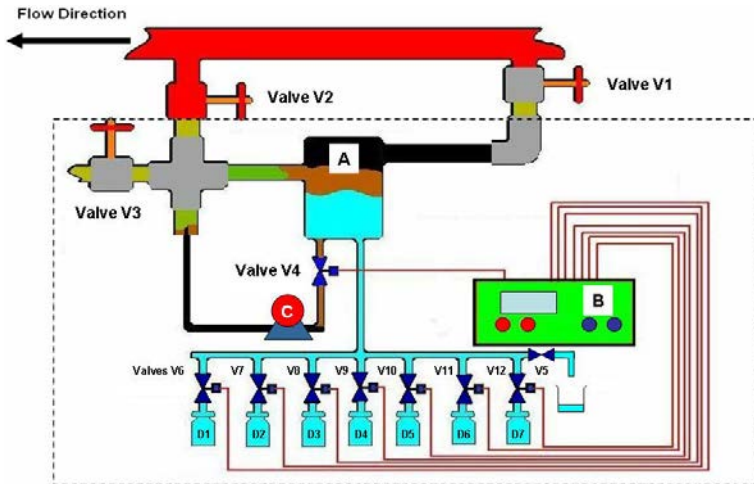(2)    The produced fluid will charge the separator A and the oil and water separate continuously by gravity.

FIG. 20. Schematic diagram of an automatic sampler for water from an oil well.

(3)  The separated 'oil' phase on top of the separator is pumped back to the bypass pipeline through valve V2 when keeping valve V3 (drainage) and valve V4 closed.

(4)  At the end of a set collection time, 'old' water from previous samplings is removed from the manifold by drainage through valve V5.

(5)  The fresh 'water' sample from the lower phase inside the separator is transferred to the sample container (D1) by gravity by opening valve V5.

(6)  After sampling, the remaining water in the separator is pumped back to the bypass pipeline by opening valve V4.

(7)  Sequences 2–6 is then repeated for the remaining sampling bottles.

(8)  Valve V3 is used for pressure release and drainage when replacing the separator equipment. Oil samples can be taken manually through valve V3 as needed.

## 2.3.2.  Measurement techniques

Measuring techniques depend on the tracers' radiological characteristics (beta, gamma or stable chemical ones), but all of them include some sample treatment prior to undertaking the measurement itself.

When counting a radioactive sample, it is well known that the instrument reading is a measure of the sample activity plus the background activity. The latter must be subtracted in order to evaluate the actual net sample activity. The background activity is usually taken to be the activity measured by using the sample taken before the injection (blank sample). If, however, the tracer does not appear

immediately (there are no canalizations), a more representative value of the background activity is obtained by measuring several of the samples and averaging the results, taking into account that the more samples, the lower the background's variation coefficient will be. The variation coefficient is the ratio between the standard deviation and the mean value.

Radioactive decay is an inherently random phenomenon that follows, strictly speaking, the binomial distribution. Nevertheless, the Poisson distribution is an excellent approach that takes into account some of the radioactive decay characteristics (the random event 'disintegration' is repeated many times and the individual probability of an atom disintegrating is very low).

Poisson distribution depends on just one parameter, generally symbolized by the Greek letter $\sigma$ and the distribution mean value and the variance are both equal to $\sigma$. This property is very useful in radioactive measurements. Once the count rate has been determined, its numerical value can be used as the expected average value and its square root as the standard deviation.

Furthermore, in the case that the number of events approaches infinity, the binomial distribution and the Poisson distribution converge towards anothers statistical distribution known as the normal distribution or Gaussian distribution, which is continuous and symmetrical around its mean value. In a normal distribution, the probability for the random variable to take values close to the mean value is very high while it approaches, asymptotically, zero for large values located in the positive and negative distribution 'tails'.

As a 'rule of thumb' it is common to require that all random variable values fall within a 2.0 standard deviation interval around the mean value. In such a case, a confidence level of 95% for the measurement is established. This means that there is a 5% probability that the 'true' mean value is outside the range given by the measured mean value by +2.0 and –2.0 standard deviations. Consequently, two measurements may be said to belong to different populations when their measured mean values differ by at least five standard deviations. This criterion is also applied to determine whether a sample is active or not, namely, that a sample has some radioactivity of its own when its count rate is five standard deviations greater that the background.

Generally, the following condition is established to calculate the lower detection limit (minimal detectable concentration), $L_D$, on the basis of the instrument background:

$$R_N > 2\,\sigma_{R_B} \tag{5}$$

This means that the sample count rate should be at least twice its own standard deviation in order to be distinguished from the background. The standard deviation is given by the following expression:

$$\sigma_{R_N} = \sqrt{\frac{R_G + R_B}{t_c}} \tag{6}$$

where

$\sigma_{RN}$   is the standard deviation for the net count rate $R_N$ (cps);
$R_G$   is the gross count rate (cps);
$t_c$   is the counting time (s);
$R_B$   is the background count rate (cps).

After some operations and approximations the following expression is obtained for $L_D$:

$$L_D = \frac{2.8}{\varepsilon\, V} \sqrt{\frac{R_B}{t_c}} \tag{7}$$

where

$L_D$   is the lower detection limit (or minimum detectable activity concentration) (Bq/L);
$R_B$   is the background count rate (cps);
$t_c$   is the counting time;
$\varepsilon$   is the detection efficiency (counts per disintegration);
$V$   is the sample volume.

As a consequence of statistical dispersion, some preprocessing of experimental data is usually needed in addition to the subtraction of background values in order to filter noise and smooth the response curves.

Finally, radioactive decay correction is needed, although in the case of tritium its half-life is long enough to avoid this kind of correction when the sampling periods last only a few months. In a general situation, an interwell study implies more than a year of sampling and tritium decays at a rate of 0.45% per month.

*2.3.2.1. Beta radioactive tracers*

The most common beta radioactive tracers for interwell studies are labelled with tritium $^3$H, $^{14}$C or $^{35}$S. All of them are usually measured by means of a liquid scintillation counting technique. A small volume of a liquid sample is mixed with a special solution known as a 'scintillation cocktail', commonly in a 20 mL light transparent (glass, polypropylene, teflon) vial. Beta particles cause emission of light when passing through and slowing down in the scintillation cocktail. These light pulses are registered by photomultipliers (PMTs) suitable for that particular photon wavelength. The light output in a pulse (light intensity) is proportional to the energy of the beta particle. This process is termed scintillation, and since it happens in liquid media, it is known as liquid scintillation.

The vial is placed inside an instrument, a liquid scintillation counter, which normally has two PMTs operating coincidentally to reduce the background. The liquid scintillation counter analyses the pulses from the PMTs and provides information about the energy of the beta particles and the rate of beta emission (activity) in the sample.

Pulses are sent to an analogue-to-digital converter where they are digitized and stored in an address memory according to their amplitudes, which are proportional to their beta energies (energy spectrum in a multichannel analyser).

In order to reduce further the background coming from natural radiation, a lead shield usually surrounds the PMTs and the vial while the sample is in the measuring position. Modern low background detection equipment also has a so-called active shield. In most cases it consists of a liquid scintillation detector surrounding the PMTs and the counting sample. This shield detector is operated in anticoincidence with the PMTs, such that any event which is registered both in the two PMTs and in the shield (cosmic rays, environmental radiation) detector simultaneously is rejected. In the case of simple non-spectrometric detection equipment (single channel analyser), the contribution of the background to the sample count rate can be further reduced by setting a counting window over only the interesting energy portion of the energy distribution. This is achieved by selecting narrow upper and lower limits. In the case of tritium, the upper gate should, for instance, be set at 19 keV.

Various processes may perturb the beta spectrum obtained in a liquid scintillation process. The most important of these are:

- *Chemiluminescence*: When different chemicals are mixed in the sample vial together with the scintillation cocktail, chemical processes may start which have relatively slow kinetics and which result in the emission of low energy photons. These photons may contribute to the very low energy end of the beta spectrum. Chemiluminescence may be reduced or completely removed

by gentle heating of the vial to 50–60°C for some minutes before counting in order to speed up the chemical process.

- *Phospholuminescence*: When a sample vial with the scintillation cocktail is exposed to white light (daylight or lamp light), the light energy may be temporarily 'stored' and slowly released during sample counting (phosphorescence). Also, this light will contribute to the very low energy end of the beta spectrum. Therefore, counting samples should always be stored in the dark for a few hours before counting starts.
- *Colour quenching*: A coloured sample liquid may absorb some of the light emitted by the scintillator. Yellowish or brown colours are the heaviest colour quenchers. Hence, attempts should be made to remove such colours during the sample preparation process and before counting.
- *Chemical quenching*: Some components in the sample may kill the energy transfer process that takes place in the scintillation cocktail and which eventually results in light emission. Such chemicals absorb the energy and release it in the form of heat. Heavy chemical quenchers include, for instance, organic compounds containing oxygen and in particular chlorine.
- *Physical quenching*: Solid particles or non-transparent emulsions in the sample may prevent light from being detected by the PMTs.

All of these forms of quenching result in a shift of the energy spectrum towards lower channel numbers because the number of photons detected by the PMTs per beta decay is reduced. Figure 21 shows in principle the effect of quenching. Quenching may change from one sample to another. Evaluation of the quenching effect is necessary in order to calculate counting efficiency.
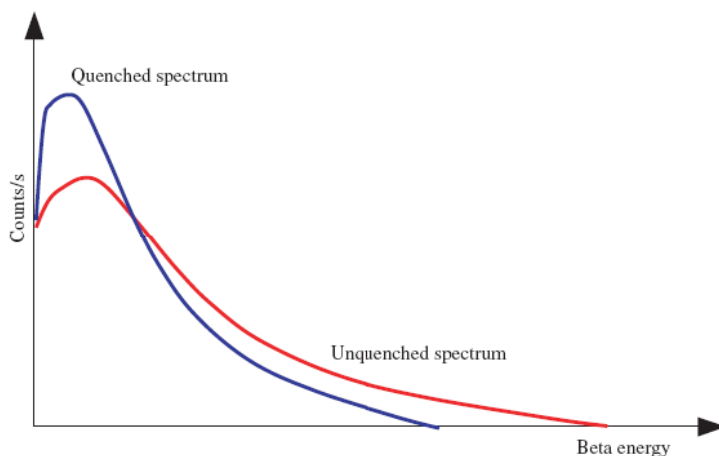


FIG. 21.  The effect of quenching on a liquid scintillation beta spectrum.

In summary, liquid scintillation counting requires careful sample preparation. Chemical separations are most often involved and when these procedures are optimized, very low detection limits may be obtained, ranging from 2 Bq/L for HTO to <0.02 Bq/L for $S^{14}CN^-$.

### 2.3.2.2. Gamma tracers

Gamma tracers are commonly measured using either solid scintillation detectors or semiconductor detectors.

*Solid scintillation detectors*: These are of different types, but the most generally applicable is the detector based on a single crystal of sodium iodide doped with traces of thallium, the so-called NaI(Tl) detector. The crystal is optically coupled to a PMT. Interaction of a gamma photon with the scintillation crystal results in the emission of light, which is detected by the PMT.

The light output is proportional to the gamma energy. The electronic system associated with the PMT analyses the pulses according to pulse amplitude (energy) and stores the results in a multichannel analyser. Thus, energy and intensity are recorded, and the result is the gamma energy spectrum of the radiation source.

The NaI(Tl) detector has a high intrinsic efficiency but limited energy resolution. The scintillation crystals are provided in different sizes. The efficiency for high gamma energies increases with detector volume.

Common counting equipment has cylindrical crystal sizes of 50 mm × 50 mm to 125 mm × 125 mm (height × diameter): the larger the crystal, the higher the price. The detectors can be made quite rugged and are suitable in field instrumentation.

*Semiconductor detectors*: Today, these are mainly based on high purity germanium crystals, so-called HPGe detectors, where a semiconductor junction is created by suitable elemental dopants on the crystal surface. A gamma ray interacting with the detector will result in an excitation of electrons from the valence band to the conduction band in the crystal, and a small electrical pulse is created in a high voltage field. The pulse height is proportional to the gamma energy. The pulses are sorted and stored in a multichannel analyser.

The intrinsic efficiency of semiconductor detectors has, for many years, been lower than that of NaI(Tl) detectors. At present, it is, however, possible to purchase detectors with efficiencies >100% relative to that of a 75 mm × 75 mm NaI(Tl) detector, but prices are very high. The main advantage of an HPGe detector is, however, its excellent energy resolution. This property may be indispensable for the analysis of complex radiation sources. HPGe detectors need cooling to the temperature of liquid $N_2$ during operation and are not generally practicable as field instrumentation.

In general, gamma tracer detection requires little sample preparation except for the extreme low energy emitters (i.e.[125]I). There are several ways to reduce the minimum detectable concentration in gamma detection:

- Increase the intrinsic detector efficiency: This is a matter of cost.
- Increase counting sample volume (constant activity concentration in the sample leads to higher total activity in the sample): There is a practical limit to the sample size.
- Optimize the counting geometry by shaping the counting sample: For a given radionuclide, a selected detection set-up and a certain sample volume, there is an optimum shape of the sample volumes. For practical reasons these are most often cylindrical shapes.
- Enrich the tracer from a large to a smaller sample volume (increased total activity for a better sample counting geometry): This requires sample treatment either by liquid evaporation or by chemical separation. Sample treatment time and cost increase.
- Reduce the background level by effective detector shielding: This is most often done by passive shielding with lead walls (5–10 cm thickness) around the detector and sample.

A typical counting set-up for a NaI(Tl) detector is shown in Fig. 22. A 1000 mL Marinelli sample container, 75 mm × 75 mm NaI(Tl) detector, Pb shield (5–10 cm), a Sn (or Cd) screen to filter Pb X rays generated by the sample activity in the Pb shield, Cu filter screen to filter away Sn (or Cd) X rays generated by the Pb X rays in the Sn (or Cd) screen.

- With NaI(Tl) detector based analytical equipment, detection limits of <0.2 Bq/L can be obtained using Marinelli beakers and reasonable counting times for common radionuclides such as [22]Na, ^{60}Co and [125]I.
- For HPGe detectors, the corresponding detection limits are <0.1 Bq/L.

## 2.3.3. Laboratory tracer analysis

### 2.3.3.1. Tracer analysis of samples from the geothermal fields

(i) Analysis of HTO

HTO in samples from geothermal fluids is analysed using liquid scintillation counting. HTO analysis is performed by a direct counting method after a sample distillation pretreatment process. In the analysis, 11 mL of
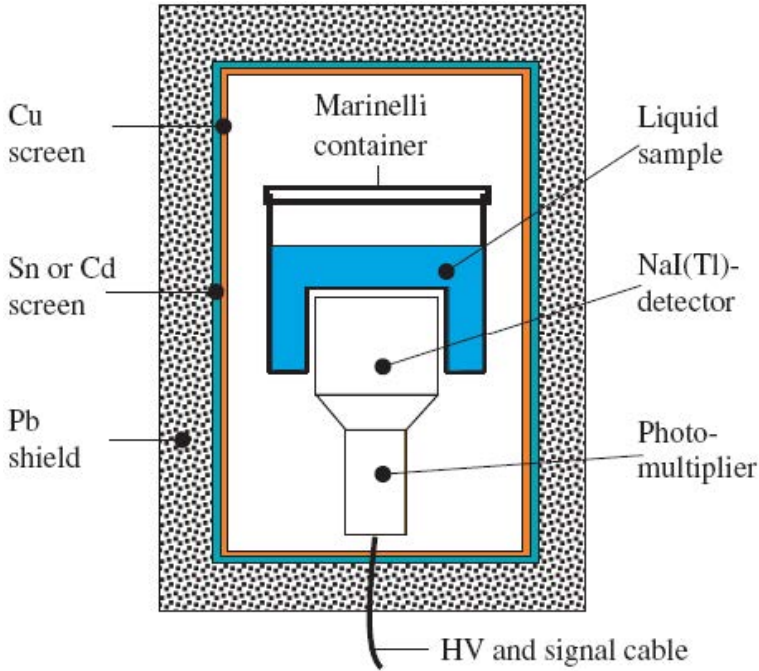
*FIG. 22. Sketch of a common set-up for counting of gamma active liquid samples.*

scintillation cocktail (Ultima Gold) is added to 10 mL of the distilled water and mixed into a 22 mL counting vial (glass or plastic) and homogenized by shaking. The counting time for each sample may, for instance, be 500 min (25 cycles, each lasting 20 min). The result is registered as counts per minute (cpm) and is subsequently converted to tritium units or becquerels per litre by taking into consideration the counting efficiency. A more detailed protocol for analysis of HTO is given in Appendix III.

(ii)   Analysis of $^{125}I^-$ tracer in water samples

Iodine-125 is a beta emitter with a half-life of 60 d. The beta decay is followed by a low energy gamma ray (35 keV). This radionuclide has a suitable half-life for short to mid-term re-injection into the geothermal field. However, the low energy characteristic makes $^{125}I^-$ difficult to detect directly in the field (on-line or in-stream). Pretreatment of the sample is needed before measurement, which is carried out either by liquid scintillation or by gamma spectrometry using a sensitive low energy gamma detector. The pretreatment is based on an upconcentration of the $^{125}I^-$ by addition of a known quantity of inactive iodide

48
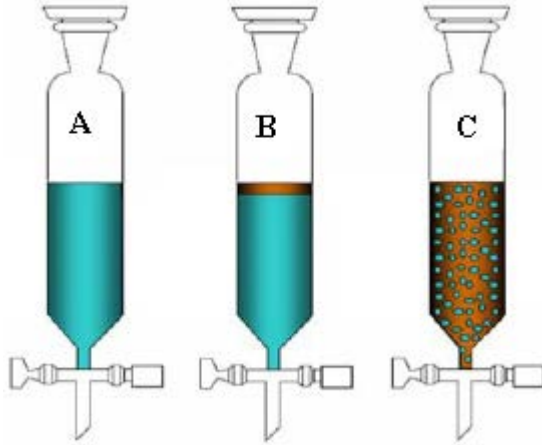
*FIG. 23.  Example of collected water samples with varying degree of oil. A is a sample typically taken from a test separator, B can be both from a test separator or from the flow line with a high water cut while C is typically from the flow line with a very low water cut.*

carrier ($^{127}I^-$), precipitation by silver as AgI followed by dissolution of the precipitate in the scintillation cocktail by addition of thiourea. The sample is then analysed by liquid scintillation counting.

All details of the analytical protocol are given in Appendix III. This protocol also includes the detailed procedure used to prepare $^{125}I^-$ for gamma spectroscopy measurement.

### 2.3.3.2.  Analysis of water tracers in samples from oilfields

(i)     Analysis of HTO

Water samples from oilfields may be of various qualities, ranging from relatively pure water (transparent liquid) via samples which contain some degree of oil to samples where the water exists mainly in an oil–water emulsion as illustrated in Fig. 23. Thus, pretreatment of the samples is needed before instrumental analysis of the beta emission (by liquid scintillation counting). The form of the pretreatment varies with the composition of the sample.

In general, for samples of type A and B, a combination of oil phase removal by pipetting and filtration followed by a distillation process is common. For samples of type C, an emulsion breaking step has to be included in the beginning before oil–water separation and eventual distillation of the resulting relatively small water volume (in most cases). Details on the analytical protocols, including pretreatments, are given in Appendix III.

(ii)    Analysis of HTO and $^{14}$C labelled alcohol in mixture

The analysis of HTO and $^{14}$C labelled alcohol in water samples from the oilfield cannot be carried out directly by liquid scintillation counting, as purification somewhat different from the procedure described above for HTO is required. The following equipment parts and the purification procedure are proposed:

*Equipment and reagents:*

(1)    Round flask 500 mL, connection size 24/40;
(2)    Fractional distillation Vigreux column, 31 cm long, cs 24/40;
(3)    Dean & Stark collector, volume 10 mL;
(4)    Water cooling system;
(5)    Heating mantle for the round flask;
(6)    Magnetic stirrer;
(7)    Liquid scintillation counter with standard vial of volume 22 mL;
(8)    Methanol and toluene reagent grade;
(9)    Scintillation cocktail, e.g. Instagel or Ultima Gold.

*Procedure:*

(1)    Sample treatment: Add 10% v/v of toluene to a water aliquot in a separation funnel and shake to extract any dispersed oil droplets into the toluene.
(2)    Transfer a maximum 10 mL aliquot of the water phase to a standard counting vial and mix with 10–12 mL of an appropriate scintillation cocktail. Shake vigorously to create a stable gel.
(3)    Store the sample in the dark at least 1 h before starting the count.
(4)    Count the sample in the liquid scintillation counter in dual label mode with the windows set at $^{3}$H and $^{14}$C. Calculate the tritium activity by correcting for the contribution of $^{14}$C in the tritium window.
(5)    To another 10 mL of the purified water phase add 3 mL of methanol and 1.3 mL of toluene and transfer the mixture into the round flask. This volume ratio of methanol and toluene creates an azeotrope.
(6)    Heat the sample very gently at low power (a few hours) to distil off the azeotrope.
(7)    Collect the distillate (about 4 mL) into the vial.
(8)    Add cocktail (10 mL) and count in dual label mode with the windows set at $^{3}$H and $^{14}$C. Calculate the $^{14}$C activity by correcting for the tritium activity in the $^{14}$C window.

# Gamma detection geometry
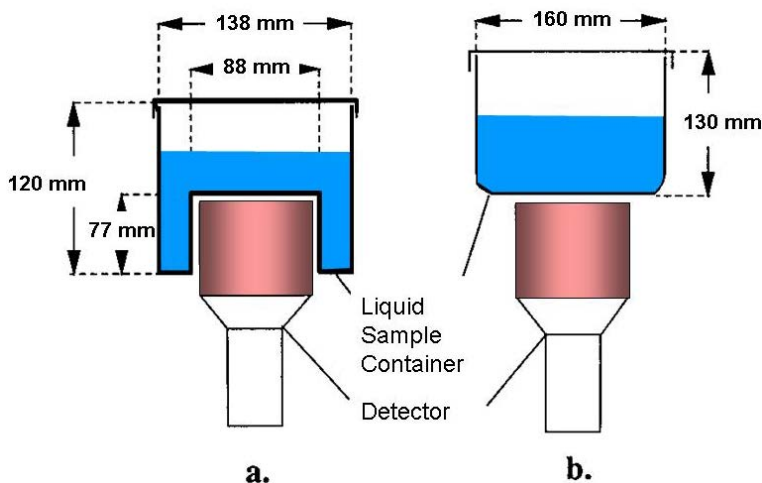## - 3x3" NaI(Tl), Marinelli and cylindrical samples

*FIG. 24. Counting geometries for liquid samples in gamma spectrometry with NaI(Tl) detectors.*

A suitable procedure for dual label counting is normally supplied with the delivery of the liquid scintillation counting equipment.

(iii)   Analysis of $^{60}$Co labelled water tracer by gamma spectrometry

The $^{60}$Co labelled water tracer is $[^{60}Co(CN)_6]^{3-}$. The $^{60}$Co emits strong gamma radiation resulting in a simple gamma spectrum (main energies at 1173 and 1332 keV).

Thus, gamma spectrometry may be a useful analytical method, also when this radionuclide is in mixtures with tritium, $^{14}$C or $^{35}$S labelled compounds, since these are pure beta emitters. Analysis of this compound in water samples may be done in different ways:

*Direct counting*

For oil samples of types A and B in Fig. 24, the simplest pretreatment procedure is to remove any visible oil layer by pipette and to filter the water through a lipophobic filter. Transfer a measured volume of water, for instance 1000 mL, to a Marinelli beaker and count with a NaI(Tl) detector, as shown in Fig. 24. A regular cylindrical beaker may also be used, but the counting

efficiency is somewhat lower. Owing to complex background radiation, an HPGe detector may be used if desired.

*Upconcentration of [$^{60}$Co(CN)$_6$]$^{3-}$ before gamma spectrometry*

- After pretreatment to remove oil, the water is percolated through an anion exchange resin in order to concentrate the tracer molecule in a small volume in the resin.
- The column can be mounted directly onto a gamma detector (NaI(Tl) or HPGe) for gamma spectroscopy measurement.
- To prepare a sample for liquid scintillation counting the [Co(CN)$_6$]$^{3-}$ on the column may be eluted with a suitable elution liquid into a small volume (a few millilitres) and mixed with a liquid scintillation cocktail. Thus, the counting efficiency is considerably improved. However, it requires that other beta emitters are not present in the sample.

A gamma spectra of $^{60}$Co accumulated with an HPGe detector with high energy resolution is compared with a gamma spectrum accumulated with a NaI(Tl) scintillation detector in Fig. 25.

The [$^{60}$Co(CN)$_6$]$^{3-}$ ion may also be detected with a liquid scintillation counter of high efficiency. It is the beta radiation and the Compton electrons which are registered. Liquid scintillation count detection is sensitive to quenching effects, as illustrated in Fig. 26 where a sample of $^{60}$Co activity is counted in a quench-free scintillation mixture and in a mixture where 8 mL of water is added. Water acts as a quenching agent in this case, resulting in a decrease in counting efficiency.

More details on the analysis of [$^{60}$Co(CN)$_6$]$^{3-}$ tracer is given in the analysis protocol in Appendix III.

(iv)   Analysis of $^{14}$C or $^{35}$S labelled SCN$^-$

Both $^{14}$C and $^{35}$S are beta emitters with similar beta energies (156 and 168 keV, respectively). Thus, they cannot be analysed simultaneously in the same counting sample. Therefore, use of these two compounds simultaneously in the same reservoir section should be avoided. If, however, both tracers are needed, it is, in principle, possible to analyse them in the same sample by special sample treatment and separation technique. The SCN$^-$ ion may be broken down to leave S in one type of molecule (e.g. $SO_4^{2-}$ by oxidation) and C in another (e.g. CN$^-$ or $CO_2$). These may be isolated separately and counting samples prepared separately for each of them. Although the process given deals exclusively with the separation, enrichment and analysis of only one of them, the basic procedure for the two is identical.
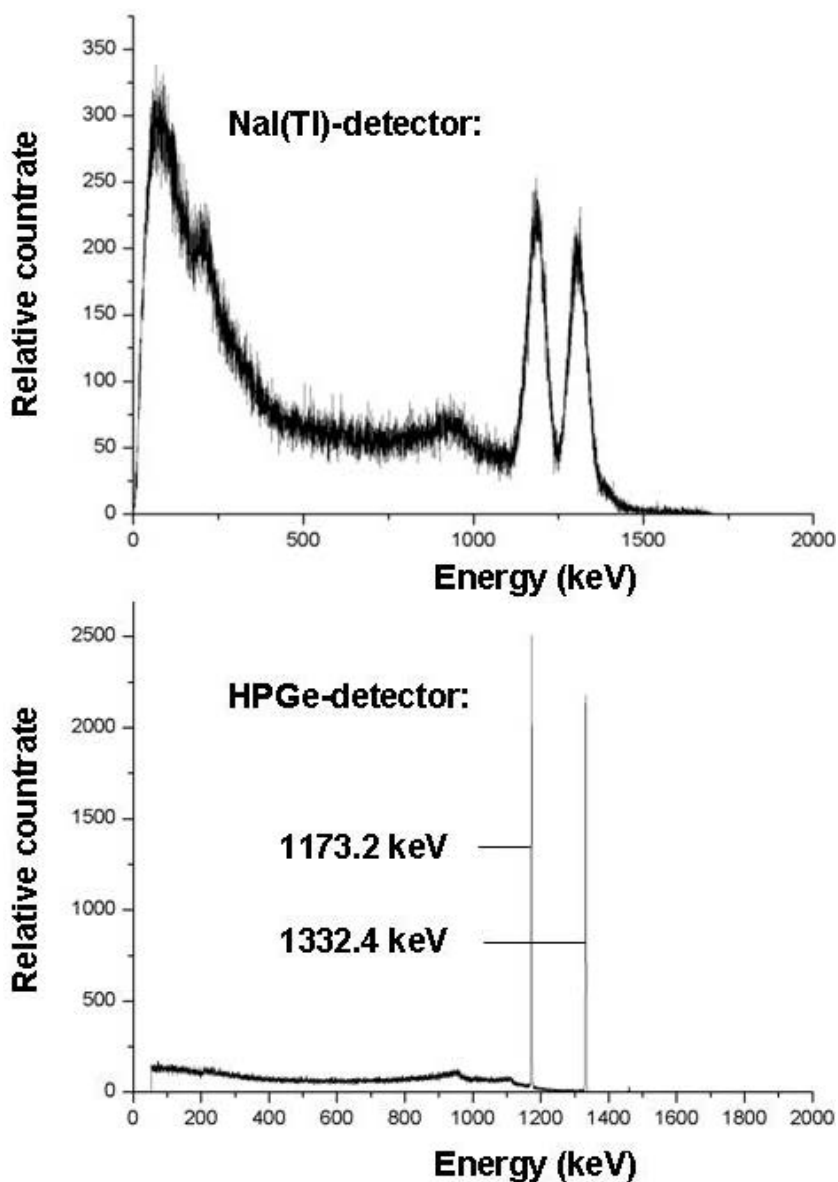
*FIG. 25. Gamma spectra of* $^{60}$*Co accumulated with a NaI(Tl) scintillation detector (top) and a high resolution HPGe detector (bottom).*

Analysis of radiolabelled $SCN^-$ in produced waters from oilfields has been described previously in the literature. Two methods are outlined, one based on liquid–liquid extraction and the other on anion exchange separation of the tracer
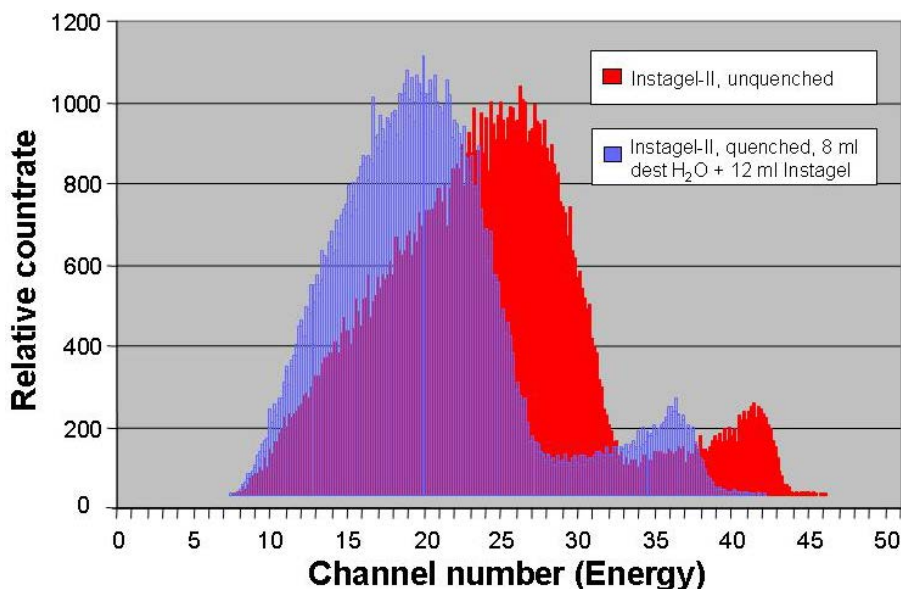
FIG. 26. Liquid scintillation spectrum of $^{60}$Co accumulated in a scintillation cocktail with no quenching (red spectrum) and in a cocktail where 8 mL of $H_2O$ is added, which acts as a quenching agent.

ions from produced water samples. A detection limit <0.01 Bq/L was obtained by using low background liquid scintillation counting equipment (Quantulus 1220). A third method proposed by the China Institute of Atomic Energy is given in detail. It is based on solvent extraction with tributyl phosphate of a metallic thiocyanate complex after the purification process of oil removal followed by filtration as described previously.

Details of the procedure are given in the analysis protocol of radiolabelled SCN⁻ in Appendix III, but the general steps include:

(1)  Removal of particles and oil droplets by filtration through 0.45 μm filter paper;
(2)  Addition of $ZnCl_2$, KSCN carrier and HCl to form $Zn(SCN)_2$ in a clear solution;
(3)  Extraction of the electrically neutral $Zn(SCN)_2$ into tributylphosphate;
(4)  Conduct of phase separation by gravity segregation or centrifugation;
(5)  Removal of sample from an aliquot of the tributylphosphate phase and mix with liquid scintillation cocktail in a liquid scintillation counting vial;
(6)  Detection of the activity by liquid scintillation counting.

(v)   Analysis $[^{60}Co(CN)_6]^{3-}$ in presence of radiolabelled $SCN^-$

The general procedure is as follows. Purify the water by removing oil as described previously. Isolate and enrich the two tracers from the bulk water volume, either sequentially or simultaneously. Two possible methods are solvent extraction and ion exchange. After the first step involving extraction/stripping or feed/elution operations, prepare samples for radioactivity detection. Ion exchange is less labour intensive than solvent extraction.

A separation procedure has recently been reported that is described in the analytical protocol for $[^{60}Co(CN)_3]^{2-}$ in presence of $^{35}SCN^-$ or $S^{14}CN^-$ in Appendix III, but the general steps include:

- Removal of particles and oil droplets by filtration through 0.45 μm filter paper.
- Preparation of an anion exchange column of the resin Dowex 2 × 8.
- Percolation of the purified sample solution through the column. The $[^{60}Co(CN)_3]^{2-}$ will bind to the resin while $^{35}SCN^-$ or $S^{14}CN^-$ will not.
- Removal of any remaining radiolabelled $SCN^-$ on the column by elution with a small volume of low concentration $NaClO_4$ solution, which is added to the raffinate.
- Concentration and purification of $^{35}SCN^-$ or $S^{14}CN^-$ in the raffinate by the procedure described for radiolabelled $SCN^-$ in Appendix III.
- Evaluation of column directly by gamma spectroscopy. In the cases where liquid scintillation counting is desirable, radiolabelled $[Co(CN)_3]^{2-}$ may be stripped from the column by, for instance, a small volume of $NH_4NO_3$ solution at medium–high concentration and mixed directly with a scintillation cocktail.
- Detection of activity by liquid scintillation counting.

The necessity for performing a separation operation is underlined in Fig. 27, where a spectrum of $^{60}Co$ is compared with a spectrum of $^{14}C$. The spectra overlap substantially. The liquid scintillation counting equipment may be run in so-called dual label mode, but the sensitivity becomes lower and the uncertainty in the results greater when spectra overlap to this extent.
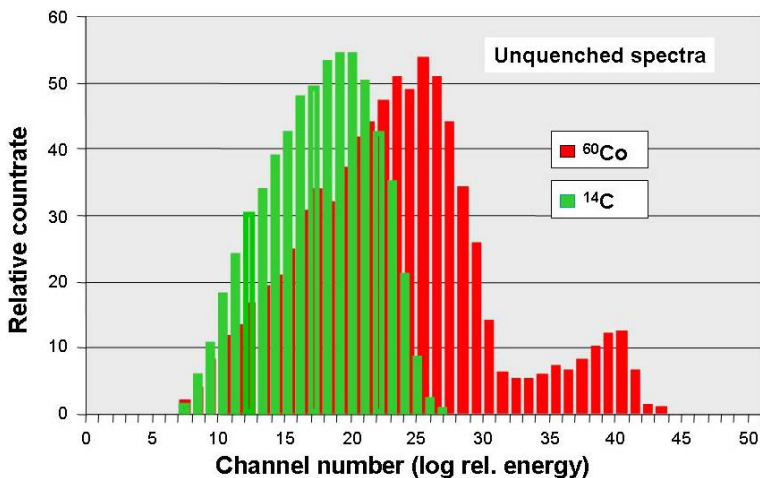
*FIG. 27. Unquenched liquid scintillation spectrum of $^{60}$Co (red) compared with an unquenched liquid scintillation spectrum of $^{14}$C (green). The spectra overlap substantially.*

### 2.3.4. Reporting of results

#### 2.3.4.1. Correcting raw data

Raw data from the analysis should be corrected before evaluation, interpretation and reporting to the end user. Examples of corrections are:

- Correction for background radiation;
- Correction for radioactive decay;
- Corrections for chemical yields and counting efficiency;
- Conversion to concentration units required by the end-user (tritium units (for tritium labelled tracers only), Bq/L, Bq/g, etc.).

#### 2.3.4.2. Data availability

Analytical results should preferably be compiled in a database system that is accessible by the end user at any time.

#### 2.3.4.3. Recording data

Data should be compiled continuously along the timeline as soon as a new analysis has been performed and presented in tables with a clear identification of

the reservoir and the well label in the table heading. Data may, in addition, be presented in the graphs or curves (production profiles for instance) for easier evaluation and interpretation (improved perception).

### 2.3.4.4. Reporting

Various types of report may be required:

- Report of the experimental activity describing the whole process up to, and including, tracer injection;
- Brief reporting (e.g. by email) upon completion of the analysis of each received batch of samples;
- Final report upon completion of the whole project which presents the full range of data and summarizes the major findings which can be extracted by a simple qualitative evaluation of the data before any quantitative interpretation.

## 2.4. DATA INTERPRETATION

### 2.4.1. Response curves

A good sampling programme and the measurement of these samples with adequate detectors (high efficiency, low background and low statistical error) is the way to obtain good response curves which form the basis for further interpretation.

### 2.4.1.1. Time response

The time response is the graphic representation of the concentration of activity (after background subtraction and decay correction) as a function of time. A preprocessing of the experimental data can also be used in order to smooth the response.

From this curve, the cumulative response (recovered activity versus time) is derived by a simple numerical integration. The application of complex integration methods is not justified because of statistical dispersion in the original data and variations in the pattern parameters.

The example illustrated in Fig. 28 was taken from an actual field exercise and shows both instantaneous and cumulative response curves to HTO injection.

Concerning the cumulative response, the following expression gives the activity recovered up to an instant, $t_i$:
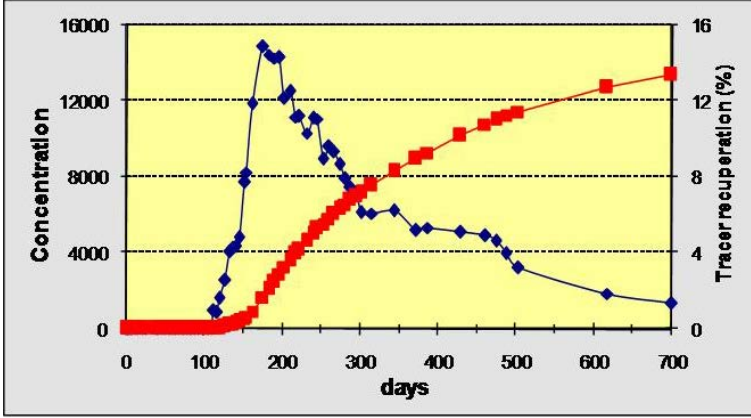
FIG. 28. Instantaneous and cumulative tracer response profile in a production well.

$$A(t_i) = \int_0^{t_i} q(t) \; C(t) \; dt \tag{8}$$

where

$A(t_i)$ is the total tracer recovery up to $t_i$ (kg or Bq);

$q(t)$ is the production water flow rate as a function of time (m$^3$/d);

$C(t)$ is the tracer concentration as a function of time (kg/m$^3$ or Bq/m$^3$);

$t_i$ is the elapsed time after the injection (d).

Information about the production flow rate is usually available in the oil company. Among the information obtained from the time response, tracer breakthrough is the first to be obtained. It is the time interval during which the tracer concentration exceeds the general background level of the samples.

The mean residence time is another important parameter. Its definition is identical to the one used in process studies, i.e. the ratio between the volume *(V)* involved in this process and the flow rate that feeds it *(Q)*.

$$\bar{t} = \frac{V}{Q} \tag{9}$$

From the experimental data, the mean residence time can be calculated as the first moment of the distribution:

$$\bar{t} = \frac{\int_0^\infty t\, C(t)\, dt}{\int_0^\infty C(t)\, dt} \tag{10}$$

The final time is the time in which the response reaches the general background level of the sample. However, in oilfield experiments it is very common to stop sampling before this point. Thus, the final time is evaluated from the extrapolated response curve. For extrapolation purposes the exponential function gives the best fit for the tail of the experimental curve.

Knowing the distance between injection and production wells it is easy to calculate the maximum, mean and minimum water velocities from the breakthrough, mean residence time and final time respectively.

The tracer recovery in each well is determined from the extrapolation of the cumulative response for time approaching infinity on the basis of the exponential approximation of the concentration curve. The fraction of injected tracer recovered in each well in the pattern ($f_i$) equals the fraction of the injected water that arrives at this well:

$$f_i = \frac{A_\infty}{A} \tag{11}$$

where $A_\infty$ is the extrapolated tracer activity recovered in the well at time infinite and $A$ is the injected activity.

The total tracer recovered in all the wells belonging to a given pattern should be identical to thequantity of tracer injected in order to obtain a perfect mass balance. However, tracer recovery is seldom higher than 80% and it can be as low as 20% for tritium, which is supposed to be an ideal tracer for water. There are three reasons for this behavior. Firstly, the tracer molecules continue moving towards second line wells and not all of them emerge from the wells immediately surrounding the injector, secondly the injected water pushes the oil to production wells and replaces it in the rock pores and finally, a fraction of the tracer mainly in the tail of the response curve suffers dilution that causes the concentration to fall under the detection limit. Sampling second line wells is a good idea in order to improve the mass balance and to gain additional information about the pattern under study.
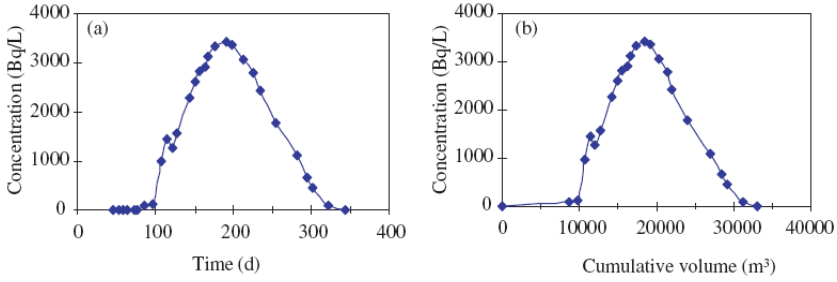
FIG. 29.  Time and volumetric tracer response profiles.

### 2.4.1.2. Volumetric response

When tracers are used to analyse industrial processes, it is common to express the tracer concentration in the system output in terms of elapsed time, and then to calculate the mean residence time, variance and other parameters related to the time response.

Although the time response is generally used in interwell studies it has some problems that reduce its usefulness. Effectively, alterations in the pattern, such as variations in the injection rate, which are very common in any oilfield, result in a biased response curve.

To avoid this inconvenience, a good alternative is to express the tracer concentration as a function of the cumulative injected or produced water volume, which is rate independent. Nevertheless, time representation is often preferred because in many cases the volumetric data are not available.

Figure 29 shows time (a) and volumetric (b) responses for the same well. It is obvious that they are nearly identical since the cumulative volume was calculated from the injection flow rate, which in this case was quite stable.

The volumetric response in a production well when an instantaneous tracer injection has been performed is a measure of the pore volume swept by the injected water.

The tracer breakthrough is sometimes used as an indicator of the swept pore volume, but the mean of the distribution is a better locator because it represents the average volume swept by the injected water and takes into account the shortest as well as the longest paths followed by the tracer. Then:

$$\bar{V} = \frac{\int_0^\infty V \, C(V) \, \mathrm{d}V}{\int_0^\infty C(V) \, \mathrm{d}V} \tag{12}$$

60

The swept volume arriving at a given well is equal to the average volume swept multiplied by the fraction of the injected water that reaches this production well ($f_i$).

### 2.4.1.3. Simplified permeability evaluation

Permeability is a property of a porous material and a measure of its capacity to transmit a fluid. Permeability is largely dependent on the size and shape of the pores in the substance and, in granular materials such as sedimentary rocks, on the size, shape and packing arrangement of the grains.

In general, permeability is evaluated in the laboratory by analysing samples taken from the oilfield, but the results obtained by this technique are subject to considerable uncertainty. Firstly, the core samples are small and limited to sectors around the wells. There is always a question about the representativeness of the sample for the reservoir. However, the use of interwell tracers allows average values of the permeability in the swept volume between wells to be derived.

On the basis of Darcy's law and many simplifications, a simple formula for permeability evaluation can be developed:

$$K = \frac{\phi\, S_w\, \mu}{\overline{t}\, \Delta P} \left(d^2 - r^2\right) \ln\!\left(\frac{d}{r}\right) \tag{13}$$

where

$K$    is the permeability;
$\phi$    is the porosity;
$S_w$    is the water saturation;
$\mu$    is the viscosity;
$r$    is the the radius of the production well;
$d$    is the the distance between the injection well and the production well;
$\Delta P$    is the differential pressure between wells;
$\overline{t}$    is the mean residence time.

Although this expression supposes a number of simplifications, it constitutes an acceptable approach from the experimental point of view. The main use is to derive comparative values related to the permeability of different layers in the same pattern or of several stratifications in a unique layer.

### 2.4.2. Interpretation

Interpretation of the response curves obtained in production wells is the final objective of an interwell study. The tracer method gives correct and comprehensive information about the reservoir's hydrodynamic parameters, allowing the reservoir engineers to understand better the phenomena and probably to increase the recovery. Four levels of complexity are generally accepted:

(1) *Qualitative*: Important information can be obtained just by looking at the response curves or by means of simple calculations. Breakthrough and mean residence times, distribution of injected water, recovered tracer mass or activity and swept volume are among these parameters.
(2) *Basic models and software*: Decomposition of complex curves into simple ones easy to approximate by elemental functions, moment determination and evaluation of statistical parameters, simple calculations and the fitting of experimental data. Anduril software (developed by Argentina) fulfils these operations and is used for simple analysis of tracer response curves.
(3) *Streamline models*: The volume under study is divided into a quasi-two-dimensional grid in small cells. Assigning to each one certain properties (pressure, permeability, porosity), streamline pictures are generated by solving the pressure equations. By this method it is possible to fit the experimental data in order to obtain structural information from the reservoir.
(4) *Reservoir simulators*: Generally, these comprise commercial and expensive software with capabilities to simulate reservoir behaviour under different conditions. Some of them have a rather basic 'tracer' option to evaluate the application of water tracers.

Analysis of the response curves consists of several steps:

(1) The simpler interpretation is the qualitative one. Just by observing the curves, the following pattern characteristics can be derived: injection water arrival time (breakthrough); high permeability channels, barriers and fractures between both wells; communications between different layers; stratifications in the same layer and preferential flow directions in the reservoir. This interpretation level is completed by means of some simple calculations from the numerical response, firstly, the determination of the mean residence time. The cumulative response can be obtained by integration of the concentration versus time curve, assuming the production flow rate is known. From this new curve, the fraction of injection water reaching each producer is easily calculated. A standard spreadsheet is the best way to make all these calculations.

(2)     A second level involves the use of basic mathematical models to fit simple response curves by means of theoretical expressions and to decompose complex responses in several simpler functions. In this way partial residence times, as well as other parameters, can be determined for each function. Mathematical models also allow the evaluation of some important parameters such as permeability and make it possible to predict the behaviour of unknown patterns.

(3)     Finally, it is possible to make use of complex mathematical models such as numerical simulators in order to achieve a more rigorous analysis. Such tracer simulators may be coupled to full field reservoir simulators where the current reservoir model is used as input (geology, stratification, etc.). This is especially useful when the well pattern is complex, the reservoir heavily faulted and there is a complex production strategy.

(4)     Reservoir simulators with a tracer option are powerful tools for determining the parameters of systems under study, for planning infill well drilling and for future tracer examinations. Well-known reservoir simulators such as ECLIPSE and VIP both have relatively simple tracer options which may be used for passive water tracers, while it is probable that the simulators from Computer Modelling Group in Calgary, Canada, represented by STARS, have the most advanced tracer simulator included. This can also be used for reversibly sorbing and phase partitioning tracers.

### 2.4.2.1.  *Example of basic analysis: First level or direct interpretation*

The concentration versus time curves (experimental response curves) are analysed to measure the main characteristics of flow in the group of wells under study (Fig. 30).

For this, 370 GBq of HTO was injected into well CnE-241. The experimental response curves give transit times and allow quantification of the injected water produced in different directions. Basic interpretation or first level interpretation allows to acquisition of qualitative and semi-quantitative information that in many cases is the only type required by the end users. Tracer sampling and measurement showed that tracer came up at three out of five production wells around the injection well. The arrows represent the fraction of the injected tracer recovered in each well.

Figure 31 presents the experimental response and cumulative curves obtained at production well CnE-324.

The experimental response curve obtained in production well CnE-324 indicates:
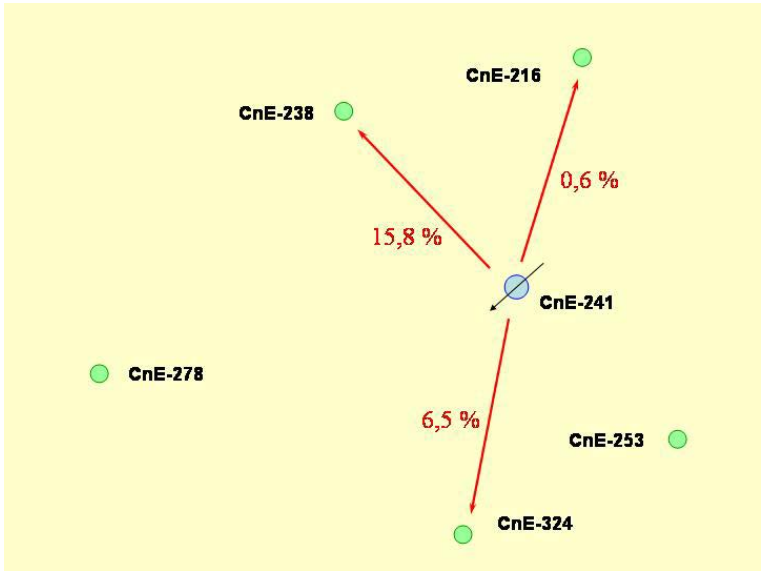
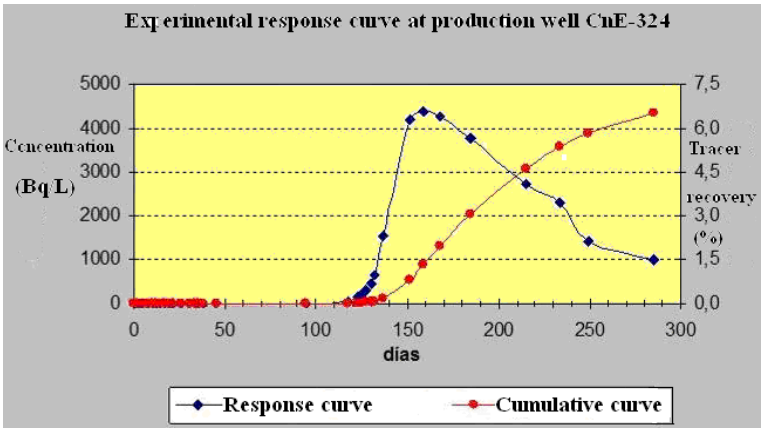*FIG. 30. Pattern under analysis.*



*FIG. 31. Response curves for well CnE-324.*

- Absence of channelling.
- Breakthrough time is 117 d.
- Time for the peak is 159 d.
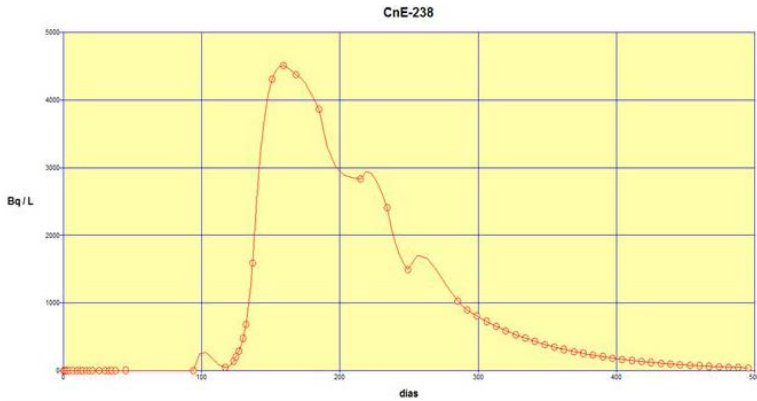- Mean residence time is 194 d.
- Tracer recovery is 6.5%.

*FIG. 32. Extrapolated response curve for well CnE-324.*

It is easy to observe that tracer sampling was interrupted before the concentration reaches background level; consequently, for more accurate results, extrapolation of the curve is required.

For this purpose, it is recommended that an exponential function be used and parameters obtained from a least squares fit using the last points in the tail of the experimental data as reference. However, extrapolation has to be used carefully and based upon the general knowledge of each particular situation in order to avoid speculation and unexpected results. Figure 32 shows the extrapolated curve generated by the Anduril software.

The new values for the parameters are:

- Breakthrough time is 117 d.
- Time for the peak is 159 d.
- Mean residence time is 217 d.
- Tracer recovery is 7.7%.

A similar treatment has been applied to other wells in the pattern shown in Fig. 30 with the following experimental results.

*Simple model analysis*

A second analytical step makes use of simple models. The response curves are decomposed in simple functions using a simple mathematical model based on the standard equations for diffusion in porous media.

TABLE 5. EXPERIMENTAL RESULTS FOR WELLS CnE-216, CnE-238 AND CnE-324

| Parameter | CnE-216 | CnE-238 | CnE-324 |
|---|---|---|---|
| Breakthrough time (d) | 117 | 117 | 117 |
| Mean residence time (d) | 176 | 213 | 217 |
| Standard deviation (d) | 24 | 63 | 64 |
| Peak time (d) | 132 | 185 | 159 |
| Final time (d) | 234 | 441 | 488 |
| Tracer recovery (MBq) | 2.2 | 67.3 | 28.5 |
| Water recovery (%) | 0.6 | 15.8 | 7.7 |

**Note:** Tracer did not arrived at wells CnE-253 and CnE-278 during the sampling period (285 d).

$$C(x,t) = C_{\text{REF}} \frac{1}{\sqrt{4\pi \dfrac{D_1}{v\,x} t_N^3}} e^{-\dfrac{(1-t_N)^2}{4\dfrac{D_1}{v\,x} t_N}} \qquad (14)$$

where

$C(x,t)$   is the tracer concentration as a function of distance and time (Bq/m$^3$);
$t_N$   is the normalized time;
$D_1$   is the coefficient of dispersion (m$^2$/d);
$v$   is the tracer velocity (m/d);
$x$   is the distance from the injection point (m);
$C_{\text{REF}}$   is the reference tracer concentration (Bq/m$^3$).

Dispersivity may be calculated by multiplying the ratio ($D_1/vx$) by the distance between the injection and production wells. Therefore, the extrapolated curve obtained before may be decomposed in two simple functions using Anduril software to give the curves shown in Fig. 33, where both functions and their sum are shown together with the experimental data.

The following table presents obtained results using Anduril software for the pair of wells CnE241-CnE324.

TABLE 6. RESULTS FOR WELLS CnE-241 AND CnE-324 USING ANDURIL SOFTWARE

| Parameter | Experimental | Model |
|---|---|---|
| Breakthrough time (d) | 117 | 117 |
| Mean residence time (d) | 217 | 212 |
| Standard deviation (d) | 64 | 65 |
| Peak time (d) | 159 | 185 |
| Final time (d) | 488 | 488 |
| Tracer recovery (MBq) | 28.5 | 25.8 |
| Water recovery (%) | 7.7 | 7.0 |
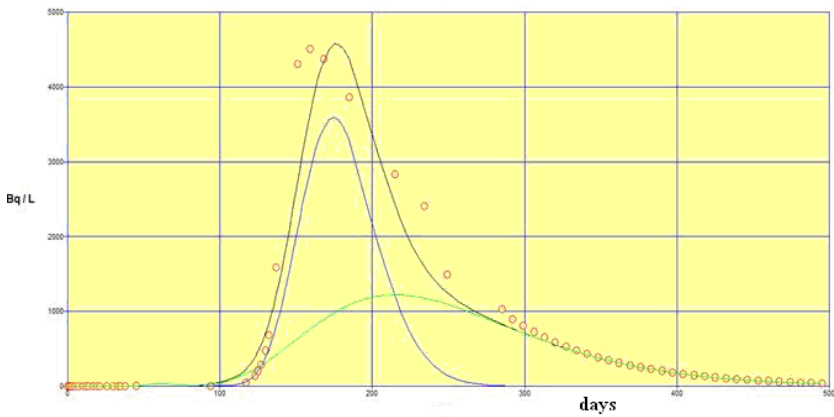


*FIG. 33. Fitting curves for well CnE-324.*

The decomposition in two curves may be explained by the fact that the tracer follows two different paths in its migration from the injector to the producer, each of them having different permeabilities.

# 3.  QUALITY ASSURANCE OF TRACERS
# AND ANALYTICAL METHODS

## 3.1.  TRACER STABILITY AND INTEGRITY

The quality of a new tracer candidate is examined by subjecting it to a test sequence where stability and associated properties are examined. Another sequence where detectability is examined and developed will only be represented here by an example where a method for analysis of radiolabelled $[Co(CN)_6]^{3-}$ and $SCN^-$ in the same sample is employed.

### 3.1.1.  Thermal degradation

The thermal stability of tracers is typically tested in batch experiments where solution aliquots of the actual tracer candidate are heat sealed in individual glass cylinders and exposed to different temperatures for different time periods. HTO is always added in a known quantity to act as a standard reference tracer. The experiments may be carried out under aerobic or anaerobic conditions. Water of different quality may be used, ranging from distilled deoxygenized water to seawater and various formation waters.

Samples are analysed with respect to the remaining original tracer concentration as a function of time at the different temperatures. The analysis is carried out by liquid scintillation counting or gamma spectrometry if the radionuclide permits.

If $R_{T_o}$ is the volume specific count rate (cps/mL) of the tracer in the original vials before the start of the experiment ($t = 0$) at temperature $T$, and $R_{Tt}$ is the volume specific count rate of the tracer after time $t$, the surviving fraction, $Y$, is found by the simple expression:

$$Y(\%) = \frac{R_{T_t} \cdot 100}{R_{T_o}} \tag{15}$$

One example of a $Y$-plot is shown in Fig. 34. For an ideal water tracer under test conditions, $Y$ should stay at ~100%. In the example given, a measurable degradation of $S^{14}CN^-$ at 120°C in seawater occurs over time.
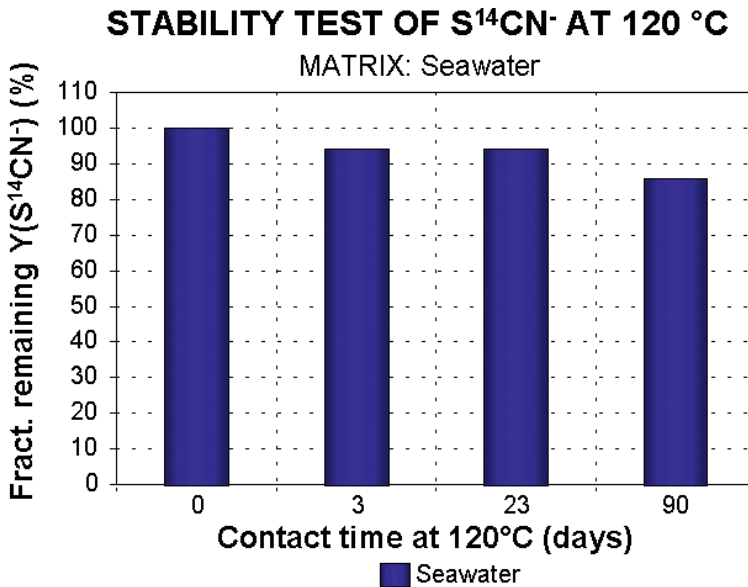
FIG. 34. Thermal stability of $S^{14}CN^-$ in seawater at 120°C expressed by the fractional remaining activity, Y, calculated from Eq. (15).

### 3.1.2. Sorption onto rock

Tracer candidates that pass the thermal stability tests mentioned above are subject to static batch sorption experiments. Crushed reservoir or reservoir-like rock is added to the same type of vial as used above. Convenient test materials are sandstone (Berea, Clashack, Bentheimer, Felser, etc.) and chalk, which represent the main reservoir rock types, and kaolinite, which represents clays that are nearly always present to some degree.

The survivability yield, Y, is calculated from Eq. (15). One example of a static sorption curve is given in Fig. 35.

As can be seen in the example given, there is a clear indication of sorption to sandstone (Clashack) whereas sorption to the other substrates is not detectable. The decrease in the Y values for chalk and clays is due to the thermal degradation data given in Fig. 35.

### 3.1.3. Stability against biodegradation

Microbial stability shows up in the tests described above owing to a substantial degree of degradation at temperatures below 70°C, while the tracer
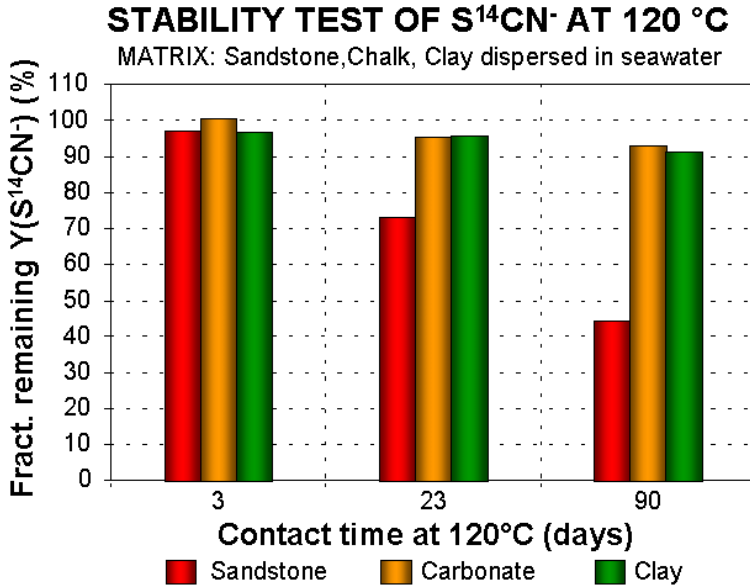
FIG. 35. *Stability of $S^{14}CN^-$ in contact with sandstone, carbonate and clay substrates at 120 °C as a function of contact time. Fractional remaining activity is found from Eq. (15).*

survivability may be better at higher temperatures. An example of this is the formate ion $H^{14}COO^-$ that seems to be degraded to $^{14}CO_2$.

It is also possible to add certain specific bacterial cultures to the vials to check the effect. The experiments may be somewhat difficult to control. Aerobic and anaerobic tests may be performed.

### 3.1.4. Partitioning between phases

Experiments should be carried out to examine the potential for tracer distribution between the water and oil phases. Three different methods are:

(1)     Static batch experiments, where phase mixing and separation takes place in a mixing apparatus and where samples can be extracted from each phase for analysis of tracer concentration. Equipment for this purpose ranges from the simplest, such as the separation funnel, to thermostatized equipment illustrated in Fig. 36 and to more complicated autoclaves where pressures can be applied if deemed necessary.
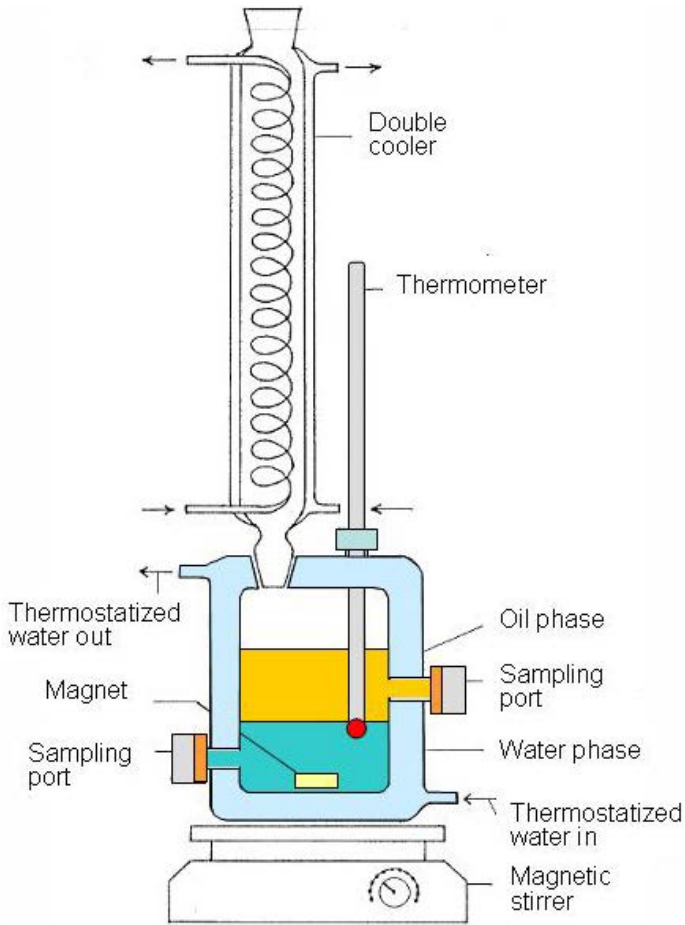
FIG. 36. Experimental set-up for studies of radiotracer partitioning between seawater and stock tank oil at temperatures <90°C and at ambient pressure.

(2)  Dynamic experiments with continuous phase mixing followed by phase separation as exemplified by the flow injection apparatus shown in Figs 37 and 38.

(3)  The dynamic or chromatographic method, where a small tracer pulse is forced through a porous medium with known oil saturation at moderate linear flow rates (25–50 cm/d) together with the standard reference non-partitioning tracer, HTO. Difference in tracer transportation time is a measure of the degree of partitioning. Various forms of flow rigs can be used for this purpose. One such piece of equipment is illustrated in Fig. 39.
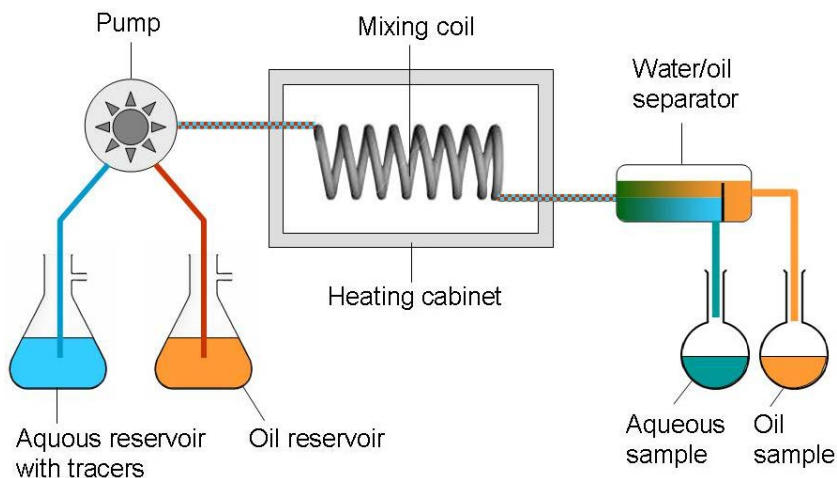
FIG. 37. *Flow equipment used for measurement of partition coefficients of tracers between water (brines) and oils at ambient pressure and moderate temperatures (<90 °C).*
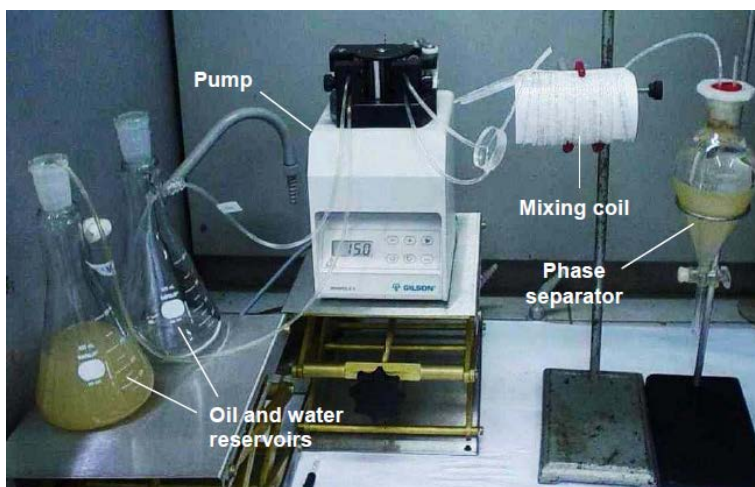


FIG. 38. *Flow equipment used for measurement of partition coefficients of tracers between water (brines) and oils at CDTN, Belo Horizonte, Brazil.*

Method (1) will give the true equilibrium partition coefficient, as will method (2) if the length of the mixing coil is sufficient to ensure full equilibrium transfer. The mixing coil may be empty (capillary) or filled with a packing material (static mixer). Method (3) will give an 'effective' partition coefficient because it includes kinetic effects such as diffusion rates and rate of exchange between phases (across liquid boundaries) and diffusion into the bulk volume as

## Oil/water partitioning experiments
### S¹⁴CN⁻ + HTO in sea water/stock tank oil
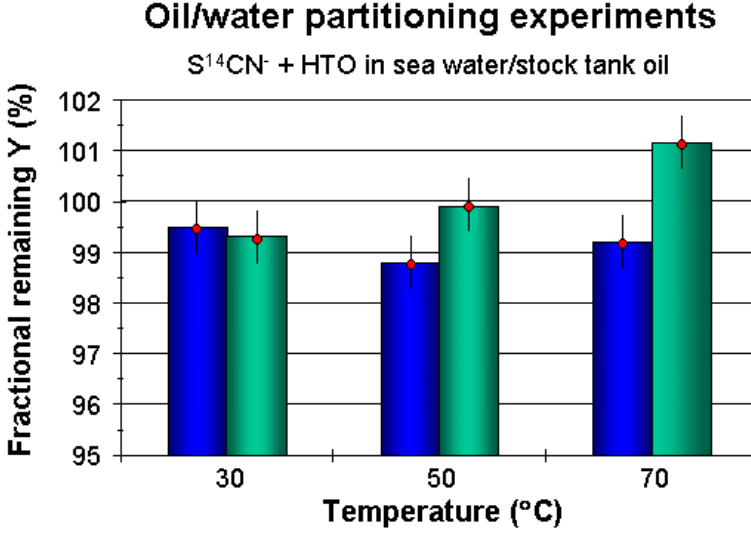
FIG. 39. *Fractional remaining activity in the water (sea water) phase after shaking with stock tank oil as a function of contacting temperature by using the simple equipment shown in Fig. 36. Blue and green bars represent two parallel experiments. Error bars are ±1σ. No partitioning is detected.*

the tracer pulse passes by. This latter may give values that are more representative for the situation in the reservoir where the tracer (in most examinations) is transported as a pulse through the porous medium. The best situation occurs when the results from both experiments match.

The degree of partitioning (partition coefficient) is expressed by:

$$K = \frac{C_{tr,o}}{C_{tr,w}} \qquad (16)$$

where $C_{tr,o}$ and $C_{tr,w}$ are concentration of the tracer in the oil phase (o) and the water phase (w), respectively.

This quantity is directly derived in method (1) above by the counting of water and oil samples. Since $C$ is proportional to the disintegration rate:

$$C_{tr,o} = R_o/\varepsilon_o \qquad (17)$$

and

$$C_{tr,w} = R_w/\varepsilon_w \qquad (18)$$

73

where $\varepsilon$ is the counting efficiency and $R$ is the count rate in the oil and water phases. Thus,

$$K = \frac{R_o \cdot \varepsilon_w}{R_w \cdot \varepsilon_o} \qquad (19)$$

In dynamic experiments, the practical partition coefficient $K'$ is derived on the basis of the recorded tracer production curve (or chromatogram). This curve is established by sampling the fluid effluent from the chromatographic column and counting by liquid scintillation counter and/or gamma spectroscopy. $K'$ can be calculated from Eq. (20):

$$K' = \frac{(V_{tr} - V_w) \cdot (1 - S_o)}{V_w \cdot S_o} \qquad (20)$$

where

$V_{tr}$    is the retention volume of the tracer candidate, i.e. the volume from the start injection to the peak maximum of the tracer production curve (which may be found by curve fitting);

$V_w$    is the retention volume of the water represented by the non-partitioning standard reference water tracer HTO;

$S_o$    is the oil saturation or fraction of oil volume occupied by oil;

$K$    $\approx 0$ for passive water tracers. Compounds with $K > 0$ are of interest for measurement of the remaining oil saturation.

A typical result for a passive water tracer is that the degree of partitioning into the oil phase is approximately 0, as illustrated for $S^{14}CN^-$ with HTO as a control in Fig. 39.

### 3.1.5. Dynamic flooding properties

Tracers which pass all the batch experiments with acceptable marks advance to the dynamic tests where their flooding properties are examined in core flooding experiments. This is the last laboratory test before final qualification in field pilot tests.
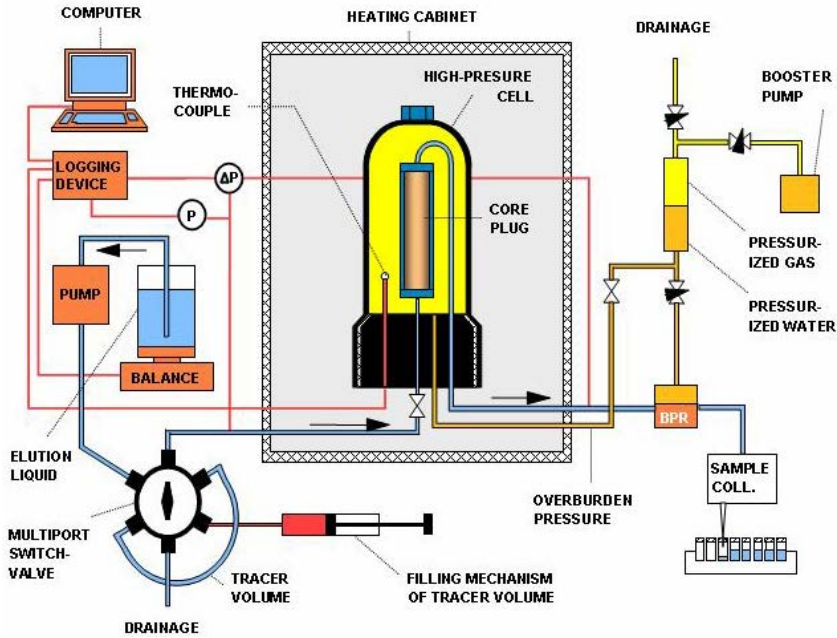
*FIG. 40. High pressure IFE-type flow rig for small (d × l = 2.5 cm × 7.7 cm) cores of reservoir or reservoir-like material for studies of dynamic properties of tracers in porous media under simulated reservoir conditions.*

### 3.1.5.1. *Experimental equipment*

Different types of equipment are available. It is common to use cores of consolidated reservoir rock or reservoir-like rock (i.e. sandstones such as Clashack, Berea, Bentheimer, Felzer, etc., and carbonates such as chalk, limestone, etc.). Core dimensions normally range from $d × l = 2.8$ cm $× 7.7$ cm to $d × l = 5.1$ cm $× 51.2$ cm.

A flow rig constructed for smaller consolidated cores is shown in Fig. 40. This is constructed to operate under simulated reservoir conditions, i.e. temperatures up to 150°C and pressures up to ~450 bar. The core is mounted in a Viton or neoprene rubber hose and an overburden pressure of ~20 bar is exerted onto the rubber hose in the external chamber in order to prevent any leakages along the surface of the core.

Instead of the permanently mounted vertical core, a Hassler cell (illustrated in Fig. 41) may be used, which permits the choice of any angle of the core from horizontal to vertical. A method has also been developed to permit the use of unconsolidated material in this equipment.
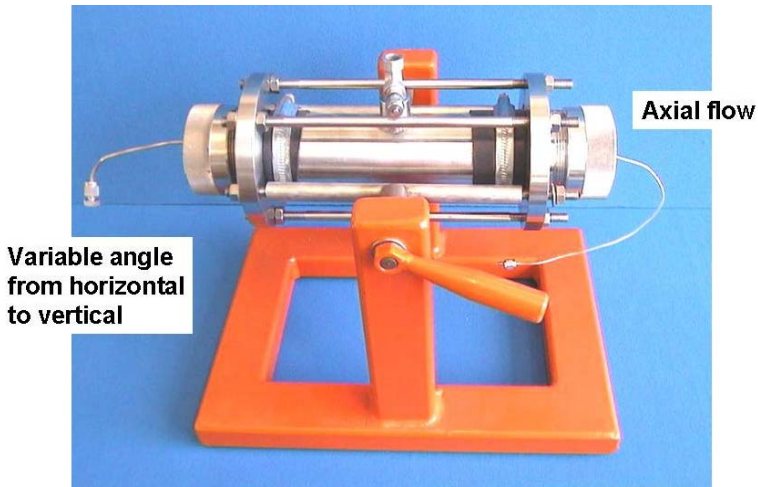
FIG. 41. High pressure Hassler-type flow rig for small (d × l = 2.5 cm × 7.7 cm) cores of reservoir or reservoir-like material for studies of the dynamic properties of tracers in porous media under simulated reservoir conditions.

Other equipment is based on the use of crushed rock material to fill chromatographic columns of varying dimensions.

Figure 42 illustrates a flow rig based on a 200 cm long chromatographic column with an internal diameter of 11 mm.

### 3.1.5.2. Further experimental details

Experiments are normally conducted with a typical linear flow rate of 25 cm/d, which corresponds to the rate of the injected flow front in the reservoir.

The most frequently used testing method utilizes pulse injection into the core. The tracer candidate is always co-injected with a standard reference tracer. For water, this is normally HTO. The production profiles of the tracer candidate and the standard reference tracer may be directly compared. Examples of such profiles are given in Fig. 3. Figure 4 shows the difference curve of the normalized production profiles.

Another method that may be used is continuous injection of a constant concentration tracer solution. Figure 43 show results from such a test at ambient temperature where $In^{3+}$ complexed with EDTA is compared with the behaviour of HTO. The curves show evidence of a slight reversible sorption of In–EDTA under the running conditions.

When a tracer candidate has also passed the dynamic tests in 'good shape', the next, and final, step is to perform a pilot test in an actual reservoir section. An

1. Electric heating elements
2. Thermally insulated column housing
3. Thermo elements
4. Air circulation pump
5. Balance
6. Column elution liquid
7. High-pressure pump
8. Piston cylinder
9. Six-port valve
10. Constant initial tracer mixture volume
11. Syringe for filling of tracer volume
12. Computer for logging
13. Differential pressure gauge
14. Collected liquid samples
15. Circulating hot air
16. Pressure equalizer
17. Back-pressure regulator
18. Sample changer
19. Nitrogen reservoir for dome pressure
20. Chromatographic column with crushed reservoir material

*FIG. 42. Flow rig for dynamic tracer testing of water tracers in columns of crushed reservoir rock or reservoir-like material under simulated reservoir conditions. The rig contains a 200 cm long thermostatized chromatographic column.*
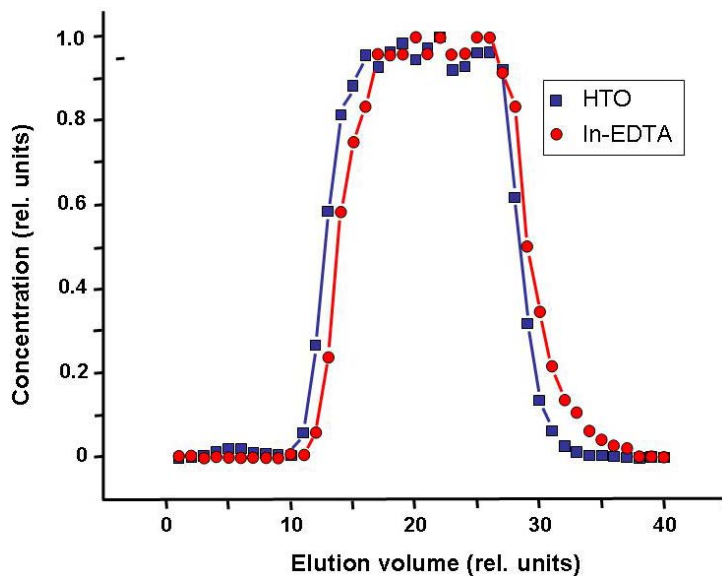


*FIG. 43. Tracer response curves of the tracer candidate In–EDTA and the reference tracer HTO in a flow experiment where the tracers have been injected simultaneously as a slug (constant concentration) and not as a short pulse. The pertinent information is in the shapes of the front and tail fractions and in the curve integrals.*

acceptable tracer performance may finally be regarded as proven after several successful experiments under reservoir conditions.

## 3.1.6. Radiochemical purity of radiolabelled tracer

For tracers composed of single atoms, such as $^{125}I^-$, $^{22}Na^+$, etc., tests are simpler than for tracer compounds based on molecular complexes. This is exemplified here with the tracer compound cobalthexacyanide ($[Co(CN)_6]^{3-}$). This molecule may be labelled with $^{56}Co$, $^{57}Co$, $^{58}Co$, $^{60}Co$ or $^{14}C$, and it may be used as the unlabelled complex. The latter requires a sensitive analytical method for Co, such as thermal neutron activation analysis. One single molecular carrier may then give rise to six different tracers. The total complex constant of this molecule ($\beta_6$) is reported to be very high ($10^{38}$–$10^{64}$) [9]. This may wrongly be interpreted as indicating that the $(CN)_6$ ligand molecule is very stable and that it will exist in this molecular form more or less regardless of the chemical environment. This argument has led to extensive and somewhat uncritical field use of radiolabelled versions of these molecules. In many cases, good results have been obtained, while in others the tracer has never been produced back. A thorough investigation of radiolabelled $[Co(CN)_6]^{3-}$ has already been conducted and a few results of this study and some complementary experiments are discussed.

The $^{60}Co$ labelled hexacyanide was purchased from one of the largest commercial producers of radiochemicals as a ready-to-inject solution. One of the quality control methods used is the electrophoresis technique. Batches purchased at different times showed different results, indicating a radiochemically impure product. A new synthesis was carried out using procedures provided by the company. Results from this experiment are shown in Fig. 44. The electrochromatogram shows a relatively broad distribution with two distinct peaks. This indicates that the $^{60}Co$ label exists in, at least, two different anionic forms. These forms are not identified; they may have different stability and chemical behaviours. The compound was then synthesized by a modified method. The modified procedure produced chromatograms similar to that shown in Fig. 45.

Cobalthexacyanide from the commercial company was then subject to thermal stability and sorption investigations. There was fast sorption onto corroded steels already at ambient temperatures, but the sorption became even more pronounced at elevated temperatures. Liquid solutions, after heating to 120°C for 24 h, were again investigated by electrophoresis. The results are shown in Figs 46 and 47.
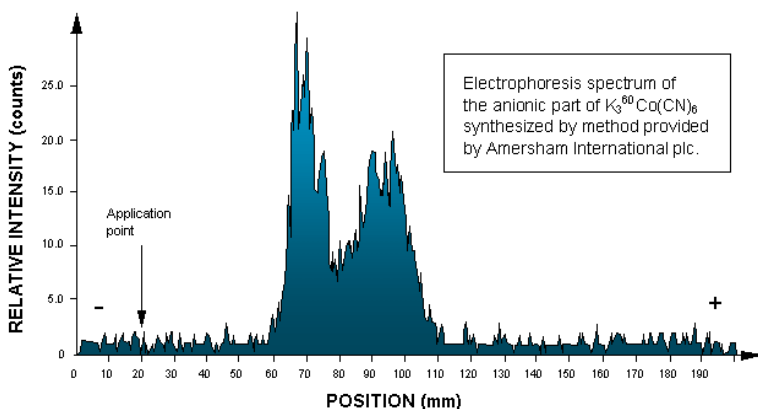
FIG. 44. Electrophoresis chromatogram of $[^{60}Co(CN)_6]^{3-}$ synthesized according to the procedure provided by a major commercial radiochemical company.
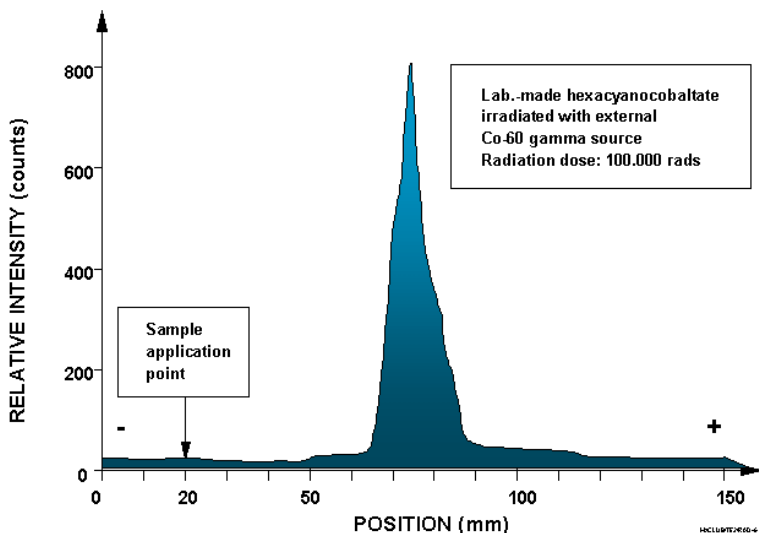


FIG. 45. Electrophoresis chromatogram of $[^{60}Co(CN)_6]^{3-}$ synthesized in a laboratory according to a revised procedure. This product has, in addition, been exposed deliberately to 105 rads of $^{60}Co$ gamma radiation in a gamma irradiation facility.

A substantial fraction is non-charged and does not move away from the application point. On the positive potential side is a relatively low and broad, nearly constant, distribution indicating different $^{60}Co$ labelled anionic forms. On the negative potential side is a substantial and broad distribution indicating various positively charged complexes where heating leads to breakdown of the
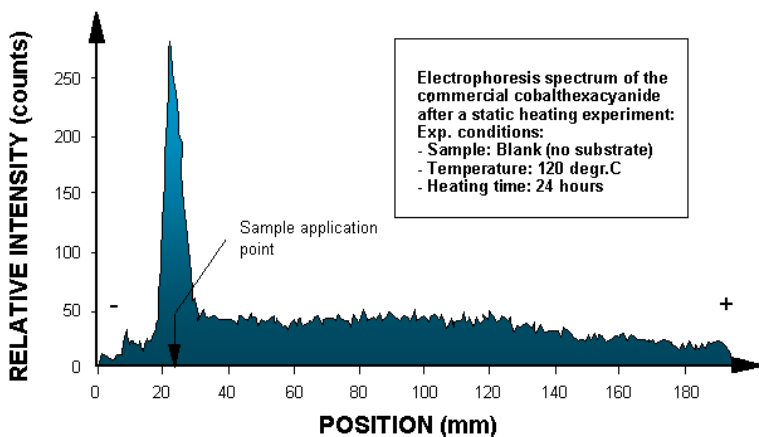
FIG. 46. Electrophoresis spectrum of $^{60}$Co-containing components in a seawater solution of commercial [$^{60}$Co(CN)$_6$]$^{3-}$ on the anionic side after a heating period of 24 h at a temperature of 120°C.
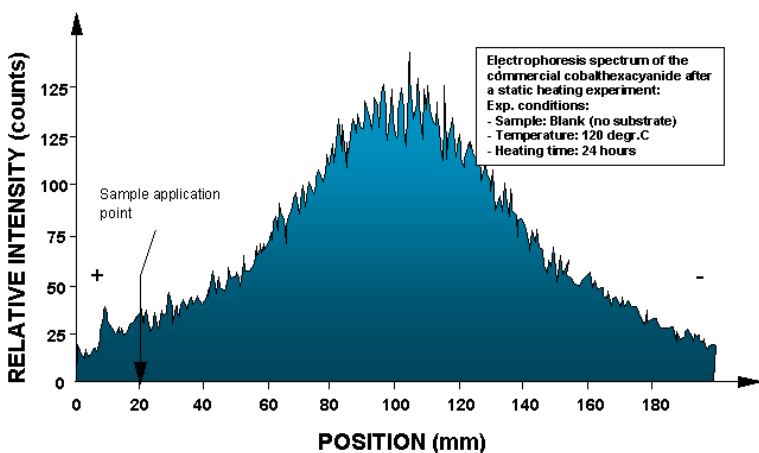


FIG. 47. Electrophoresis spectrum of $^{60}$Co-containing components in a seawater solution of commercial [$^{60}$Co(CN)$_6$]$^{3-}$ on the cationic side after heating for 24 h at 120°C.

hexacyanide complex into a range of different complexes with varying masses and charges.

The CN ligands may be exchanged to some degree with Cl$^-$, OH$^-$ or even H$_2$O to saturate the coordination number of 6. This leads to complexes of different charges and different chemical properties. The referred experimental investigations showed that the quality control on the radiochemical purity is very

important, and the purity of $[Co(CN)_6]^{3-}$ should be ensured at the start of any field application. This tracer compound should not be used at reservoir temperatures >90°C.

## 3.2. ANALYSIS OF RADIOLABELLED $[Co(CN)_6]^{3-}$ AND SCN$^-$ IN THE SAME SAMPLE

The $[Co(CN)_6]^{3-}$ complex is of interest as a basic carrier of the five different radionuclides $^{56}Co$, $^{57}Co$, $^{58}Co$, $^{60}Co$ and $^{14}C$. The first four are gamma emitters while the latter is a pure beta emitter.

In actual field situations, $[Co(CN)_6]^{3-}$ may be used in areas where $^{35}SCN^-$ or $S^{14}CN^-$ have been applied simultaneously. Since the thiocyanate tracers have to be analysed by liquid scintillation counting the presence of $[Co(CN)_6]^{3-}$, regardless of the radiolabel, will disturb the counting of the thiocyanate. For gamma emitting labels, the analysis may be performed by gamma spectrometry, but if the label on the $[Co(CN)_6]^{3-}$ is $^{14}C$, there will be a mutual disturbance of the two radiolabelled complexes. Therefore, there was a need to develop radiochemical procedures to separate cobalthexacyanide and thiocyanate at the tracer level in produced water and results of attempts at this separation have been reported.

A method was developed for quantitative analysis using 1000 mL of sea water (as a substitute for produced water) containing a mixture of SCN$^-$ and $[Co(CN)_6]^{3-}$ produced by enrichment procedures and preconcentration into samples small enough to be measured by liquid scintillation counting. The sample volume for liquid scintillation counting should not exceed 8–10 mL, since this is normally the maximum water sample volume dissolved by modern scintillation cocktails (12 mL) for ordinary 22 mL scintillation vials.

The main hypothesis was to take advantage of the difference in anionic charges to obtain a separation. The test sequence involved the following:

- Screening tests used to find a selective separation procedure for $[Co(CN)_6]^{3-}$ by the use of $^{60}Co$ labelled complex as a tracer. The separation is based on either solvent extraction or ion exchange techniques.
- Testing of different stripping or elution agents in order to minimize the degree of quenching in the final counting samples.
- Checking the absorption and stripping/elution characteristics of SCN$^-$ in the $[Co(CN)_6]^{3-}$ method.
- Performing separation experiments on an actual sample containing both tracers labelled with $^{60}Co$ and $^{14}C$.

The screening experiments with $^{60}$Co were measured by gamma spectroscopy using a lead shielded, high resolution semiconductor detector and $^{14}$C was measured with a liquid scintillation counter.

### 3.2.1. Separation methods

#### 3.2.1.1. Solvent extraction method

The procedure was as follows: A series of 5 mL samples of seawater were doped with tracer quantities of $^{60}$Co labelled $[Co(CN)_6]^{3-}$ and pH adjusted in the range pH1–7 by addition of HCl. Each sample was then contacted in a separator funnel with 5 mL of organic phase (kerosene) containing the extraction agent. The funnel was then vigorously shaken by a mechanical shaking machine for a predetermined time of 3 min at room temperature, which is sufficient to reach extraction equilibrium. After phase separation (by gravity), 1 mL samples were extracted from both phases and measured for radioactivity.

For the high gamma energies of $^{60}$Co (1173 keV and 1332 keV), correction for differences in counting efficiency due to sample density is not needed. In addition, when equal volumes of the two phases are used in the counting procedures, the distribution ratio (D value) can be determined from the raw counting rates by the formula:

$$D = \frac{R_{org}}{R_{aq}} \tag{21}$$

where $R_{org}$ is the net counting rate of the organic sample and $R_{aq}$ is the net counting rate of the aqueous sample.

The quantity extracted from one extraction operation of aqueous and organic phases is expressed as $E(\%)$ by the formula:

$$\%E = \frac{D}{\dfrac{V_{aq}}{V_{org}} + D} \cdot 100\% \tag{22}$$

where $V_{aq}$ and $V_{org}$ are the volumes of the aqueous and organic solutions, respectively.

For high values of $D$, it is possible to obtain a substantial volume reduction and enrichment factor by using a volume ratio $V_{aq}/V_{org} = 10$ or higher. For equal volumes of the organic and aqueous phases, the formula simplifies to:

$$\%E = \frac{D}{1+D} \cdot 100\% \tag{23}$$

For even further enrichment, it is necessary to strip the activity back to an aqueous phase with a high stripping efficiency and perform a new extraction sequence on this strip solution with a volume ratio $V_{aq}/V_{org} \gg 1$. As an example, for D = 10 and $V_{aq}/V_{org} = 10$, it is possible to obtain a volume reduction of 10 and an enrichment factor of 5 after one extraction. After a stripping with 100% efficiency and a new extraction with the same volume ratio, a volume reduction of 100 and an enrichment factor of 25 will be obtained. For higher D values, the enrichment factor will be higher.

Therefore, the stripping efficiency was also screened with a few stripping agents.

The extractions performed here are based on so-called ion pair formation and the extraction agents are all amines of different kind, which, as a rule, have been conditioned with 0.1M $H_2SO_4$. Data for extraction and stripping systems are found in Table 7.

TABLE 7. EXTRACTION AND STRIPPING SYSTEMS

| Extractant | Type | Producer | Concentration | Stripping agent tested |
|---|---|---|---|---|
| Primene JM-T | Primary amine | Rohm and Haas | 10% in kerosene | No stripping |
| Amberlite LA-2 | Secondary amine | Rohm and Haas | 10% in kerosene | 1.8M $H_2SO_4$ |
| Amberlite LA-2[a] | Secondary amine | Rohm and Haas | 10% in kerosene | 3.5M $H_2SO_4$ |
| Alamine 336 (>95% trioctylamine) | Tertiary amine | Henkel Corp. | 10% in kerosene | 6M $NH_3$, 1M $K_2(COO)_2$ |

[a]  Without pretreatment with 0.1M $H_2SO_4$.

### 3.2.1.2. Anion exchange method

The general procedure was as follows. The anion exchange resin based on a copolymer of styrene and divinylbenzene was immersed in water for 24 h for full swelling before loading onto a column made of polyethylene. The resin was then washed with 10M HCl to convert it into the Cl⁻ form, followed by ion exchanged water until pH 7 is reached in the water eluate.

For experiments where the main purpose was the separation of $[Co(CN)_6]^{3-}$, the column had dimensions $\emptyset = 5$ mm and $L = 25$ mm, corresponding to a resin volume of ~0.5 mL. For the experiments where the main purpose was absorption of SCN⁻, the column dimensions were $\emptyset = 6$ mm and $L = 300$ mm, corresponding to a resin volume of ~8.5 mL. A sample volume of 100–1000 mL of seawater containing radiotracer was passed through the columns. Flow rates were kept at ~0.5 mL/min.

Absorption yield (%) is expressed as:

$$Y_{abs} = \frac{R_{cs,feed} - R_{cs,raf}}{R_{cs,feed}} \cdot 100\% \tag{24}$$

where $R_{cs,feed}$ denotes the net sample counting rate per mL (proportional to activity concentration (Bq/mL) of the feed solution and $R_{cs,raf}$ denotes the net sample counting rate per millilitre of the raffinate.

Elution yield is determined as:

$$Y_{elut} = \frac{R_{cs,elut}}{R_{cs,feed} \cdot Y_{abs}/100} \cdot 100\% \tag{25}$$

where $R_{cs,elut}$ denotes the net sample counting rate per mL of the eluate.

The separation factor of $[Co(CN)_6]^{3-}$ and SCN⁻ in the complete ion exchange procedure (feed plus elution) is then defined as:

$$\alpha_{Co}^{SCN} = \frac{Y_{abs,SCN} \cdot Y_{elut,SCN}}{Y_{abs,Co} \cdot Y_{elut,Co}} \tag{26}$$

All anion exchangers are of the amine type. The main parameters are given in Table 8.

TABLE 8. ANION EXCHANGERS USED

| Resin used | Type | Producer | Elution agents tested |
|---|---|---|---|
| Amberlite IR45, 50–100 mesh | Weak base, $-NH_2$ | Rohm and Haas | No elutions performed |
| Lewatit MP60, 50–100 mesh | Weak base, $-NH_2$ | Bayer AG | No elutions performed |
| Dowex 1 × 2, 50–100 mesh | Strong base, quaternary amine | Dow Chemical | 4M $NH_4Cl$+2M HCL, 12M HCL, 65% $HNO_3$ |
| Dowex 1 × 2, 200–400 mesh | Strong base, quaternary amine | Dow Chemical | $NH_4Cl$ (saturated), 65% $HNO_3$ |
| Dowex 2 × 8, 100–200 mesh | Strong base, quaternary amine | Dow Chemical | 70% $HClO_4$, HI (conc.), 96% $H_2SO_4$, 12M HCl, 32.5% $HNO_3$, 2.5M $NH_4NO_3$, 5M $NH_4NO_3$, 7.5M $NH_4NO_3$, 10M $NH_4NO_3$ |
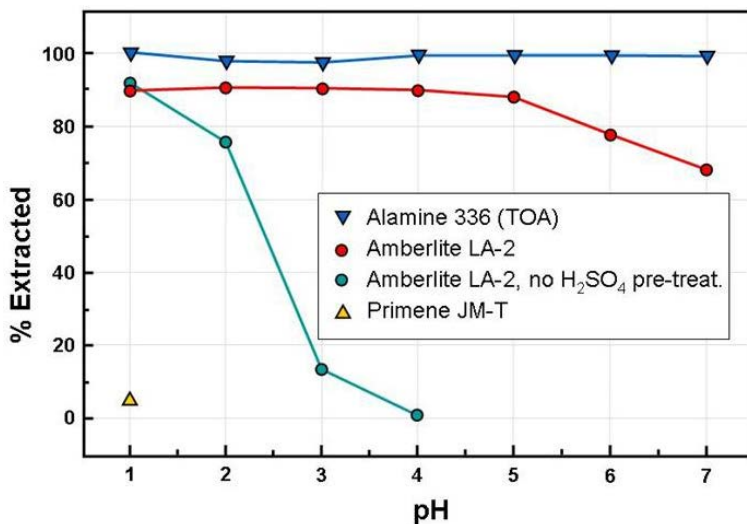
FIG. 48. *Extraction yield for the [Co(CN)$_6$]$^{3-}$ complex as a function of pH using four different extraction agents (10%) in kerosene.*

### 3.2.2. Comparison of the methods

#### 3.2.2.1. Results of solvent extraction method

Results from the liquid extraction of [Co(CN)$_6$]$^{3-}$ are shown in Fig. 48. The primary amine, Primene JM-T, extracted only minor quantities at pH1. At higher pH values, the extraction was not detectable. The secondary amine, Amberlite LA-2, without H$_2$SO$_4$ pretreatment shows as expected a reasonably high extraction at pH1, but has a strongly falling tendency towards higher pH values while the same resin with H$_2$SO$_4$ pretreatment maintains a high extraction yield until pH5 but decreases at higher pH values. Only the tertiary amine extractant, Alamine 336, extracted the Co complex strongly (near 100%) over the whole pH1–7 range.

Since Alamine 336 contains a basic nitrogen atom in the amine group, it may react with a variety of inorganic and organic acids to form amine salts, which are capable of undergoing ion exchange reactions with a host of other anions. As such, Alamine 336 is a liquid ion exchanger operated in a solvent extraction system. The general reactions, which are shown in Table 9, illustrate the two steps protonation and anion exchange:

After extraction, the organic phases containing Amberlite LA-2 and Alamine 336 were tested for stripping by the agents listed in Table 8. Ammonia could be used for stripping the Co complex from the Amberlite phases, while

## TABLE 9. PROTONATION AND ION EXCHANGE: GENERAL REACTIONS

| | |
|---|---|
| Protonation of resin by acid HA (HCl) | 1. $[R_3N]_{org} + [HA]_{aq} \leftrightarrows [R_3NH^+A^-]_{org}$<br>2. $[R_3N]_{org} + [HCl]_{aq} \leftrightarrows [R_3NH^+Cl^-]_{org}$ |
| Anion exchange | 3. $[R_3NH^+A^-]_{org} + [B^-]_{aq} \leftrightarrows [R_3NH^+B^-]_{org} + [A^-]_{aq}$<br>4. $3[R_3NH^+Cl^-]_{org} + [Co(CN)_6]^{3-}_{aq} \leftrightarrows \{[R_3NH^+]_3[Co(CN)_6]^{3-}\}_{org} + 3[Cl^-]_{aq}$ |

$K_2(COO)_2$ (potassium oxalate) could be used for stripping Co complex from both for the Amberlite and Alamine phases. For Alamine 336, for instance, the type of stripping agent to be recommended depends on the overall recovery process. In general, basic stripping agents, which reverse the protonation reaction, show the best stripping efficiency.

Two alternative mechanisms for stripping $[Co(CN)_6]^{3-}$ are:

(1)   $2\{[R_3NH^+]_3[Co(CN)_6]^{3-}\}_{org} + 3[K_2(COO)_2]_{aq} \leftrightarrows 3[R_3N]_{org}$
        $+ 3[H_2(COO)_2]_{aq+org} + 2K_3[Co(CN)_6]_{aq}$

(2)   $2\{[R_3NH^+]_3[Co(CN)_6]^{3-}\}_{org} + 3[K_2(COO)_2]_{aq} \leftrightarrows 3\{[R_3NH^+]_2[(COO)_2^{2-}]\}_{org}$
        $+ 2\{K_3[Co(CN)_6]\}$
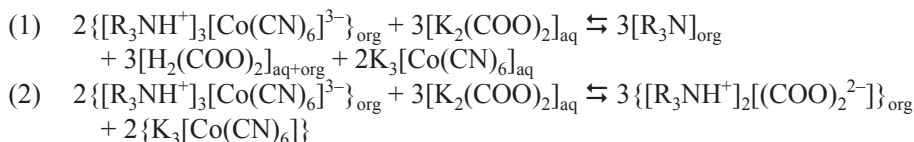
### 3.2.2.2. Results of anion exchange method

(1)   $[Co(CN)_6]^{3-}$

Table 10 gives the ion exchange yields for tracer concentration of $[Co(CN)_6]^{3-}$ on various ion exchange resins with a feed volume of 100 mL.

### TABLE 10.  THE ION EXCHANGE YIELDS FOR THE RESINS

| Anion resin | Anion exchange yield ($Y_{abs}$ (%)) |
|---|---|
| Amberlite IR45 | 40.7 |
| Lewatit MP60 | 2.6 |
| Dowex $1 \times 2$ (50–100 mesh) | 95.9 |
| Dowex $1 \times 2$ (200–400 mesh) | 100 |
| Dowex $2 \times 8$ (100–200 mesh) | 100 |
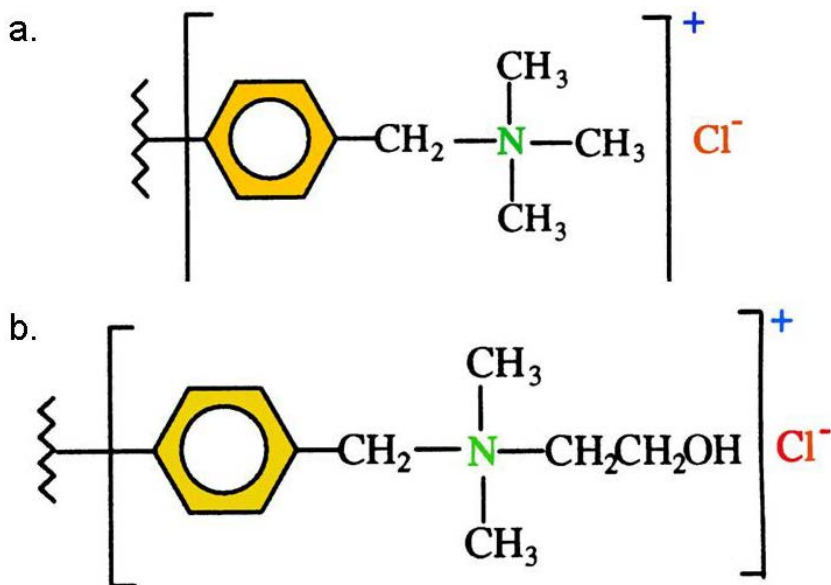
*FIG. 49.  Functional group of Dowex 1 (a) and Dowex 2 (b).*

It is obvious from the data in Table 10 that the strong base resins are superior to the weak base ones. Although both Dowex 1 and Dowex 2 are strong bases and quaternary amines, there is a difference in the functional groups:

- The functional (or ionogenic) group of Dowex 1 (Fig. 49(a)) is $-CH_2-N+(CH_3)^3$.
- For Dowex 2 the ionogenic group (Fig. 49(b)) is $-CH_2-N+(CH_3)^2-C_2H_4OH$.
- This latter structure implies that the base strength is somewhat lower than for the first structure. This is not seen in the ion exchange yield but became evident in the succeeding stripping process.

Table 11 shows that elution of $[Co(CN)_6]^{3-}$ from the Dowex 2 resin is easier than from the Dowex 1 resin both for strong $HNO_3$ and HCl elution agent solutions reflecting the somewhat weaker basicity of Dowex 2.

(2)   $SCN^-$

A method for isolation and upconcentration of $SCN^-$ from sea water (produced water) has previously been published and is based on the use of the

TABLE 11.  ELUTION YIELDS FOR $[CO(CN)_6]^{3-}$ FROM DOWEX $1 \times 2$ AND DOWEX $2 \times 8$ WITH TWO DIFFERENT STRONG MINERAL ACIDS

| Elution agent | Elution yield ($Y_{elut}$ (%)) | |
| --- | --- | --- |
| | Dowex 1 | Dowex 2 |
| 12M HCl | 24.7 | 63.4 |
| 14.5M $HNO_3$ | 52.3 | 80.3 |
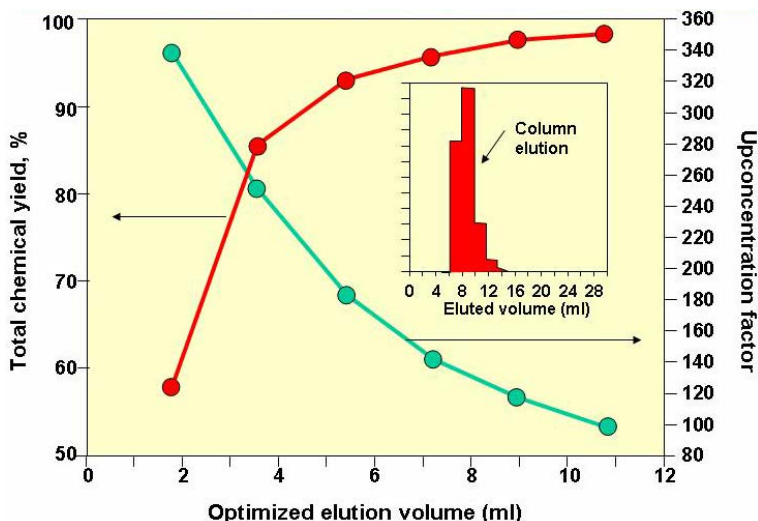


FIG. 50. Absorption yield of radiolabelled $SCN^-$ on BioRad AG1 is ~98.5% for a sample volume of 1000 mL of tracer-containing brine (seawater salinity).

anion exchange resin BioRad AG1, which is, in principle, equivalent to Dowex 1. Figure 50 shows the stripping yield (green curve) with 2.8M $NaClO_4$ as the stripping agent and the total chemical yield (red curve) of the $SCN^-$ separation and enrichment process, both as a function of the collected volume of the eluate. The elution peak is shown in the inset.

The performance of $SCN^-$ on the Dowex $2 \times 8$ resin with the column dimension described earlier was checked and the separation factor from $[Co(CN)_6]^{3-}$ with various elution agents investigated. Results of elution yields and separation factors are given in Table 12.

Figure 51 illustrates the absorption characteristics for $[Co(CN)_6]^{3-}$ and $SCN^-$ on the Dowex $2 \times 8$ column and compares these data with the sorption characteristics of $SCN^-$ on the BioRad AG1 column.

TABLE 12. ELUTION EFFICIENCY OF $[Co(CN)_6]^{3-}$ AND $SCN^-$ ON A DOWEX 2 × 8 (ø = 5 mm, l = 25 mm (100–200 MESH)) COLUMN AND THE SEPARATION FACTORS OBTAINED

| Elution agent | Elution yield ($Y_{elut}$ (%)) | | Separation factor ($\alpha_{Co}^{SCN}$) |
|---|---|---|---|
| | $[Co(CN)_6]^{3-}$ | $SCN^-$ | |
| $Na_3PO_4$ (saturated) | ≈0 | 3.4 | — |
| 1M $NH_4NO_3$ | 5 | 85 | 17.0 |
| 1.5M $NH_4NO_3$ | 7 | 95 | 13.6 |
| 0.1M $NaClO_4$ | 2 | 60 | 30.0 |
| 0.2M KI | 5 | 88 | 17.6 |
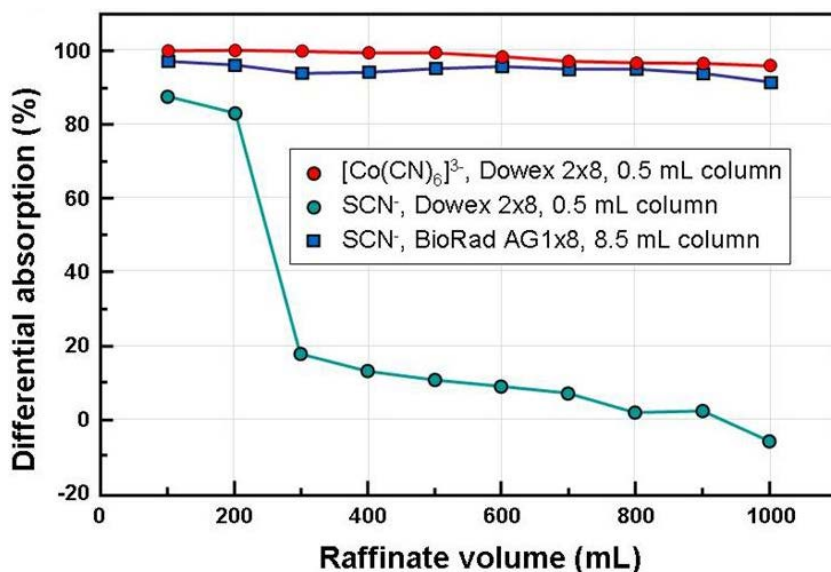


FIG. 51. Absorption yield of $[Co(CN)_6]^{3-}$ and $SCN^-$ on the 0.5 mL Dowex 2 ×8 (100–200 mesh) column, and for $SCN^-$ on the 8.5 mL BioRad AG1 column, as a function of raffinate volume (or original sample size) for tracer-containing seawater samples.

It is obvious from the data that $SCN^-$ experiences a rather fast breakthrough on the 0.5 mL Dowex 2 × 8 column, so the separation from $[Co(CN)_6]^{3-}$ will be substantial in the absorption process.

*3.2.2.3. Evaluation of the separation methods*

Both solvent extraction and ion exchange procedures may be used for entrapment, enrichment and separation of $[Co(CN)_6]^{3-}$ and $SCN^-$ tracers from saline waters (sea water or formation water). It seems, however, that the ion exchange procedures are the least labour intensive.

The results reported indicate a higher solvent extraction yield for $[Co(CN)_6]^{3-}$ with strong basic extractants rather than weak ones for the prevailing experimental conditions. This is valid both for the liquid extraction agents and for the solid anion exchangers tested. In the ion exchange processes, it is found that $[Co(CN)_6]^{3-}$ is more strongly absorbed by Dowex $1 \times 2$ than by Dowex $2 \times 8$, although the absorption yields are close to 100% for both under the prevailing conditions. Their relative absorption strengths appear through their ability to release the tracer again by various elution agents.

The difference in the degree of cross-linking between the Dowex $1 \times 2$ and Dowex $2 \times 8$ resins would favour the kinetics of the $\times 2$ resin. However, for reasonable flow rates, the kinetics is not an issue. Since the Dowex $2 \times 8$ resin shows the highest elution yield (which was previously concluded to be due to the difference in the functional groups), use of the Dowex $2 \times 8$ resin is recommended for the actual separation process.

The remaining $SCN^-$ on the Dowex $2 \times 8$ ion exchanger after sample loading may be eluted selectively and with high elution efficiency by 10 mL of 0.1M $NaClO_4$. This eluate may be added to the raffinate after the sample loading process and used as a feed to the BioRad AG1 column for separation and enrichment of the $SCN^-$ tracer along the lines already outlined.

From a 1000 mL sample, the total recovery (chemical yield) is >65%. Since the volume is reduced by a factor of 100, the enrichment factor is >65. By optimizing the process, it is probably possible to double this figure, especially by selecting carefully only the elution volume containing the bulk of the tracer peak. In this way, the volume may perhaps be reduced by a factor of 2–3 with a slight reduction in chemical yield.

The $[Co(CN)_6]^{3-}$ complex may be stripped from Dowex $2 \times 8$ by, for instance, 10 mL 5M $NH_4NO_3$ (acceptable for modern scintillation cocktails) with an efficiency of 75%. The overall chemical yield will, therefore, be >75%. From the same sample size as for $SCN^-$, the volume reduction will amount to a factor of 100 and the corresponding enrichment factor to >75. It is also possible to improve this figure by optimization of the procedure along the same lines as described for $SCN^-$.

# Appendix I

# CASE STUDIES

## I.1.  CASE 1: DIADEMA OILFIELD (ARGENTINA)

The study began in January 2006 when 740 GBq of HTO was injected into well I-103, 750 kg of ammonium thiocyanate into well I-124 and 40 L of uranine into well I-125, all of the wells belonging to the Diadema oilfield in the province of Chubut, Argentina. The patterns involved in the operation can be seen in Fig. 52.

The response curves are shown in Fig. 53 where the tracer concentrations are represented in a relative way (activity and mass). The ordinate scale is logarithmic.
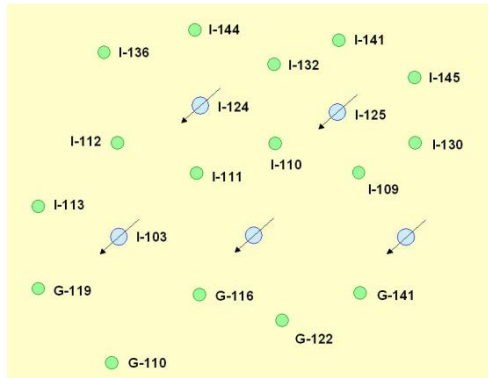


*FIG. 52.  Well pattern in the Diadema oilfield.*

TABLE 13. MAIN  PARAMETERS  OF  DIADEMA  WELL  PATTERN *(average values)*

| Parameter | Value | Parameter | Value |
|---|---|---|---|
| Layer thickness | 10 m | Permeability | 0.1–1 Darcy |
| Layer porosity | 30% | Injection flow rate | 270 m$^3$/d |
| Water saturation | 50% | Injection pressure | 34 kg/cm$^2$ |
| Distances (injection–production) | 250 m | Temperature | 50°C |
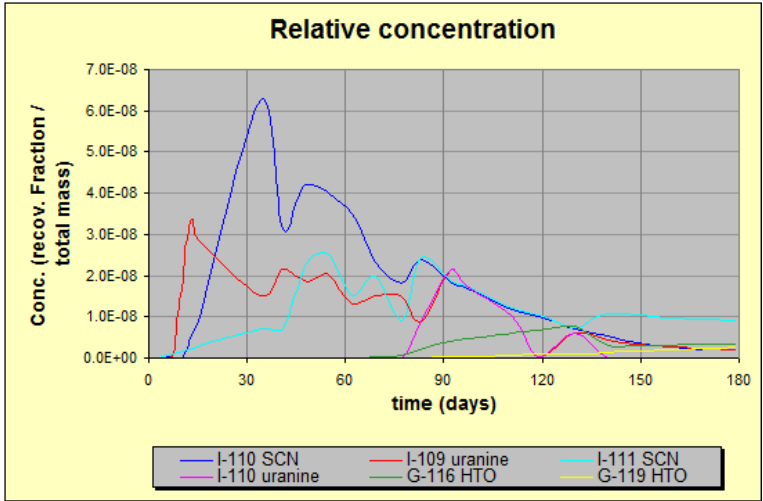
*FIG. 53.  Relative concentration curves (Diadema oilfield).*
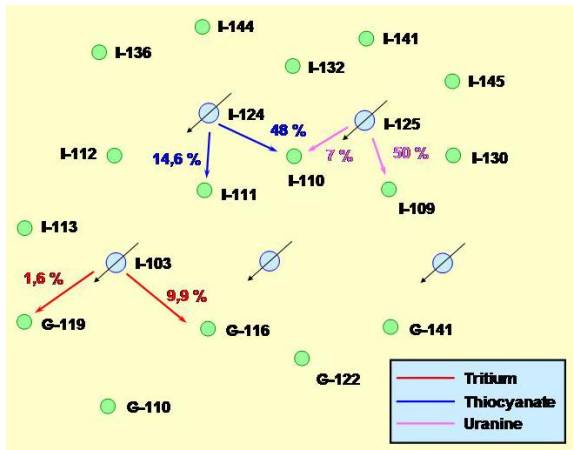


*FIG. 54.  Tracer distribution in the Diadema oilfield.*

The tracers are moving mainly to the south, as can be seen in Fig. 54, where only those wells with a recovery mass or activity of more than 1% are reported.

Breakthrough times were in the range of 48–72 d for HTO, 11–34 d for ammonium thiocyanate and 8–83 d for uranine. Tracer recovery ranged around 0.2–10% for HTO, 15–48% for ammonium thiocyanate and 0.1–50% for uranine for those wells in which tracer was detected.
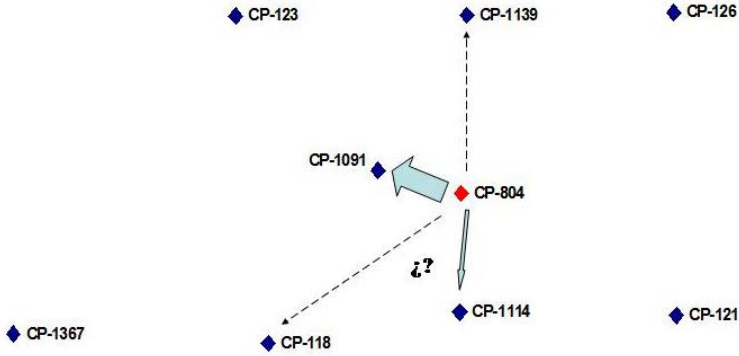
*FIG. 55.  Well pattern in the Carmopolis oilfield.*

TABLE 14.  MAIN PARAMETERS OF CARMOPOLIS WELL PATTERN *(average values)*

| Parameter | Value | Parameter | Value |
|---|---|---|---|
| Layer thickness | 10 m | Distances (injection–production) | 205 m |
| Layer porosity | 17% | Injection flow rate | 83 m³/d |
| Water saturation | 62.8% | | |

I.2.  CASE 2: CARMOPOLIS OILFIELD (BRAZIL)

In the pattern shown in Fig. 55, well CP-804 was injected with 55.5 GBq of HTO.

The response curves are shown in Fig. 56 where the tracer concentrations are represented in a relative way as tracer daily fractional recovery (TDFR) according to Eq. (27).

$$TDFR = \frac{1}{m_{\text{tracer-inj}}} \frac{\Delta m_{\text{tracer-rec}}}{\Delta t} = \frac{C_{\text{tracer-sample}} \cdot q_{\text{water-producer}}}{m_{\text{tracer-inj}}} \qquad (27)$$

This way of expressing concentration is used in several other examples.
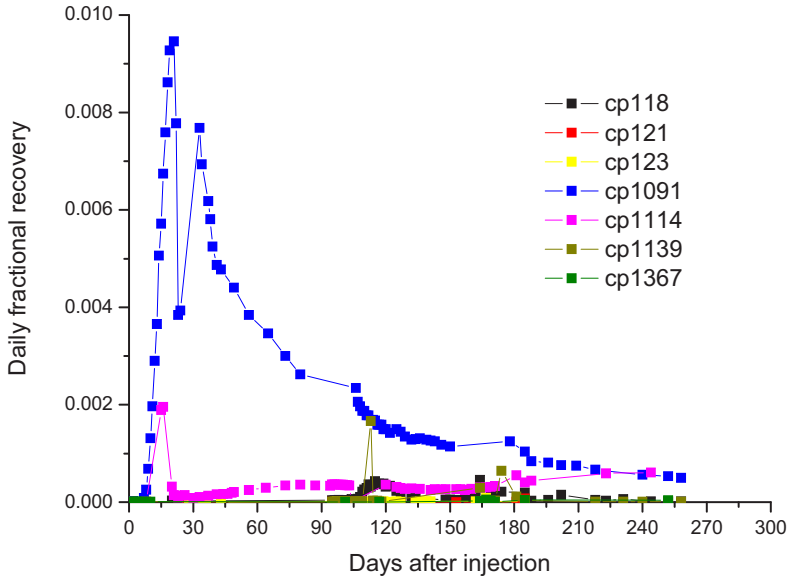
FIG. 56. Tracer daily fractional recovery curves (Carmopolis oilfield).
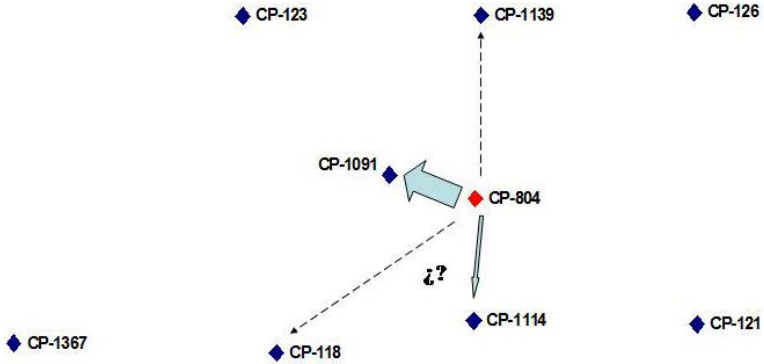


FIG. 57. Tracer distribution in the Carmopolis oilfield.

Figure 57 shows that the tracer is moving mainly in the direction of well CP-1091.
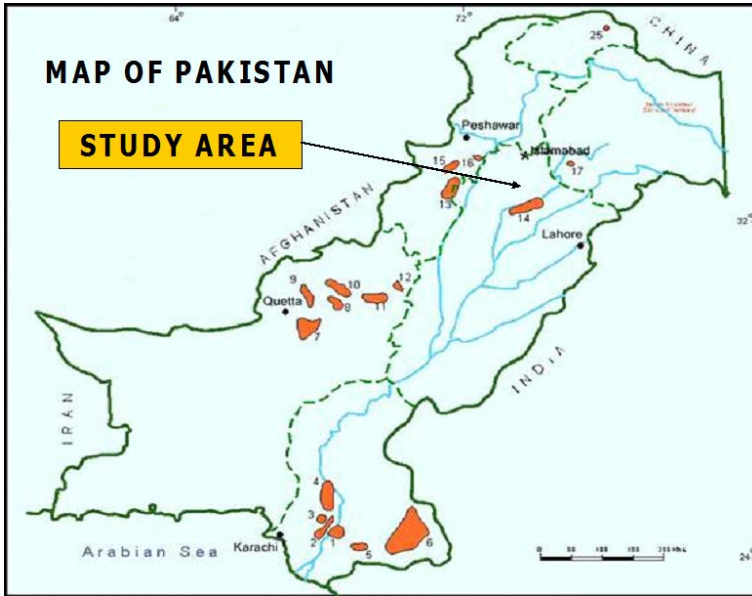
*FIG. 58. Map of Pakistan showing the study area.*

## I.3. CASE 3: FIMKASSAR OILFIELD (PAKISTAN)

### I.3.1. Introduction

Radiotracer applications for interwell communication studies were carried out in two oilfields in Pakistan. The study area consists of two oilfields (oilfield 1 and oilfield 2) and is shown in Fig. 58.

### I.3.2. Tracer test in oilfield 1

The study is being carried out in the Fimkassar oilfield, which is operated by the Oil and Gas Development Co. Ltd. This oilfield is located in the Potowar Basin, about 100 km southwest of Islamabad. The field has two production wells (wells 1 and 2) and the third well (well 3) is used as an injection well for water flooding. A fourth well was drilled but it was 'dry' and was capped. The pattern and the location of the wells are shown in Fig. 59.

97
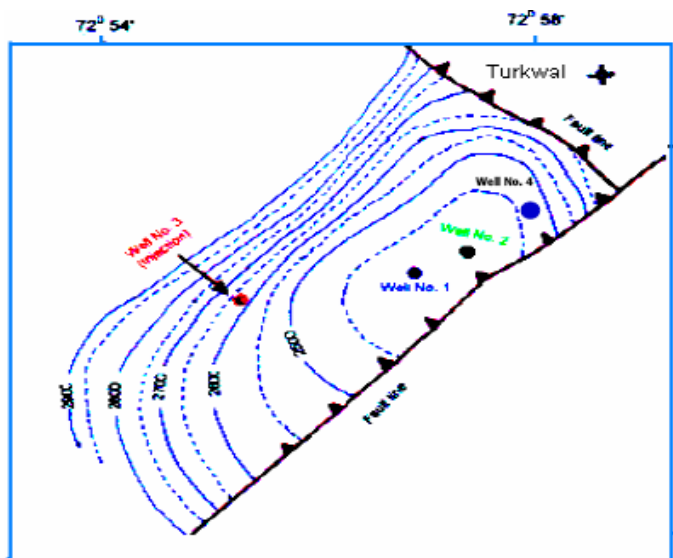
*FIG. 59. Well pattern, Fimkassar oilfield.*

*Objectives*

The main objectives of the study were to:

- Determine breakthrough time between injection and production wells;
- Assess the contribution of injected water towards the production well and investigate the presence of quick channelling between the injection and production wells;
- Determine the swept volume of the reservoir by injected water;
- Assess the efficiency of injected fluid to increase the reservoir pressure;
- Assess the relative contributions of injected water and formation water in the produced water.

Monthly sampling of producer wells and the injection well was carried out and samples were analysed for tritium ($^3$H) and stable isotopes ($^2$H, $^{18}$O) using liquid scintillation counting and isotope ratio mass spectrometry, respectively. Radiotracer and stable isotope data were processed and analysed and these data are displayed in Figs 60 and 61.

The work related to this oilfield is complete and the results are as follows:

- Breakthrough time is 252 d.
- Water produced in well 1 has an 85% contribution of fresh injected water.
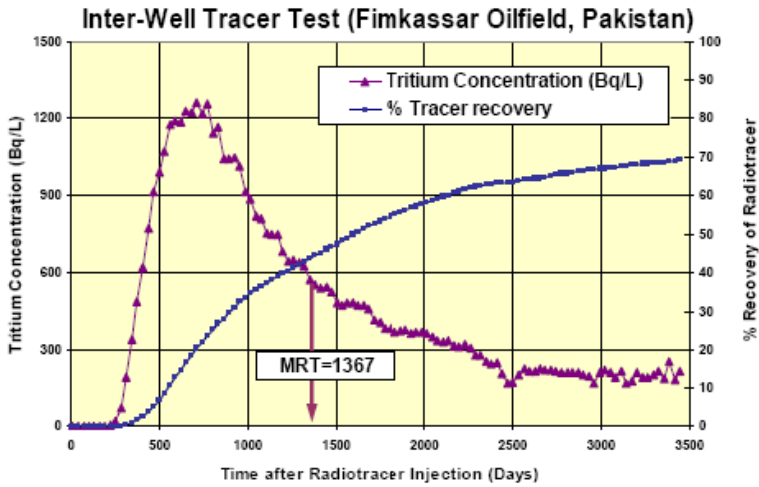
FIG. 60.  Tracer response curve and tracer recovery (Fimkassar oilfield).
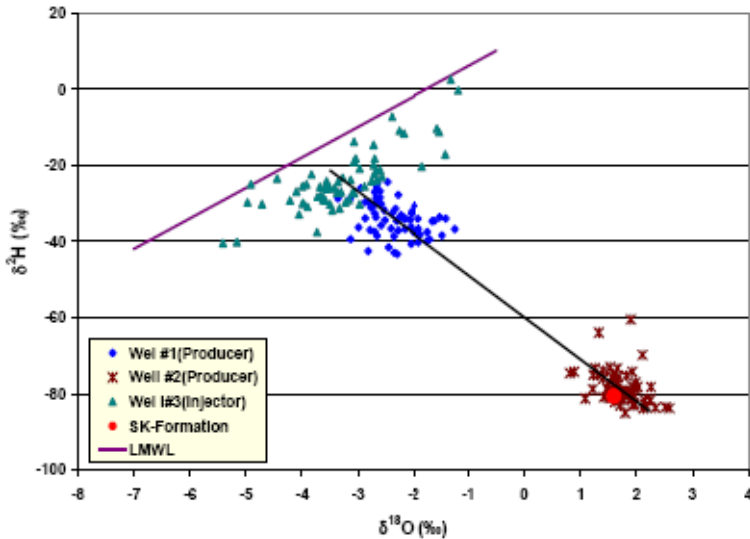


FIG. 61.  Stable isotope data delineating different water sources.

- Mean residence time of tracer (water) is 1367 d.
- Mean injected water volume is 2 497 864 $m^3$.
- Mean produced water volume is 460 711 $m^3$.
- Maximum and mean velocities of injected water are 10.3 m/d and 1.9 m/d, respectively.
- Tracer recovery is ~69%.

Considering a mean produced water volume of 460 711 m$^3$ and 69% recovery of radiotracer from well 1, the mean swept volume is determined as 317 891 m$^3$. This is the average volume of the reservoir swept by injected water.

- After initial reduction in breakthrough time, the injection water has swept a large volume and there appears to be no channels connecting the injection well and production well 1.
- No injected tracer was detected in well 2.
- The tracer response shows that the water flood regime was not managed properly in the initial stages that changed the hydrodynamics of the reservoir and affected the production.
- The water in the formations is meteoric water, recharged from northern parts of the country.

### I.3.3.  Tracer test in oilfield 2

The experience gained through the work carried out in oilfield 1 strengthened the capabilities of the tracer group at PINSTECH and resulted in better cooperation and enhanced acceptance of the technology by the end user. This provided an opportunity to extend radiotracer applications to another oilfield. Oilfield 2 is situated about 20 km away from oilfield 1. There are four production wells and two injection wells in this field. The pattern of wells is shown in Fig. 62. The distance between injection wells and production wells varies from 1125 to 3975 m and the depth of the wells varies from 4068 to 4267 m below mean sea level.

*Objectives*

The objectives of this study were to:

- Determine the breakthrough time between the injection and production wells;
- Assess the contribution of injected water in the production wells;
- Determine relative contribution of injected water and formation water to individual production wells;
- Investigate the presence of channels (if any) between the injection and production wells;
- Determine the mean residence time of floodwater in the reservoir;
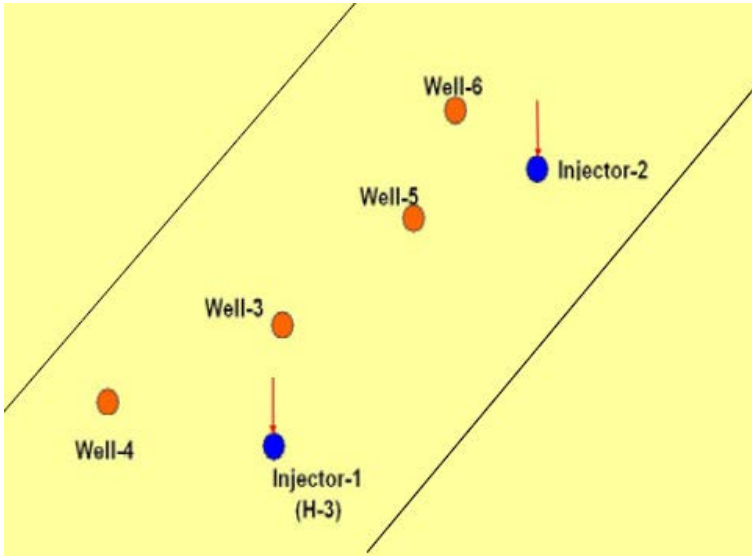- Determine the percentage radiotracer recovery and the swept volume by floodwater.

*FIG. 62. Pattern of wells in oilfield 2.*

Tritium (as HTO) was injected in well 1 through a bypass loop and production wells 3, 4, 5 and 6 were monitored for tracer response. Tracer breakthrough was recorded in well 3 in 17 d. However, no tracer breakthrough was observed in production wells 4, 5 and 6 up to June 2008. Stable isotopes of water ($^2$H and $^{18}$O) were also utilized to identify different water sources and their relative contributions to produced water. The data are shown in Figs 63 and 64.

The work related to oilfield 2 is in progress and the results obtained to date are as follows:

- The breakthrough time of well 3 is 17 d.
- The early breakthrough in well 3 indicates the channelling effect between injection well and production well 3.
- Mean residence time of tracer with respect to injection well 1 and production well 3 is 127 d.
- The volumetric response of tracer has determined that mean produced water volume from well 3 is 52 000 m$^3$, which was achieved in 136 d after radiotracer injection and 301 d since water injection was started. These figures are in good agreement with a mean residence time of 121 d.
- The volumetric response of tracer has determined that mean injected water volume from injection well 1 is 200 490 m$^3$, which was achieved in 131 d after radiotracer injection and 301 d since water injection was started. These figures are again in good agreement with a mean residence time of 127 d.
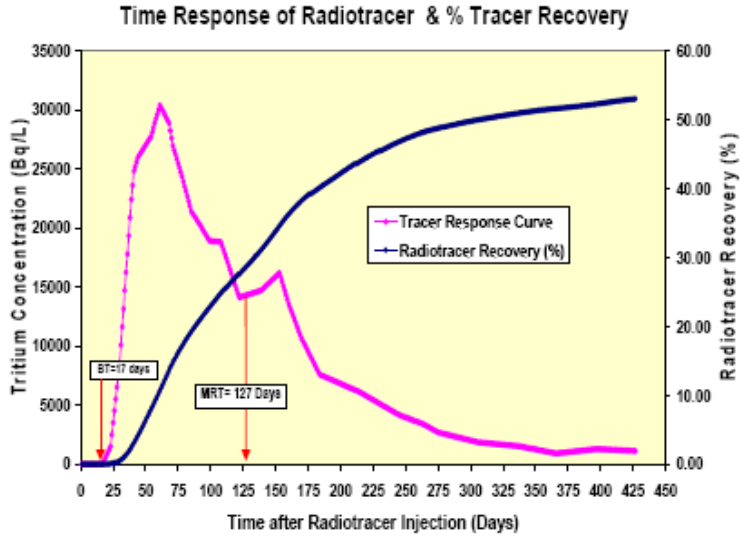
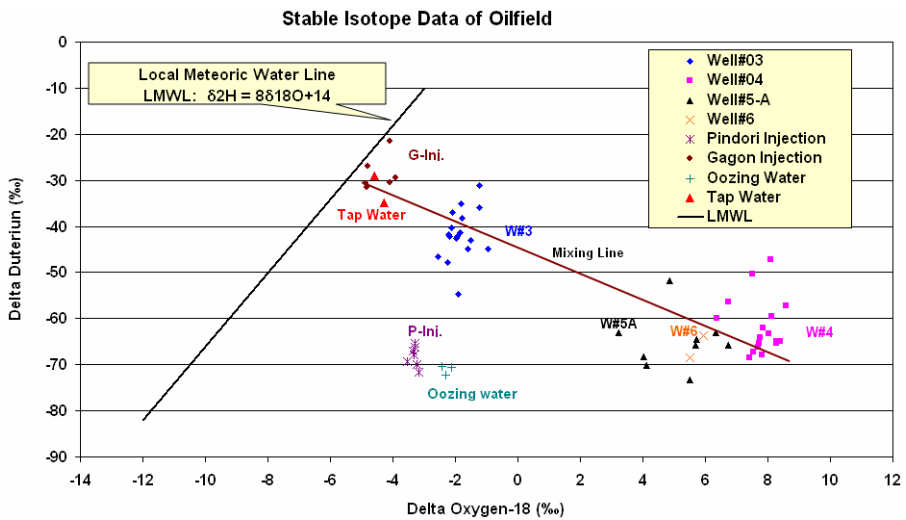FIG. 63. Tracer response of well 3 and tracer recovery (%).



FIG. 64. Stable isotope data of oilfield 2.

- The maximum and mean velocities of injected water between injector well 1 and producer well 3 are 80.9 m/d and 110.8 m/d, respectively.
- About 53% of injected tracer has been recovered through producer well 3 within 427 d of radiotracer injection (up to 15 May 2008).

102

- Considering a mean produced water volume of 52 000 m$^3$ and 53% recovery of radiotracer from well 3, the mean swept volume is determined as 27 560 m$^3$. This is the average volume of reservoir swept by injected water which was produced by well 3.
- No radiotracer breakthrough was detected in wells 4, 5A and 6 up to 15 May 2008.
- Relative contributions of injected water and formation water to production well 3 are 77% and 23%, respectively.

### I.3.4. Conclusions

The tracer test carried out in both oilfields provided excellent data, which can be used to validate modelling software. The highlighting point of these tracer tests was that the conjunctive use of the stable isotopes of water ($^2$H and $^{18}$O) along with radiotracer provided very useful supplementary information, giving more credibility to tracer technology as applied to interwell communication studies. Therefore, stable isotopes can be successfully applied for interwell communication studies where there is reasonable difference in stable isotope indices of injection and formation waters. Further, stable isotopes are unique tools to identify different sources of groundwater.

### I.4. CASE 4: LAHENDONG GEOTHERMAL FIELD (INDONESIA)

#### I.4.1. Tritium tracer test in Lahendong geothermal field

The Lahendong geothermal field is located in North Sulawesi province at an elevation of 800–1100 m above mean sea level and is producing about 20 MW(e) of electricity annually.

Tritium tracer with an activity of 629 GBq (17 Ci) was injected into LHD-7 injection well in July 2006. Monitoring of tritium tracer has been done in several production wells surrounding LHD-7. The tracer monitoring in production wells LHD-8, LHD-11, LHD-12 and LHD-15 was done periodically every two weeks during the first three months after injection, and then periodically every month.

Tritium in water samples was analysed using a Packard-TR 1900 liquid scintillation counter. The direct counting method was used and samples were distilled before counting. A 10 mL sample of distilled water and 11 mL of Instagel cocktail (Ultima Gold) were added to the counting vial and homogenized by shaking. The counting time for each sample was 20 min and the counting rate was converted to tritium units.

## I.4.2. Results and discussion

Table 15 shows the result of tritium tracer in Lahendong geothermal field, whereas Fig. 65 shows the plot of time versus tracer concentration curve.

TABLE 15. MONITORING RESULTS OF TRITIUM TRACER IN LAHENDONG GEOTHERMAL FIELD

| Production wells | Tritium concentration (tritium units) | | | | |
|---|---|---|---|---|---|
| | LHD-8 | LHD-11 | LHD-12 | LHD-15 | LHD-10 |
| Background | 0.53 | 0.24 | 0.25 | 0.43 | 0.12 |
| Time (d) | | | | | |
| 3 | 0.74 | 0.38 | 0.31 | 0.72 | |
| 21 | 1.05 | 1.18 | 0.95 | 1.15 | |
| 33 | 1.59 | 1.33 | 1.21 | 1.21 | |
| 47 | 1.6 | 1.04 | 1.98 | 3.59 | |
| 61 | 1.05 | 4.2 | 6.57 | 4.18 | |
| 65 | 3.61 | 3.23 | 3.03 | 5.05 | |
| 81 | 0.84 | 0.85 | 1.72 | 1.24 | |
| 95 | 0.47 | 1.7 | 1.42 | 1.21 | |
| 121 | 0.84 | 0.93 | 1.19 | 1.7 | |
| 148 | 1.33 | 2.34 | 1.9 | 1.9 | |
| 226 | | | 1.57 | 5.51 | 1.47 |
| 252 | | | 5.06 | 4.11 | 5.51 |
| 309 | | | 4.5 | 7.39 | 4.76 |
| 342 | | | 12.57 | 20.29 | 24.14 |
| 370 | | | 112.47 | 112.5 | 112.17 |
| 405 | | | 125.19 | 174.4 | 227.78 |
| 433 | | | 75.84 | 69.19 | 69.88 |
| 472 | | | 73.65 | 38.58 | 18.22 |
| 508 | | | 39.59 | 30.73 | 40.62 |
| 625 | | | 25.08 | 11.04 | 16.7 |
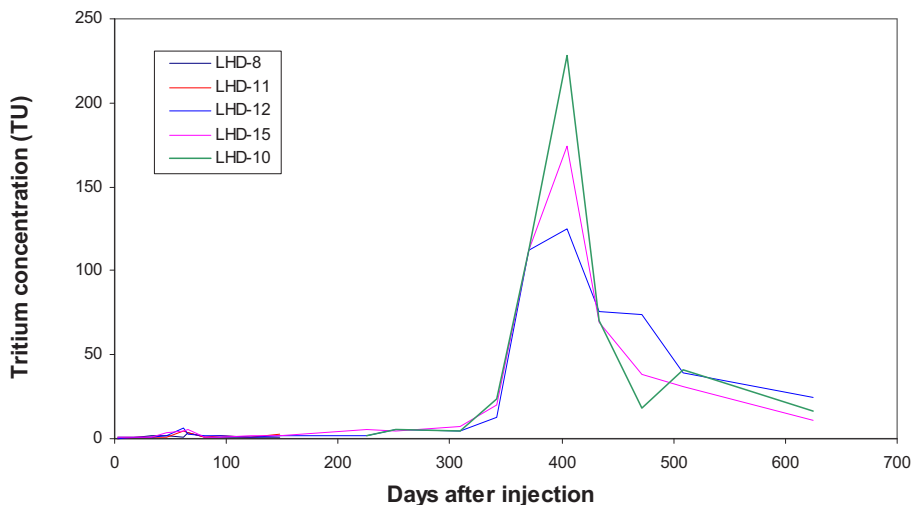
FIG. 65. Tritium concentration in monitored production wells.

Figure 65 shows that tritium concentration in monitored production wells fluctuated around background value until 300 d after injection. Tracer breakthrough occurred in 309 d after tracer injection. The tracer concentration peak of the response curves of three wells (LHD-10, LHD-12 and LHD-15) was recorded around 400 d after injection with a maximum tritium concentration of 228 tritium units.

### I.4.3.   [125]I tracer test in Dieng geothermal field

Dieng geothermal field is located in central Java. It has more than 15 production wells and 3 injection wells. It produces about 60 MW(e) of electricity annually. In August 2007, 5.6 Ci of ^{125}I tracer was injected in the well HCE-29. The same injection method as tritium injection in Lahendong was applied to this field. The sampling and subsequent measurements were carried out for a period of 135 d after injection.

*Analysis of [125]I*

Isotope ^{125}I is a low energy gamma emitter (35 keV) with a half-life of 60 d. On the basis of its half-life, ^{125}I is a suitable radiotracer for short to mid-term reinjection into a geothermal field. However, the low energy characteristic makes ^{125}I difficult to detect directly in the field. Pretreatment of sample and use of a

sensitive detector, i.e. liquid scintillation counter, are required in order to analyse this tracer activity.

The procedure used to analyse $^{125}$I is as follows:

- The samples (2 L) are delivered in plastic bottles and are weighed to determine their volumes accurately. A known quantity of inactive iodide (5 mg) is added to act as carrier, as well as to ensure that the final precipitate is of sufficient mass (about 10 mg) to be reliably filtered and weighed. The samples are then filtered if inspection reveals any debris or cloudiness, and NaOH is added to make the samples slightly alkaline (~pH9).
- The iodide is then oxidized to iodate with $KMnO_4$ and allowed to stand for about 20 min. At the same time, any sulphide present (which would form $Ag_2S$ precipitate in competition with AgI) is oxidized to sulphate. A longer standing time might be used if organic matter is present or if there is a high sulphide concentration.
- The iodate (including the carrier) is then reduced back to iodide by adding an acid mixture ($HNO_3$ and HF) followed by $Na_2SO_3$ solution. The HF is included to inhibit formation of silica, which would clog filters and interfere with the weight of the final precipitate. Sulphate is unaffected by this step, thus effectively removing sulphide interference. After standing, the solution is filtered to remove any traces of silica which might have formed.
- An excess of $AgNO_3$ solution is added soon after the filtration to form a precipitate of AgI. Because AgI is much less soluble than AgCl, it is precipitated preferentially despite the approximately thousand-fold excess of chloride ions. However, small quantities of AgCl (and AgBr) are formed. After standing in the dark, the precipitate is filtered through cellulose acetate paper under vacuum. The AgCl and AgBr are then removed by washing with ammonia. The precipitate, now pure AgI, is then passed quickly through a further oxidation–reduction cycle for purification purposes before being dried and weighed.
- The precipitate is then dissolved in the liquid scintillation cocktail. This is done by inserting the rolled filter paper into the cocktail vial, adding about 20 mg of acidified thiourea to complex the AgI, and then immersing the vial in an ultrasonic bath to disperse the AgI into the cocktail. The paper is translucent and should be left in the vial (20 mL). The precipitates are dried and weighed.
- The analytical yield is calculated by dividing the mass of iodide in the AgI precipitate by the quantity of iodide added plus that known from prior analysis to be in the sample, typically 0.1–0.2 mg/L.

Table 16 presents the sample counting rates obtained at different production wells. It shows that during 135 d of monitoring, the $^{125}$I tracer appears at wells HCE-7A, HCE-7B, HCE-7C, HCE-9B and HCE-28A. Figure 66 shows the tracer experimental response curve obtained at the production well HCE-28A.

## I.5.   CASE 5: LEYTE GEOTHERMAL FIELD (PHILIPPINES)

### I.5.1.   Problem

The Tongonan-1 sector of the Leyte geothermal production field (LGPF) in the Philippines (Fig. 67) has been experiencing declines in output in some of its production wells, which have been mainly attributed to injection returns from brine injected into one of the wells situated near the production area. Routine production well chemistry monitoring indicated physicochemical changes in the production wells attributed to migration of the reinjected brine back to the production sector since 2001, when the injection load from South Sambaloran was transferred to Tongonan-1.

TABLE 16. CONCENTRATION OF $^{125}$I IN PRODUCER WELLS *(net cpm/g)*

| Monitoring period (d) | Well | | | | |
|---|---|---|---|---|---|
| | HCE-7A | HCE-7B | HCE-7C | HCE-9B | HCE-28A |
| 7 | — | 715 | 887 | 445 | — |
| 14 | 2804 | 246 | 460 | — | — |
| 22 | — | 244 | — | 508 | — |
| 57 | 2351 | — | — | 212 | 1387 |
| 71 | 1712 | 189 | 483 | 721 | 126 |
| 92 | 89 | — | — | — | 8792 |
| 107 | — | 216 | 291 | 157 | 2367 |
| 121 | 409 | — | — | — | 760 |
| 134 | 436 | 107 | 218 | 210 | 268 |
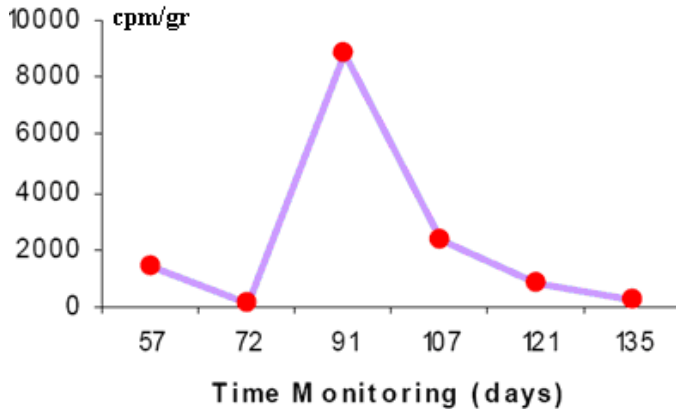
*FIG. 66. Tracer experimental response curve obtained at the production well HCE-28A.*
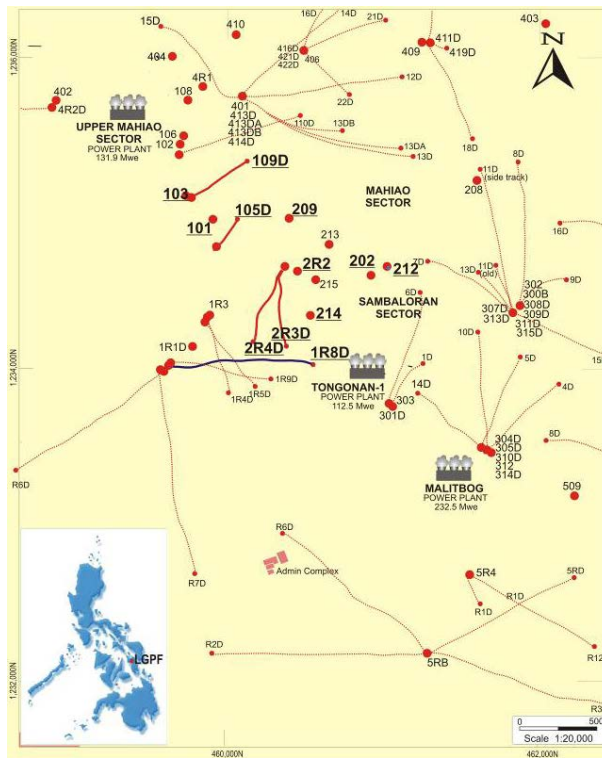


*FIG. 67. Location map of the LGPF showing tracks of wells drilled (in red lines). Inset delineates the area where the tracer test was conducted. Well 1R8D is the tritium injector well.*

## I.5.2.  Methodology

HTO (10 Ci) was injected into well 1R8D on 12 July 2006. Ten production wells were chosen for tracer breakthrough monitoring. These are wells 101, 103, 105D, 109D, 202, 209A, 212, 214, 2R2, 2R3D and 2R4D. Wells 105D, 103 and 109D were selected on the basis of their rapid physicochemical response, employing 1R8D as a reinjection well. Wells with considerable steam fraction (enthalpy of 1800–2700 kJ/kg) were selected deliberately to determine the behaviour of tritium in the vapour phase. However, a few watery wells were also included in the programme to determine tritium's fractionation between the water and vapour phases.

As a basis for selecting samples from 'watery' wells, 1,5-naphthalene disulphonate (NDS) was injected on 14 June 2006, one month prior to the injection of tritium in 1R8D. The watery wells that showed NDS breakthroughs were chosen for tritium analysis (i.e. 2R3D, 2R4D, 202, 214). Moreover, the results of NDS tracer were also used to compare and/or confirm the tritium data collected.

Continuous sampling was conducted for a year in the selected monitor wells. However, analysis was terminated for the wells which did not yield positive tritium returns after six months from injection. Tritium was analysed at the Philippine National Research Institute and at CAIRT, Jakarta, Indonesia. The NDS analysis, on the other hand, was done at the LGPF Geoservices Laboratory using high performance liquid chromatography.

Data reduction, both for tritium and NDS, was achieved using the Anduril 2.3 package specifically designed for radioactive tracers. NDS data were processed using the ICEBOX software package (United Nations University Geothermal Training Programme, 1994) and Anduril 2.3. Results from both software packages revealed almost identical values.

## I.5.3.  Results and discussion

### I.5.3.1.  Tracer recovery

Among the ten wells monitored for a year, three wells (W2R3D, 214 and 202) yielded positive results for tritium tracer. These same wells also yielded positive returns with NDS. These returns confirmed the communication between the injector well 1R8D and the nearby production wells.

Figure 68 shows the results of the NDS tracer test. Among the wells in Tongonan-1 nearest to 1R8D, wells 2R3D and 2R4D showed NDS breakthrough starting about 19 d after injection. Well 214 manifested breakthrough 40 d after injection, while breakthrough in well 202 occurred much later, at 131 d.
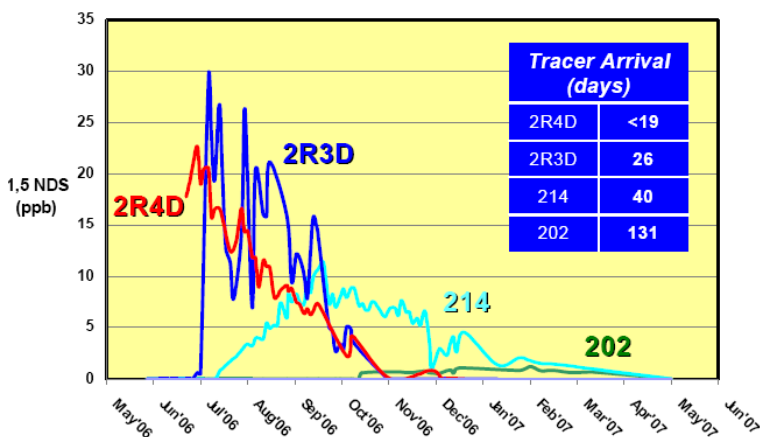
*FIG. 68. Plot showing the breakthrough of wells from NDS tracer injected into well 1R8D.*

The wells which showed NDS breakthrough also showed positive returns with tritium; among the wells monitored, these are the only wells which gave tritium breakthrough. Tritium in well 2R3D appeared 28 d after injection; while it appeared in wells 214 and 202, 61 D and 189 d after injection, respectively. The vapour rich wells (i.e. 101, 105 and 109D) did not show a positive manifestation of tritium, even after six months of monitoring, thus analysis in these wells was terminated after December 2006 (Fig. 69).

Tritium and NDS returns in wells 2R3D and 2R4D exhibit sharp breakthroughs at the start and gradually tapered off over time. This is opposed to the relatively semi-broad nature of the graphs for wells 214 and 202. Figure 70 shows the processed curve for well 2R3D for both tritium and NDS tracers. The plots show that there are two pulses of tritium and NDS that entered the well.

Well 214 showed two pulses of HTO breakthrough, while only one pulse was detected for NDS (Fig. 71).

Reduction of HTO and NDS curves in well 202 showed only one pulse for both (Fig. 72). Further, the recovery yield for both NDS and tritium were different. Using the Anduril software, the tracer recovery for tritium was 0.4% for well 2R3D, while wells W214 and W202 both gave yields of 0.1%. NDS recovery, on the other hand, was 1.3% for well 2R3D, 0.2% for well 214 and 0.1% for well 202. On the basis of these results, NDS recovery was higher by almost 100% for wells 2R3D and 214, while recovery was the same for well 202, the well furthest from the injector.
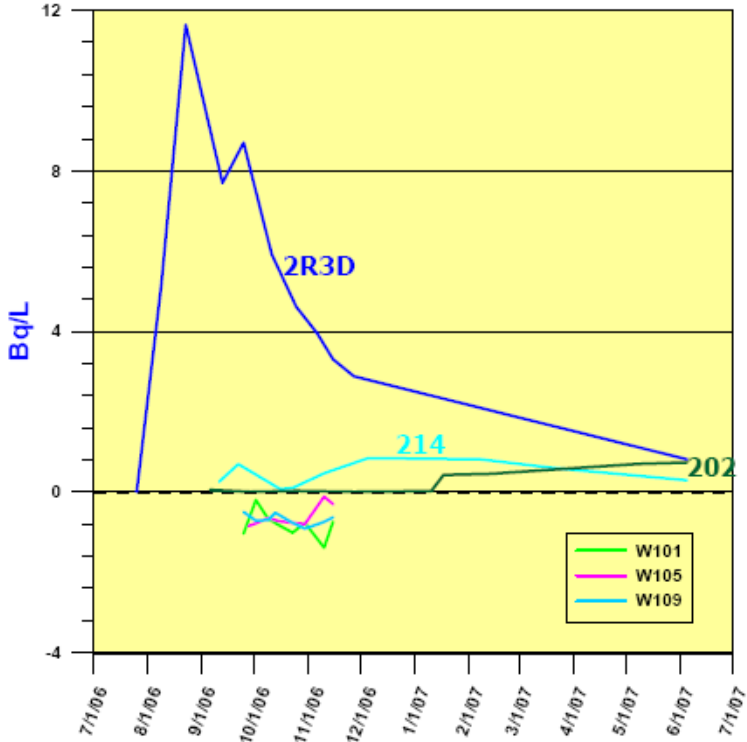
110

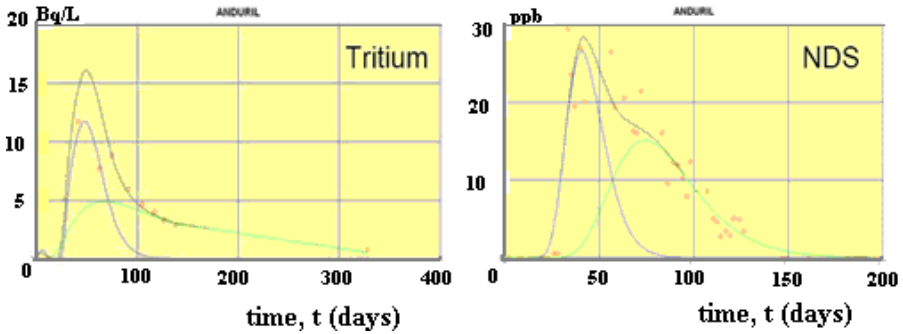FIG. 69.  Plot of wells monitored for tritium breakthrough.



FIG. 70.  Processed curve for well 2R3D using Anduril software, showing the two pulses of tritium and NDS recoveries (blue and green curves). The black curve represents the sum of both pulses.
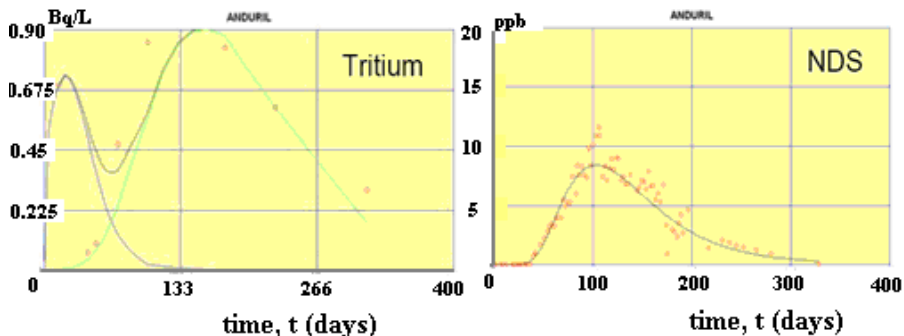
FIG. 71. Tritium and NDS curves for well 214. The black curve (tritium) represents the sum of the pulses (green and blue curves). Only one pulse was processed for NDS.
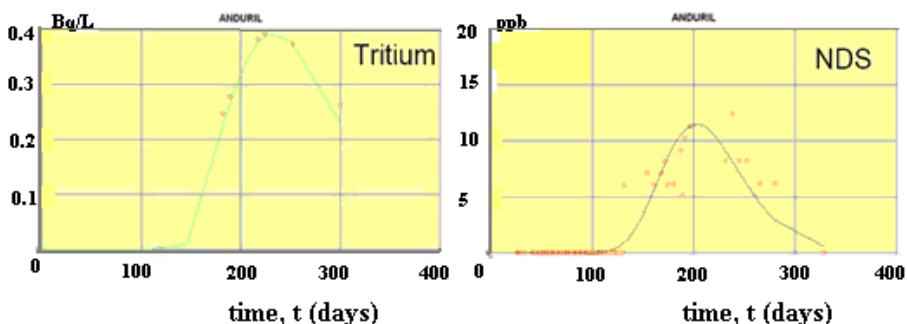


FIG. 72. Tritium and NDS curves for well 202, showing only one pulse for both tracers.

### I.5.3.2.  Tracer movement

Structural correlation indicates that the main conduit of the tritium and the NDS from 1R8D to the production wells is the Sambaloran Fault. Figure 73 shows the schematic of the likely path of the tritium-bearing fluid. By first order of approximation, it is logical to think that wells 2R3D and 2R4D would yield the tracer first since these are situated nearest the injector well. It should then follow that the tracer recovery would diminish from well 2R3D towards well 202.

Figure 74 shows the cross-section and the structures intersected by wells where tritium and NDS were detected. As shown, the Sambaloran Fault is the only structure intersected by the wells which showed breakthroughs. Thus, it is the likely conduit of the tritiated brine.

Considering the proximity of the injector well, 1R8D, with the nearest monitor production well, 2R3D/2R4D, at ~140 m (well bottom separation), a much higher recovery of tracer was expected than was actually measured.
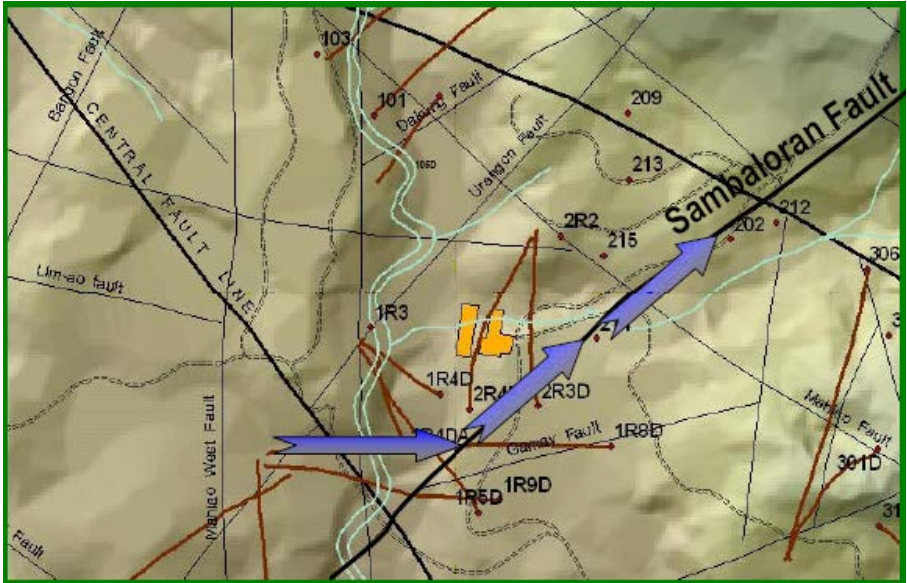
FIG. 73. Map showing the projected path of the tritiated/NDS fluids from 1R8D.
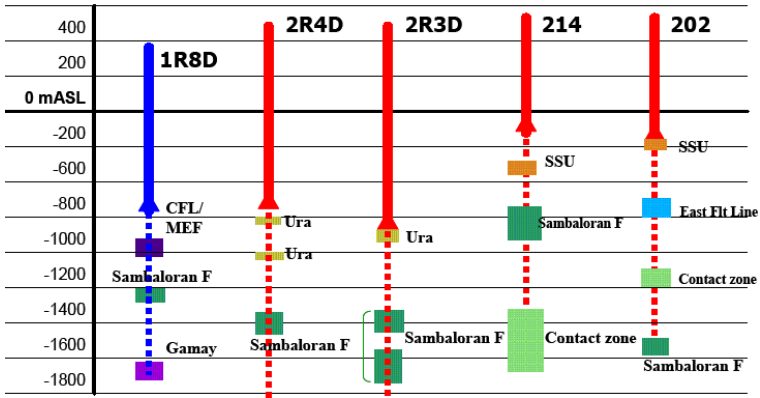


FIG. 74. Cross-section of the wells showing the structures intersected. Highlighted in dark green are the intersects of the Sambaloran Fault. (CFL — Central Fault Line; MEF — Mahiao East Fault; Ura — Urangon Fault; SSU — South Sambaloran Unit).

Similarly, the tracer recoveries in wells 214 and 202 are considered low since there were already chemical and thermal indications as early as 2002 that when 1R8D was commissioned for brine injection (from South Sambaloran production wells in an adjacent sector), brine returns were then observed in wells 214 and 202, amongst others.
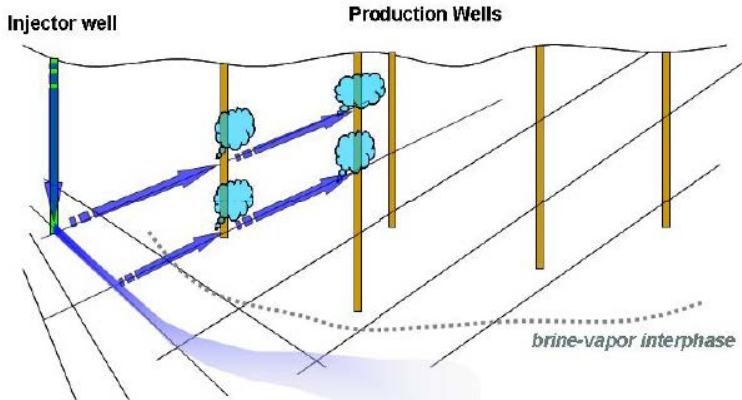
*FIG. 75. Schematic diagram of the possible path of the tritium injected into well 1R8D.*

Although wells 202, 214 and 2R3D have brine returns based on geochemical monitoring and tracer breakthrough, the low tracer recovery suggest that these wells are still predominantly fed by the upper steam zone. This implies that most of the tritium is still in the deeper portion of the reservoir, along with the liquid zone. This is corroborated by flow measurements showing medium to high enthalpy discharges at the well head (W214 ~2500–2700 kJ/kg enthalpy, W202 ~2000–2200 kJ/kg, 2R3D ~1800–1900 kJ/kg).

Tritium, on the other, has a fractionation factor of 1. Thus, equal concentrations go to the water and vapour phases. The low recovery seen in wells 2R3D, 214 and 202 may suggest that the 10 Ci injection is insufficient.

The two pulses seen in wells 2R3D and 214 imply that the first pulse passed through the structural conduit, the Sambaloran Fault, from 1R8D and the second pulse which occurred at a later period could mean that the tracer travelled with the brine to the deeper part of the reservoir and later flashed and again passed through another conduit to appear in these wells (Fig. 75).

It has been reported that the northern Tongonan wells, 101 and 105D, showed declines in their gas concentrations and geothermometers, and this was attributed to the injection returns from well 1R8D. The discharges from these wells remained dry despite the prognosticated brine returns simply because of their shallow production zones, which are tapping the degassed steam from the Tongonan injection sink.

On the basis of the above-mentioned scenario, the absence of tritium in wells 105D, 101 and 109D could indicate two things. Firstly, there may not have been enough tritium injected into well 1R8D to effect a breakthrough in these northern Tongonan wells. Secondly, the current preferential flow of the tracer and the brine returns is to the east through the Sambaloran Fault, as indicated by the
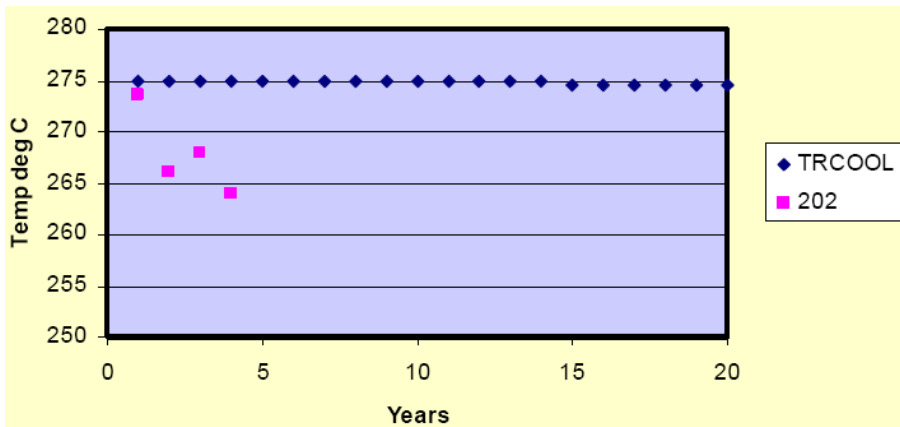
114

FIG. 76. Plot of simulated temperature using the TRCOOL program compared with actual temperatures (TQuartz) in well 202.

early tracer breakthroughs in the wells along the structure. Thus, breakthrough of the tracer to the northern Tongonan wells could be observed much later. However, as shown by chemical changes in these wells, with the use of well 1R8D, the connection between these wells cannot be discounted.

Using minimal tracer recovery experimental data, no decline in temperature was observed in TRCOOL simulation (Fig. 76). Thus, no historical match was processed for the wells, in terms of cooling or thermal decline. The ~10°C decline in the fluid temperature (based on TQuartz) of well 202 did not match the cooling prediction based on tritium and NDS recoveries.

These observations and processed data could, therefore, imply one, or a combination, of the following: (i) tritium injected may have been insufficient to be detected in the monitor wells, however short their distances are; (ii) because of the nature of NDS tracer, monitoring in a highly two phase environment will give minimal recovery; (iii) the chemical breakthroughs observed in previous years could mean that well 1R8D is not the sole source of brine/cold waters capable of effecting such changes in thermal and chemical parameters.

## I.5.4. Conclusions

The injection of tritium in the LGPF has indicated the applicability of tritium as tracer, as it has been detected in three wells. Its low recovery, however, could be due to insufficient concentration injected into well 1R8D. It could also indicate that there is significant dispersion or diffusion of tritium within the reservoir, such that its occurrence in other wells could occur at a much later date.

However, if insufficient concentration was injected, there is a possibility that the tritium injected will not find its way out of the reservoir.

The absence of processed historical matching (Fig. 76) in terms of thermal decline in the wells monitored for tracer could indicate that there are other sources of brine/cooler waters that effected a change in the wells. The tracer tests conducted for tritium in LGPF were able to detect the connection between the injector and the production wells monitored.

HTO with an activity of 10 Ci was injected into well 1R8D and tritium was detected at three monitor wells: 2R3D, 214 and 202.

These wells lie directly on the north-east path of the tritium derived from well 1R8D, along the Sambaloran Fault. The other monitor wells, which are situated to the north of the injector, did not manifest any tritium breakthrough one year after injection. The recovery in these wells, however, is only 0.1–0.4%. Near simultaneous NDS tracer test injected into the same well revealed positive breakthroughs, with recoveries slightly higher at 0.1–1.3%. Both tritium and NDS yielded the highest recovery at well 2R3D, the well nearest the injector.

The tracer results showed the hydrological connection between the wells monitored. The very low recovery, however, suggests other possible paths of the fluids from 1R8D. This was not established in the monitoring programme conducted. Nonetheless, the exercise demonstrated that tritium can indeed be utilized as a tracer in a vapour dominated environment. The major consideration here would be the cost of the tritium and the analysis.

## I.6.  CASE 6: TUHA OILFIELD (CHINA)

### I.6.1.  Problem

A field tracer experiment was commenced by the Tuha Oil Company on 10 July 2005. The objectives of the experiment were:

— To validate $^{14}C$ tagged KSCN and $^{60}Co$ tagged $K_3[Co(CN)_6]$ as interwell water tracers;
— To evaluate the water injection processes;
— To reveal the features of reservoir heterogeneity.

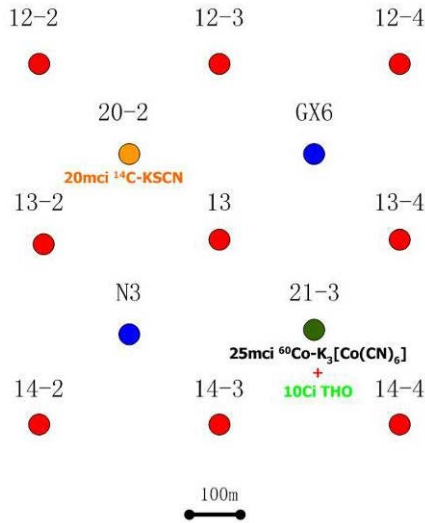Figure 77 shows the well pattern and the tracer injection wells.

*FIG. 77. Well pattern and tracer injection wells in the Tuha oilfield.*

### I.6.2. Tracers and tracer injection

As indicated in Fig. 77, three radioactive tracers were used in the test, HTO, $^{14}C$ tagged KSCN and $^{60}Co$ tagged $K_3[Co(CN)_6]$. In the test, 20 mCi of $^{14}C$ tagged KSCN was injected into well 20-2 on 10 July 2005, and 10 Ci of HTO, together with 25 mCi of $^{60}Co$ tagged $K_3[Co(CN)_6]$, was injected into well 21-3 on 11 July 2005.

### I.6.3. Tracer responses

All tracers were detected in corresponding production wells:

- The $^{14}C$ from well 20-2 was found on 30 January 2006 at well 12-3, 204 d after injection.
- The HTO from well 21-3 was found on 30 November 2005 at well 13-4, 141 d after injection, and was found on 23 January 2006 at well 13, 195 d after injection.
- The $^{60}Co$ from well 21-3 was found on 05 January 2006 at well 13-4, 177 d after injection.

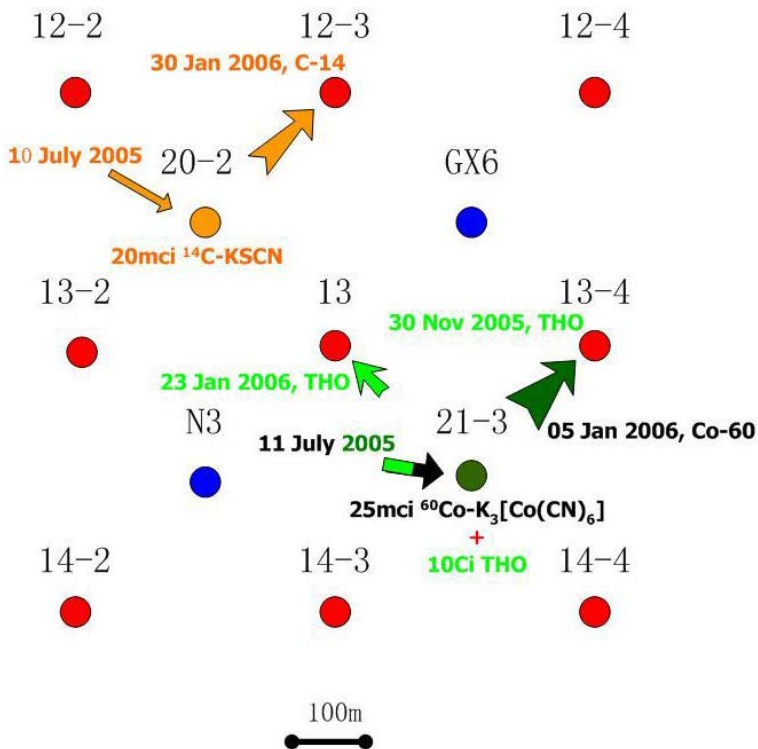Tracer injection and directional tracer movements are shown in Fig. 78.
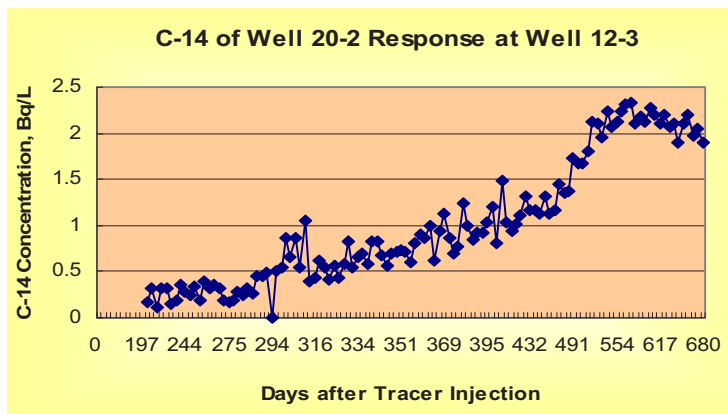
*FIG. 78. Schematic map of tracer movement.*



*FIG. 79. Carbon-14 of well 20-2 response at well 12-3.*

PORO software simulation was used for tracer data treatment. Tracer response curves are shown in Figs 79 and 80.
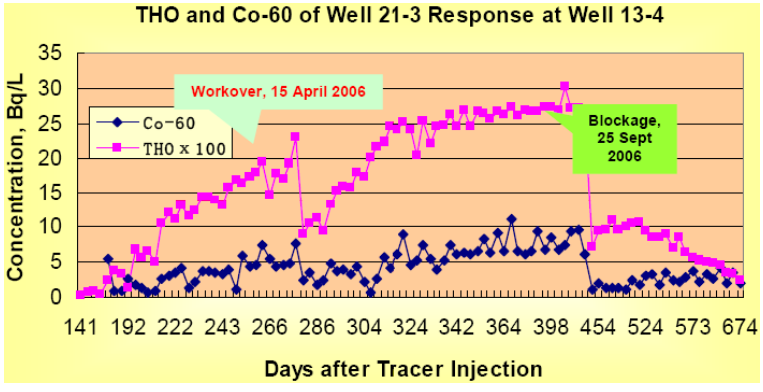
*FIG. 80. HTO and $^{60}$Co of well 21-3 response at well 13-4.*

## Appendix II

## LABORATORY INTERCOMPARISON

The experimental laboratory intercomparison tests ('round robin' test) reported here were twofold: (i) analysis of HTO in different waters and (ii) analysis of HTO plus $^{14}CH_3OH$ in mixtures in different waters. The first test sequence was organized by Norway while the second was arranged by Vietnam.

## II.1. LABORATORY INTERCOMPARISON TEST ON HTO ANALYSIS

### II.1.1. Preparation of samples

The following series of samples were prepared at IFE, Norway:

- Series 1, samples 1A–1E: Distilled tap water with added and calibrated quantities of HTO. Sample volume was 100 mL each.
- Series 2, samples 2A–2E: Distilled tap water with a quenching agent added and calibrated quantities of HTO. Sample volume was 100 mL each.
- Series 3, samples 3A–3E: Artificial Gullfaks (Norwegian oilfield) formation water with added and calibrated quantities of HTO. Sample volume was 250 mL each.
- Series 4, samples 4A–4E: Real formation water (Tordis oilfield, Norway) which has been in contact with 'live' oil. A calibrated quantity of HTO was added. Sample volume was 250 mL each. For the concentration of some main ions, see Table 17.

The samples were calibrated with certified Wallac and Packard secondary standard tablets using Quantulus 1220 liquid scintillation counting equipment. Six packages of 20 water samples each were shipped to the various participating laboratories on 18 May 2006. Results were requested by 15 September 2006.

### II.1.2. Experimental parameters used at each participating laboratory

Table 18 lists the experimental parameters used in different laboratories.

## TABLE 17. SALINE WATER COMPOSITIONS

| Series 3: Artificial Gullfaks formation water, salts dissolved in distilled tap water | | Series 4: Tordis produced water (samples have been in contact with live oil) | |
|---|---|---|---|
| NaCl | 41.04 g/L | $Na^+$ | 12 400 ppm |
| KCl | 0.635 g/L | $K^+$ | 230 ppm |
| $MgCl_2 \cdot 6H_2O$ | 2.546 g/L | $Ca^{2+}$ | 800 ppm |
| $Na_2SO_4$ | 0.047 g/L | $Mg^{2+}$ | 175 ppm |
| $NaHCO_3$ | 0.212 g/L | $Ba^{2+}$ | 30 ppm |
| | | $Sr^{2+}$ | 150 ppm |
| | | $Cl^-$ | 21 000 ppm |
| | | $SO_4^{2-}$ | 23 ppm |

## TABLE 18. EXPERIMENTAL PARAMETERS USED AT THE DIFFERENT LABORATORIES ON COMPLETION OF THE ROUND ROBIN TEST

**Brazil,** CDTN Radiochemistry Laboratory

| | |
|---|---|
| Sample treatment: | 1A–3E: No treatment, 4A–4E: Distillation |
| Calibration: | Dilutions from NIST SRM 4926E, 3 Sept 1998 |
| Equipment/method: | Quantulus 1220, 22 mL PE vials |
| Scintillation cocktail: | Optiphase HighSafe III, C/W = 12/10 |
| Counting time: | 12 × 10 min = 120 min |
| Background coun trate: | 1.89 ± 0.49 cpm |

**Indonesia,** Hydrology and Geothermic Laboratory Center for the Application of Isotope and Radiation Technology, National Nuclear Energy Agency

| | |
|---|---|
| Sample treatment: | Distillation of all samples |
| Calibration: | Dilutions from NIST SRM 4926D-11, 25 July 1989 |
| Equipment/method: | Packard 1900 TR, PP vials |
| Scintillation cocktail: | Ultimo Gold, C/W = 11/10 |
| Counting time: | 720 min |
| Background count rate: | 2.98 ± 0.29 cpm |

TABLE 18.  EXPERIMENTAL PARAMETERS USED AT THE DIFFERENT LABORATORIES ON COMPLETION OF THE ROUND ROBIN TEST (cont.)

**China,** Industrial Application of Radioisotopes, China Institute of Atomic Energy

| | |
|---|---|
| Sample treatment: | All samples filtered with 0.45 µm filter. No distillation |
| Calibration: | H-3 Standard Sample Series, National Institute of Metrology |
| Equipment/method: | Wallac 1414, Win Spectral, PP vials |
| Scintillation cocktail: | Optiphase HighSafe III, C/W = 2/1 |
| Counting time: | 60 min |
| Background count rate: | 8 cpm |

**Argentina,** Porous Media Group, Comahue National University

| | |
|---|---|
| Sample treatment: | Distillation of all samples |
| Calibration: | No direct calibration. Based on internal non-quenched spectra and measured quenching parameters |
| Equipment/method: | Wallac 1414, Win Spectral, PP vials |
| Scintillation cocktail: | Optiphase HighSafe II, C/W=16/4 |
| Counting time: | 90 min |
| Background countrate: | 34 cpm |

**Vietnam,** Centre for Applications of Nuclear Technique in Industry, NRI

| | |
|---|---|
| Sample treatment: | A1–E2: No treatment. 3A–4E: Both with and without distillation |
| Calibration: | No direct calibration. Based on internal non-quenched spectra and measured quench curves |
| Equipment/method: | Packard TriCarb 2900TR |
| Scintillation cocktail: | Instagel Plus, C/W = 12/8 |
| Counting time: | 90 min |
| Background count rate: | 12 cpm |

**Pakistan,** Radioisotope Hydrology Laboratory, Pakistan Institute of Nuclear Science
and Technology

| | |
|---|---|
| Sample treatment: | A1–2E: No treatment. 3A–3E: Distilled, 4A–4E: Filtered and distilled |
| Calibration: | NIST SRM 4926D-15, 3 September 1998 |
| Equipment/method: | Packard TriCarb 3170, 22 mL PE vials |
| Scintillation cocktail: | Ultima Gold, C/W = 12/8 |
| Counting time: | $10 \times 50$ min |
| Background count rate: | 1.1 cpm |

**Norway,** Department for Reservoir and Exploration Technology, Institute for Energy
Technology

| | |
|---|---|
| Sample treatment: | 1A–3E: Filtering (0.45 μm), 4A–3E: Filtering and distillation |
| Calibration: | Wallac and Packard secondary standard tablets (with expiring date). Check with internal quench parameters and with addition of internal standard |
| Equipment/method: | Quantulus 1220, 22 mL PP vials |
| Scintillation cocktail: | Ultima Gold, C/W = 12/8 |
| Counting time: | 3 h |
| Background count rate: | Undistilled blank: $2.1 \pm 0.5$ cpm, distilled blank $1.8 \pm 0.5$ cpm |

## II.1.3. Results

Results from the various laboratories are summarized in Table 19. All datasets except the one from Argentina are internally relatively consistent and also relatively close to the nominal values.

Figure 81 compares the country results for each of the samples and Fig. 82 compares the results for each country with the nominal values of the tracer concentration in radar plots with a logarithmic concentration axis. In Fig. 82, a horizontal bar has been inserted showing a symmetric realistic $2\sigma$ error of $\pm 5\%$ around the nominal value. This value is derived mainly from a realistic assessment of the uncertainty in the accuracy of the secondary standard.

TABLE 19.  EXPERIMENTAL RESULTS FROM PARTICIPATING ANALYTICAL LABORATORY

Measured concentration (Bq/L)

| No. | Brazil | | Indonesia | | China | | Argentina | | Vietnam | | Pakistan | | Norway | | Nominal |
|---|---|---|---|---|---|---|---|---|---|---|---|---|---|---|---|
| | Conc. | $1\sigma$ | Conc. | $1\sigma$ | Conc. | $1\sigma$ | Conc. | $1\sigma$ | Conc. | $1\sigma$ | Conc. | $1\sigma$ | Conc. | $3\sigma$ | Conc. |
| 1A | 91.4 | 11.8 | 92.0 | 8.6 | 68.9 | 5.4 | 4607.0 | 25.0 | 74 | 3 | 95.5 | 0.9 | 100.4 | 4.3 | 101.0 |
| 1B | −3.1 | 6.0 | 2.6 | 0.5 | 2.1 | 3.8 | 4172.0 | 24.0 | 2 | 3 | 0.0 | 1.0 | 0.1 | 1.8 | 0.1 |
| 1C | 710.7 | 23.6 | 660.1 | 61.5 | 526.0 | 13.7 | 4693.0 | 25.0 | 510 | 9 | 681.8 | 3.7 | 725.6 | 10.3 | 734.5 |
| 1D | 5.1 | 4.2 | 6.4 | 0.8 | 24.8 | 4.4 | 4268.0 | 24.0 | 6 | 5 | 6.1 | 1.1 | 4.9 | 2.3 | 5.5 |
| 1E | 14.7 | 4.4 | 18.6 | 1.9 | 14.4 | 4.2 | 4252.0 | 24.0 | 16 | 4 | 19.3 | 2.1 | 19.2 | 2.7 | 20.2 |
| 2A | 696.9 | 37.4 | 665.5 | 61.5 | 532.0 | 14.0 | 4982.0 | 26.0 | 508 | 6 | 675.2 | 3.7 | 742.5 | 10.3 | 734.5 |
| 2B | 14.7 | 5.9 | 20.4 | 2.0 | 28.7 | 4.7 | 4279.0 | 24.0 | 14 | 6 | 18.6 | 1.4 | 19.9 | 2.7 | 20.2 |
| 2C | 88.3 | 9.6 | 94.3 | 8.7 | 72.1 | 5.7 | 4911.0 | 26.0 | 70 | 5 | 94.3 | 0.9 | 99.4 | 4.3 | 101.0 |
| 2D | −4.1 | 4.8 | 1.9 | 0.6 | nd | nd | 3913.0 | 23.0 | 2 | 2 | 0.8 | 0.8 | 0.8 | 2.2 | 0.1 |
| 2E | 2.5 | 6.4 | 6.4 | 0.8 | 13.9 | 4.1 | 4357.0 | 24.0 | 5 | 4 | 6.3 | 1.3 | 6.0 | 2.3 | 5.5 |
| 3A | 44.6 | 8.2 | 46.0 | 4.3 | 48.3 | 5.0 | 9780.0 | 36.0 | 34 | 6 | 41.9 | 1.6 | 46.5 | 3.3 | 44.1 |
| 3B | 8.5 | 6.3 | 30.3 | 2.8 | 7.4 | 3.9 | 8575.0 | 34.0 | 18 | 6 | 8.4 | 1.4 | 11.7 | 2.5 | 11.0 |

TABLE 19. EXPERIMENTAL RESULTS FROM PARTICIPATING ANALYTICAL LABORATORY (cont.)

| No. | Measured concentration (Bq/L) | | | | | | | | | | | | | | |
|-----|--------|------|-----------|------|--------|------|-----------|------|---------|------|----------|------|--------|------|---------|
| | Brazil | | Indonesia | | China | | Argentina | | Vietnam | | Pakistan | | Norway | | Nominal |
| | Conc. | $1\sigma$ | Conc. | $1\sigma$ | Conc. | $1\sigma$ | Conc. | $1\sigma$ | Conc. | $1\sigma$ | Conc. | $1\sigma$ | Conc. | $3\sigma$ | Conc. |
| 3C | 106.2 | 15.7 | 78.7 | 7.3 | 75.5 | 5.7 | 9679.0 | 36.0 | 77 | 4 | 99.0 | 3.3 | 110.6 | 4.5 | 110.2 |
| 3D | −2.4 | 5.7 | 23.9 | 2.2 | 2.5 | 3.9 | 7393.0 | 31.0 | 5 | 2 | 2.9 | 1.0 | 0.4 | 2.1 | 0.1 |
| 3E | 355.8 | 18.7 | 215.2 | 19.9 | 268.0 | 9.7 | 8013.0 | 33.0 | 253 | 12 | 335.2 | 3.5 | 383.3 | 7.7 | 367.3 |
| 4A | −2.4 | 6.5 | 26.5 | 2.5 | 4.2 | 3.8 | 8543.0 | 33.0 | 2 | 2 | 2.8 | 0.9 | 0.1 | 2.0 | 0.1 |
| 4B | 5.6 | 5.9 | 33.1 | 3.1 | 28.5 | 4.4 | 7707.0 | 32.0 | 8 | 6 | 9.1 | 2.1 | 9.7 | 2.4 | 9.2 |
| 4C | 349.0 | 18.7 | 234.4 | 21.7 | 276.0 | 10.0 | 8688.0 | 34.0 | 236 | 10 | 333.3 | 2.8 | 374.5 | 7.5 | 367.3 |
| 4D | 32.6 | 9.5 | 46.6 | 4.4 | 26.7 | 4.3 | 9306.0 | 35.0 | 25 | 9 | 39.1 | 2.7 | 35.0 | 3.0 | 36.7 |
| 4E | 83.8 | 8.9 | 78.0 | 7.2 | 69.3 | 5.3 | 9163.0 | 35.0 | 64 | 8 | 92.3 | 2.9 | 91.9 | 4.1 | 91.8 |
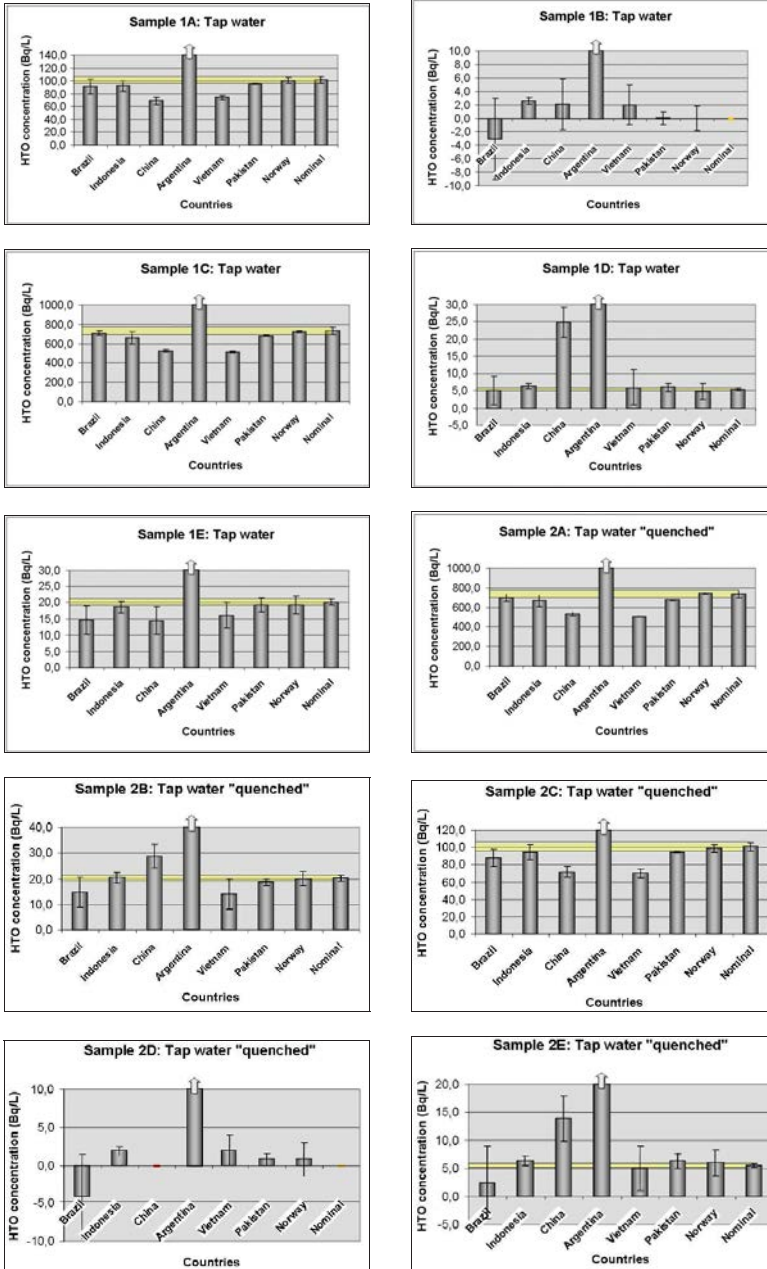
*FIG. 81. Bar plot of HTO laboratory tests for different participating countries compared with the nominal value of each sample (yellow bar). Width of bar represents uncertainty in nominal value (cont. on p. 127).*
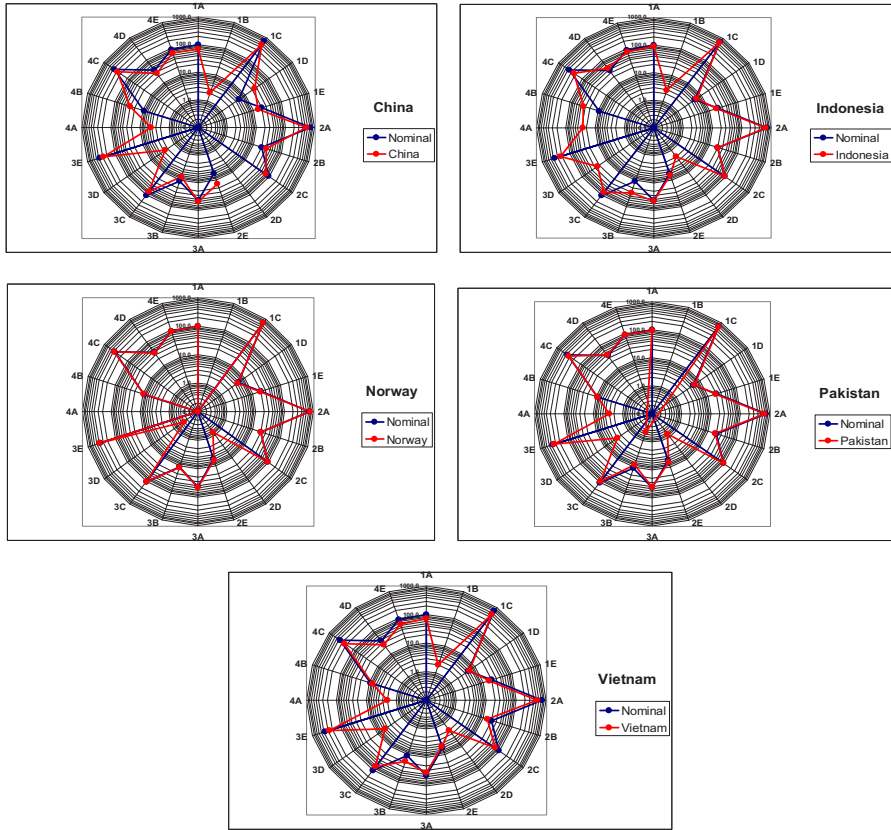
126
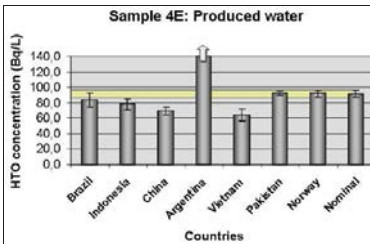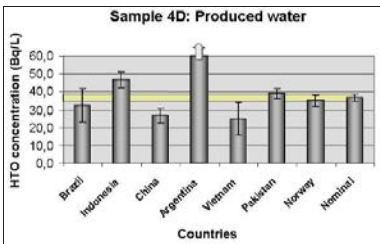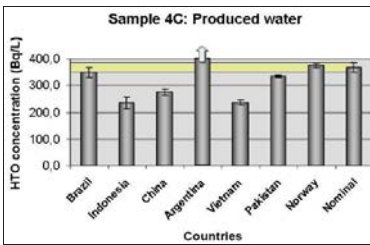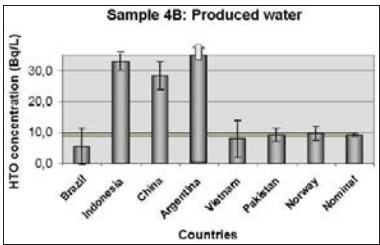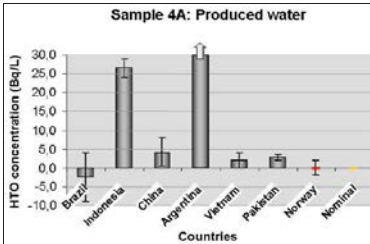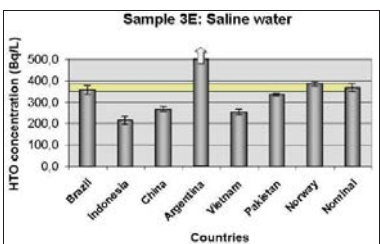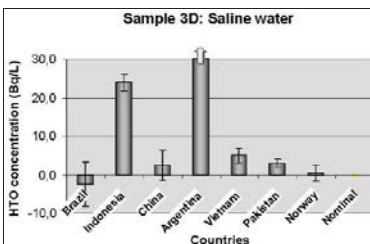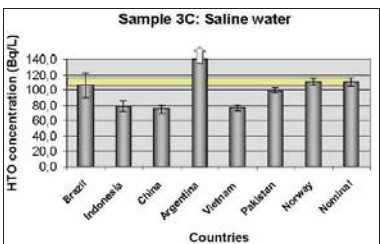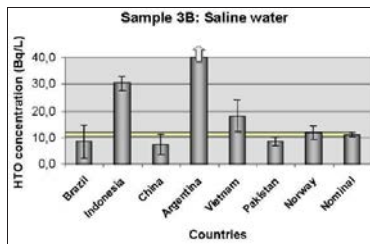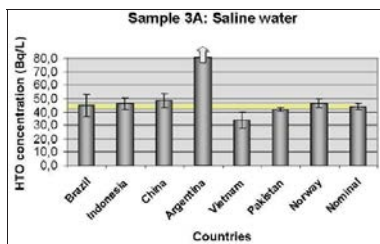
*FIG. 82. Radar plots of results for each country with the nominal values of the tracer concentration.*

A few difficulties prevail:

- The high values reported from Argentina may possibly be explained by contamination of the samples. When the samples were received in Argentina, they were erroneously stored in a room with about 80 Ci of HTO for tracer injection. Samples were stored for about 14 d before being analysed.
- For higher HTO concentrations, China and Vietnam are consistently reporting values that are too low. This problem may be due to erroneous calibration at higher concentrations. If that is the case, the problem may be rectified by making a new calibration with new certified standards.
- Indonesia, although having reported the lowest background counting rate of all the laboratories, seems to have a problem with the low content samples of brine and produced formation water.

### II.1.4.  Conclusion

The round robin test conducted has been a useful exercise. The main conclusion from the test is that all laboratories seem to handle this kind of analysis in a satisfactory manner.


## II.2.  LABORATORY INTERCOMPARISON OF ANALYSIS OF HTO AND $^{14}$C TAGGED METHANOL

### II.2.1.  Sample preparation

Samples were prepared by the Tracer Laboratory of the Centre for Applications of Nuclear Techniques in Industry (CANTI), Dalat, Vietnam, by adding various quantities of HTO and $^{14}$C-MeOH standard solutions into injection water (Table 20) to get the concentrations of HTO and $^{14}$C-MeOH in samples ranging from zero to a few hundreds of becquerels per litre and from zero to 74 Bq/L, respectively.

Samples were prepared in 10 sets. Each set contained 15 samples stored in polyethylene bottles. Seven sets were sent to seven laboratories on 28 January 2008. One set in a glass bottle was left at the Tracer Laboratory (CANTI) for analysis and the rest were stored in CANTI for further reference (preserved samples). Instructions for the analysis of HTO and $^{14}$C-MeOH in mixture in brine by distillation were prepared by CANTI and sent by email to participating laboratories on 19 February 2008.

### II.2.2.  Summary of reported results

Table 21 shows the summary of reported results.

TABLE 20.  INJECTION WATER (PROCESSED BRINE) COMPOSITIONS

| Composition | Concentration | Composition | Concentration |
|---|---|---|---|
| Salinity | 17 g/L | $Ca^{2+}$ | 209 mg/L |
| $Na^+$ | 5063 mg/L | $Cl^-$ | 9424 mg/L |
| $K^+$ | 188 mg/L | $SO_4^{2-}$ | 1150 mg/L |
| $Mg^{2+}$ | 600 mg/L | $NO_3^-$ | <1 mg/L |
| $Br^-$ | 31 mg/L | | |

TABLE 21. REPORTED RESULTS

| Country | HTO | $^{14}$C-MeOH | Applied distillation | Date of measurement |
|---|---|---|---|---|
| Argentina | Good, consistent | Undetectable | Y | 23 June 2008 |
| Brazil | Good, consistent | Detectable | Y | |
| China | High value, contamination? | Undetectable | Y | |
| France | Good, consistent | Detectable | N | 27 February 2008 |
| Indonesia | Good | Not measured | | |
| Norway | Good, consistent | Detectable | N | |
| Pakistan | Good, high error? | Undetectable | Y | |
| Vietnam | Good | Detectable | Y | 21 January 2008 |

## II.2.3. Discussion of results

### II.2.3.1. HTO

Results of HTO analysis from the laboratories are summarized in Table 22.
Figure 83 presents a summary of the results for HTO from all participants
and for each sample. The nominal value is presented as the red bar with the error
of 5% as an uncertainty of the secondary standard. The errors in results as
reported by the authors were presented in error bars as 3σ. Figure 84 compares
the results for each laboratory with the nominal values for HTO concentration in
radar plots with a logarithmic scale.

Discussion

- All HTO analytical data are acceptable in terms of consistency and are
  relatively close to the nominal values, except for the results from China,
  which show high values in comparison with the nominal ones. In general,
  the overall uncertainty of analytical results of tracer laboratories matches
  the requirement of field works as well.
- The results for HTO reported by China are generally higher than the
  nominal values. This may possibly be due to contamination of samples.
- The inconsistency of the Indonesian results on samples with low
  concentration could be due to high background from liquid scintillation
  counting or the luminescence effect.

### II.2.3.2. $^{14}$C-MeOH

The results from the analysis of $^{14}$C-MeOH are not consistent with nominal
values in most cases (Table 23). Some of the participants reported that they could
not find any $^{14}$C-MeOH in any of the samples while others reported a low
concentration of $^{14}$C-MeOH in comparison with the nominal value for some
samples. Some laboratories did not apply the enrichment process (distillation) to
measure low concentrations of $^{14}$C-MeOH while others attempted to distill
samples but still found zero or low concentrations.

The results reported from Vietnam are acceptable. Measurements were carried
out soon after receipt of the samples, on 21 January 2008. Upon receipt of various
comments from participating laboratories regarding the difficulties of measuring
$^{14}$C-MeOH in the samples, CANTI's tracer laboratory was requested to measure a
stored reference set of samples (29 June 2008). The new analysis showed the same
difficulty or problem previously observed and reported by the other laboratories.
There was close to zero activity of $^{14}$C in the stored samples (Table 24).

TABLE 22. ANALYTICAL RESULTS OF HTO FROM PARTICIPATING LABORATORIES

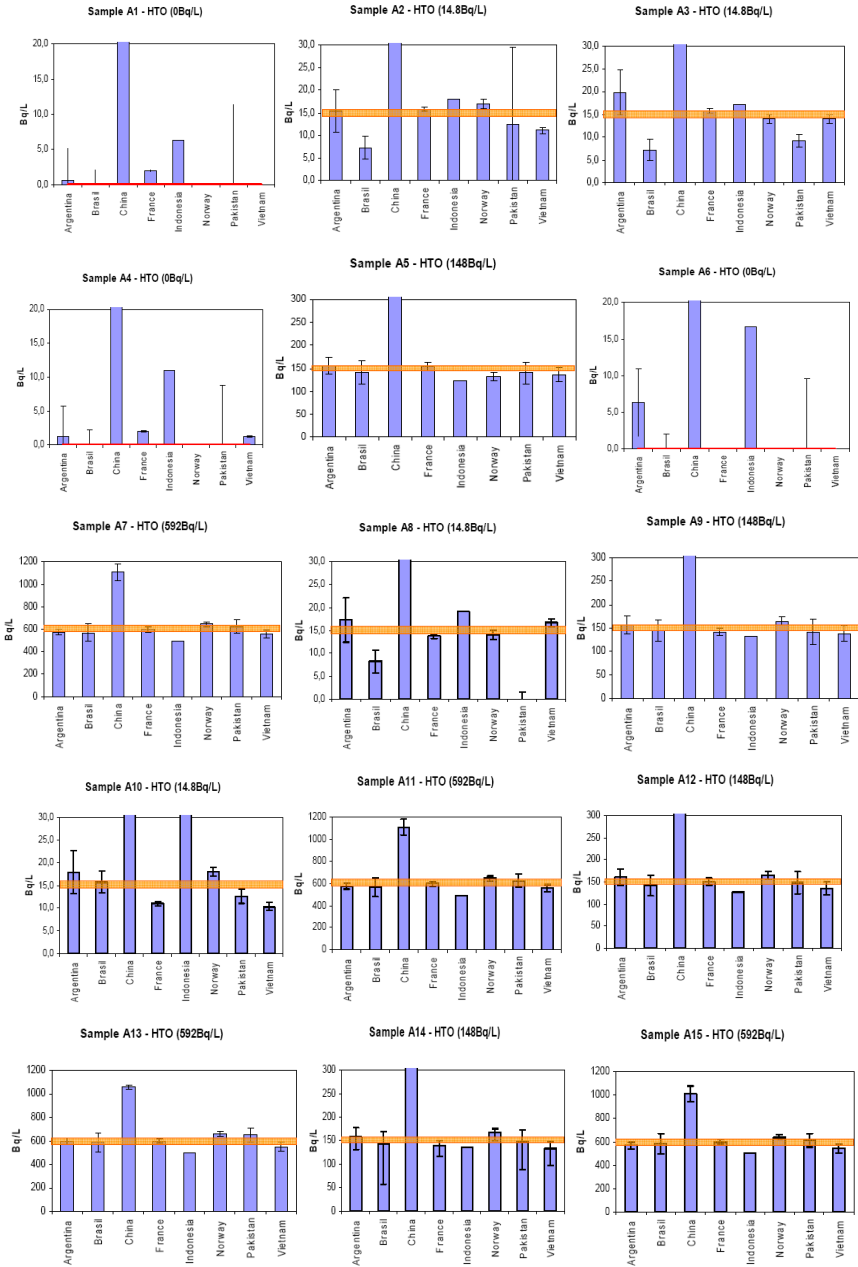| No. | Prep. conc. ±1σ (Bq/L) | Measured concentration ±1σ (Bq/L) | | | | | | | |
|---|---|---|---|---|---|---|---|---|---|
| | | Argentina | Brazil | China | France | Indonesia | Norway | Pakistan | Vietnam |
| A1 | 0.0 | 0.6±4.5 | <3±2.1 | 251±6.1 | 2.0±0.1 | 6.2 | <2 | 0±3.8 | 0.0 |
| A2 | 14.8±0.7 | 15.4±4.7 | 7.2±2.5 | 288±7.0 | 15.8±0.5 | 18.1 | 17±1.0 | 12.4±5.7 | 11.1±0.7 |
| A3 | 14.8±0.7 | 19.8±4.8 | 7.2±2.4 | 275±6.7 | 15.8±0.5 | 17.1 | 14±1.0 | 9.2±5.5 | 14.0±0.9 |
| A4 | 0.0 | 1.3±4.5 | <3±2.2 | 249±6.0 | 2.0±0.1 | 11.0 | <2 | 0.0±2.9 | 1.3±0.1 |
| 2A5 | 148±7 | 155±6.3 | 140.8±8.5 | 453±10 | 154±3.0 | 122 | 132±3.0 | 139.7±8.1 | 135±5.2 |
| A6 | 0.0 | 6.3±4.6 | <3±2.1 | 229±5.6 | <2 | 16.7 | <2 | 0.0±3.2 | 0.0 |
| A7 | 592±30 | 57±59.5 | 568±26 | 1110±26 | 597±8.0 | 490 | 649±7.0 | 622.8±18.9 | 558±12 |
| A8 | 14.8±0.7 | 17.3±4.7 | 8.2±2.6 | 276±6.7 | 13.8±0.2 | 19.2 | 14±1.0 | 0.0±3.3 | 16.8±1.1 |
| A9 | 148±7 | 157±0.3 | 145±7.5 | 428±9.7 | 142±0.3 | 131 | 165±3.0 | 142.1±8.9 | 138±5.5 |
| A10 | 14.8±0.7 | 17.9±4.7 | 15.7±2.4 | 242±6.1 | 11.0±2.0 | 32.5 | 18±1.0 | 12.6±6.1 | 10.4±0.6 |
| A11 | 592±30 | 582±9.5 | 600±28 | 998±25 | 583±8.0 | 497 | 647±7.0 | 645.1±19.9 | 551±12 |
| A12 | 148±7 | 160±6.3 | 142±8.0 | 477±11 | 150±3.0 | 126 | 165±3.0 | 148.5±8.4 | 134±4.9 |
| A13 | 592±30 | 598±9.6 | 588±28 | 1060±5.5 | 600±8.0 | 497 | 660±7.0 | 651.9±20.5 | 550±12 |
| A14 | 148±7 | 159±6.3 | 144±8.2 | 433±9.7 | 140±3.0 | 135 | 167±3.0 | 148.5±8.3 | 132±4.9 |
| A15 | 592±30 | 568.3±9.4 | 586±29 | 1010±23 | 600±8.0 | 504 | 641±6.0 | 613.1±19.7 | 543±12 |

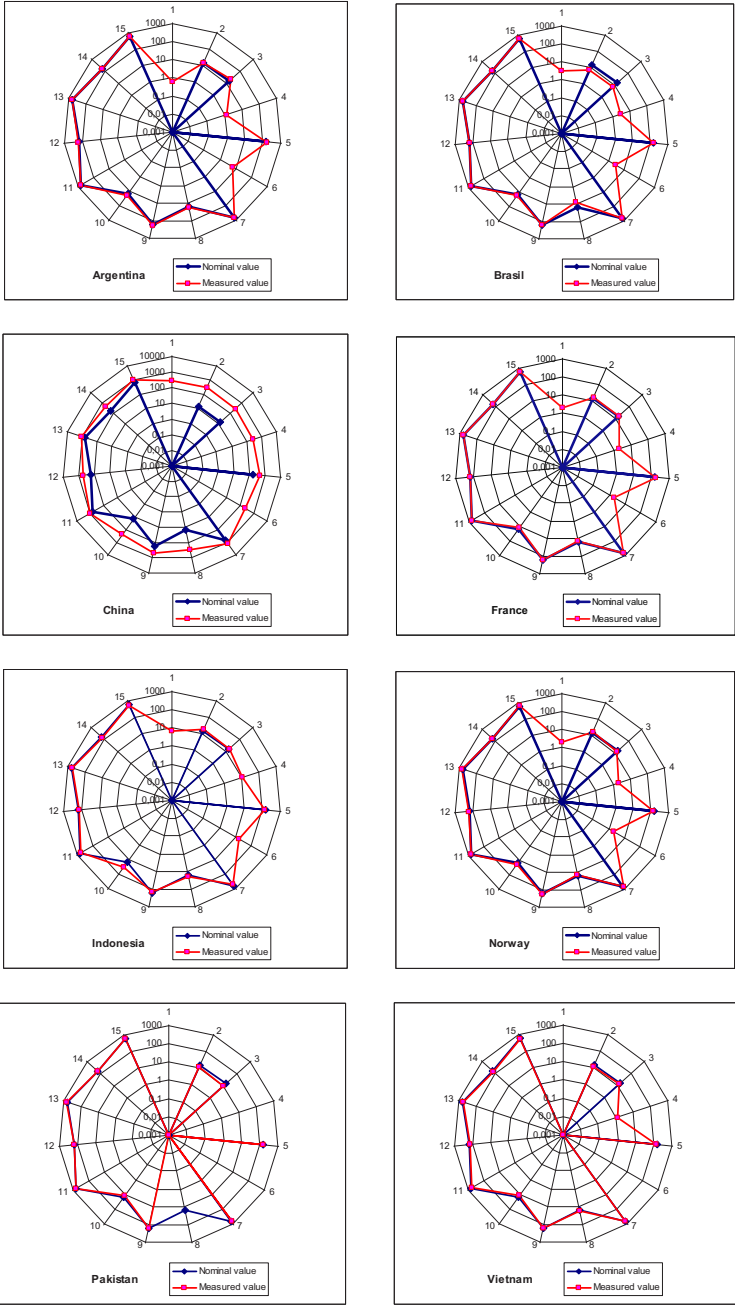FIG. 83. HTO analytical results.

133

*FIG. 84. Radar plot representation of the datasets.*

TABLE 23.  ANALYTICAL RESULTS OF ^{14}C-MEOH FROM PARTICIPATING LABORATORIES

| No. | Prepared conc. ±1σ (Bq/L) | Measured concentration ±1σ (Bq/L) | | | |
|-----|---------------------------|-------|--------|--------|---------|
|     |                           | Brazil | France | Norway | Vietnam |
| A2  | 0.74 ± 0.4                | n.d. ±1.4 | <0.005 | | 0.78 ± 0.23 |
| A3  | 0.0                       | 0.8[a] ± 1.5 | <0.005 | | 0.32 |
| A4  | 7.4 ± 0.4                 | 2.9[a] ± 1.6 | <0.005 | | 6.20 ± 0.46 |
| A5  | 0.0                       | n.d. ± 1.6 | <0.005 | | 0.21 |
| A6  | 74 ± 4                    | 6.95 ± 0.44 | 37.8 ± 0.40 | 32 ± 1.5 | 76.92 ± 4.92 |
| A7  | 0.0                       | 0.9[a] ± 1.5 | <0.005 | | 0.12 |
| A8  | 7.4 ± 0.4                 | n.d. ± 1.6 | 0.46 ± 0.01 | | 8.95 ± 0.68 |
| A9  | 0.74 ± 0.04               | n.d. ± 1.4 | <0.005 | 32 ± 1.5 | 0.94 ± 0.15 |
| A10 | 74 ± 4                    | n.d. ± 1.5 | 46.9 ± 0.50 | | 65.44 ± 5.17 |
| A11 | 0.74 ± 0.04               | 0.4[a] ± 1.5 | <0.005 | | 0.81 ± 0.13 |
| A12 | 7.4 ± 0.4                 | n.d. ± 1.4 | 0.21 ± 0.01 | | 6.08 ± 0.82 |
| A13 | 7.4 ± 0.4                 | n.d. ± 1.5 | <0.005 | | 8.26 ± 1.10 |
| A14 | 74 ± 4                    | 1.0[a] ± 1.4 | 22.75 ± 0.33 | 14.5 ± 1.2 | 71.37 ± 3.75 |
| A15 | 74 ± 4                    | 0.2[a] ± 1.4 | 18.11 ± 0.31 | 18 ± 1.2 | ± 6.85 |

[a]  Values below detection limit.

TABLE 24. ANALYTICAL RESULTS FROM TRACER LABORATORY (CANTI) FOR TWO DIFFERENT MEASUREMENTS

| No. | Prepared conc. (Bq/L) | ^{14}C-MeOH concentration (Bq/L) (Measured 21–25 January 2008 Glass bottles. Distillation procedure applied) | ^{14}C-MeOH concentration (Bq/L) (Measured 29 June to 4 July 2008 PE bottles. Distillation procedure applied) |
|-----|-----------------------|------------------------------------------------------------------------------------------------------------|-------------------------------------------------------------------------------------------------------------|
| A1  | 0.74                  | 0.94 | 0 |
| A2  | 0.74                  | 0.68 | 0 |
| A3  | 0                     | 0    | 0 |

TABLE 24. ANALYTICAL RESULTS FROM TRACER LABORATORY (CANTI) FOR TWO DIFFERENT MEASUREMENTS (cont.)

| No. | Prepared conc. (Bq/L) | $^{14}$C-MeOH concentration (Bq/L) (Measured 21–25 January 2008 Glass bottles. Distillation procedure applied) | $^{14}$C-MeOH concentration (Bq/L) (Measured 29 June to 4 July 2008 PE bottles. Distillation procedure applied) |
|---|---|---|---|
| A4 | 7.4 | 6.20 | 0 |
| A5 | 0 | 0 | 0 |
| A6 | 74.0 | 76.92 | 0.92 |
| A7 | 0 | 0 | 0 |
| A8 | 7.4 | 8.95 | 0 |
| A9 | 0.74 | 1.08 | 0 |
| A10 | 74 | 65.44 | 0.2 |
| A11 | 0.74 | 0.81 | 0 |
| A12 | 7.4 | 6.08 | 0 |
| A13 | 7.4 | 8.26 | 0 |
| A14 | 74.0 | 53.52 | 0.77 |
| A15 | 74.0 | 91.39 | 0.51 |

However, the standard solution prepared for making samples that was stored in glass ampoules were also tested and it gave results consistent with the nominal values determined before. It seems that methanol had escaped by diffusion through the polyethylene bottle.

The standard solutions of HTO and $^{14}$C-MeOH were supplied from American Radiolabelled Chemicals (ARC), United States of America (Table 25). Samples were prepared by CANTI by adding various quantities of HTO and $^{14}$C-MeOH standard solutions into injection water (processed brine) to obtain the requisite concentrations of HTO and $^{14}$C-MeOH in samples in the range from zero to a few hundreds of becquerels per litre and from zero to 74 Bq/L, respectively.

TABLE 25.  ORIGINAL STANDARD SOLUTIONS OF HTO AND $^{14}$C-MEOH

| Original standard | Supplier | Model/lot number | Solvent | Concentration (Bq/mL) | Calibration date |
|---|---|---|---|---|---|
| HTO | ARC | ART 0194A /Lot: 070427 | Water | 3.7E7 ± 1% | 13 August 2007 |
| $^{14}$C-MeOH | ARC | ART 0194A /Lot: 070305 | MeOH | 3.7E6 ± 1% | 19 February 2007 |

## II.3.  LABORATORY INTERCOMPARISON OF PRODUCTION CURVES WITH THE ANDURIL SOFTWARE PROGRAM

### II.3.1.  Introduction

Interwell passive tracer testing is a powerful tool for the evaluation of secondary recovery projects in oilfield reservoirs. In these projects, water injected into injector wells push the oil to the producer wells from which it is extracted. The water injected patterns are usually very complicated because of the natural heterogeneity of the reservoirs and the mobility differences between water and oil. Channelling of water between injector and producer wells is a very common problem that conspires against achieving acceptable sweep efficiencies. The interwell tracer tests permit this problem to be detected and also to allow some reservoir parameters to be determined.

Owing to the elevated uncertainty associated with the reservoir knowledge, especially later to the waterflooding, there is no need, in an initial phase of interpretation, to assume a very detailed model. Therefore, a simple moment analysis or an analytical solution from a one dimensional model can provide acceptable results about the average residence times and water volumes in many cases.

### II.3.2.  Objectives

In consequence, employment of the Anduril 2.3 simulator was proposed for estimating the principal parameters from data recorded from an interwell tracer test performed in an oilfield in Argentina. The Anduril 2.3 program has capabilities for both temporal and volumetric analyses. In this instance, it was used to determine the following parameters between different pairs of wells:

- Breakthrough time;
- Mean residence time;
- Peak maximum time;
- Final time;
- Tracer recovery.

From the above mentioned parameters, the following volumetric parameters can be obtained:

- Breakthrough volume;
- Mean swept volume;
- Injected volume at peak;
- Maximum injected volume;
- Pore volume swept between wells.

These parameters are proportional to the ones in the first list (water flow rate is the proportionality factor).

### II.3.3.  Results for wells K-301, K-329, K-300, K-166 and K-24

A laboratory intercomparison test was performed where the same set of data was provided by Argentina to coordinated research projects participants. Results from using the Anduril 2.3 software on these data are displayed in Figs 85–89.

### II.3.4.  Discussion

The values of the obtained parameters were very similar for all the users of the Anduril software.

However, a problem was detected in relation to the computation of the 'final time'. The strong differences in the calculated cumulative tracer recovery of well K-301 indicated that an appropriate final time must be chosen.

It is opportune to highlight that an elemental moment analysis may be used to calculate temporal and volumetric moments. The use of analytical solutions allows the number of producing layers (by a deconvolution process) to be identified and, thereby, the moments (and the associate parameters) for each layer to be calculated.
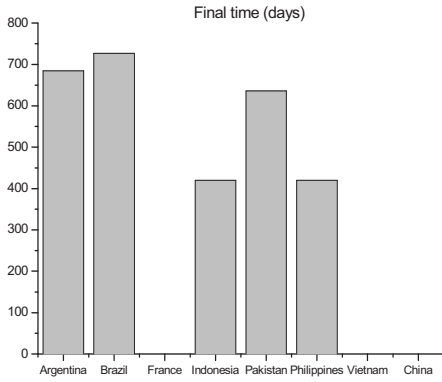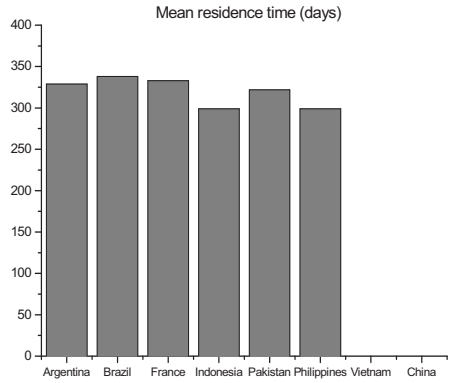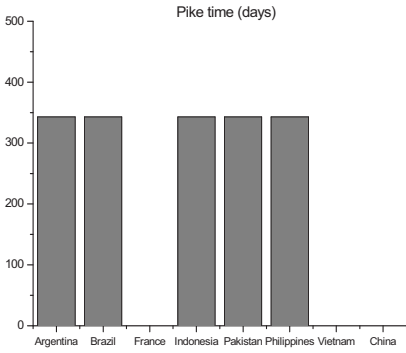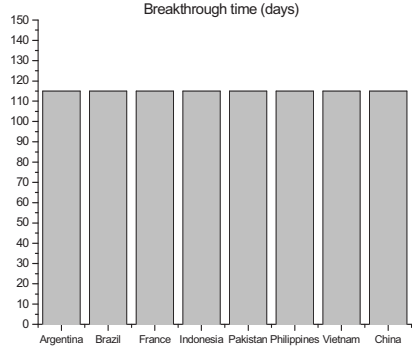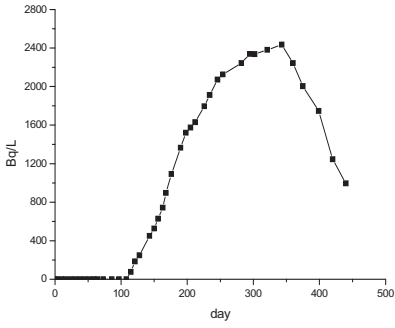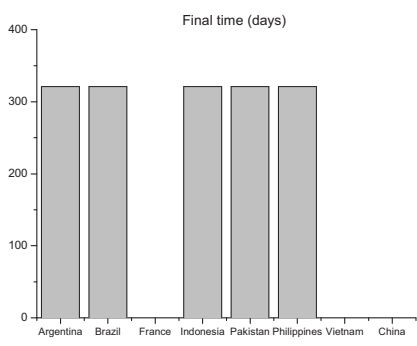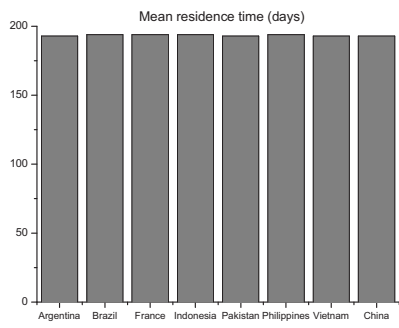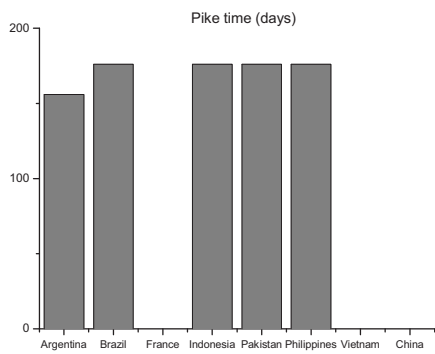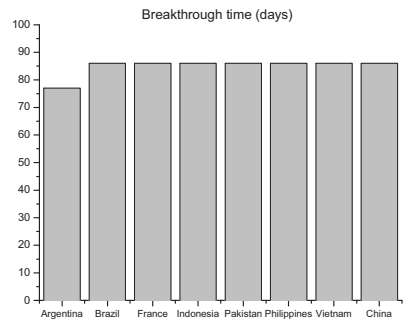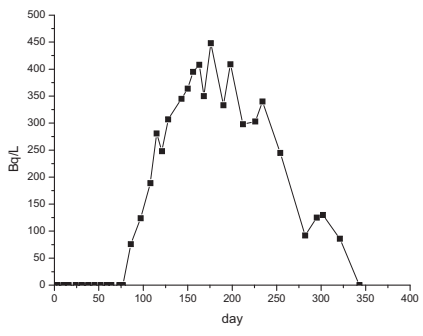
*FIG. 85. Anduril 2.3 analysis of well K-301.*
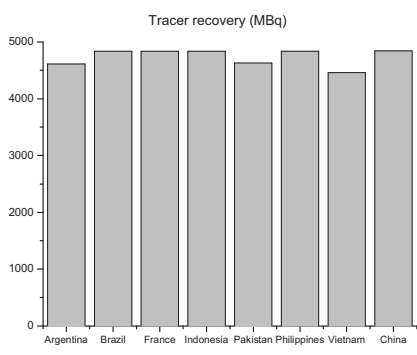
FIG. 86.  Anduril 2.3 analysis of well K-329.

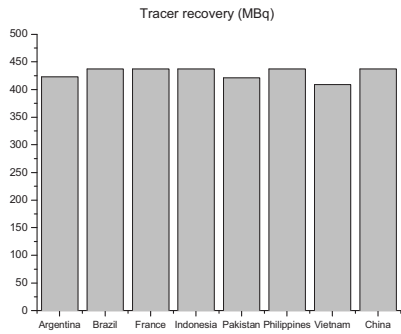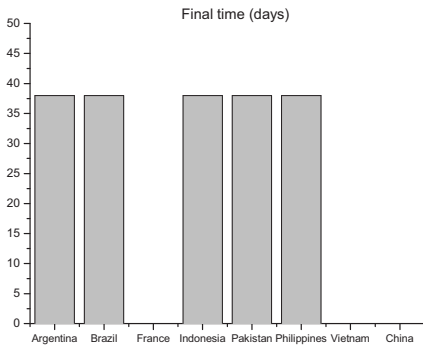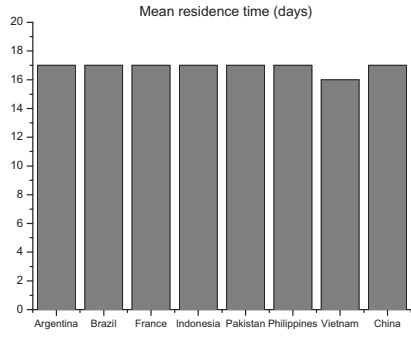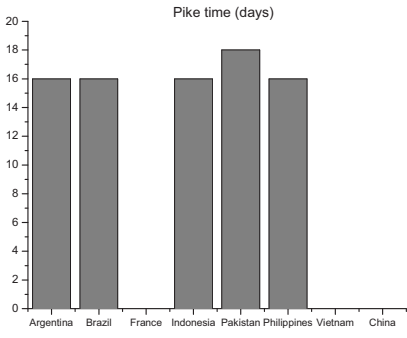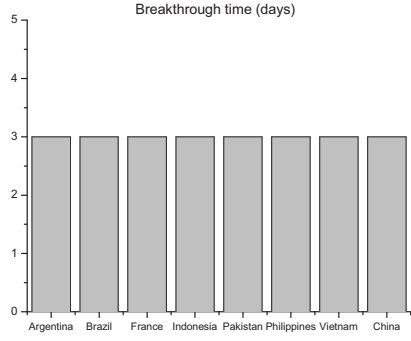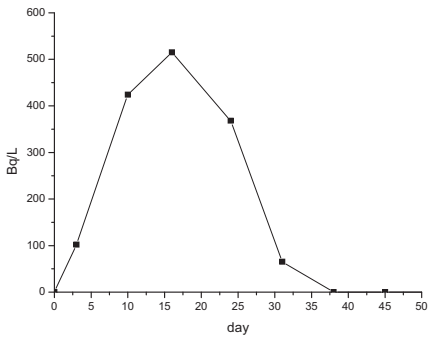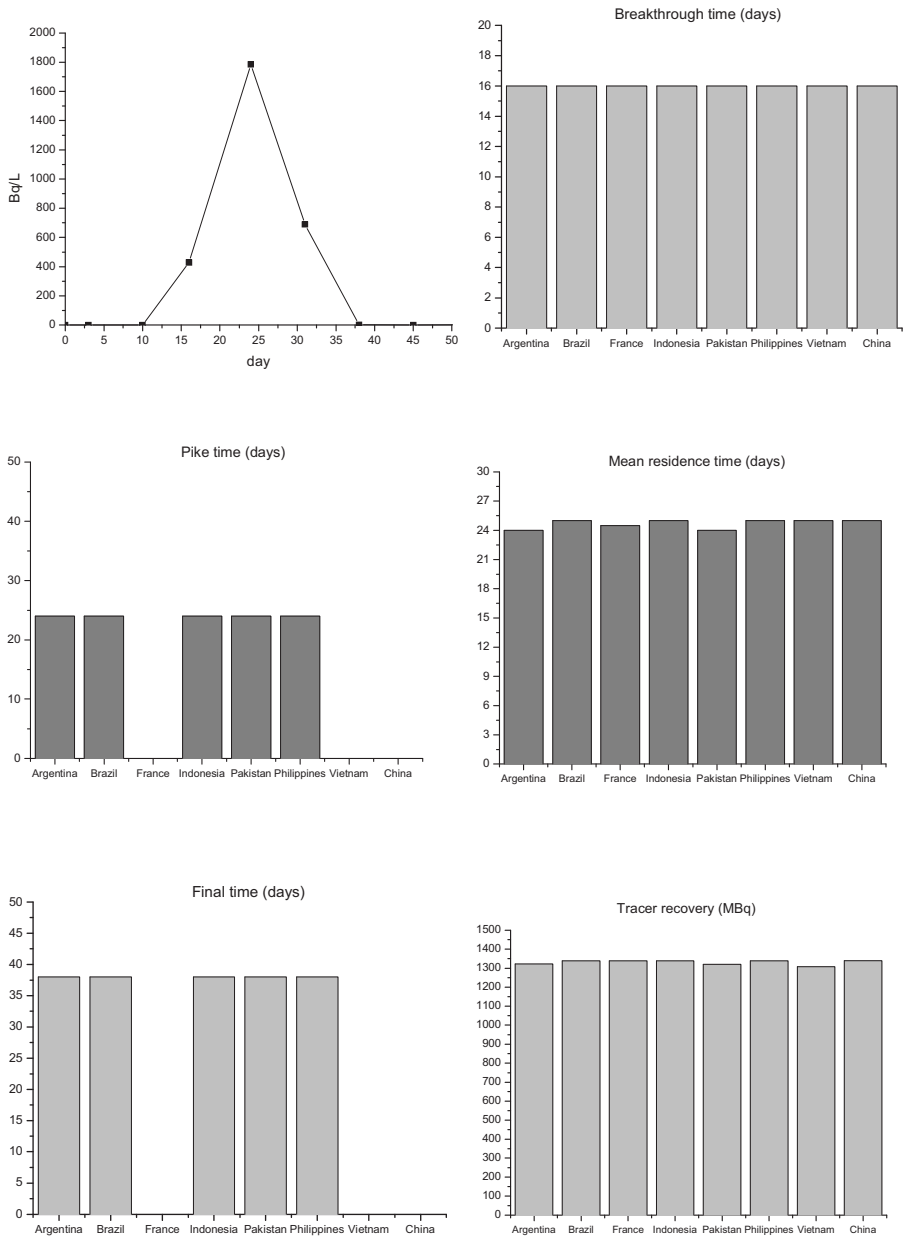FIG. 87. Anduril 2.3 analysis of well K-300.

*FIG. 88. Anduril 2.3 analysis of well K-166.*
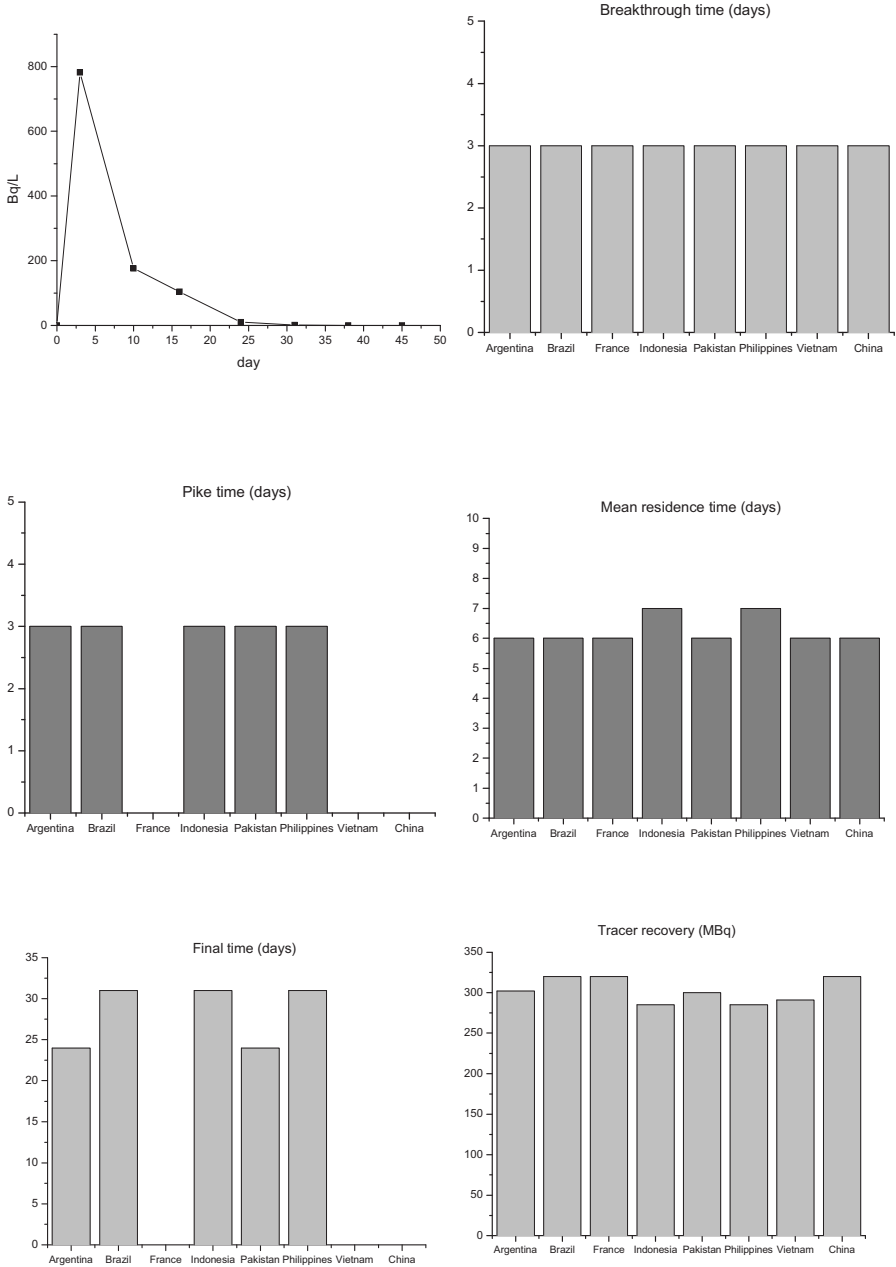
FIG. 89. Anduril 2.3 analysis of well K-24.

143

However, it should be noted that the analytical solutions from one dimensional models are less dispersive than the reality (which is two or three dimensional). Also, the one dimensional models cannot consider the 'areal extension' of the tracer flow (identical to the water flow). Consequently, very important parameters such as layer thickness and layer permeability cannot be calculated.

**Appendix III**

**PROCEDURES FOR PREPARATION AND
ANALYSIS OF RADIOTRACERS**


III.1.  PREPARATION FOR RADIATION SAFETY OF RADIOTRACER
 TESTS

### III.1.1.  Introduction and general comments

Tracer techniques have wide application in petroleum exploration and production. For several decades, well-to-well tests have been used to study the movement of injected fluids through reservoirs. When properly carried out, such investigations can render information on the reservoir structure and fluid flow behaviour that could not have been obtained by other means. HTO is regarded as the standard reference tracer for water. With regard to safety, HTO is the most favourable radioactive water tracer generally available. However, there are other applicable radiolabelled water tracers, some of which are labelled with pure beta emitters such as $^{14}$C and $^{35}$S and some with both beta and gamma emitters such as $^{58}$Co, $^{60}$Co and $^{131}$I, while others emit only gamma radiation (electron capture decay) such as $^{57}$Co and $^{125}$I.

This appendix attempts to cover both the more general parts of the safety consideration as well as aspects that are nuclide specific for the individual radionuclide. In order to avoid an overly complicated treatment, tritium is considered to represent the beta radiolabels and $^{60}$Co to represent the gamma emitting radiolabels.

Radioactive tracer injection can be carried out in a safe manner with little impact on the environment. A typical safety report has to be prepared for the approval of the radiation protection authority and for the acceptance of end user management. The report contains:

- The design of the tracer experiment (calculation of tracer quantities, description of practical procedures for tracer preparation, transport and injection, sampling procedures, etc.);
- The description of safety precautions during handling and treatment of HTO during the whole operation.

To perform tracer injection in a safe manner, the injection equipment should have a sound design and meet pressure and temperature requirements. It should be properly tested before injection and operated by well-trained personnel. If

these requirements are satisfied, an injection of radioactive and non-radioactive tracers can be carried out with very little risk.

Experience has shown that typically 370–3700 GBq (10–100 Ci) of HTO is injected into an injection well for interwell investigation in oilfields. A typical quantity for a $^{14}C$ or $^{35}S$ labelled tracer is 3.7–37 GBq (0.1–1 Ci) and the same for a gamma emitting tracer. A common design for an injection device for beta emitting tracers is presented in Fig. 7. This equipment can be operated in a bypass mode to the main injection line or by application of a high pressure pump. The pneumatically operated Maximator pump, which can be seen in Fig. 12, can deliver up to 10 L/min at a working pressure of 200 bar; lower at higher pressures. The pump is normally run at a rate of 5 L/min. The available pneumatic pressure for operation of the pump should be at 7–10 bar.

### III.1.2. Radiation safety considerations

Injection of a radioactive tracer into a hydrocarbon reservoir at high pressure entails handling of materials with properties that are unfamiliar to most laypersons. As radioactive material in quantities used for injections is potentially dangerous, it is important that it be treated properly. In an injection project, safety considerations should have already been taken into account when the tracer is selected and the quantities fixed. During transport and storage at the well head site, the safety aspect should be borne in mind and safety precautions should be taken according to international rules and regulations.

*III.1.2.1. Quantity of radioactivity*

A quantity of radioactive material is characterized by the number of nuclear disintegrations or transformations that occur within a specified time interval. The parameter is termed the disintegration rate, $D$, and the unit for this quantity is the becquerel (Bq), which is equal to one nuclear transformation per second. Another unit that is still in use is the Curie, equal to $3.7 \times 10^{10}$ disintegrations per second (dps). Following on, the:

- Activity concentration, $A_c$, has the dimension dps per unit mass (or unit volume) of a sample (i.e. Bq/g or Bq/mL).
- Specific activity, $A_s$, has the dimension of dps per unit mass of the inactive counterpart of the tracer atom or molecule. For HTO, the dimension is Bq/g $H_2O$ or Bq/mL $H_2O$.

For HTO in pure water, $A_c = A_s$. For HTO in aqueous mixtures with other water soluble components, $A_c \neq A_s$.

*III.1.2.2. Radiation doses*

When ionizing radiation from a radioactive material passes through a mass of some other material, the radiation will interact with the atoms of the material in different ways. The net result is that energy will be absorbed in the material. The quantity of energy that is absorbed per unit mass is termed the absorbed dose and is measured in gray (Gy), whereby 1 Gy = 1 joule/kg. The old unit RAD is still in use, whereby 1 RAD = 0.01 Gy.

The biological effect of the radiation does not depend solely on the absorbed dose, but also on the quality factor of the radiation. For small dose rates of beta and gamma radiations, this quality factor is set to 1 (for alpha particles, neutrons, etc., the quality factor is >1). The absorbed dose multiplied by the quality factor renders the equivalent dose, which is measured in sievert (Sv). The old unit REM is still in some use: 1 REM = 0.01 Sv.

Humans are continuously receiving radiation doses from ambient (natural and artificial) sources. For most people these doses are in the range 3–5 mSv per year. Approximately 60–70% of this dose is caused by inhalation of radon ($^{222}$Rn) from materials in the surroundings which contain uranium (decay of $^{238}$U). For comparison, 5 mSv corresponds to the dose that a person receives from the intake of 300 MBq of HTO. For members of the public, the International Commission on Radiation Protection has recommended the use of 1 mSv/y, averaged over 5 years, as a limit for radiation doses caused by application of radioactive material or other types of ionizing radiation.

A material emitting ionizing radiation will create an absorbed dose rate that is usually measured in Gy/h. The corresponding equivalent dose rate is measured in Sv/h or the smaller units μSv/h, or mSv/h.

Injection of a radioactive tracer into a hydrocarbon reservoir at high pressure entails handling of materials with properties that are unfamiliar to most people. As radioactive materials in quantities used for injections are potentially dangerous, it is important that they are treated properly. In an injection project, safety consideration should already have been taken into account when the tracer is selected and the quantities fixed. During transport and storage at the well head site, the safety aspect should be borne in mind and safety precautions should be taken according to international rules and regulations.

*III.1.2.3. The 'as low as reasonably achievable' (ALARA) principle*

Use of radioactive material has to be approved by a competent authority in the country concerned. One of the main principles governing the utilization of radioactive material is that it shall not pose danger to persons, neither those working with the materials nor the general public. In addition, the radiation doses

to which workers and the public are exposed should be within the limits set by laws and regulations.

Another principle is that use of radioactive material will be accepted only when the benefit is considerable, after having taken economic as well as health and environmental aspects into consideration.

A third principle is that when using radioactive material every effort should be made to keep the quantity of radioactivity to be used and the resulting radiation doses ALARA.

*III.1.2.4. Dangerous quantities of radioactivity*

In March 2002, the IAEA's Board of Governors approved a Safety Requirements publication entitled Preparedness and Response for a Nuclear or Radiological Emergency [22]. This publication established the requirements for achieving an adequate level of preparedness and response for a nuclear or radiological emergency in any Member State. Amongst other things, the publication specifies requirements for emergencies involving a dangerous source. The Requirements define a dangerous source as one "*that could, if not under control, give rise to exposure sufficient to cause severe deterministic effects*". The Requirements then go on to define a severe deterministic effect as one that "*is fatal or life threatening or results in a permanent injury that decreases the quality of life*".

The operational definition of a dangerous source is known as the D value. The D value is that quantity of radioactive material, which, if uncontrolled, could result in the death of an exposed individual or a permanent injury that decreases that person's quality of life.

For the purposes of determining D values, the exposure scenarios that were used fall into two groups: one for material that has not been dispersed and one for material that has been dispersed.

Different numerical values are provided for each of these groups:

- The $D_1$ value is the activity of a radionuclide in a source that, if uncontrolled but not dispersed (i.e. it remains encapsulated), might result in an emergency that could reasonably be expected to cause severe deterministic health effects.
- The $D_2$ value is the activity of a radionuclide in a source that if uncontrolled and dispersed might result in an emergency that could reasonably be expected to cause severe deterministic health effects.
- The D value is the lowest value of the $D_1$ and $D_2$ values for a radionuclide.

For pure beta emitters $D_1$ values do not apply in this actual radiotracer application. For gamma tracers, both $D_1$ and $D_2$ values apply. The quantities (activity) of radionuclides typically used in interwell tracer examinations are evaluated against their recommended D values.

### III.1.2.5. Shielding of gamma radiation

Doses to humans during handling and injection of gamma emitting radiotracers may be reduced by passive shielding, e.g. lead. A narrow beam of monoenergetic photons with an incident intensity $I_0$, penetrating a layer of material with mass thickness $d$ and density $\rho$, emerges with intensity $I$ given by the exponential attenuation law

$$\frac{I}{I_0} = \exp(-\mu_{\mathrm{m}} d) \tag{28}$$

where $\mu_{\mathrm{m}} = \mu/\rho$ is the mass attenuation coefficient (cm$^2$/g), $\mu$ is the linear attenuation coefficient (cm$^{-1}$) and $\rho$ the material density (g/cm$^3$). The mass thickness $d = x\rho$ (g/cm$^2$) where $x$ is the distance or the linear thickness in the material (cm). Introducing the term $d = x\rho$ into Eq. (28) and solving for $x$ gives:

$$x = \frac{\ln(I/I_0)}{\mu_{\mathrm{m}}\rho} = \frac{\ln(I/I_0)}{\mu} \tag{29}$$

Mass attenuation coefficients for lead ($\rho = 11.35$ g/cm$^3$) [23] have been reconstructed from the plot given for lead and used to calculate the linear attenuation coefficients for the main gamma energies of the various radionuclides used as radiolabels and treated below.

### III.1.2.6. Characteristics of the various radiotracers and the D values of their radiolabels

(a)   Tritium label

HTO is water in which one of the atoms of the ordinary hydrogen isotope $^1$H is replaced by an atom of another hydrogen isotope $^3$H, also known as tritium. This hydrogen isotope is radioactive with a half-life of 12.32 y.

Tritium disintegrates through a process where beta particles with energies up to 18 keV are emitted. Owing to its low energy, the penetrative power of beta

radiation from tritium is low: a sheet of paper can stop the particles. Thus, there will, in practice, be no radiation from a tritium tracer outside its containments, e.g. bottles, tubes and pipelines. Tritium does not emit gamma radiation. However, during the use of HTO as a water tracer, the injection process is often monitored by adding a modest quantity (10–100 kBq) of $^{131}I^-$ to the primary tracer mixture (i.e. a tracer in the tracer) in order to facilitate the monitoring of the injection process itself.

 The only way of receiving a radiation dose from tritium is by intake, i.e. through mouth or by inhalation. As the tracer is kept in a closed system during the injection process, there is, generally, no possibility of HTO intake under normal conditions.

Tritium is common in the environment. It is produced continuously in the atmosphere from cosmic ray interaction with atmospheric molecules. Tritium is also generated in nuclear power production and in nuclear bomb tests. The global inventory of tritium is in the order of $5 \times 10^{10}$ GBq. Approximately 99% of the tritium inventory is in the form of HTO. The concentration of $^3H$ in sea water off the coast of northern Europe is in the order of 1 kBq/m$^3$. The water volume of the North Sea is approximately $5 \times 10^{13}$ m$^3$, and the inventory of tritium in this sea volume is, therefore, in the order of $5 \times 10^7$ GBq.

For tritium labelled radiotracers, the $D_2$ value applies. Table 1 [24] gives $D_2(^3H) = 2 \times 10^3$ TBq, which is about 500 times higher than the upper estimate of applied quantities of HTO per injection in oil reservoirs. For tritiated methanol, $CH_2TOH$, which is also a useful water tracer under certain conditions, the normally injected quantities are a factor of 10 lower than for HTO. Accordingly, it may be concluded that the tritium activities described here do not approach being defined as dangerous quantities.

(b)   $^{14}C$ and $^{35}S$ labels

Typical water tracers labelled with $^{14}C$ is thiocyanate, $S^{14}CN^-$, and cobalthexacyanoferrate, $Co[(CN)_5{}^{14}CN]^{3-}$, while a typical water tracer with the $^{35}S$ label is $^{35}SCN^-$. In water solutions, these are all anions and not volatile.

Carbon-14 is produced naturally in the upper atmosphere by the reaction of neutrons originating from cosmic rays with nitrogen and, to a lesser extent, with oxygen and carbon. The natural steady state inventory of $^{14}C$ in the biosphere is about $10^{19}$ Bq, or 10 EBq (about 300 million Ci), most of which is in the oceans. Large quantities of $^{14}C$ have also been released to the atmosphere as a result of nuclear weapon testing. Weapon testing through 1963 added about $3.5 \times 10^{17}$ Bq, or 350 PBq (about 9.6 million Ci), an increase of 3% above natural steady state levels. Carbon-14 is also made commercially for use in medical, biological or technical tracer research described in this publication.

Carbon-14 is produced in nuclear reactors by the capture of neutrons by nitrogen, carbon, or oxygen present as components of the fuel, moderator, or structural hardware.

Carbon-14 is a pure beta emitter with a half-life of 5730 y and a maximum energy of $E_{\beta max}$ = 156.4 keV. The range of these beta particles in air (20°C) is 22 cm and in stainless steel or Monel <50 µm. Hence, the beta particles do not penetrate the walls of the combined transport and injection container.

The only way of receiving a radiation dose from the $^{14}$C labelled molecules described above during the injection phase is by intake (e.g. through mouth) or by liquid spillage on the skin. As the tracer during the injection process is kept in a closed system, there is, generally, no possibility of tracer intake or human skin contamination under normal conditions.

For $^{14}$C on this basis the $D_2$ value applies. This value is $D_2(^{14}C) = 50$ TBq ($1.35 \times 10^3$ Ci) as compared with the actual injection quantities of 3.7–37 GBq (0.1–1.0 Ci) which is more than a factor of a 1000 lower. Hence, it may be concluded that the $^{14}$C activities described do not approach levels defined as dangerous.

For $^{35}$S labelled SCN$^-$, the same evaluation and conclusion as for $^{14}$C is valid. Also, $^{35}$S is a pure beta emitter with a half-life of 87.4 d and with a maximum beta energy of $E_{\beta max}$ = 167 keV, close to that of $^{14}$C.

The $D_2$ value is also similar, $D_2(^{35}S) = 60$ TBq ($1.62 \times 10^3$ Ci) as compared with the actual injection quantities of 3.7–37 GBq (0.1–1 Ci), which gives the same conclusion as for $^{14}$C above.

(c)    Gamma emitting labels

Each of the labels $^{57}$Co, $^{58}$Co, $^{60}$Co, $^{125}$I and $^{131}$I will be treated separately.

Cobalt-57 is produced in charged particle reactions at accelerator facilities (for instance by the reactions $^{55}$Mn($\alpha$,2n), $^{56}$Fe(d,n) or $^{59}$Co(p,3n) plus beta decay) and there is no sizable production (or natural inventory) in either the biosphere or geosphere. It decays by 100% electron capture with a half-life of 271.74 d. The main gamma energies are low, the four strongest being 14.4 keV (9.16%), 122.1 keV (85.60%), 136.5 keV (10.68%) and 692.4 keV (0.15%).

Being a gamma emitter, special precautions have to be taken during injection operations. It is possible to apply the injection apparatus shown in Fig. 7 with some extra shielding on the injection container and eventually also on the injection tubing (see below). Alternatively, a method such as the one illustrated in Fig.10 is applicable.

Radiation dose may be received directly from the tracer container (external radiation) by spillage on skin and clothes and by oral intake of radioactive liquids. Given that the tracer during the injection process is kept in a closed system, there

is, generally, no possibility, of oral intake of the tracer or of skin and clothing contamination under normal conditions.

The $D_1$ and $D_2$ values are different in this case. The proposed values are $D_1(^{57}Co) = 7 \times 10^{-1}$ TBq (about 20 Ci) and $D_2(^{57}Co) = 4 \times 10^2$ TBq (about $1.1 \times 10^3$ Ci), respectively [24]. Considering that a typical injection quantity is 3.7–37 GBq (0.1–1.0 Ci), which is only a factor 20–200 lower than the given $D_1$ value, measures should be taken to reduce the dose rate from the injection solution during handling and injection. Radiation dose can most effectively be minimized by passive shielding of the injection container, for instance, by lead. The linear attenuation coefficient for the most intense gamma ray at 122.1 keV in lead is calculated to be $\mu_{122keV}(Pb) = 36.3$ cm$^{-1}$. The half-thickness and the thicknesses needed to reduce the radiation intensity by factors of 100 and 1000, respectively, are $x_{0.5} = 1.9 \times 10^{-3}$ cm, $x_{100} = 0.127$ cm and $x_{1000} = 0.190$ cm.

For a dispersed source, however, where the $D_2$ value applies, the injection quantity is a factor of more than 1000 lower.

Cobalt-58 is produced in charged particle reactions at accelerator facilities (for instance by the reactions $^{55}Mn(\alpha,n)$ or $^{57}Fe(d,n)$ or by fast (14 MeV) neutron reactions (for instance $^{59}Co(n,2n)$ or $^{58}Ni(n,p)$)) and there is no sizeable production (or natural inventory) in either the biosphere or geosphere. It decays by 85% electron capture and 15% positron emission and has a half-life of 70.86 d. The main photon energies are 511 keV annihilation radiation (29.8%) and 810.76 keV (99.45%).

Being a gamma emitter with intermediate energies, the same general comments as given for $^{57}Co$ above apply also for $^{58}Co$. Owing to somewhat different decay characteristics and higher gamma energies, the D values are lower at $D_1 = 7 \times 10^{-2}$ TBq (about 2 Ci) and $D_2 = 7 \times 10^1$ TBq (about 2000 Ci), respectively.

Since a typical injection quantity is 3.7–37 GBq (0.1–1.0 Ci), which is only a factor 2–20 lower than the given $D_1$ value, measures must also be taken to reduce the dose rate from the injection solution during handling and injection. For lead shielding, the linear attenuation coefficient for the most intense gamma ray at 810.76 keV is calculated to be $\mu_{810keV}(Pb) = 0.94$ cm$^{-1}$. The half-thickness and the thicknesses needed to reduce the radiation intensity by factors of 100 and 1000, respectively, are $x_{0.5} = 0.74$ cm, $x_{100} = 4.9$ cm and $x_{1000} = 7.3$ cm.

For a dispersed source, however, where the $D_2$ value applies, the injection quantity is a factor of more than 1000 lower.

Cobalt-60 is produced in thermal neutron reactions in a nuclear reactor ($^{59}Co(n_{th},\gamma)$) or by fast (14 MeV) neutron reactions (e.g. $^{60}Ni(n,p)$ or $^{63}Cu(n,\alpha)$) and there is no sizable production (or natural inventory) in either the biosphere or geosphere. It decays by 100% beta emission and has a half-life of 5.27 y. The main gamma energies are 1173.2 keV (99.85%) and 1332.4 keV (99.98%).

Being a strong and relatively high energy gamma emitter, the same general comments as given for $^{57}$Co and $^{58}$Co above also apply for $^{60}$Co. The decay characteristics are different from the two gamma emitters described above and the D values are even lower than for $^{58}$Co: $D_1 = 3 \times 10^{-2}$ TBq (about 0.8 Ci) and $D_2 = 3 \times 10^1$ TBq (about 800 Ci), respectively. Since a typical injection quantity is 3.7–37 GBq (0.1–1.0 Ci), which is in about the same region as the given $D_1$ value, measures must also be taken to reduce the dose rate from the injection solution during handling and injection. For lead shielding, the linear attenuation coefficient for the most intense gamma ray at 1332.4 keV is calculated to be $\mu_{1332\text{keV}}(\text{Pb}) = 0.72$ cm$^{-1}$. The half-thickness and the thicknesses needed to reduce the radiation intensity by factors of 100 and 1000, respectively, are $x_{0.5} = 0.97$ cm, $x_{100} = 6.5$ cm and $x_{1000} = 9.7$ cm.

For a dispersed source, however, where the $D_2$ value applies, the injection quantity is a factor of about 800 lower.

Iodine-125 is produced in charged particle reactions at accelerator facilities (for instance by the reactions $^{123}$Sb($\alpha$,2n), $^{126}$Te(p,2n) or $^{127}$I(p,3n plus beta decay) or by thermal neutron reactions in a nuclear reactor ($^{124}$Xe(n$_{\text{th}}$,$\gamma$) plus beta decay) and there is no sizeable production (or natural inventory) in either the biosphere or geosphere. It decays by 100% electron capture and has a half-life of 59.4 d and the main photon energies are the tellurium X rays K$_{\alpha2}$ = 27.2 keV (40.1 %), K$_{\alpha1}$ = 27.4 keV (74.0%), K$_{\beta3}$ = 30.9 keV (6.83%) and K$_{\beta1}$ = 31.0 keV (13.2%) and the gamma ray at 35.5 keV (6.68%).

Owing to the low photon energies, external radiation from a source of $^{125}$I is relatively low and it is easily shielded. The D value for a closed source is $D_1 = 10$ TBq (270 Ci). However, because of the biological effect of iodine (for instance accumulation of I$^-$ in the thyroid gland), the $D_2$ value is much lower than for the radionuclides previously discussed: $D_2 = 0.2$ TBq (5.4 Ci).

The external radiation dose is easily shielded by a modest amount of shielding material. For lead shielding, the linear attenuation coefficient for the most intense gamma ray at around 30 keV is calculated to be $\mu_{30\text{keV}}(\text{Pb}) = 204$ cm$^{-1}$. The half-thickness and the thicknesses needed to reduce the radiation intensity by factors of 100 and 1000, respectively, are $x_{0.5} = 3.4 \times 10^{-3}$ cm, $x_{100} = 2.3 \times 10^{-2}$ cm and $x_{1000} = 3.4 \times 10^{-2}$ cm. Dose may also be received by spillage on skin and clothes and by oral intake of radioactive liquids or inhalation of iodine in elemental (I$_2$) form (I$^-$ may be easily oxidized in the environment). Therefore, it is especially important to ensure no liquid leakage occurs during the handling and injection processes.

Iodine-131 is mainly produced by thermal fission of $^{235}$U or by reactions induced by thermal neutrons in a nuclear reactor ($^{130}$Te(n$_{\text{th}}$,$\gamma$) plus beta decay), and there is no sizeable production (or natural inventory) in either the biosphere or geosphere. It decays by 100% beta emission and has a half-life of 8.02 d and

the main gamma energies are 284.3 keV (6.22%), 364.5 keV (81.5%) and 637.0 keV (7.16%).

The chemistry and the physiological processes and reactions of $^{131}I^-$ are the same as for $^{125}I^-$. Owing to the higher gamma energies, the D values are relatively low: $D_1 = D_2 = 0.2$ TBq (5.4 Ci). Since normal injected quantitites are in the range 3.7–37 GBq (0.1–1.0 Ci), strict measures must be taken to reduce any risk of excessive doses.

External radiation dose may be reduced by proper shielding. For the most intense gamma ray at 364.5 keV, the linear attenuation coefficient is calculated to be $\mu_{364keV}(Pb) = 2.8$ cm$^{-1}$. The half-thickness and the thicknesses needed to reduce the radiation intensity by factors of 100 and 1000, respectively, are $x_{0.5} = 0.25$ cm, $x_{100} = 1.6$ cm and $x_{1000} = 2.4$ cm.

### III.1.3. Radiation exposure and chemical hazards in a designed injection process

*III.1.3.1. Exposure in a normal situation*

For pure beta radioactive tracers used in a normal situation, there will be no exposure to radiation during transport and injection because the soft beta radiation will not penetrate the walls of the bottles and equipment in which the tracers are kept before injection.

For gamma radioactive tracers, appropriate shielding has to be applied to reduce the dose to the personnel involved to below an acceptable limit.

*III.1.3.2. Exposure due to a transport accident*

For pure beta radioactive tracers, the tracer is shipped in a sealed 95 mL Monel bottle surrounded by water absorbent material and placed in a steel container. This container is again placed in a steel barrel surrounded by shock absorbing Ethafoam.

For gamma radioactive tracers, the volume of the tracer solution will be similar to the beta emitting tracers, i.e. 50–75 mL, and the packaging and containment are the same except for a higher level of shielding surrounding the inner steel container in order to give an acceptable transportation index (see necessary shielding thicknesses above).

If an accident occurs during the transport of the tracers, the radioactive material is supposed to be retained in its containment. Even in a major accident it is very unlikely that radioactive material will be dispersed. The situation will be dealt with in a normal way according to national and international laws and rules.

*III.1.3.3. Exposure due to release of radioactive tracer during injection*

There are two scenarios that could result in the release of tracer:

(1) Very small leakages of tracer containing liquid at tube connections, etc.
(2) Breakage or destruction of injection equipment due to some accident onboard the platform.

(a) Scenario 1

As a general rule, injection of radioactive tracers should always be performed by at least two persons with the necessary technical skills and safety competences. One person is implementing the injection process while the other is handling monitoring instruments and safety precaution equipment.

In case a leakage occurs, valve B (Fig. 7) connecting the tracer injection equipment to the water injection pipe on the platform will be closed. This will stop the leakages and the released fluid will be removed and treated as contaminated material by operators carrying personal protective equipment. It is supposed that this type of tracer dispersion will not cause any significant exposure to radiation or intake of radioactive material by the operators.

(b) Scenario 2

If a serious accident (e.g. an explosion) occurs in the vicinity of the injection site during the few seconds when the tracer is being flushed from the tracer bottle to the water injection pipe, causing destruction of the injection equipment, there could probably be a release of tracer.

It could also be envisaged that a valve or pipeline failure on the high pressure side would cause extensive leakage in the form of an unidirectional ejection of tracer-containing fluid.

The action to be taken, if possible, in this case will be to stop the flow through the injection cylinder by closing valve B. Then the injection equipment and the site will be flushed with large quantities of water to disperse the tracer into the sea (for offshore installations). As the tracer will be diluted with water very rapidly in this case, it is believed that there will be no significant intake of tracer by the operators. If the injection operator, who wears the mandatory protective water repellent clothing, has been splashed by tracer-containing fluid, the nearby support person immediately starts decontamination of the operator according to established procedure, including dousing of the operator with water followed by removal of the protective clothing. The support person also operates

monitoring equipment to ensure that the operator is clean before they leave the injection site.

In the case of onshore operations, injection equipment should be mounted in a trough in order to collect any spillage from the injection equipment itself. In addition, the nearby surface area should be covered with a plastic sheet with absorbent tissue paper on top to collect any spillage and facilitate site decontamination after a spillage. If soil contamination occurs, the area should be evacuated for a time long enough that the remaining activity in the soil has either evaporated (in the case of volatile tritiated liquids) or disappeared deeper into the ground (in the case of non-volatile beta and gamma emitting tracers). Surface monitoring of gamma radiation and/or vapour samples taken by radiation safety workers and analysed with respect to the content of volatile tritium labelled tracers will decide when the area is opened for general and normal work.

*III.1.3.4. Worst case accident*

Since HTO is the most frequently used water tracer, as an example, the possible dose to the operating personnel in the case of a worst case accident is discussed.

In the case of spillage of HTO, some of the water will evaporate and there will be tritiated vapour in the air. As vapour can be inhaled, a spillage of the total volume of HTO should be considered as the worst case scenario.

In the injection cylinder, the 2000 GBq of HTO will be diluted to approximately 75–100 mL. If this water evaporates and mixes with 500 m$^3$ of air (e.g. a volume of air 10 m × 10 m × 5 m), the tritium concentration in the air will be 4 GBq/m$^3$ or 4 MBq/L. If a person stays in this atmosphere for one minute and inhales 20 L of air and the entire vapour in the inhaled air is retained in the lungs, the intake of tritium will be 80 MBq. The annual limit of intake of tritium (from HTO) by professional workers as recommended by the ICRP is 1000 MBq. Thus, the calculated figure in the example above corresponds to approximately 8% of the annual limit of intake.

The worst case scenario for intake will occur if a beam of HTO is directed towards the faces of the operators handling the injection equipment. However, the operators will wear visors, masks and protective clothing, and they are well trained to deal with such situations. Taking into consideration that the total release of tracer can hardly occur unless there is a serious accident in the vicinity or some serious breakdown of the injection equipment at the time of injection, the worst case scenario described is very unlikely to arise. An accident causing destruction of injection equipment and the release of tracer will probably be more dangerous than the release of the radioactive tracer.

### III.1.3.5. *Sampling of produced water*

The concentrations of tracer in the sampled water will be very low. For HTO, it will be in the range of 200–300 Bq/L at maximum (top of the tracer recovery curve). For other tracers which have been injected in lower quantities, the concentration will be correspondingly lower. Sampling will not require any special protection equipment such as breathing apparatus or rubber gloves.

### III.1.4. **General safety measures**

### III.1.4.1. *Well-trained personnel*

The injections will be carried out by trained personnel from the tracer company. Most often, personnel from the oil or operator company are also present. As previously mentioned, two persons from the tracer company will participate in the injection programme. Both will have considerable experience in the technical application of radioactive tracers in industry and offshore activities. Before the injection work is started, a safety meeting will be held for the operater company's crew where personnel from the tracer company will discuss their work and the safety aspects of the tracer injections.

### III.1.4.2. *Urine samples*

Owing to the very low penetration power of beta radiation, the radiation from $^3$H, $^{14}$C or $^{35}$S intake cannot be registered by ordinary dose meters or radiation detectors. In order to be able to document possible radiation doses to personnel, or more likely, to document the absence of such doses in the case of tracer leakage, all operator company crew members that have to remain at the injection site will be asked to deliver urine samples. These samples will be analysed by liquid scintillation counting by a competent and independent health and safety laboratory. Analysis of urine samples is the most practical method for checking the intake of pure beta emitting radionuclides. Urine samples are taken before and after injection.

### III.1.4.3. *Precautions at the injection site*

The area around the injection sites will be roped off and appropriate warning signs will be set up. Only personnel taking part in the injection work will be allowed to remain at the site. Water hoses that can deliver copious quantities of water should be placed at the injection site. Thus, any spill of tracers can be

washed away. In the case of onshore operation, the nearby surface area should be covered by plastic sheets with water absorbent tissue on top.

### III.1.4.4. Personal protection equipment

The injection crew must carry visors and masks during the critical phases of the injection. Rainsuits or water repellent clothes should be worn in case of spillage of tracer solution.

### III.1.4.5. Equipment for injection and monitoring

Before the injection of tracer takes place, the complete injection equipment will have been pressure tested and checked for proper functioning. The tracer solution will be delivered in a closed Monel bottle that will be connected directly to the injection equipment before the valves on the bottle are opened. Thus, the radioactive material will not be exposed to the environment or to the personnel.

Tracer injection will be carried out either by connecting the injection equipment as a bypass to the main injection tubing or by pumping water from a 200 L container through the injection module and into the injection line using a high pressure pump. The pumps are pneumatically and not electrically driven in order to reduce the risk of sparks igniting any gas leakage from the nearby petroleum operations. The injection of the water tracer is expected to last 1.5 h. The main injection (99.9% of the tracer) takes place in a few minutes and the remaining time is used to clean out traces of radioactivity from the injection system.

Decontamination of the equipment and the site (if needed in case of accidents) will be carried out by personnel from the tracer company. In order to check water samples for radioactivity, a portable liquid scintillation counter will be available at the well head site.

### III.1.5. Impact on the environment

### III.1.5.1. General

Since HTO is the most frequently used water tracer and, in addition, applied in the highest quantities per injection (in becquerels), it is used here as an example on discussion of the environmental impact of such operations.

Sea water contains low concentrations of practically all radioactive nuclides present globally. The radionuclide $^3H$ is also present in sea water. In the North Sea, the concentration of $^3H$ is in the order of 1 Bq/L. During injection, there will normally be no release of tracer into the sea from offshore installations. However,

in case of an abnormal situation arising involving spillage of tracer, then the spilt tracer will be dispersed into the sea. The impact on the environment caused by this type of tracer discharge therefore has to be evaluated.

### III.1.5.2. Impact of an accident during injection

(a)   Worst case from radioactive tracer discharge into the sea

The worst case impact on the environment will occur if a whole portion of tracer has to be discharged into the sea.

(b)   Impact on the European population from HTO discharge

The following is an example on how this has been evaluated for a typical North Sea situation.
The report NRPB-R109 from the British National Radiological Protection Board, A Model to Calculate Exposure from Radioactive Discharges into the Coastal Waters of Northern Europe, contains a suitable model for calculations of dose commitments to the people in the region.

### III.1.5.3. Dose commitment from 3700 GBq of HTO

From the NRPB-R109 report, it is possible to calculate that a discharge of 1 GBq in one year gives a collective intake of 57.07 Bq over a period of 50 years. From this, 2000 GBq of HTO gives a collective intake of 211 159 Bq. A discharge of 50 MBq HTO gives a dose commitment equal to 1 mSv. Thus, the collective intake of 211 160 Bq originating from a discharge of 2000 GBq gives a dose commitment of $4.2 \times 10^{-6}$ mSv.

### III.1.6. Test procedure for injection of HTO

A typical check list for testing the injection equipment shown in Fig.7 prior to injection is:

(1)  With all the valves on the injection module in the closed position, the injection line pressure is applied to the module by opening valve 2 and by starting the pneumatic pump and opening valve 1.
(2)  Check for leakage on the tube fittings connecting the injection module to the injection line. If necessary tighten the leaking connections.
(3)  Close valve 2.

(4) The relief valve is set to 30 MPa (350 bar). Check that it does not relieve at working pressure.

(5) Open valves D and B. Check for leakages.

(6) Remove drain plug and open valve C slightly to check for flow through the module.

(7) Close valve C and replace drain plug.

(8) Close valve D and open valve 2. The two manometers on the module will now read injection line pressure.

(9) After having passed through the steps 1–8 successfully, close all valves. The module is now ready for installation of the tracer bottle.

(10) Bring the tracer bottle to the site.

(11) Check that the wire seal between the valves on the bottle is not broken.

(12) Remove the plugs from the two valve outlets.

(13) Connect the bottle to the injection module.

(14) Starting with all valves closed, open valves 1 and E and check for leakages.

(15) Close valve E and open valves D and F. Check for leakages.

(16) Close valves 1, D, F and check that all other valves are closed.

(17) Having passed the above steps successfully, the tracer injection module is ready for injection of tracer.

### III.1.7. Injection of tracer

*III.1.7.1. Safety measures*

Check that water hoses are available and connected to the supply. Check that the operators have the required personal safety equipment and that the injection site is roped off.

*III.1.7.2. Injection procedure*

(1) Starting with all outlets from the module plugged and all valves closed, then start the pump and bring it up to the injection line pressure. Open valves 1, B and 2.

(2) Open valve D slightly, close it and read the manometer pressures.

(3) Open valves E and F. Then open valve D slightly to admit pressure to the tube section between valves F and H. Close valve D and check for leakages.

(4) Break the wire seal on the tracer bottle and carefully open valve G while looking for possible leakage at the ends of the bottle. If leakage occurs, close valve G immediately and then close all other valves.

(5) If there are no leaks, open valve H and the tracer solution will be pressed into the injection pipe.

(6) Check by means of the gamma monitoring equipment that the tracer is transferred to the water injection line.

(7) After 30 min a sample should be collected from the injection water that has been diverted through the tracer bottle. The sample should be checked for tracer by means of the portable liquid scintillation counter.

(8) If the samples show that the tracer concentration in the water which has passed through the injection module is sufficiently low, the injection can be stopped and all valves closed. However, the injection should last for at least one hour before it is terminated.

(9) Disconnect the injection module and check for radioactivity at the outlet/inlet opening on the injection line.

(10) The injection module can now be decontaminated and prepared for another injection.

## III.1.8. Decontamination

Personnel from the tracer group will clean all equipment and, if necessary, all areas that have been contaminated by radioactive material. Sweep tests will be performed in order to ensure successful decontamination. Equipment that cannot be decontaminated at the platform will be packed according to the rules and sent to the institute for further cleaning or storage.

The radioactive and non-radioactive tracer injections that are described in this report will not have environmental consequences.

When transport, storage and handling of the tracers are carried out according to laws, rules and regulations, the tracer injections can be performed in a safe manner. Under normal circumstances there will be practically no radiation exposure to the operators or to the general public.

## III.2. ANALYSIS OF HTO IN SAMPLES OF PRODUCED WATER

### III.2.1. General

HTO or $^1H^3HO$ is a commonly used radiotracer in many industrial applications, particularly in interwell communication studies (water flooding) during enhanced oil recovery operations in oilfields and various investigations in geothermal fields. Tritium is a radioactive isotope of hydrogen, which decays by emission of very low energy beta particles ($E_{max.}$ = 18.6 keV) and has a half-life of 12.3 y). As tritium emits a very low energy beta particle, it cannot be measured on-site or on-line. The samples are required to be taken to the laboratory for measurement by liquid scintillation counter. A liquid scintillator is added to the

sample vial, which acts as a detector for beta particles. When beta particles interact with the scintillator, it emits scintillation photons, which are, in turn, detected by two PMTs placed around the sample vial. The unit of tritium commonly used in hydrology is the tritium unit. One tritium unit represents the ratio of tritium in common hydrogen atoms as: 1 tritium unit $= 10^{-18}$ [$^3$H]/[$^1$H].

The unit of tritium measurement commonly used in industrial applications, including the oil industry, is becquerel per kilogram (Bq/kg) or becquerel per litre (Bq/L). One becquerel is equal to one disintegration per second. One tritium unit is equal to 0.11919 Bq/L.

### III.2.2. Registration and storage of samples

Each sample arriving in the laboratory should be properly registered. A suitable sample registration form (consisting of sample identification code, description of sampling well/station with its location, name of project, date of sampling, date of sample receipt in laboratory and name of receiving person with their signature) should be used to maintain the sample record.

Check that bottles are not leaking. Store the bottles in proper conditions away from heat sources and direct sunlight. Samples should not be stored in rooms/buildings where artificial tritium compounds are, or have been, handled (contamination risk).

### III.2.3. Water sample preparation

For relatively pure water samples (type A), the procedure is as follows:

(1) Filter the sample through a lipophobic filter to remove any traces of dispersed oil droplets and any suspended particles.
(2) The oilfield samples usually contain high salt contents and chemical load. This raises the quenching effect profoundly during sample measurement, which introduces inaccuracy in the results. Though correction factors for chemical quenching can be applied to rectify the quenching effect, it is always desirable to avoid such complicated processes. For this reason, samples are distilled before measurement. All necessary glassware should be thoroughly washed and dried to avoid contamination. Therefore, transfer preferably 250 mL of the water filtrate into a 500 mL round flask.
(3) Assemble the distillation equipment as shown in Fig. 90.
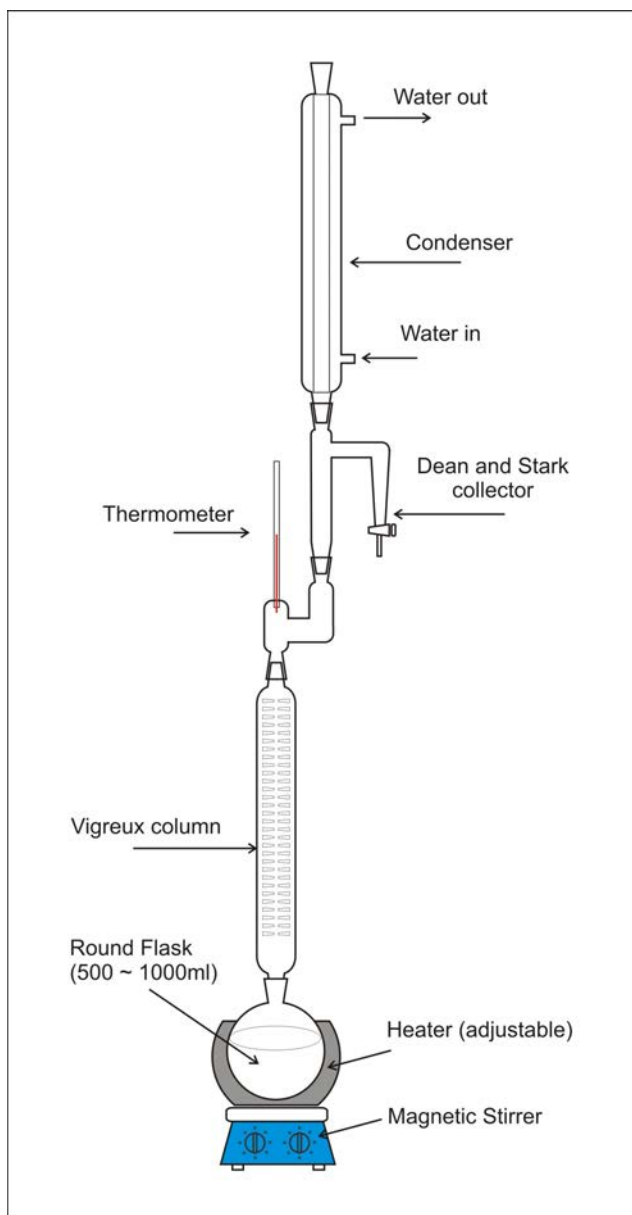(4) Distil with gentle boiling and collect distilled water in the sidearm of the glass equipment.

*FIG. 90. Distillation equipment is used for preparation of liquid scintillation counting samples of HTO from samples of produced water.*

(5) Discard the two first fractions of the distilled water because these may contain volatile hydrocarbon components which have been dissolved in the original water sample and which may quench the scintillation process.

(6) Collect the third 8–10 mL sample for analysis. If, for any reason, the water sample cannot be analysed the same day that it is purified and distilled, the samples (vials) should be stored in the refrigerator until they are prepared for counting.

(7) Mix with 10–12 mL of an appropriate scintillation cocktail which is able to accommodate about 50% of water without a detrimental decrease in counting efficiency, for instance Ultima Gold.

(8) Store the counting sample for at least 1 h in the dark in order for any chemiluminescense or phosphorescence to die out before starting the counting sequence.

(9) Three background samples ('dead' water) and three standard samples with known activity on a given date are prepared and counted along with the produced water samples.

(10) If variable quenching is suspected in the produced water samples, a correction has to be made for the corresponding varyiable counting efficiency. Most modern liquid scintillation counting equipment provides an instrumental quench correction method. In case this is not the case, the quench correction can most easily be performed by the internal standard method. After having counted the samples, a known activity of a non-quenching tritium compound (standard solution) is added to each vial and counted again.

This gives the counting efficiency directly according to the formula:

$$\varepsilon = \frac{R_{x+s} - R_x}{D_s} \tag{30}$$

where

$R_x$    is the background corrected counting rate of the produced water sample;

$R_{x+s}$    is the background corrected counting rate of the sample after addition of a known quantity of standard;

$D_s$    is the disintegration rate of the added quantity of standard (Bq).

The activity of tritium in the original sample, $D_x$ (Bq), can then be calculated by:

$$D_x = \frac{R_x}{\varepsilon} \qquad (31)$$

and the activity concentration, $D_{xc}$ in Bq/L, in the produced water by:

$$D_{xc} = \frac{D_x \cdot V_x}{1000} \qquad (32)$$

where $V_x$ is the volume of the water in the counting sample in millilitres.

For samples with a visible layer of oil (type B), remove the oil layer on top of the water with a pipette, then carry out the same procedure as outlined in point 1 above.

For the most difficult samples consisting largely of an oil–water emulsion (type C), the first step is to break the emulsion in order to sample any water dispersed in the oil. There are a variety of commercial emulsion breakers available (a chemical supplier can assist).

Then carry out the same procedure as for point 1 above, with the modification which takes into consideration the volume of water available after emulsion breaking may be limited, i.e. a few millilitres only. In that case, the distillation process may be omitted or performed in miniaturized equipment.

### III.2.4. Sample enrichment

It is possible to enrich HTO in water by electrolysis of the water to produce hydrogen and oxygen gases. In this process, water containing the lighter hydrogen atoms $^1H$ and $^2H$ are preferentially removed from the water, leaving an electrolyte which is increasingly enriched in HTO. Starting with a volume of 250 mL, it is possible to reach an enrichment factor of 25–35, depending on the equipment and procedure used. However, in all cases where HTO is added artificially as a tracer to water, there is not much gain in this enrichment technique because the natural HTO content is increased, as well as the background. Thus, the quality of the analysis is not improved even though the number of counts increases. Sample enrichment is indispensable when analysing natural samples that have low contents of tritium, however.

### III.2.5. Calibration method

Normalization of a liquid scintillation counter is done using unquenched sealed standards of $^{14}$C, tritium and background supplied by a commercial company (e.g. Packard Instrument Co.) The samples and standards are usually counted for a preset time of 50 min and the whole batch is cycled 10 times. Thus, each sample/standard is counted for a total time of 500 min (the sample counting time and the number of cycles can be adjusted as per requirement). The samples with higher counts can be counted for shorter times and for fewer repeat cycles). The data are statistically evaluated by applying Chauvenet's criterion and rejecting outliers. This is followed by the calculation of the mean background count rate, the net mean count rate of the standard and the net count rates of unknown samples.

Uncertainty in the tritium activity is calculated by combining the uncertainties of all the factors involved (net counts per minute of counting standard, activity of counting standard, net counts per minute of sample, weights and decay correction) and using the error propagation law.

### III.3. ANALYSIS OF RADIOLABELLED ($^{14}$C or $^{35}$S) SCN$^-$ IN SAMPLES OF PRODUCED WATER

### III.3.1. Method

The tributylphosphate solvent extraction method was developed for $^{14}$C or $^{35}$S labelled SCN$^-$ enrichment. The recovery efficiency of S$^{14}$CN$^-$ or $^{35}$SCN$^-$ is about 90%. The enriched sample is measured by liquid scintillation counting. Essentially, the method consists of three steps:

(1)  Sample purification by filtration;
(2)  Tributylphosphate solvent extraction;
(3)  Liquid scintillation counting.

### III.3.2. Equipment and reagent

- pH meter, balance (1/10 000), 0.45 μm paper filter, funnel, flask (1000 mL), pipette, electromagnetic stirring device, liquid scintillation counter.
- Tributylphosphate (A.R.), ZnCl$_2$ (A.R.), HCl (A.R.), KSCN (A.R.).

```
                    ┌──────────────────┐
                    │   1000mL brine   │
                    └──────────────────┘
                              ↓
              ┌───────────────────────────────┐
              │ Filtration by 0.45 µ m filter paper │
              └───────────────────────────────┘
                              ↓
            ┌───────────────────────────────────┐
            │ Add 5g ZnCl₂, 0.1g KSCN and 1mol HCl │
            └───────────────────────────────────┘
                              ↓
              ┌───────────────────────────────┐
              │  Add 10mL TBP and stir 30 minutes │
              └───────────────────────────────┘
                              ↓
               ┌─────────────────────────────┐
               │   Keep to phase separation  │
               └─────────────────────────────┘
                              ↓
┌────────────────────────────────────────────────────────────────┐
│ Take 8mL of the upper phase +12 mL cocktail (ULTIMA-GOLD LLT) for LSC │
└────────────────────────────────────────────────────────────────┘
```
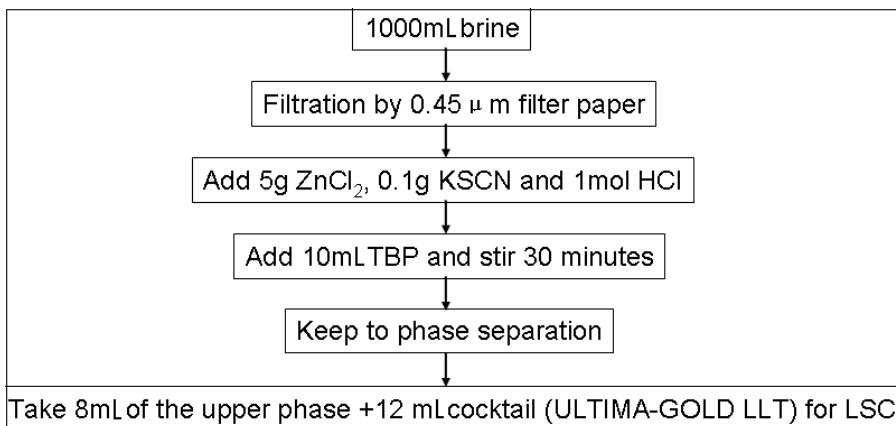
*FIG. 91. Analytical procedure for analysis of radiolabelled $SCN^-$ in samples of produced water.*

### III.3.3. Analytical procedure

The analytical procedure is shown in Fig. 91.

### III.3.4. Recommendations

It is recommended that a reference solution (sample with known tracer concentration in the brine of the target reservoir) should be prepared and applied in an actual scale test, in order to obtain very reliable results through the use of the above analytical procedures. The concentration of the tracer in the reference solution should be at a similar level to that in the samples collected from the field.

## III.4.  ANALYSIS OF RADIOLABELLED $[Co(CN)_6]^{3-}$ IN SAMPLES OF PRODUCED WATER

There are several radioisotopes that can be used to label the $[Co(CN)_6]^{3-}$ compound: $^{56}$Co, $^{57}$Co, $^{58}$Co, $^{60}$Co and $^{14}$C.

### III.4.1. Method

Enrichment of radiolabelled $[Co(CN)_6]^{3-}$ in reservoir brine is conducted by anion exchange column chromatography. The absorption efficiency of the
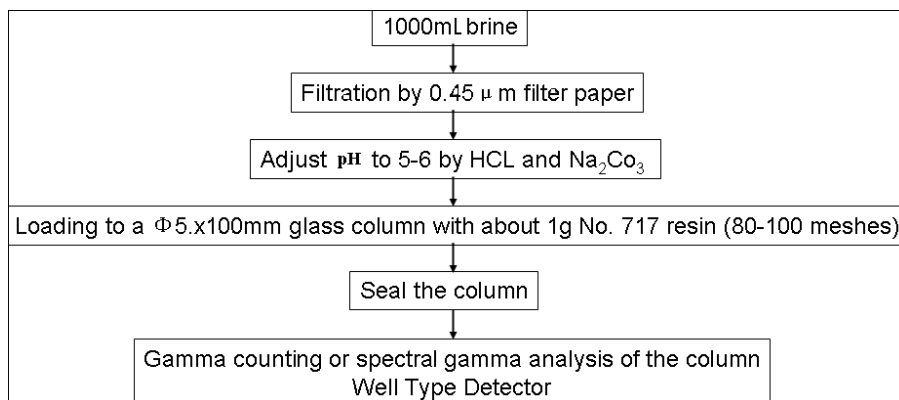
FIG. 92. Analytical procedure for analysis of radiolabelled $[Co(CN)_6]^{3-}$ in samples of produced water.

$[Co(CN)_6]^{3-}$ to the resin is more than 99%. The analysis method consists of three steps:

(1) Sample purification by filtration;
(2) Use of No. 717 anion exchange resin column enrichment;
(3) Gamma counting or spectral gamma analysis.

### III.4.2. Equipment and reagent

- pH meter, balance (1/10 000), 0.45 μm filter paper, funnel, flask (1000 mL), pipette, 5 mm × 100 mm glass column, spectral gamma analyser or gamma counter (well-type detector is recommended).
- No. 717 anion exchange resin (Beijing Analytical Reagent Factory), HCl (A.R.), $Na_2CO_3$ (A.R.).

### III.4.3. Analytical procedure

The analytical procedure is shown in Fig. 92.

### III.4.4. Recommendations

It is recommended that a reference solution (sample with known tracer concentration in the brine of the target reservoir) should be prepared and applied in an actual scale test in order to obtain very reliable results through use of the

above analytical procedures. The concentration of the tracer in the reference solution should be at a similar level to that in the samples collected from the field.

## III.5. ANALYSIS OF RADIOLABELLED ALCOHOLS

### III.5.1. Tritium and $^{14}$C analysis in alcohol

The presence of tritium and $^{14}$C in alcohol in a water sample taken from the oilfield cannot be analysed directly by liquid scintillation counting; it needs to be purified using the distillation process described below.

### III.5.2. Equipment and reagents

- Round flask 500 mL, connection size 24/40;
- Fractional distillation Vigreux column 31 cm long, connection size 24/40;
- Dean & Stark collector sized 10 mL;
- Cooling system;
- Heater;
- Magnetic stirrer;
- Liquid scintillation counter with standard 10–20 mL vial;
- Methanol and toluene reagent grade;
- Cocktail Instagel or Ultima Gold.

### III.5.3. Procedures

(1) Sample treatment: Add 10% v/v of toluene and extract water by funnel.
(2) Place water sample in standard vial with appropriate cocktail to count $^3$H and $^{14}$C directly on liquid scintillation counter at dual label mode. Calculate tritium (HTO) activity with correction for $^{14}$C in methanol contribution.
(3) Add 3 mL of methanol and 1.3 mL of toluene to water sample in the round flask.
(4) Add a magnetic stirring bar to the round flask on the distillation system.
(5) Heat the sample at low power to distil for 5 h.
(6) Collect the distillate (about 4 mL) into the counting vial.
(7) Add cocktail and count by dual label mode with liquid scintillation counter.
(8) Calculate the $^{14}$C activity (from $^{14}$C-MeOH) using the appropriate correction for HTO influence.
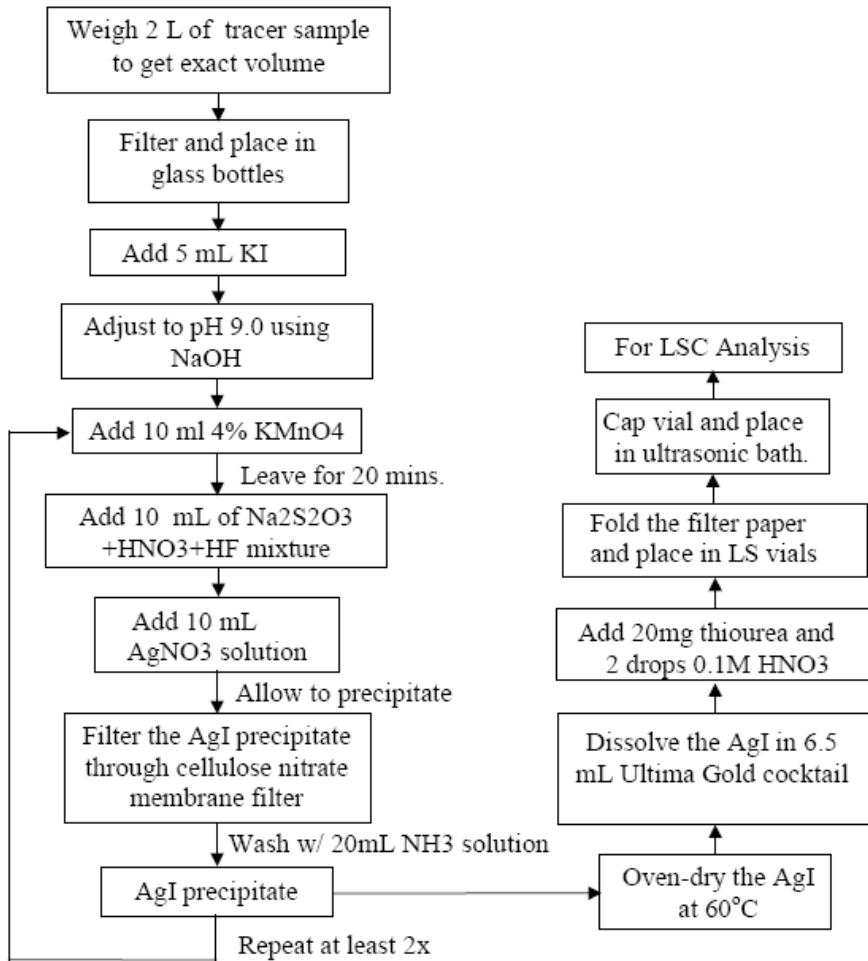
FIG. 93. Flow chart of water sample pretreatment for analysis of tracer levels of $^{125}I^-$ in samples from geothermal wells.

## III.6. ANALYSIS OF RADIOIODINE ($^{125}I^-$ or $^{131}I^-$) IN SAMPLES OF PRODUCED WATER

### III.6.1. Analysis by chemical treatment of water sample for detection with liquid scintillation counter

There are several procedures for sample treatment, one of which is described below. The flow chart of this analytical procedure is shown in Fig. 93.

(1) The samples (2 L) are delivered in plastic bottles and are weighed to determine their volumes. A known quantity of inactive $I^-$ (5 mg) is added to act as a carrier, as well as to ensure that the final precipitate is of sufficient mass (about 10 mg) to be reliably filtered and weighed. The samples are then filtered if inspection reveals any debris or cloudiness, and NaOH is added to make the samples slightly alkaline (~pH9).

(2) The $I^-$ is then oxidized to $IO_3^-$ with $KMnO_4$ and allowed to stand for about 20 min. At the same time, any sulphide present ($S^{2-}$, $HS^-$ or $H_2S$, which would form an $Ag_2S$ precipitate in competition with AgI) is oxidized to $SO_4^{2-}$. A longer time might be used if organic matter is present or if there is a high sulphide concentration.

(3) The $IO_3^-$ (including the carrier) is then reduced back to $I^-$ by addition of an acid mixture ($HNO_3$ and HF) followed by $Na_2SO_3$ solution. The HF is included to inhibit formation of silica ($Si(OH)_x$), which would clog filters and interfere with the weight of the final precipitate. The $SO_4^{2-}$ is unaffected by this step, thus effectively removing sulphide interference. After standing, the solution is filtered to remove any traces of $Si(OH)_x$ which might have formed.

(4) An excess of $AgNO_3$ solution is added soon after the filtration to form a precipitate of AgI. Because AgI is much less soluble than AgCl, it is precipitated preferentially despite the approximately thousand-fold excess of chloride ions. However, small quantities of AgCl (and AgBr) are formed. After standing in the dark, the precipitate is filtered through cellulose acetate paper under vacuum. The AgCl and AgBr are then removed by washing with ammonia. The precipitate, now pure AgI, is then passed quickly through a further oxidation–reduction cycle for purification purposes before being dried and weighed.

(5) The precipitate is then dissolved in the liquid scintillation cocktail. This is done by inserting the rolled filter paper into the cocktail vial, adding about 20 mg of acidified thiourea and then immersing the vial in an ultrasonic bath to disperse the AgI into the cocktail. The AgI dissolves to form the silver complex $Ag[SC(NH_2)_2]_2^+$. The paper is translucent and should be left in the vial (20 mL). The precipitates are dried and weighed.

(6) The analytical yield is calculated by dividing the mass of iodide in the AgI precipitate by the quantity of iodide added plus that known from prior analysis to be in the sample, typically 0.1–0.2 mg/L.

## III.6.2. Analysis of $^{125}$I by gamma spectrometry

The procedure for $^{125}$I analysis using gamma spectrometry and a multichannel analyser is as follows:
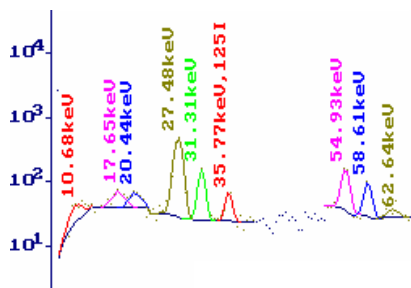
FIG. 94.  The photon–photon coincidence method spectrum of $^{125}$I. The 35.5 keV gamma ray of $^{125}$I is 93% converted. Intense production of tellurium X rays shown as two peaks at 27.5 and 31.3 keV in the spectrum. Sum coincidence peaks are also shown (between 50 and 65 keV).

(1)    Filter the brine sample (1 L) by using 0.45 µm pore size filter paper.
(2)    Adjust to pH6–7 by adding HCL or $Na_2CO_3$.
(3)    Prepare an anion exchanger column with diameter 5 mm and 100 mm length (various resins are available commercially, e.g. Dowex 1, BioRad 1). Mesh size can be 80–100, and cross-linking ×8.
(4)    Percolate the solution through the column at a slow rate (a few millilitres per minute).
(5)    Seal the column at both ends.
(6)    Count the column in a detector set-up (preferably a well-type HPGE detector) connected to the multichannel analyser multichannel analyser by the gamma–gamma (photon–photon) coincidence method, where the sum coincidence between the X rays and between the X ray and the gamma ray are measured.

A photon spectrum from the use of the photon–photon (sum) coincidence method is shown in Fig. 94.

## Appendix IV

## SOFTWARE PACKAGES

IV.1.  ANDURIL DISPERSION SIMULATOR

### IV.1.1.  Anduril software

Anduril is a software package for basic data treatment and preliminary interpretation based on the standard equations for convection–diffusion in porous media. Figure 95 shows the main window of the Anduril 2.3 software.

The main data (time, concentration and water flow rate in the producing well) is introduced in a grid manually or by a copy and paste operation from an ordinary spreadsheet. The information can also come from a pre-existing file. Water volume may be used as an independent variable instead of time. The software also needs the injected activity and the radioisotope (tritium is the default), the background concentration and the baseline expressed as a real constant multiplied by the background. Experimental concentration values below this line are not taken into account.
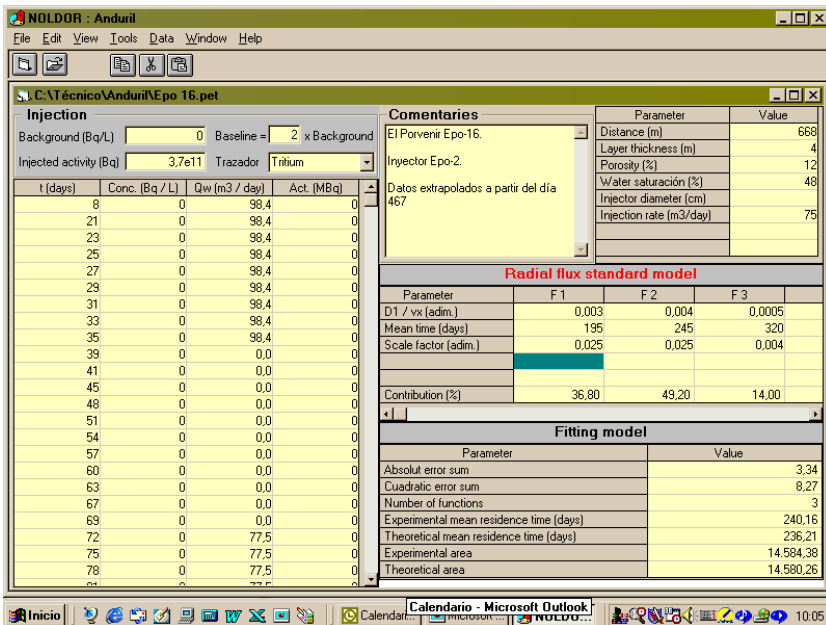


*FIG. 95.  Anduril 2.3 main window.*

173

- As a general rule for further calculations, the distance between wells, layer thickness, porosity and water saturation should be written, while the inclusion of some other parameters will depend on the selected model. Finally, any additional information may be included as a 'commentary' in an appropriate text box.
- Original concentrations are corrected for internal calculations or graphic operations both by background and by radioactive decay. However, the information remains unchanged in the main grid.
- The experimental data can be filtered in order to eliminate the quick and random alterations that could mask the true values. The fast Fourier transform is the mathematical tool used for the purpose of eliminating higher harmonics. The experimental curve can also be extrapolated.
- The software calculates and plots the tracer recovery as a function of time or volume. Tracer concentration is also plotted. The main statistic parameters are also evaluated.
- The response curve can be decomposed in several simple functions following the classical dispersion function. This operation can be performed manual or automatically. Error information is shown in both cases so as to enable the user to correct the 'fit' parameters in order to identify the best approach. Graphic representation of simple functions can be presented as well as numerical information on each curve.
- This software includes many other options, such as the calculation of sweep volume, breakthrough time, final time and mean residence time and a function to calculate the activity to be injected in future experiments.

A pattern of oil secondary recovery in which water is pumped into an injection well that is surrounded by several production wells can be modelled as a system ruled by radial flow. In such a case, the tracer concentration, as a function of time and space, can be analysed by means of the classical dispersion equation for one dimensional flow:

$$D\frac{\partial^2 C}{\partial x^2} - v\frac{\partial C}{\partial x} = \frac{\partial C}{\partial t} \tag{33}$$

the solution of which is:

$$C(x,t) = C_{REF} \frac{1}{\sqrt{4\pi \frac{D_1}{v\,x} t_N^3}} e^{-\frac{(1-t_N)^2}{4\frac{D_1}{v\,x} t_N}}$$

(34)

where

$C_{(x,t)}$ is the tracer concentration as a function of distance and time (Bq/m$^3$);

$t_N$ is the normalized time;

$D_1$ is the coefficient of dispersion (m$^2$/d);

$v$ is the tracer velocity (m/d);

$x$ is the distance from the injection point (m);

$C_{REF}$ is the reference tracer concentration (Bq/m$^3$).

The normalized time is the ratio between the time and the mean residence time of the tracer, and:

$$C_{REF} = F \frac{A}{\pi\,x^2\,h\,\phi\,S_w}$$

(35)

where

$A$ is the injected activity (Bq);

$h$ is the thickness of the layer (m);

$\phi$ is the average porosity;

$S_w$ is the water saturation;

F is a constant.

The denominator represents the volume of free water in a cylinder whose radius is the distance between the injection and the production wells and whose height is the layer thickness.

Single response curves can be easily fitted by the model adopted by Anduril. However, in the case of complex response curves with multiple relative maxima, it is convenient and necessary to decompose them into simple functions in order to extract conclusions related with the behaviour of each of them.

Working area
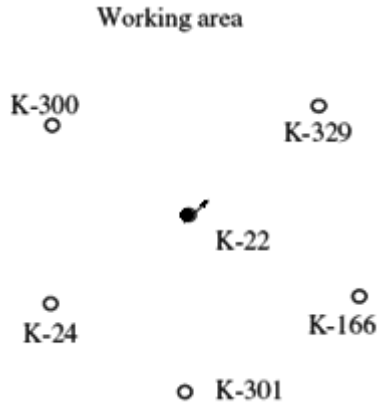


*FIG. 96. Well pattern for case study 1.*

## IV.1.2. Case studies using Anduril software

*IV1.2.1. Case study 1*

Figure 96 shows a well pattern of a reservoir sited in southern Argentina, where an interwell study by means of radiotracers was performed some years ago.

Since HTO was the selected tracer, the liquid scintillation technique was used for measurement. Because of operative limitations in the laboratory measurement, samples were not distilled before counting and, in addition, a short count time was used. For that reason the detection limit was much higher than usual. The detection parameters were:

- Background = 20 cpm;
- Efficiency = 0.28 (counts/disintegration);
- Count time = 10 min;
- Volume of the sample = 8 mL;
- Detection limit = 29.5 Bq/L.

From the detection limit, the mean output concentration was fixed at ten times this value (295 Bq/L), which leads to an activity of 167 GBq (4.5 Ci). In fact, 10 Ci of HTO was injected into well K-22 using the bypass device. Figure 97 shows an example of the tracer concentration and cumulative response curves for well K-329, whose output was followed during a full year and belongs to the K-22 pattern.

The first information obtained in production well K-329 from a quick analysis of the response curve using Anduril software was:
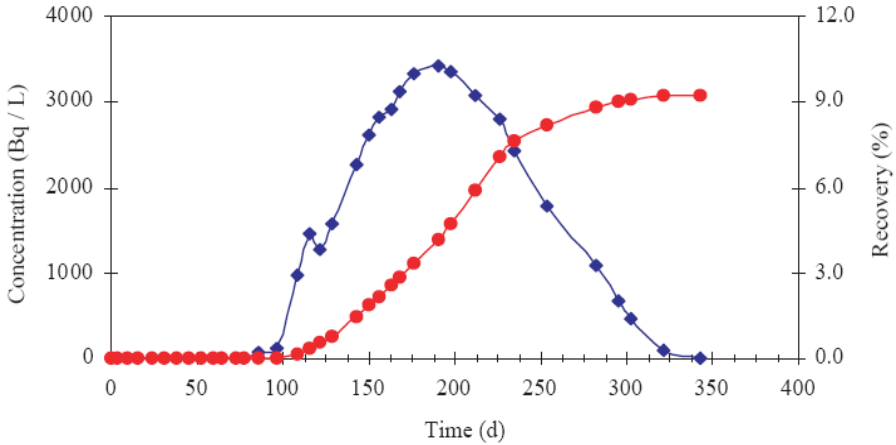
*FIG. 97. Instantaneous (left hand scale) and cumulative (right hand scale) response curves (well K-329).*

- Breakthrough = 86 d;
- Mean residence time = 193 d;
- Final time = 321 d;
- Tracer recovery = 9.2%.

The distance between wells K-22 and K-329 is 251 m, thus, the calculated minimum, medium and maximum water velocities are 0.78 m/d, 1.3 m/d and 2.9 m/d, respectively. Permeability was also evaluated by Anduril software using Darcy's law. A value of 282 mD was obtained, which appeared reasonable to reservoir engineers.

Anduril software was used to model the experimental response curve obtained by sampling in production well K-329. A radial dispersion model was applied. Figure 98 indicates a good fit.

The model gives the following parameter values for the dynamics of tracer movement between injection well K-22 and production well K-329:

- Breakthrough = 75 d;
- Mean residence time = 210 d;
- Final time = 410 d;
- Tracer recovery = 9.1%.
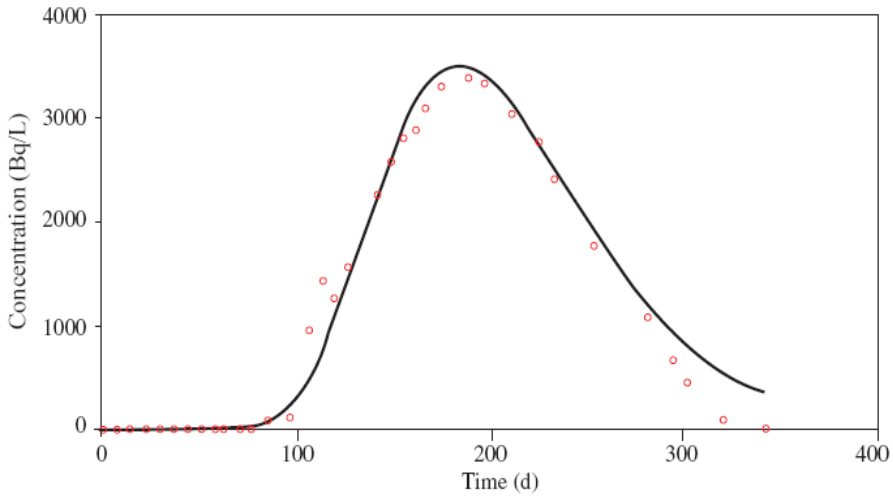
FIG. 98. Radial dispersion model approach (well K-329).
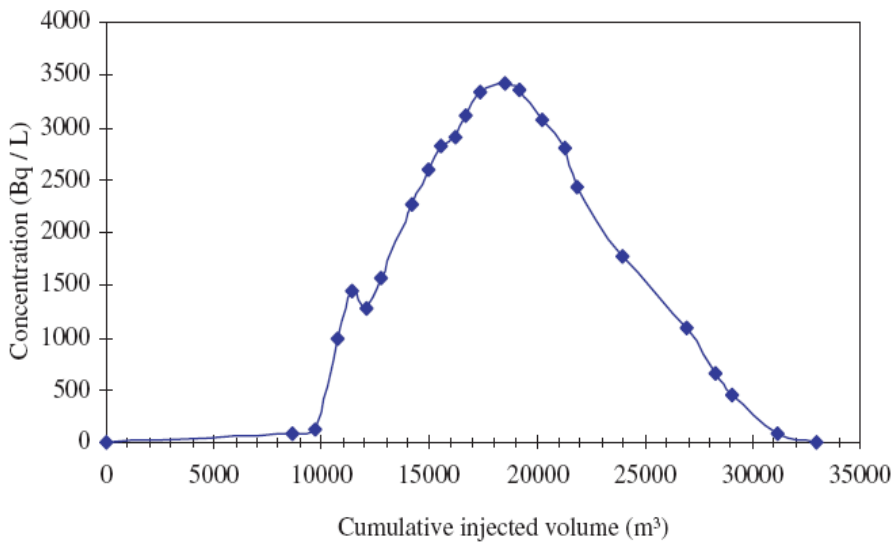


FIG. 99. Volumetric response curve (well K-329).

The volumetric response curve for well K-329 appears in Fig. 99, given in terms of the cumulative injected volume. Reservoir information extracted from the tracer response curve in well K-329 is:

178

- Breakthrough = 86 d;
- Mean volume = 19.073 m$^3$;
- Swept volume = 1.775 m$^3$.

The last value is the pore volume swept from the injector to the production well (K-329) and equals the mean volume multiplied by the recuperation factor (0.092).

*IV.1.2.2. Case study 2*

Complex response curves can be obtained in some cases due to the mixed response from different layers. Anduril software can be used to decompose a complex response curve into several simple curves. These simple curves are supposed to represent tracer movement in a unique layer. Modelling each of the simple curves provides the mean residence times and the quantity of tracer recovered from each layer.

An example of this methodology is shown in Fig. 100 in which the complex response of a production well was approached using four simple functions (Fig. 101) based on the radial model. A possible explanation of the tracer behaviour could be that it reached the production well by following four paths of different permeability belonging to a unique layer.

The parameters of each function are given in Table 26.
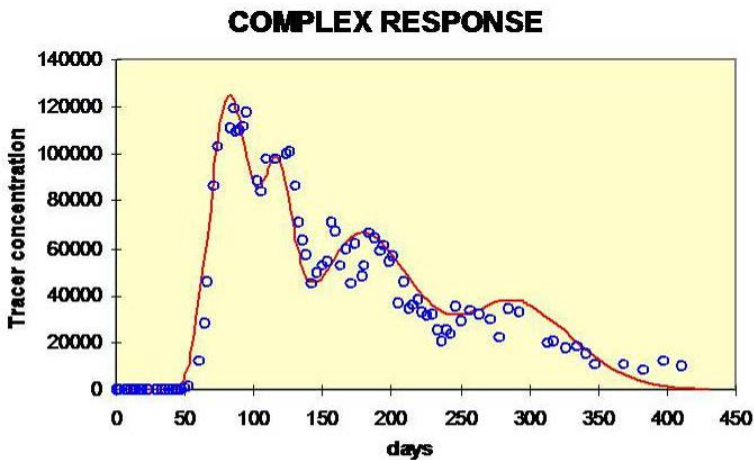


*FIG. 100. Complex response and its theoretical approach.*

## SIMPLE FUNCTIONS
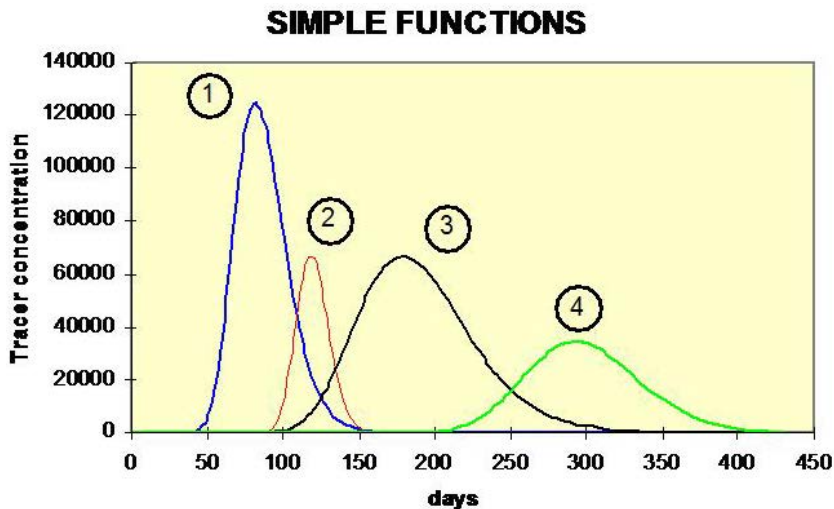


*FIG. 101. Individual theoretical functions.*

TABLE 26.  COMPLEX RESPONSE MODELLED BY FOUR FUNCTIONS

| Curve | $D_1/vx$ | $t_{mean}$ (d) | $f_i$ |
|---|---|---|---|
| 1 | 0.020 | 87 | 0.292 |
| 2 | 0.004 | 120 | 0.105 |
| 3 | 0.020 | 190 | 0.384 |
| 4 | 0.008 | 300 | 0.219 |

Some 46% of the total quantity of tracer recovered in this well related to the injected activity. The parameter $f_i$ is the contribution of each path expressed as a fraction of that percentage and was evaluated from the area under each curve. Dispersivities may be calculated by multiplying the ratio $D_1/vx$ by the distance between the injection and the production wells.

## IV.2.  PORO STREAMLINE SIMULATOR

### IV.2.1.  Data interpretation: Conversion from raw data to information

The importance of interwell tracer testing in oil exploitation is indicated by the great number of tests conduced worldwide over the last 40 years. Normally,

water is injected into injector wells to 'push' the oil to the producer wells, from which it is extracted. The end of the secondary recovery process occurs when the water cut increases to the point where water injection becomes economically inefficient to continue further. At this stage, the fluid flow in the reservoir consists mainly of injection water. The oil remaining in the reservoir is largely stagnant (residual saturation) in the swept volume but can also comprise larger untouched oil volumes. This incomplete sweeping of the oil is a consequence of the natural heterogeneity of the reservoirs and the usually unfavourable mobility differences between water and oil. Hence, channelling of water between injector and producer wells is a very common problem that counteracts achieving acceptable sweep efficiencies.

The interwell tracer tests permit detection of this problem and also determination of some parameters of the watered zones, which are necessary for corrective action. Owing to the considerable uncertainty associated with fluid flow knowledge in the water flooding process, there is insufficient basis for assuming a very detailed reservoir model. Therefore, a 'kit' of simple methods can provide acceptable information, including moment analysis and Brigham based analysis.

### IV.2.1.1. Moment analysis method

The moment analysis method was originally developed for closed reactor vessels [25, 26], but has been applied to the more general conditions of open boundaries [27] for characterization of fractured media under continuous tracer reinjection [28, 29] and for estimation of flow geometry [30, 31]. Certain restrictions are inherent in the calculation, for example, steady state conditions and conservative tracer behaviour are assumed a priori. Nevertheless, the method has a rigorous mathematical basis and has been extensively validated analytically and experimentally.

The governing equations used in moment analysis are based on knowledge of the residence time distribution of the tracer, defined as:

$$E(t) = \frac{C(t).q_{inj}}{M_{inj}} \tag{36}$$

where $C$ is the collected sample tracer concentration (ppm, ppb, Bq/L, etc.), and $Q_{inj}$ and $M_{inj}$ are the injection water flow rate (m$^3$/d) and the injected tracer quantity (kg, g, Bq, etc.), respectively.

If the tracer experimental curve is not fully recorded (which is very frequently experienced because of limited the sample collection and analysis), it is important to employ some criteria for extrapolating.

The parameters of the experimental residence time distribution curve are calculated by the moment method. The $n$th moment of a residence time distribution curve is defined as:

$$t^n = \frac{\int_0^\infty t^n \cdot E(t) \cdot dt}{\int_0^\infty E(t) \cdot dt} \tag{37}$$

The zero moment (equivalent to the fractional cumulative recovery of the tracer) is:

$$\frac{m_{rec}}{M_{inj}} = \int_0^\infty E(t) \cdot dt \tag{38}$$

The first moment (equivalent to the residence mean time) is:

$$t^* = \frac{\int_0^\infty t \cdot E(t) \cdot dt}{\int_0^\infty E(t) \cdot dt} \tag{39}$$

IV.2.1.2. Pore volume determination

Pore volume determination is based on the knowledge of the zero and the first moments. It is calculated from:

$$Vp = \frac{m_{rec}}{M_{inj}} q_i t^* \tag{40}$$

The calculated pore volume represents only the watered pore volume. The complementary volume occupied by the oil cannot be reached by a passive tracer.

### IV.2.1.3. Calculating flow geometry

It has been proposed that the flow and the storage (pore volume) geometry of the formation can be estimated directly from a tracer test [30, 31]. The cumulative flow capacity at any streamline 'i' of a formation ($F_i$) is the sum of the contribution of each streamline that has a velocity greater than the 'i' and is normalized by the ensemble properties. Darcy's law gives:

$$F_i = \frac{\sum\limits_{j=1}^{i} \dfrac{k_j A_j}{l_j}}{\sum\limits_{j=1}^{N} \dfrac{k_j A_j}{l_j}} \qquad (41)$$

The cumulative storage capacity of these streamlines ($\Phi_i$) is simply the sum of their individual pore volumes:

$$\Phi_i = \frac{\sum\limits_{j=1}^{i} Vp_j}{\sum\limits_{j=1}^{N} Vp_j} \qquad (42)$$

These can be estimated from a tracer test, where $\Phi_i$ is the incremental first moment calculated at the time $t$ and normalized by the true first moment:

$$\Phi_{(t)} = \frac{\int\limits_{0}^{t} E(\tau)\tau\,\mathrm{d}\tau}{\int\limits_{0}^{\infty} E(t)t\,\mathrm{d}t} \qquad (43)$$

The cumulative flow capacity is simply the cumulative tracer recovery at time $t$ normalized by the complete recovery:

$$F_{(t)} \cong \frac{\int\limits_{0}^{t} E(\tau)\,\mathrm{d}\tau}{\int\limits_{0}^{\infty} E(t)\,\mathrm{d}t} \qquad (44)$$
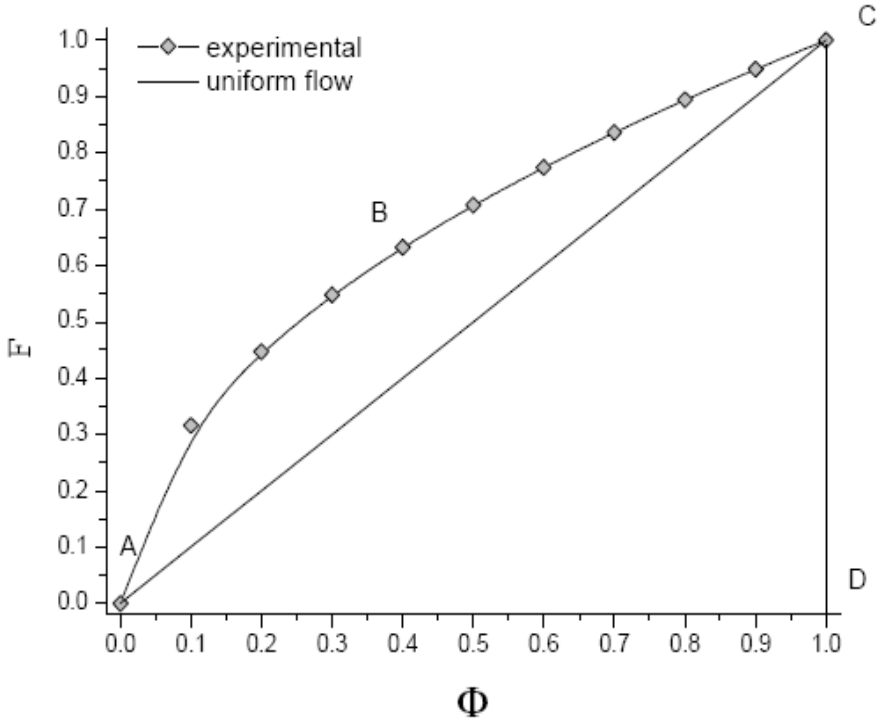
FIG. 102. (F,Φ)-plot showing a hypothetical experiment and uniform flow cases.

Flow and storage capacities are most often plotted in a (F,Φ)-plot. The shape of a (F,Φ)-plot is useful as a diagnostic tool indicating what fraction of the pore volume contributes to what fraction of the fluid flow. The (F,Φ)-plots are widely used in oil reservoir engineering. Figure 102 illustrates the (F,Φ)-plot showing experimental values compared with the case of uniform flow (parallel equidistant streamlines).

### IV.2.1.4. Estimating heterogeneity

Two common measures of heterogeneity can be obtained from the (F,Φ)-plot: the Lorentz coefficient ($L_c$) and the Dykstra Parsons coefficient ($V_{DP}$) [32]:

$$L_c = 2\left\{\int_0^1 F \, d\Phi - \frac{1}{2}\right\} \tag{45}$$

184

$$V_{DP} = \frac{F'\big|_{\Phi=0.5} - F'\big|_{\Phi=0.841}}{F'\big|_{\Phi=0.5}} \tag{46}$$

- $L_c$ varies between 0 and 1, with 0 representing a homogeneous flow field.
- $F'$ is the derivative of $(F, \Phi)$. It is evaluated at the mean (0.5) and at one standard deviation below the mean (0.841).

### IV.2.1.5. Volumetric fluid sweep efficiency

Volumetric fluid sweep efficiency is a measure of efficiency for use of the injected fluid. It expresses that fraction of the injected water which is actively contributing to pushing the original fluids in the reservoir. Using the concept of streamlines and the definition of '$F$' above, it is possible to estimate sweep efficiency directly from a tracer test.

The $F(t)$ term can be interpreted as the fraction of streamlines that have 'broken through' and have started to produce injected fluid. These streamlines are not contributing further to sweeping of the reservoir. In the opposite sense, at the beginning, all the injected water is active and the sweep efficiency must be at a maximum. Hence, sweep efficiency can be expressed in terms of fractional tracer recovered and injection rates:

$$E_V(t + \Delta t) = E_V(t) + \frac{q_{inj}}{V_p} \frac{m}{M_{inj}} \Delta t \left[1 - F(t + \Delta t)\right] \tag{47}$$

Sweep efficiency is typically reported as a function of dimensionless time or time normalized by the total pore volume:

$$t_D = \frac{q_{inj}}{V_p} \frac{m}{M_{inj}} t = \frac{t}{t^*} \tag{48}$$

### IV.2.1.6. Limitations of the method

- Conservative tracer travelling jointly with the water bulk flow is required.
- Steady state flow is necessary.
- The necessity for extrapolation of the tracer records (tracer production curve). Sampling for tracer is frequently terminated long before the tracer concentration falls to zero. Because the first moment is a time weighted average, failure to include late time data leads to the underestimation of

both mean residence time and pore volume. A decline pattern composed of exponential terms is most commonly observed.
- The difficulty of distinguishing between the imposed flow geometric effects (resulting from the injection pattern) and heterogeneity effects.
- The estimations can be erroneous if the tracer does not move with the 'bulk flow'. This happens, for example, in double porosity rocks with diffusion in the secondary porosity.

**IV.2.2. Brigham based method**

This method is based on an analytical model which was developed in a sequence of papers starting with Refs [33–36].

In the assumed model, the reservoir is considered a 'layer cake' of homogeneous, non-communicating layers. The injected tracer pulse is distributed among the layers in accordance with the flow conductivity (permeability and thickness) of each layer. The tracer material in a layer moves in the reservoir toward the producer wells and is broadened by longitudinal dispersion in the direction of movement. The combined tracer response from all the layers makes up the response curve of tracer concentration as a function of the cumulative volume of water injected or produced. The peak height, the breakthrough time and the shape of the produced tracer response curve can be computed from the quantity of tracer injected, the formation properties and the well pattern geometry.

The initial model was expanded by Abbaszadeh-Dehghani and Brigham, who presented analytical solutions of tracer breakthrough curves for a number of balanced patterns with a rigorous treatment of the effects of tracer dispersion [35].

The tracer response curves from all homogeneous and balanced patterns analysed by the authors can be correlated into a single curve using a dimensionless pore volume parameter ($V_{pD}$) given by:

$$V_{pD} = \frac{V_p - V_{pBT}}{1 - V_{pBT}} \tag{49}$$

Firstly, Abbaszadeh-Dehghani and Brigham found an analytical expression for the displacing fluid cut '$f_D$' for all the balanced patterns [35]:

$$f_D = 1 - \frac{1}{2}\left\{\exp\left[-1.810\left(V_{pD}\right)^{0.530}\right] + \exp\left[-0.715\left(V_{pD}\right)^{0.972}\right]\right\} \tag{50}$$

When a 'slug' of tracer with a pore volume equal to $V_{pT}$ and an initial concentration of $C_0$ is injected into a pattern, the effluent tracer concentration profile from the reservoir is the difference between two pattern breakthrough curves (in the absence of mixing or any other transport process). That is:

$$\frac{C}{C_0} = f_D(V_p) - f_D(V_p - V_{pT})$$

(51)

The mixing of a tracer with reservoir fluid during its transport through a porous medium is due partially to molecular diffusion and partially to mechanical or hydrodynamic dispersion. On the basis of experimental results, the effect of molecular dispersion on mixing in field tracer tests can be neglected with a good approximation. Also, it is possible to neglect the transverse mixing. Furthermore, to simplify the derivation of tracer mixing expressions without losing too much accuracy, mixing is considered to be related in a linear fashion to the interstitial pore velocity, $u$, so that the dispersion coefficient is:

$$K = \alpha u$$

(52)

Considering convection and hydrodynamic dispersion as the dominant transport processes, it is possible to write the tracer mass balance equation as:

$$K\frac{\partial^2 C}{\partial x^2} - u\frac{\partial C}{\partial x} = \frac{\partial C}{\partial t}$$

(53)

For a small slug tracer injection, whose length is infinitesimal compared with the distance between wells and defining a coordinate, $s$, along each streamline ($s$ replace $x$), the resulting solution is:

$$\frac{C(s,t)}{C_0} = \frac{\Delta s}{\sqrt{2\pi\sigma^2}}\exp\left[\frac{(s-\bar{s})^2}{2\sigma^2}\right]$$

(54)

where $\Delta s$ is the width of a stream tube occupied by an undiluted tracer slug at the distance, $\bar{s}$, and $\sigma$ is the variance of the tracer distribution profile that includes changes for mixing and the geometry of the stream tubes, where:

$$\sigma^2 = 2\alpha u^2(\bar{s}) \int_0^{\bar{s}} \frac{ds}{u^2(s)} \qquad (55)$$

For a given pattern geometry the tracer response curve from a homogeneous layer is a function of the Peclet number, $a/\alpha$, where $a$ is the distance between producers and $\alpha$ is the dispersivity of the formation. As an example, the concentration for a balanced five spot pattern is expressed by:

$$C(V_\mathrm{p}) = 0.577266\, C_0 F_\mathrm{r} \sqrt{\frac{a}{\alpha}} \int_0^{\frac{\pi}{4}} \frac{\exp\left\{-\dfrac{0.645776}{Y(\psi)} \dfrac{a}{\alpha} \left[V_\mathrm{pBT}(\psi) - V_\mathrm{p}\right]^2\right\}}{\sqrt{Y(\psi)}}\, d\psi$$

$$(56)$$

The $Y(\varPsi)$ term is a hyperelliptical integral that results from the mixing integral and $V_\mathrm{pBT}(\varPsi)$ is the pore volume injected at breakthrough of the streamline, $\varPsi$.

The $F_\mathrm{r}$ term is the tracer size expressed as a fraction of displaceable pattern pore volume:

$$F_\mathrm{r} = \frac{V_\mathrm{T}}{A\phi h S_\mathrm{w}} \qquad (57)$$

where

$V_\mathrm{T}$    is the tracer slug volume injected into the pattern;
$A$    is the area of the pattern;
$\varPhi$    is the porosity of the layer;
$h$    is the layer thickness;
$S_\mathrm{w}$    is the water saturation.

*IV.2.2.1.  Limitations of the method*

The model is based on a number of assumptions, mainly: (i) flow in parallel non-communicating aerially homogeneous layers, (ii) constant water saturation, $S_\mathrm{w}$, and (iii) regular and balanced patterns. These assumptions are acceptable in cases where they represent the situation of an ideal reservoir. By comparing the experimental tracer records with those of the Abbaszadeh-Dehghani and Brigham

model [35, 36], it is possible to derive how far the true situation deviates from the ideal one. Nevertheless, some additional considerations may be easily included in the model. The effects of adsorption and radioactive decay were analysed by Abbaszadeh-Dehghani [37]. Tracer partition between the water and hydrocarbon phases was considered by Tang [38].

### IV.2.3. Streamlines computation

The PORO software is based on principles similar to those reported by Abbaszadeh-Dehghani and Brigham [35, 36], but includes no regular and unbalanced injection patterns, anisotropic permeabilities and faults effects. The strategy is based on the computation of the streamlines and the numerical evaluation of the convection diffusion equations on each stream tube. In this process, the time is converted to frequency, employing Fourier transforms. All the numerical computations are made using FORTRAN.

It is considered that, in a mature secondary recovery project, only water is flowing and that the stationary state has been reached. Therefore, if there is a horizontal, homogeneous and non-isotropic layer, then the Darcy velocity components are [39]:

$$v_x = \frac{1}{2\pi h} \frac{K_{max}}{K_{min}} \sum_{j=1}^{N} q_j \frac{(x - x_{wj})}{C}$$

$$v_y = \frac{1}{2\pi h} \frac{K_{max}}{K_{min}} \sum_{j=1}^{N} q_j \frac{(y - y_{wj})}{C}$$

(58)

where

$$C = \left[ (x - x_{wj}) \cos\theta + (y - y_{wj}) \sin\theta \right]^2 +$$
$$\frac{K_{max}}{K_{min}} \left[ -(x - x_{wj}) \sin\theta + (y - y_{wj}) \cos\theta \right]^2$$

(59)

where

| | |
|---|---|
| $j$ | is the well index; |
| $N$ | is the number of wells; |
| $x$ and $y$ | are the spatial coordinates; |

189

$x_{wj}$ and $y_{wj}$     are the well coordinates;

$q_j$     is the water flow rate;

$h$     is the layer thickness;

$K_{max}$ and $K_{min}$ represent the permeabilities associated with the spatial principal directions;

$\theta$     is the angle between the principal and ordinary axes.

Equation (60) was obtained from the non-isotropic version of the Laplace equation:

$$K_{max}\frac{\partial^2 p}{\partial X^2} + K_{min}\frac{\partial^2 p}{\partial Y^2} = 0 \tag{60}$$

where $X$ and $Y$ are the spatial coordinates related to the principal axis.

When sealing faults are present, additional 'image wells' are included in Eq. (60) for confining the flux. The streamlines are computed from the Eq. (60), by solving:

$$v_x = \phi\left(\frac{\partial x}{\partial t}\right); \quad v_y = \phi\left(\frac{\partial y}{\partial t}\right) \tag{61}$$

where $\varPhi$ is the porosity. The boundary conditions at the beginning of each streamline are:

$$\left.\begin{aligned} x_i &= x_{wI} + r_{wI}\cos\left(\theta_i\right) \\ y_i &= y_{wI} + r_{wI}\sin\left(\theta_i\right) \end{aligned}\right\} \quad i = 1,2,...,N_{sl} \tag{62}$$

and, at the end of each streamline:

$$r_{wP} = \sqrt{(x_i - x_{wP})^2 + (y_i - y_{wP})^2}, \quad i = 1,2,...,N_{sl} \tag{63}$$

In Eq. (62),

$$\theta_i = i\frac{2\pi}{N_{sl}}$$

190
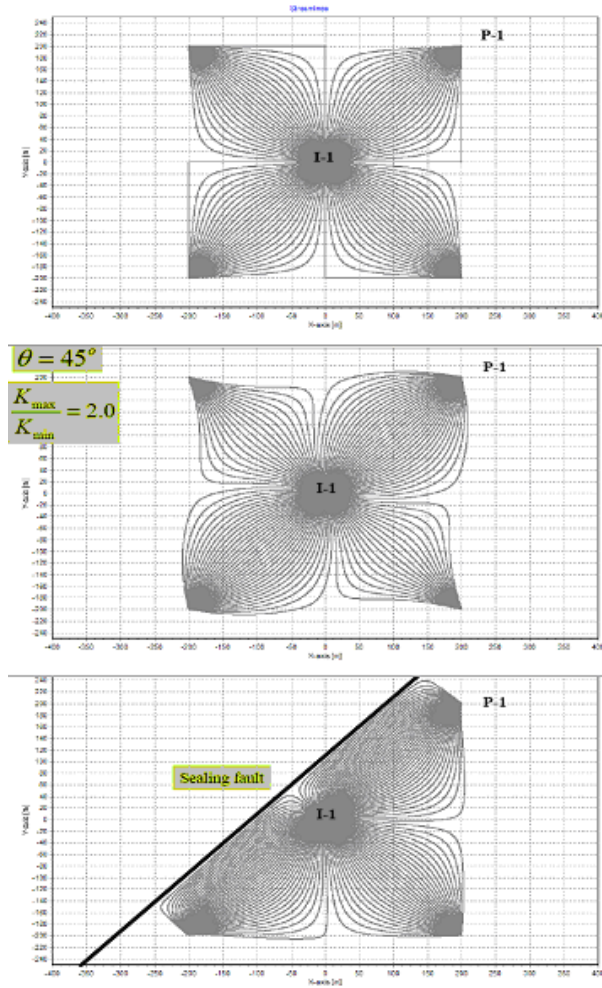
*FIG. 103. Streamlines generated by PORO.*

is the starting angle of the streamline (i), $N_{sl}$ is the number of streamlines, and $x_{wI}$ and $y_{wI}$ are the spatial coordinates of the injection well. In Eq. (63), $r_{wP}$ is the radius of the production well, and $x_{wP}$ and $y_{wP}$ are its spatial coordinates.

For illustrating the results, Fig. 103 shows the obtained streamlines of a five spot pattern for an isotropic, balanced case (above), non-isotropic balanced case (half) and sealing fault case (under).

*IV.2.3.1. Tracer transport*

On each streamline, the tracer transport problem can be considered as one dimensional. Hence, a new spatial coordinate, $s$, (along each streamline) must be defined, satisfying:

$$v_i = \phi \left( \frac{ds_i}{dt} \right); \quad i = 1, 2, ..., N_{\text{sl}} \tag{64}$$

with the boundary condition: $s_i(0) = 0$.

As in the Abbaszadeh-Dehghani and Brigham model, the convection diffusion equation governs the tracer transport along each streamline:

$$\phi \frac{\partial C_i}{\partial t} + v_i \frac{\partial C_i}{\partial s_i} = \alpha_{\text{L}} v_i \frac{\partial^2 C_i}{\partial s_i^2}; \quad i = 1, 2, ..., N_{\text{sl}} \tag{65}$$

where $\alpha_{\text{L}}$ is the longitudinal dispersivity.

By considering that $C(s, \omega)$ is the Fourier transform of $C(s, t)$:

$$C(s, \omega) = \frac{1}{\sqrt{2\pi}} \int_{-\infty}^{+\infty} C(s, t) e^{-i\omega t} dt \tag{66}$$

and taking into account the fundamental property:

$$i\omega C(s, \omega) = \frac{1}{\sqrt{2\pi}} \int_{-\infty}^{+\infty} \frac{\partial C(s, t)}{\partial t} e^{-i\omega t} dt \tag{67}$$

it is possible to write the Eq. 67 as:

$$\alpha v(s) \frac{\partial^2 C(s, \omega)}{\partial s^2} - v(s) \frac{\partial C(s, \omega)}{\partial s} - i\omega \phi C(s, \omega) = 0 \tag{68}$$

Converting the spatial variable, $s$, in a discrete form:

$$C_i = C(i\Delta s, \omega) \approx C(s, \omega) \tag{69}$$

the first spatial derivative can be written as:

$$\frac{\partial C(s,t)}{\partial s} = \frac{1}{\Delta s} C(s+\Delta s,t) - \frac{1}{\Delta s} C(s,t) \approx \frac{1}{\Delta s} C_{i+1} - \frac{1}{\Delta s} C_i = \left(\frac{\partial C}{\partial s}\right)_i \tag{70}$$

and the second spatial derivative:

$$\frac{\partial^2 C(s,t)}{\partial s^2} = \frac{1}{\Delta s}\left(\frac{\partial C}{\partial s}\right)_{i+1} - \frac{1}{\Delta s}\left(\frac{\partial C}{\partial s}\right)_i$$

$$\approx \frac{1}{\Delta s^2} C_{i+2} - \frac{2}{\Delta s^2} C_{i+1} + \frac{1}{\Delta s^2} C_i = \left(\frac{\partial^2 C}{\partial s^2}\right)_i \tag{71}$$

Finally, it becomes:

$$\alpha v(s)\left(\frac{1}{\Delta s^2} C_{i+2} - \frac{2}{\Delta s^2} C_{i+1} + \frac{1}{\Delta s^2} C_i\right) - v(s)\left(\frac{1}{\Delta s} C_{i+1} - \frac{1}{\Delta s} C_i\right)$$

$$- i\omega\phi C_i = 0 \tag{72}$$

and:

$$C_i = \frac{\left(2v(s)\alpha + v(s)\Delta s\right)\cdot C_{i+1} - \alpha v(s)\cdot C_{i+2}}{\alpha v(s) + v(s)\Delta s - i\omega\phi\Delta s^2} \tag{73}$$

The input boundary condition (in the Fourier domain) is:

$$C(0,\omega) = f(\omega) = \frac{\sqrt{2}C_0 e^{-i\omega T/2}}{\omega\sqrt{\pi}} \sin\frac{\omega T}{2} \approx C_1 = f(\omega) \tag{74}$$

where $C_0$ is the pulse height and $T$ its lifetime.
At the output, a 'flow' condition was imposed:

$$\frac{\partial C(L,\omega)}{\partial s} = \frac{1-k}{\alpha} C(L,\omega) \approx \frac{1}{\Delta s} C_N - \frac{1}{\Delta s} C_{N-1} = \frac{1-k}{\alpha} C_{N-1} \tag{75}$$

where $N$ is the greatest value taken by the index, $i$.

This equation can be written as:

$$C_{N-1} = \frac{C(N)}{f(k)}, \quad f(k) = 1 + \frac{(1-k)\Delta s}{\alpha} \tag{76}$$

By solving these equations, it is possible to obtain the $C(L,\omega)$ for each streamline. After this, by composing the individual responses and returning to the time domain, the program obtains the complete tracer response.

To illustrate the final result, Fig.104 shows the tracer records (expressed as daily fractional recovery) of a five spot pattern (for an isotropic balanced case). It can be seen how the layer thickness controls the breakthrough, the peak position and the broadness of the tracer records.

Dispersivity controls the breakthrough, the broadness and, to a slight extent, the peak position of the tracer records. The effect of anisotropy (for wells along the direction of $K_{max}$) is opposite to that of the dispersivity. While increased dispersivity results in greater peak width, increased anisotropy reduces the peak width. Figure 105 illustrates the tracer records for an isotropic case and a non-isotropic case.
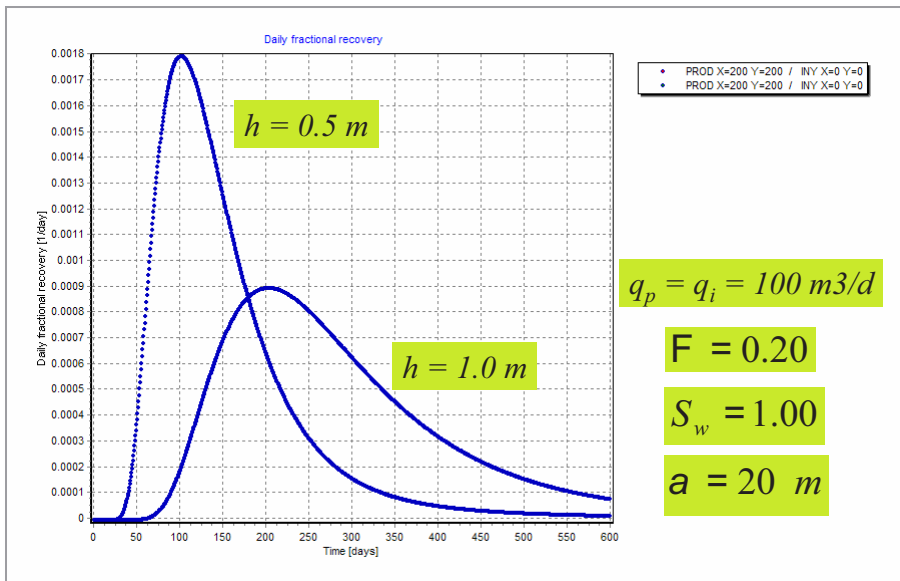


FIG. 104. Daily fractional recovery of a five spot pattern (for an isotropic balanced case). Influence of layer thickness.
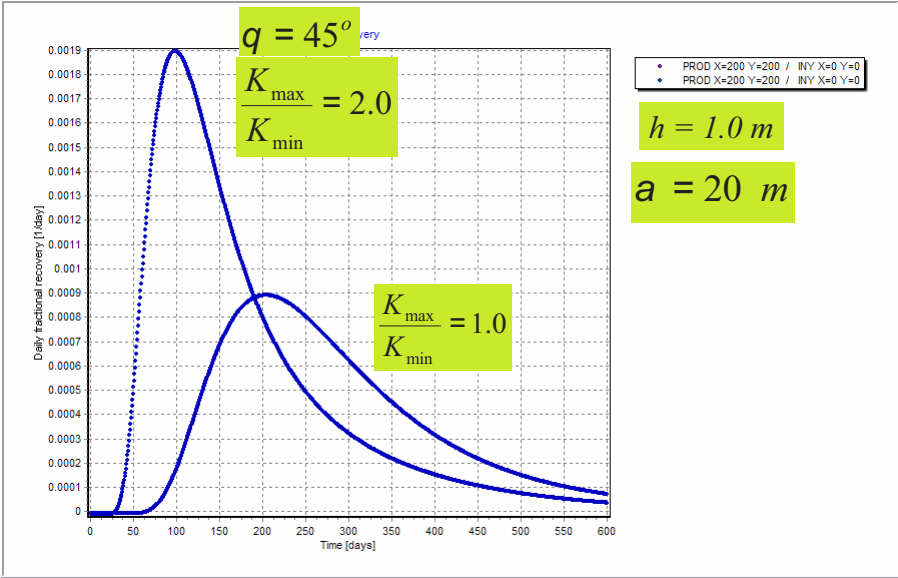
*FIG. 105. Daily fractional recovery of a five spot pattern (for a non-isotropic balanced case). Influence of $K_{max}/K_{min}$.*

Additionally, the presence of a sealing fault enhances the injection water support in the producers located in the same fault block as the injector, especially in the wells along the fault (e.g. P-1 in Fig. 106).

The effect on the daily tracer recovery is similar to that caused by anisotropy (on well P-1), giving earlier breakthrough and peak position, but reducing the peak width. Finally, sometimes the lack of tracer (or the scarce production of tracer) in a producer, may be the consequence of actions outside the involved injectors. As a consequence, the tracer daily fractional production in well P-1 is strongly reduced (Fig. 106).

### IV.2.4. PORO limitations

Although some limitations of the original models persist in PORO (flow in parallel no communicating areally homogeneous layers, constant water saturation, $S_w$, conservative tracer travelling jointly with the bulk water flow and steady state flow) it constitutes an advancement in the sense that it incorporates very common aspects of the reservoirs, such as non-regular unbalanced patterns, anisotropy and sealing faults. Also, it is important to highlight that the model may be easily extended for incorporating adsorption, radioactive decay and tracer partitioning in the same way as in the Abbaszadeh-Dehghani and Brigham model
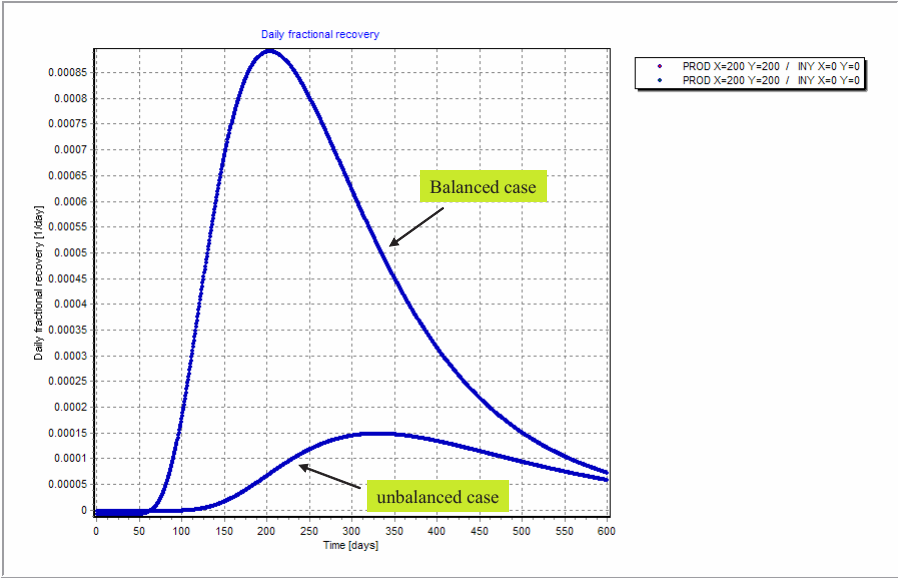
*FIG. 106. Daily fractional recovery of well P-1 with balanced and unbalanced conditions.*

[35, 36] and also it can incorporate the transport of tracers in stationary gas flow [40].

## IV.2.5.  PORO: Installation and use

*IV.2.5.1.  Installation*

Installation is an almost automatic process. In the CD there is an 'auto run' file that starts installation some seconds after having inserted the disk in the CD drive. However, in case this file does not work properly, installation can be started by clicking in the Windows start menu at the 'run' option. Then browse for CD drive and the 'setup.exe' file. Accepting will force the installation sequence to start.

The set-up software has been written in Spanish but most steps are performed without human participation. First of all, eight auxiliary files are copied from the CD to the hard disk in order to prepare installation. Once files have been copied, the 'welcome' window appears, recommending closure of any open application.

Instalación de PORO TracerSim 2.0 (english)
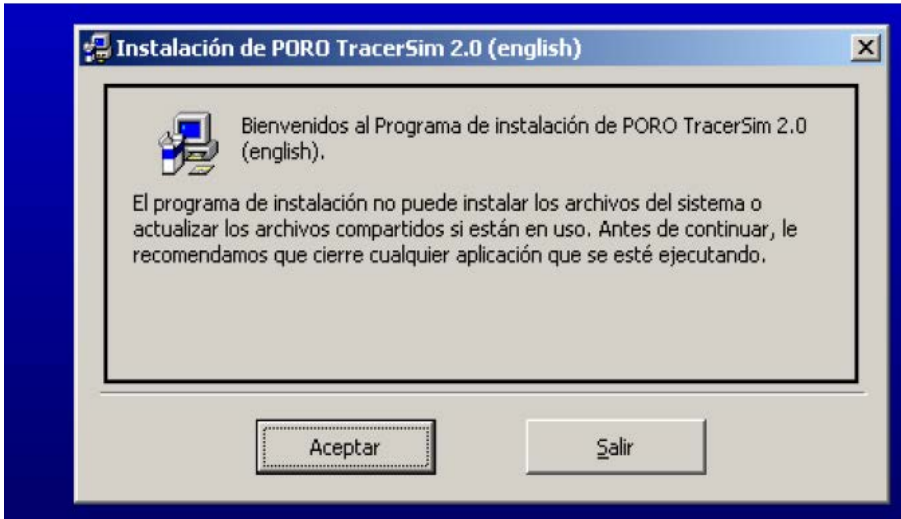
After accepting, the installation windows open. To install PORO TracerSim 2.1 in the default folder, click on the icon, otherwise click in the Cambiar directorio button.



Instalación de PORO TracerSim 2.0 (english)
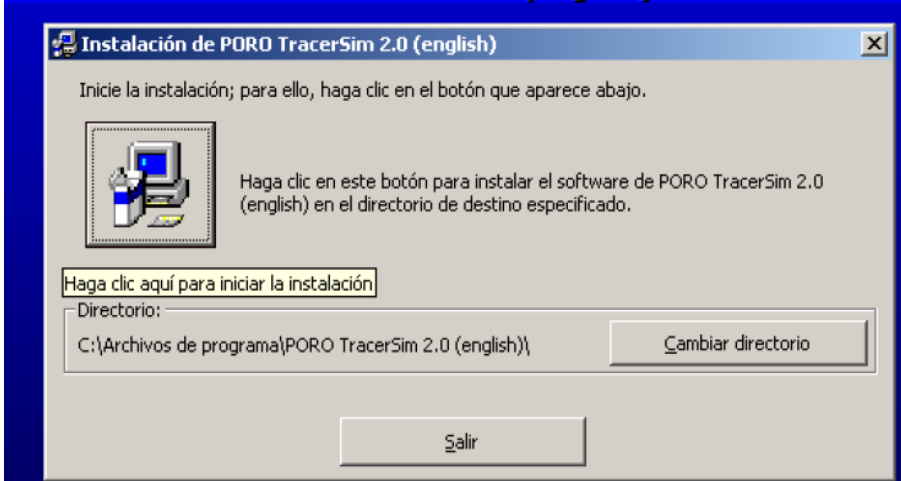
- The first step is to select a program group for adding a shortcut for PORO TracerSim.
- The second step is the installation itself. An advance bar is shown.
- Finally, a new window appears indicating that installation was completed successfully.

To remove PORO TracerSim 2.1, open the control panel and select Add or Remove program options and follow the instructions.

*IV.2.5.2. How to use PORO 2.1*

What is the work space?
PORO TracerSim allows use of a work space, that is, the field in which the wells and faults are inserted. Its definition is simple, only the coordinate limits of the area of interest need be entered in the text boxes.
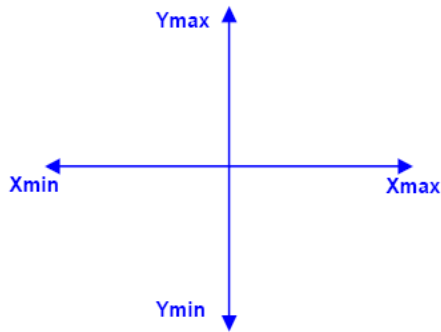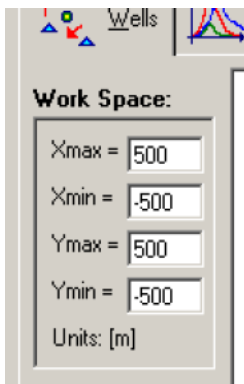


While working, the work area may be modified as required.
Another way to modify the work space is by clicking the Setup menu and then on the calculation and graph parameters, or directly by clicking the following icon.

Help
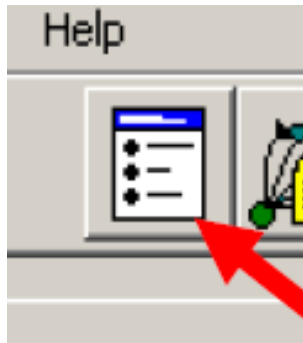
The following dialog box will be shown where the values of the work space can be changed.

**Calculation and Graph parameters**
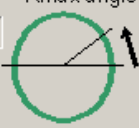
**Problem parameters:**

Dispersivity = 7    [m]    Porosity = 0.2

Water saturation [SW] = 1

Injected mass of tracer = 100    [Kg]    Tracer
○ Chemical
○ Radioactiv

Injection time = 0.5    [days]

Thickness = 1    [m]

Permeabilities relationship = 1
   [r = Kmax/Kmin]

Kmax angle = 0    [º]

Kmax angle

**Work space:**

Xmax = 500
Xmin = -500
Ymax = 500
Ymin = -500
Units: [m]

**Time answer:**

Number of points = 1000

Initial time = 0
Final time = 1000
Units: [days]

**Frequency setup:**

wi = 0.0001    [1/day]    Steps by decade = 100
wf = 1    [1/day]    Equalizer = 1

How are the wells inserted?

To insert a well, either PRODUCTOR or INJECTOR, the corresponding icon of the bar of elements on the left side of the screen should be selected.
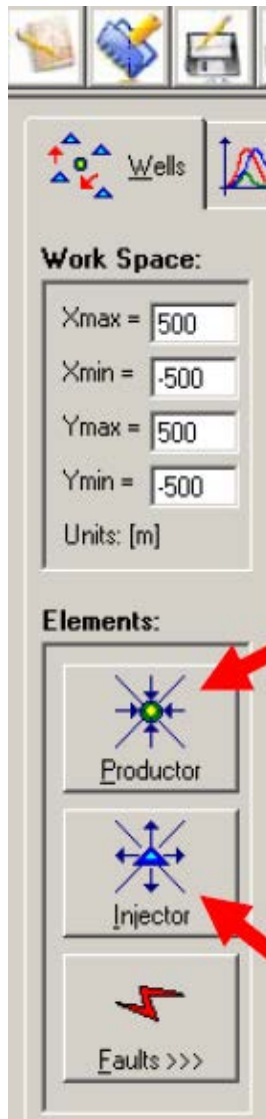
Then a dialog box appears where the following data must be entered:

- Well flow rate (without +/-, the program set depends on whether the well is PRODUCER or INJECTOR);
- Position in X;
- Position in Y.



It is not necessary to enter the X and Y positions with the keyboard, the mouse can be used anywhere in the field or work space and the values in the dialog box will change automatically. The coordinates of the mouse pointer in the position indicator can be followed.
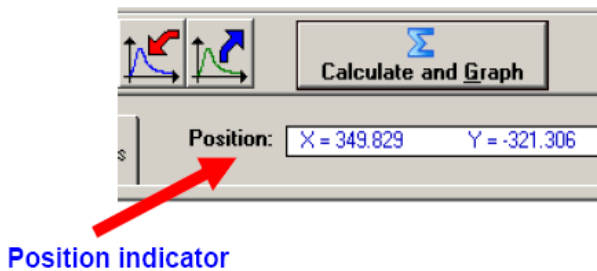


Once writing values, click on the Accept button, and the element will be inserted. In the field or work space an image appears in the corresponding place that allows selecting whether the well is a PRODUCTOR or an INJECTOR:

How to delete a well?

Right-click the corresponding image of the well to be deleted and then the menu appears by which the selected well can be eliminated.

How to amend the wells inserted?

To modify a well already inserted, click on the image of the well. The same table which was used to insert the well appears. This enables the values to be corrected, and then press Accept.

How are the faults inserted, modified and removed?

Click on the button Faults.[1]A list of inserted faults is now shown in the field or work space. By clicking on the New Fault button the following box appears.



Faults are inserted in a manner similar to the wells by writing the positions of two points that define the line of the fault in the following box. To use the mouse instead just click on Position X in the text box of POINT 1 and then click on the position of the field or work space. The values for X and Y will be written automatically.

To insert POINT 2, click on the Position X text box of POINT 2, and then perform the same operation as for the first point. The values can be changed at any time, until the right position is found. In the field or work space, the following image appears:



---
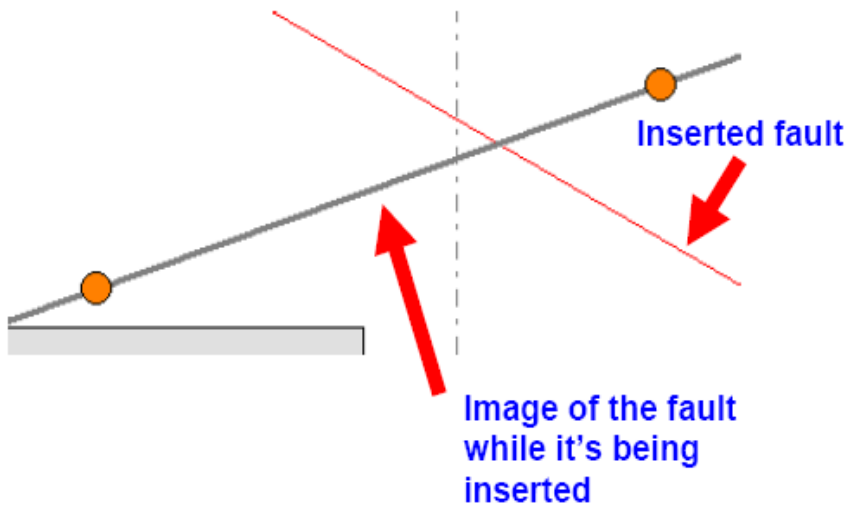
[1] It must be ensured that, prior to calculation, no wells are included behind the fault (or faults). PORO reserves this region for the 'image wells' (which are automatically generated by PORO).

To remove an already inserted fault, click on the corresponding fault in the list of faults and then on the Eliminate button in the same box.

To modify an already inserted fault, double-click on the corresponding fault in the list of faults, or select with a single click the fault, and click on the Modify button. A box appears similar to the one which appears when a new fault is being inserted. Only the values of the X and Y coordinates of both points defining the line of the fault should be modified. The mouse should be used in the same way as that for inserting a new fault.

**IV.2.6. Calculation and graph parameters**

Click on the Setup menu and then in calculation and graph parameters, the following dialog box will appear.



This allows the line thicknesses of curves to be modified. As explained above, also from here, new limits for the work space can be set. Further, it allows modification of streamlines and colours of the daily fractional recovery curves.

For the latter, another practice option is available. By clicking on the coloured squares which are in the Wells button on the left of the window, this can be done in a more practical way.
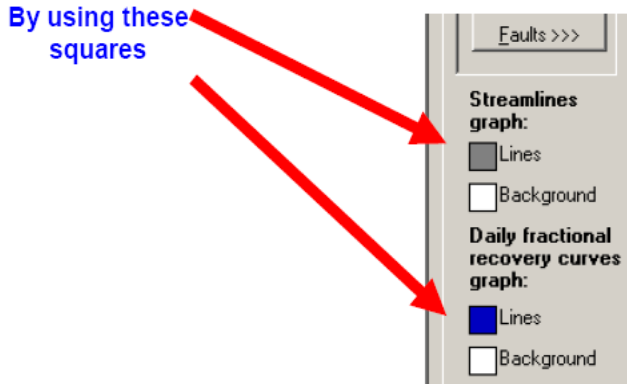


### IV.2.6.1.  Problem parameters

Here, the values of dispersivity and porosity must be entered. The injected mass of tracer and the time of injection must also be entered. The type of tracer to use can be either chemical or radioactive. There is another, more practical, way to amend the problem parameters, by clicking on the appropriate button.
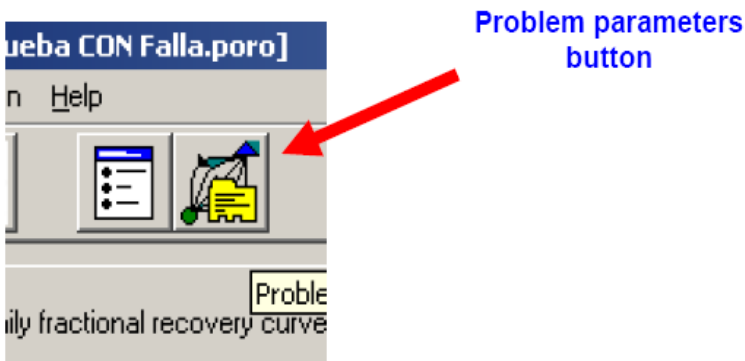
The following dialog box is where all the changes that are required can be made.
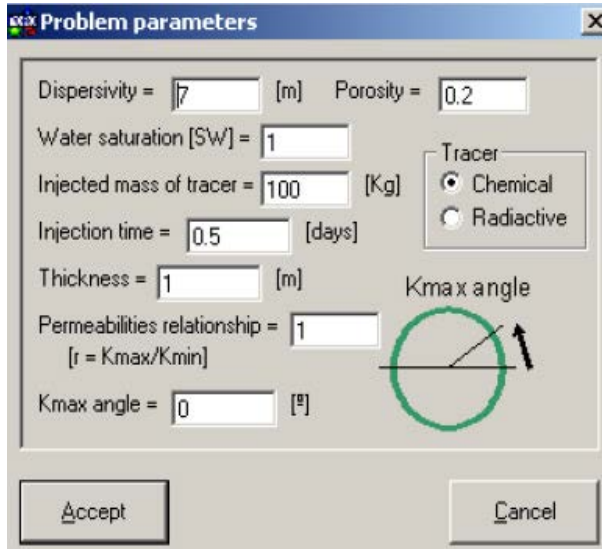


- *Streamline calculation*: Values required for defining the number of streamlines of the problem are the angle swept by them and the distance between two successive points on one line. It also requires the total number of points to be entered.
- *Time answer*: The range of times to be displayed in the daily fractional recovery curve is entered.
- *Frequency set-up*: These are values required by the program for the calculations. The method of calculation works in the frequency domain and these values are needed. By setting them, it is possible to find better solutions to the problem being considered.

How to calculate the daily fractional recovery curves?

Once all the elements (production wells, injection wells and faults) have been inserted, select a PRODUCTOR and an INJECTOR. A red square or circle around the element indicates that this element has been selected, as shown in the following image.
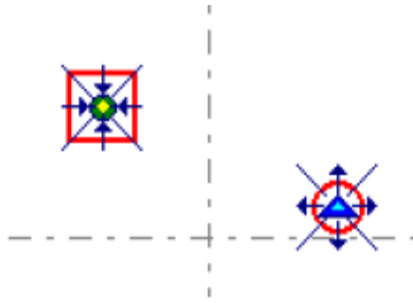
Note the difference between the production well (square) and the injection well (circle).

Verify that the parameters of the calculation are the correct ones and that the wells are not inserts on both sides of a fault (otherwise, incorrect values will be found on the other side of the fault).

Then click the Calculate and Graph button, to display a dialogue box that prompts whether to continue or not. Click Yes. The program will then begin to calculate the streamlines and the daily fractional recovery curves.
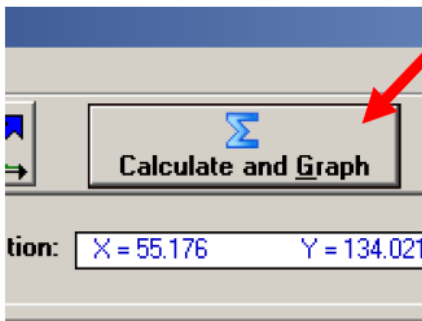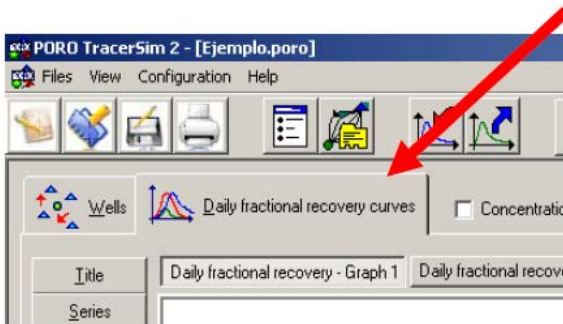
If you click on the Daily fractional recovery curves button, an image similar to the following will appear.
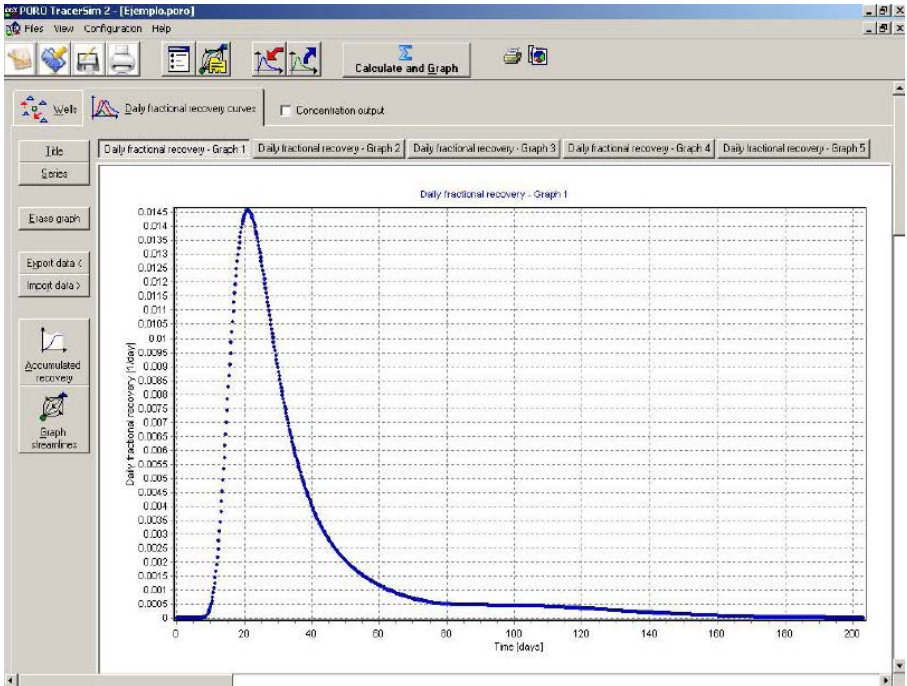


Notice that two icons appear in the toolbar. One allows printing and the other copying the image displayed on the screen.
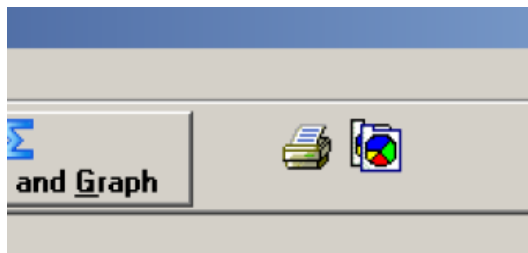
*IV.2.6.2. Multiple daily fractional recovery graphs*

See the upper section of the frame.
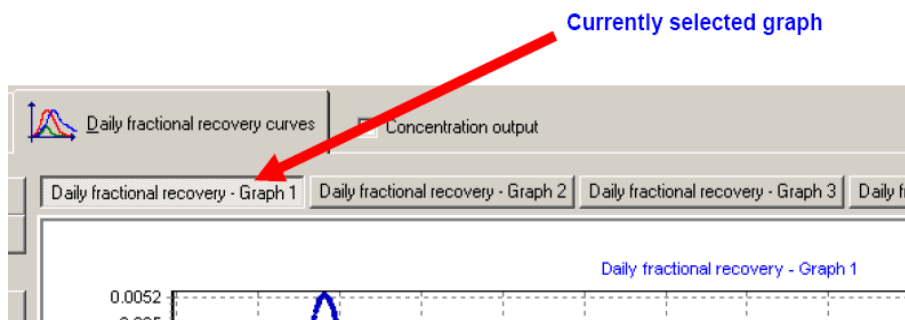


PORO TracerSim allows the creation of five different graphs. For example, if it is desired to calculate and show another daily fractional recovery curve of a different well, in another graph, then click on the Graph 2 button. Then return to the Wells button, and make the selection of the corresponding wells. Following a click on the Calculate and Graph button, a dialog box will be displayed that will give the option to continue or not. Click Yes. In this way, the program will begin to calculate the streamlines and the daily fractional recovery curves of the new well, and the result will be shown in Graph 2 (without erasing the other generated graphs).

*IV.2.6.3. Concentration output*

To show a concentration graph, click in the Concentration output checkbox.
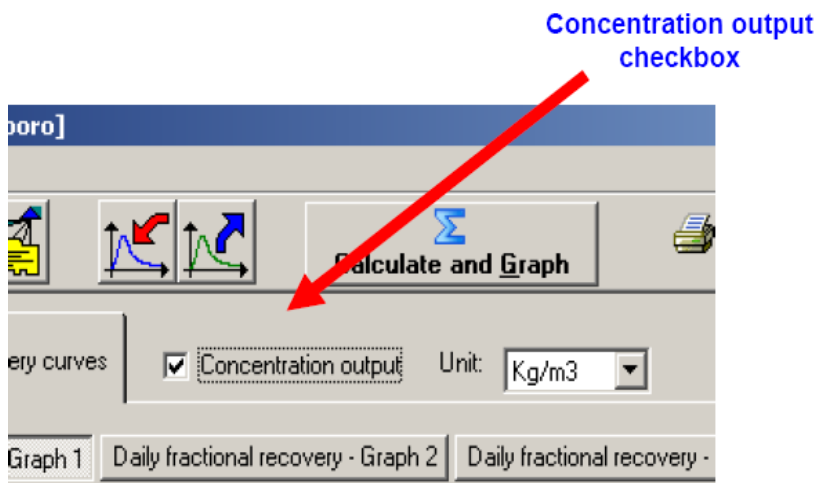
Note that PORO makes it possible to select and modify the unit of the output parameter. In this case, when the tracer is chemical, the unit is mass per unit volume. For a radioactive tracer, the unit will be in becquerel per unit volume.

### IV.2.6.4. Accumulated recovery

Once the daily fractional recovery curve has been drawn, then click on the Accumulated recovery button.
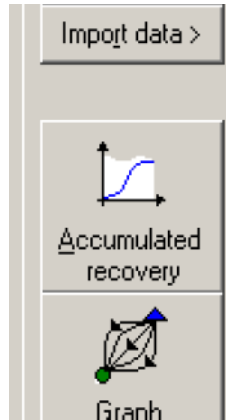


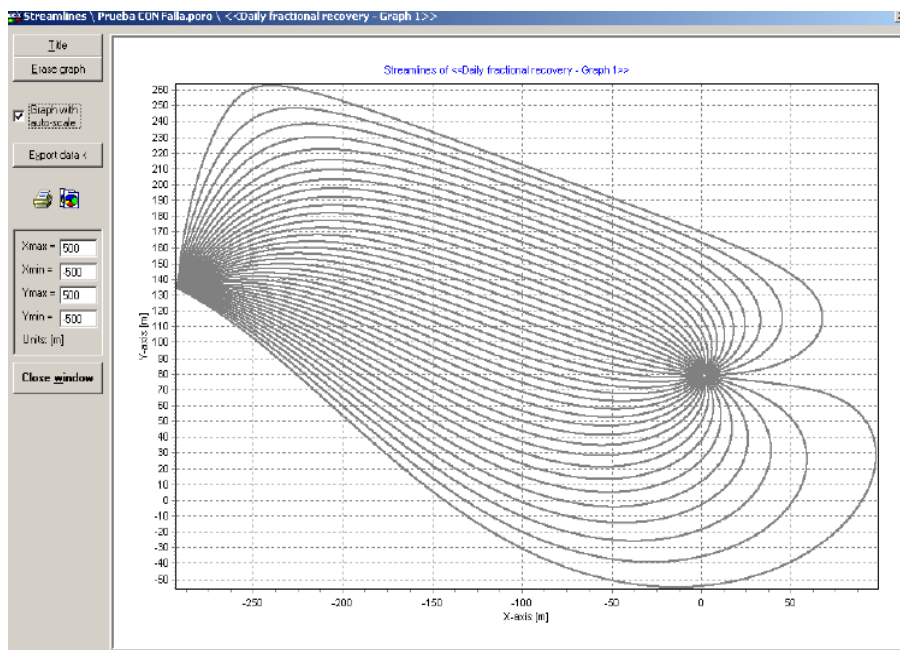The accumulated recovery will be shown in a special window, as shown below.
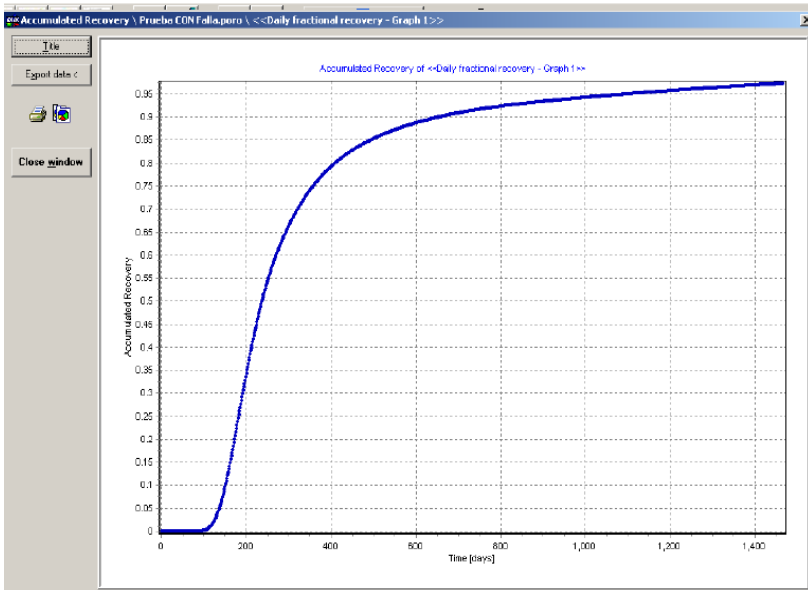
It is possible to copy or print an image of this window.

How to graph the streamlines?

To present a graph with the streamlines of the selected wells, click on the button Graph streamlines, as shown below.



Then, the streamlines will be presented in a window, as shown below.

New, Open, Save, Save as, Print

PORO TracerSim allows the creation of new documents, saving and printing them, in the same way as many other programs that run with the same operative system. The files with which PORO TracerSim works have the extension 'PORO'.

## IV.2.7. PORO software applicability

PORO is a semi-analytical simulator for tracer flux in an oil reservoir that supposes homogeneous and non-isotropic horizontal layers in which several vertical sources and sinks are present. The conceptual model is based on the analytical solutions of Darcy and convention diffusion equations. This simple model is more applicable than a more detailed one because of the high level of uncertainty in the reservoir description, especially after the water flooding in oil secondary recovery projects. The quality of the results was checked by comparing the simulator predictions with experimental results from laboratory and field exercises under different conditions.

How does PORO work?

The PORO simulator allows the evaluation of the principal parameters of the watered layers, by matching the experimental data on the basis of:

- A number of vertical injector wells (with arbitrary coordinates);
- A number of vertical producer wells (with arbitrary coordinates);
- Uniform water flow rates;
- Homogeneous horizontal layers;
- Non-lateral boundaries or sealing faults as boundaries;
- Anisotropy (the $K_{max}/K_{min}$ ratio and the direction of $K_{max}$ must be specified, $K$ being the permeability).

The PORO simulator works by taking into account:

- That the wells are 'vertical lines' sources or sinks (cylindrical geometry);
- Analytical solutions for the velocity field (and the superposition principle);
- The generation of the streamlines between each injector and the connected producers;
- The solution of the convection diffusion equation on each streamline and computing the overall concentration in each producer.

For solving the convection diffusion equation, PORO converts the time into frequency (by Fourier transform) and transforms the space into a discrete one along each streamline. Finally, a simple scheme of finite differences is employed.

The overall concentration is converted in daily fractional recovery of tracer (TDFR) that is defined as follows:

$$\text{TDFR} = \frac{1}{m_{\text{tracer-inj}}} \frac{\Delta m_{\text{tracer-rec}}}{\Delta t} = \frac{C_{\text{tracer-sample}} \cdot q_{\text{water-producer}}}{m_{\text{tracer-inj}}} \qquad (77)$$

Prior to starting the simulation, the following information has to be entered:

- The type (injector or producer) and the coordinates of the wells;
- The water flow rates of each well;
- The layer thickness, porosity and water saturation;
- The layer dispersivity (in oilfield scale, it is in the order of 10% of the distance between wells);
- The anisotropy ratio ($K_{\text{max}}/K_{\text{min}}$) and the direction of $K_{\text{max}}$;
- The sealing faults, if any;
- The time and frequency ranges (between 0.00001 and 1 for the conventional oilfield scale);
- The number of streamlines and the distance between consecutive points in each streamline.

Preparation of a software package for covering the tracer dynamics in all rock reservoir situations is a difficult, but necessary task. The most frequent cases include water stationary fluxes in which a conservative tracer moves in approximately horizontal and homogeneous layers (with simple primary porosity). These cases can be interpreted acceptably by the methods discussed here. Also, absorption, partition in the hydrocarbon phase, radioactive decay and tracers in stationary gas flows can be easily included in the models. However, it is very frequent to find cases in which the tracer moves in rocks with double porosity, particularly along conductive fractures [41–45]. Other anomalous cases are related to the tracer flow in 'wormholes', which are typical in unconsolidated sands and heavy oil reservoirs [46, 47]. Finally, it is necessary to include other geometries for covering 3-D flows and 2-D special cases, such as flow in horizontal wells.

conductive fault

Injector

Producer
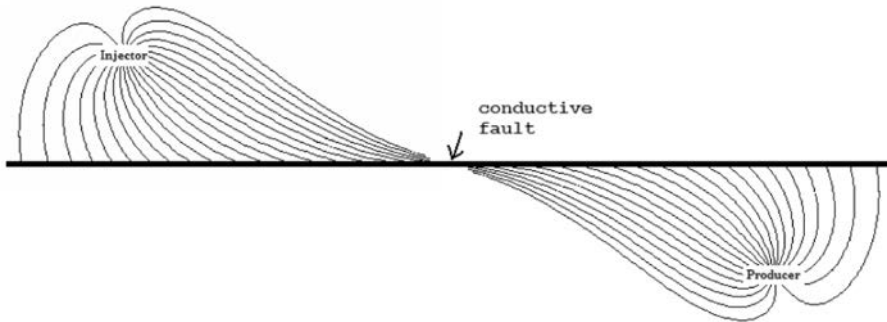
## IV.2.8. Validation of PORO

### IV.2.8.1. Interpretation of experimental field data

Some field tracer experimental data has been analysed using the PORO simulator. Some of them are described below as case studies. In all cases, the first step in the simulation was carried out under the following conditions:

- Residual oil saturation ($S_w = 1 - (S_{or} - S_{wi})$);
- Total layer thickness watered ($h = h_{max}$);
- Reported porosity;
- Nominal water flow rates;
- 100% tracer recovery;
- No faults;
- No anisotropy;
- Dispersivity equal to 10% of the distance between wells.

Case application 1: Carmopolis oilfield (Brazil)

The pattern is illustrated in Fig. 107. The layer thickness is 10 m, the porosity 17%, the water saturation 63%, the injection flow rate 83 m³/d and the injected activity 55.5 GBq.

In the first step of the simulation of well CP-1091, using the parameters reported by the oil company, it was observed that the simulated tracer breakthrough time was double the experimental value.

Additionally, the measured cumulative tracer recovery in the well was 55.33% (extrapolated to 60%) instead of the simulated value (43.80%). It is believed that this difference is due to the fact that the streamlines were too 'open' because only the water flow rates in the wells were taken into account in

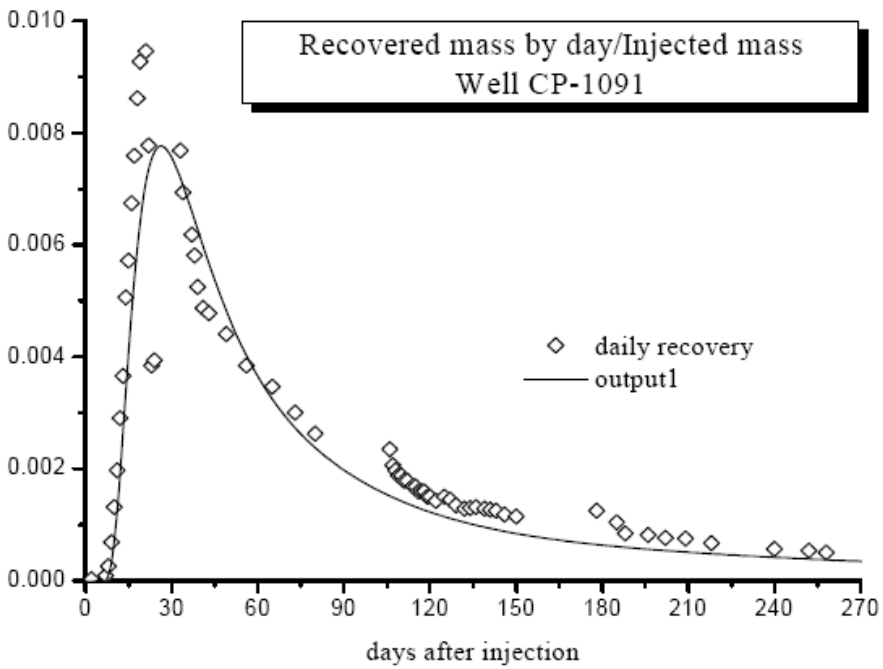FIG. 107.  CP-804 pattern (Carmopolis oilfield, Brazil).



FIG. 108.  Tracer records in the well CP-1091.

calculating their paths. Introducing modifications to confine the streamlines simulation became more realistic (Fig.108).

Thickness, water saturation and porosity values used in the second step of the simulation were provided by the company. The dispersivity value was in
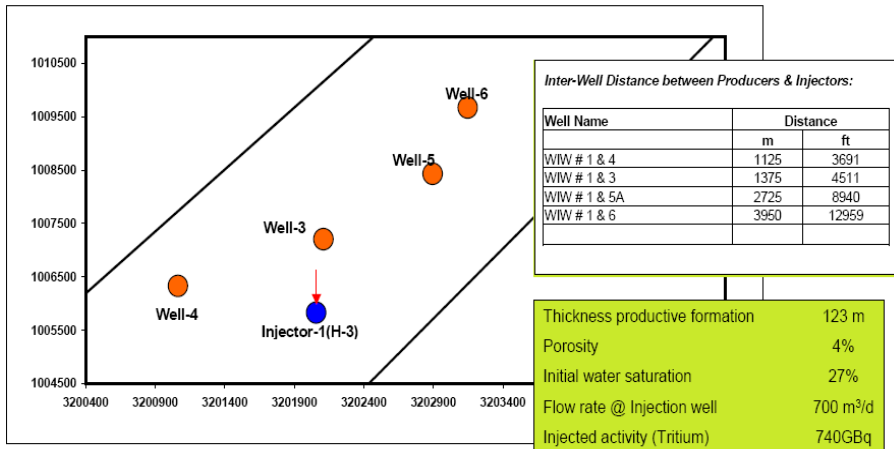
*FIG. 109. Well 1 pattern (Pindori oilfield, Pakistan).*

agreement with the criteria requiring that it must be equivalent to 10% of the distance between wells.

Case application 2: Pindori oilfield (Pakistan)

The pattern and the reservoir parameters are illustrated in Fig. 109. Up to day 150 after HTO injection, the only well in which tracer had been detected was well 3. On day 60, the injection conditions were modified, introducing strong perturbations in the tracer record. For that reason, only its non-perturbed portion was considered for this study.

Figure 110 shows both the experimental and the simulated tracer responses under the mentioned conditions.

The PORO simulator allowed an acceptable fit to the experimental records to be obtained by employing the reported injection water flow rate and the same water flow rates for all the producer wells. A layer thickness of only 0.35 m was used.

However, the simulation predicts a quick tracer breakthrough in well 4, which is not in agreement with actual tracer behaviour. Several reasons may be responsible for the lack of tracer detection in this well, such as different location of the fault, anisotropy and low water flow rate to the well. Additional information will be necessary for selecting the right scenario for this case.

Case application 3: Chinese oilfield

Figure 111 shows the pattern of injection and production wells where the tracer test was run.
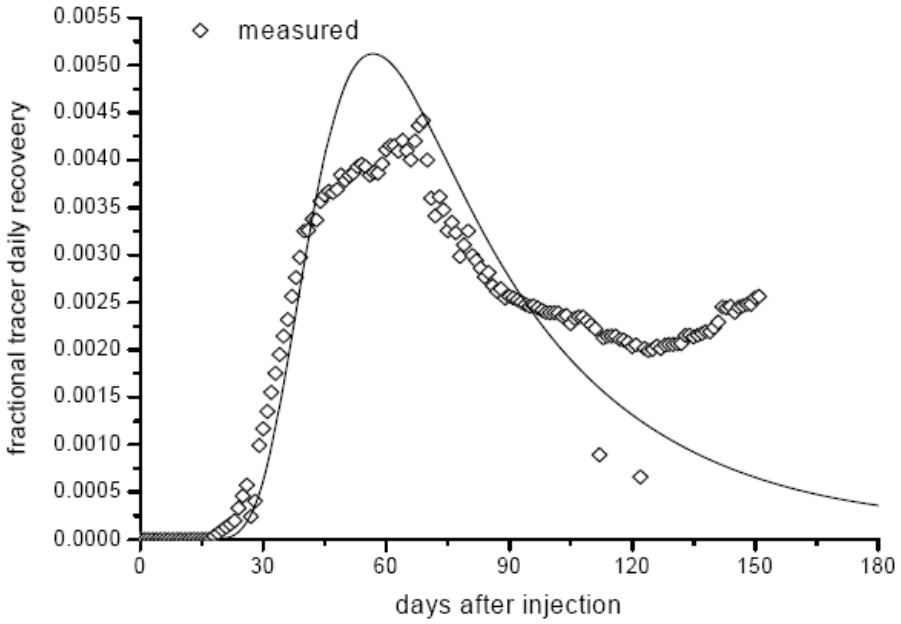
*FIG. 110. Tracer records in well 3.*



The selected injectors are the wells 20-2 and 21-3.

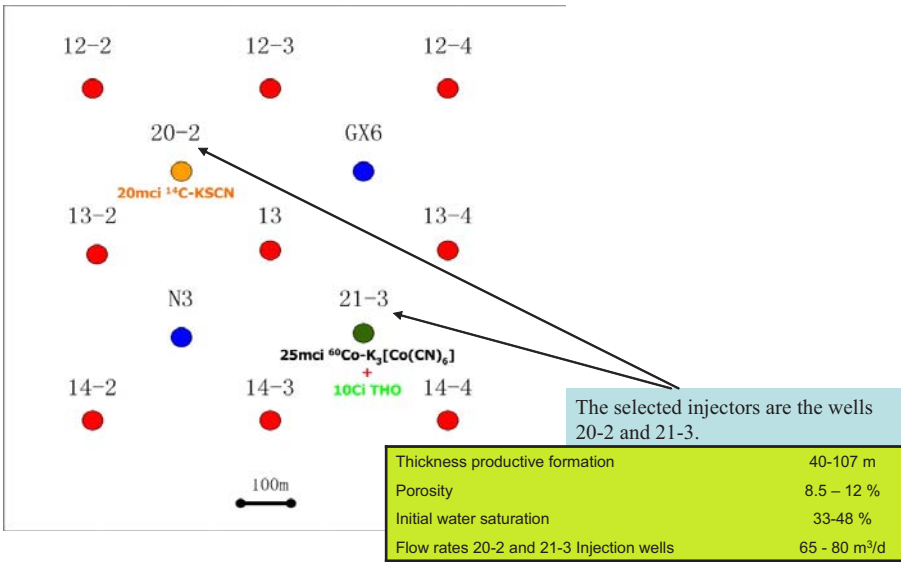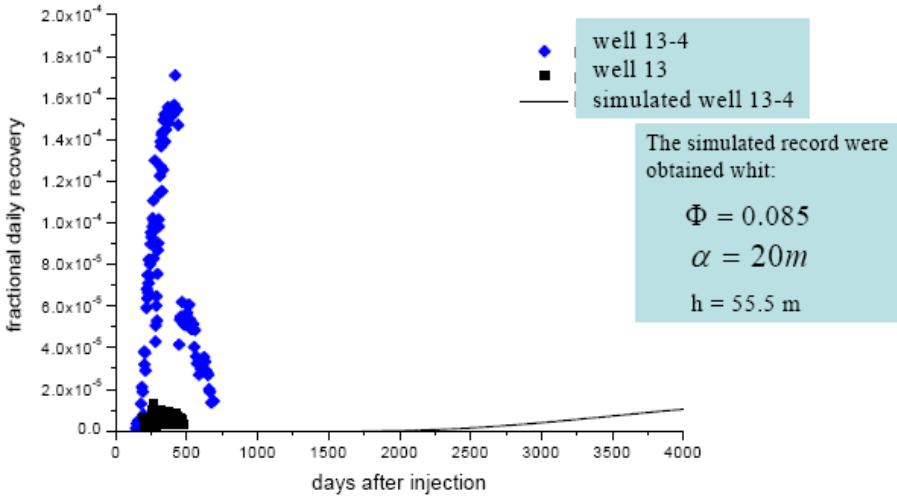| | |
|---|---|
| Thickness productive formation | 40-107 m |
| Porosity | 8.5 – 12 % |
| Initial water saturation | 33-48 % |
| Flow rates 20-2 and 21-3 Injection wells | 65 - 80 m³/d |

*FIG. 111. Wells 20-2 and 21-3.*

FIG. 112. Tracer records in well 21-3 mesh.

Up to two years after the tracer injection, only three wells had detected tracer breakthrough: wells 12-3, 13-4 and 13. The simulation for the well 13-4 using the parameters provided by the oil company is shown as a black line in Fig. 112.

To obtain a better fit to the experimental data of well 13-4, the layer thickness was reduced from 55.5 m to 3.2 m, resulting in the curve given in Fig. 113. However, the simulation predicted a very significant production of tracer in well 14-4, which did not occur.

A similar situation appears in the mesh of well 20-2. It is possible to fit the tracer record of well 13-3, but the simulator predicts significant tracer production in well 13-2, which is absent (Figs 114 and 115).

A scenario which assumes strong anisotropy along the direction between wells 21-3 and 13-4 (or wells 20-2 and 12-3) is proposed. However, in this case, in the simulation there is tracer production in wells 14-3 and 13-2 (tracer response was undetected in these wells). In consequence, the only way to avoid tracer production in wells 14-3 and 13-2 is to assume that the injectors located to the south of these wells have higher water injection rates.

For example, if the injection water flow rates of the injectors located to the south are duplicated, it is possible to obtain a good fit for the tracer record of well 13-4. A satisfactory fit of simulated response and experimental data (for wells 12-3 and 20-2) was obtained (Fig. 116).
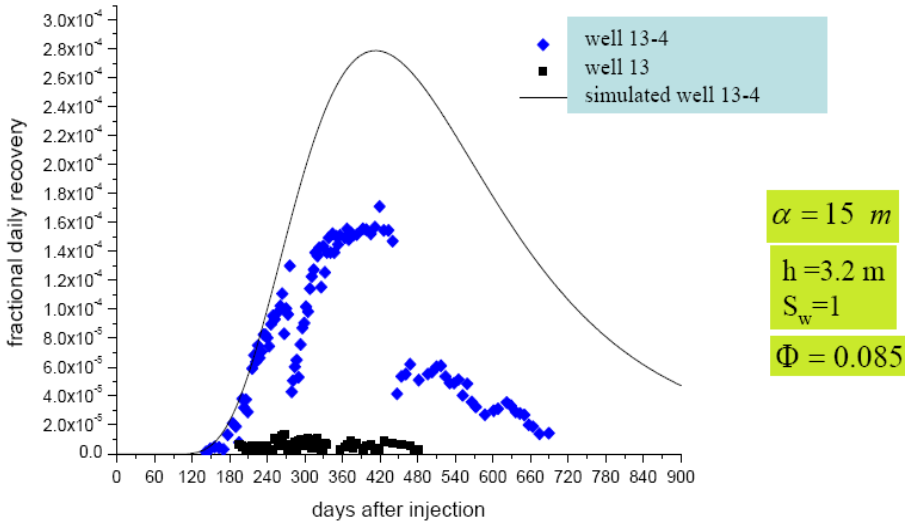
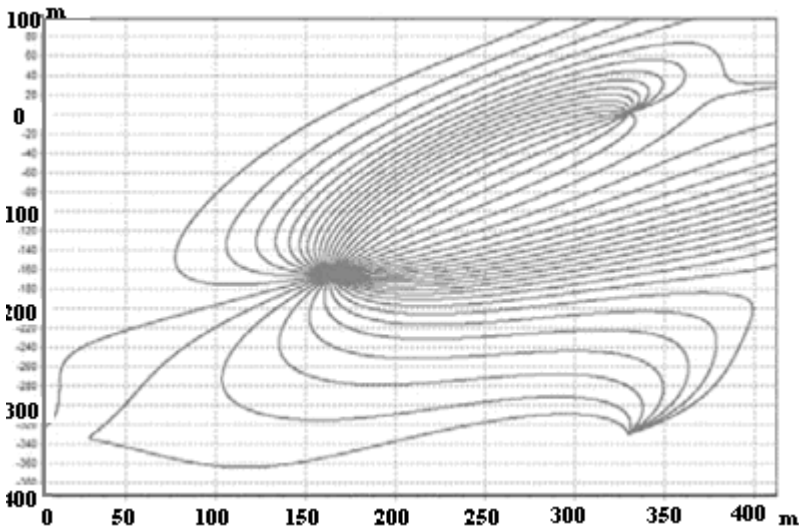*FIG. 113. Tracer records in the well 3 with the new, reduced, thickness layer.*
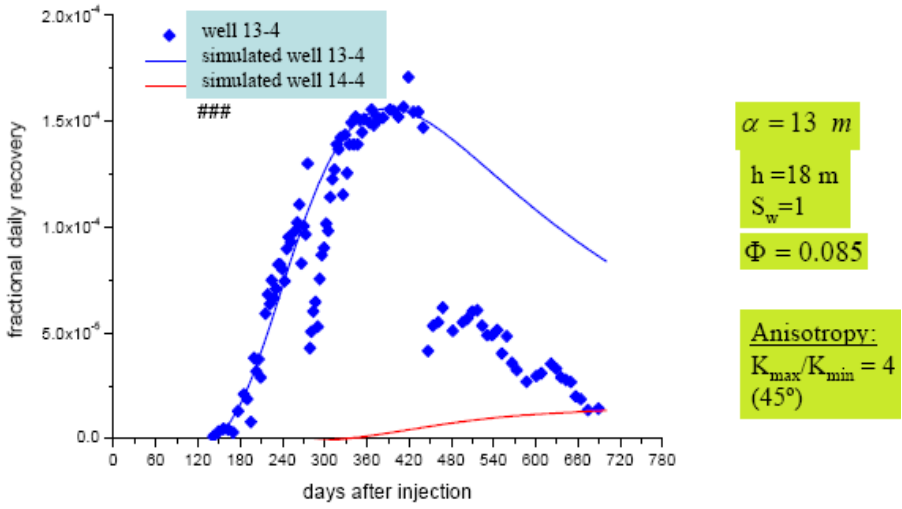


*FIG. 114. Streamlines in well 21-3 mesh.*

218

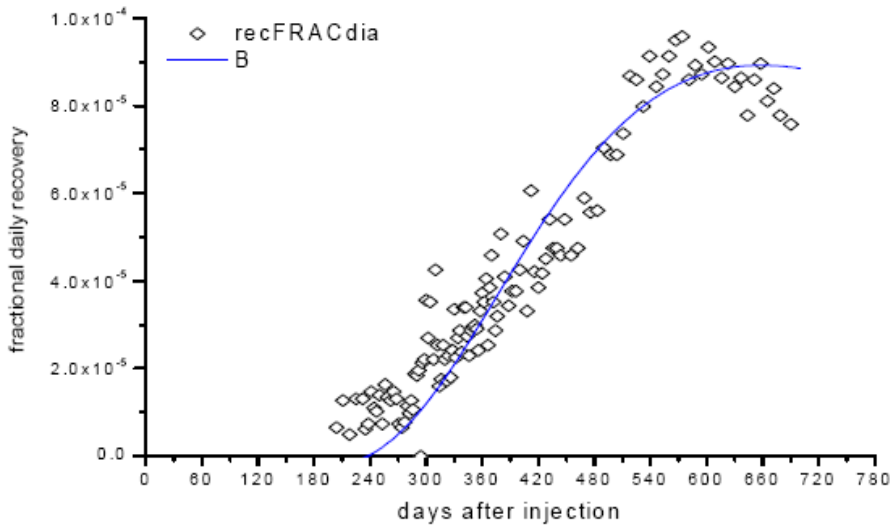FIG. 115.  *Experimental and simulated tracer records for well 13-4.*



FIG. 116.  *Experimental and simulated tracer records for well 12-3.*

219

Case application 4: Interpretation of tracer experiments in laboratory model of non-boundary conditions

*Introduction*

The interpretation of tracer experiments in interwell communications is much more complex than those obtained in industrial devices because oilfields and geothermal fields are non-boundary systems and little information about their internal structure is available; the curves are often incomplete, operating parameters change during the experiment and, finally, the percentage of tracer recovery is very low. In order to simplify the approach, an intercomparison of the software packages has been made on the experimental data obtained previously on a laboratory scale.

To achieve this purpose, the results from tracer experiments carried out in a laboratory model in the Commissariat à l'Energie Atomique in Grenoble, France, were used. To obtain the simulated tracer records the following conditions were considered:

- Water saturation ($S_w = 1$);
- Total layer thickness watered ($h = 0.8$ m);
- Reported porosity (0.35);
- Nominal water flow rates (injector: 107 mL/min, producers: 26.8 mL/min);
- Tracer recovery of 81.06% (in agreement with the reported values);
- No faults;
- No anisotropy;
- Dispersivity (estimated).

*Experimental set-up and data treatment*

The five spot set-up (Fig. 117) has been designed using a large rectangular vessel of 160 cm × 95 cm × 80 cm. It has been filled manually with sand with a density of 1.8 g/cm$^3$ and an average granulometry of 0.75 mm ($d_{10} = 0.5$ mm, $d_{50} = 0.75$ mm, $d_{90} = 0.90$ mm). The size of the five spot is only 40 cm square to avoid boundary effects with 5 wells of 40 mm diameter.

It should be noted that the studied five spot used to analyse this effect is not symmetrical. The bed of sand is initially saturated with water.

Four experiments have been conducted, three experiments with stagnant water inside the bed and flow rates of 107 cm$^3$/min (exp. 1), 107 cm$^3$/min (exp. 2), 184 cm$^3$/min (exp. 3) at the injected wells. The fourth experiment has been conducted with a linear velocity of the water table of 2 m/d. The experimental data treatment has been revised; curves have been time and area
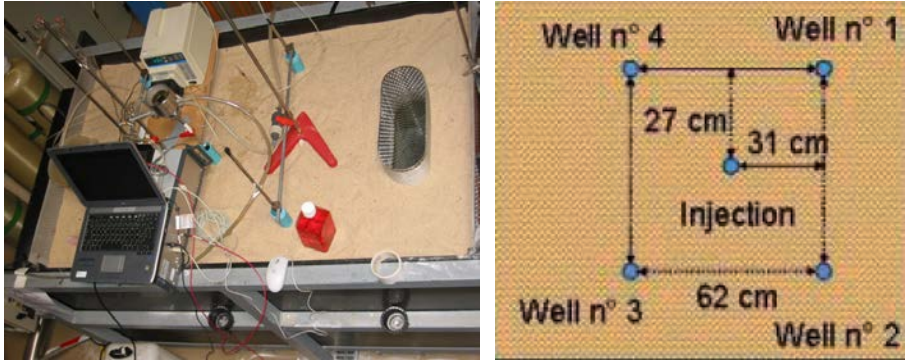
*FIG. 117. Photo and scheme of the five spot set-up.*
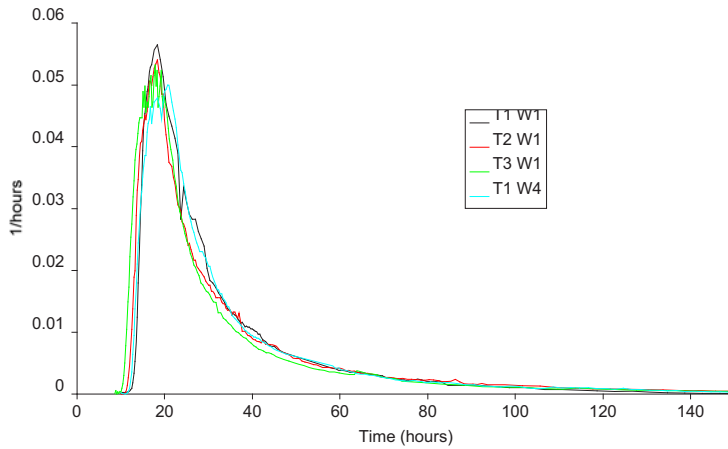


*FIG. 118. Superposition of time and area normalized tracer curves obtained for well 1 for three experiments and well 4 for one experiment.*

normalized in order to overcome the apparent discrepancy due to the non-homogenous radial injection. It should be noted that interpretation of tracer experiments in oilfields should take into account the near impossibility of having uniform radial distribution of the tracer injection. In some extreme cases, this may explain the low tracer recovery observed.

Figure 118 shows the superposition of the tracer responses at well 1 for the three static experiments and one of the curves obtained for well 4.

*FIG. 119. Comparison between experimental data and simulations obtained with PORO.*
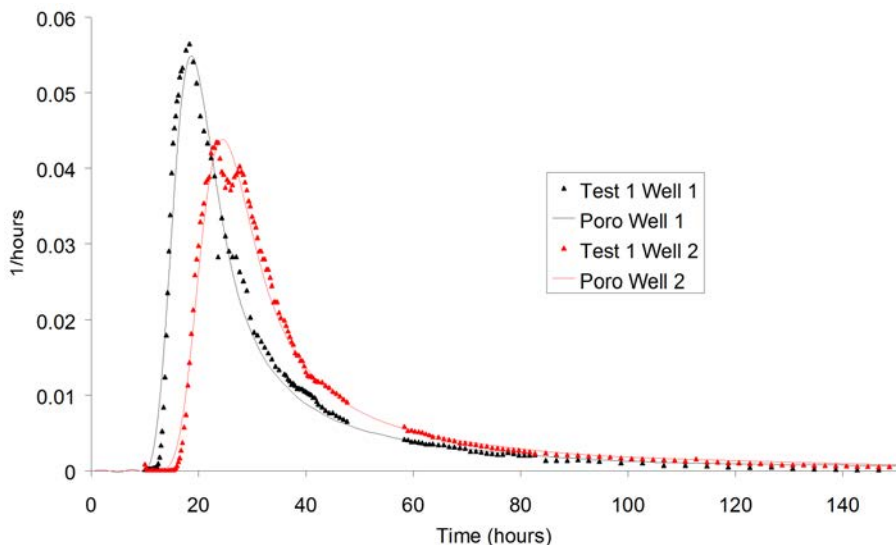
*Intercomparison of models and software packages*

Four models and/or software packages have been tested, the Brigham model, PORO software (Streamlines approach), and the simple diffusion model using two different CFD software packages (Comsol and Castem).

PORO software was used successfully to simulate the experimental data. Figure 119 shows the good agreement obtained for wells 1 and 2. These simulations permitted the estimation of the porosity of the sand bed as 40%. The dispersivity was estimated to be 6 mm, this value being consistent with the characteristic of the sand bed.

Figure 120 shows the good agreement between experimental data and CFD simulations using the two CFD codes (Castem CEA made, 'finite element toolbox' and Comsol multipurpose finite element package, Comsol group, Sweden). However, it should be pointed out that the CFD code will be time consuming and more difficult to use for actual complex oil field simulations.

Finally, Fig. 121 shows comparison between the PORO and Brigham models, with several dispersivities (from 1 to 100 m) for a five spot configuration. If the tendencies of the two models are similar, the dispersions of the curves are different due to the original hypothesis of the two models.
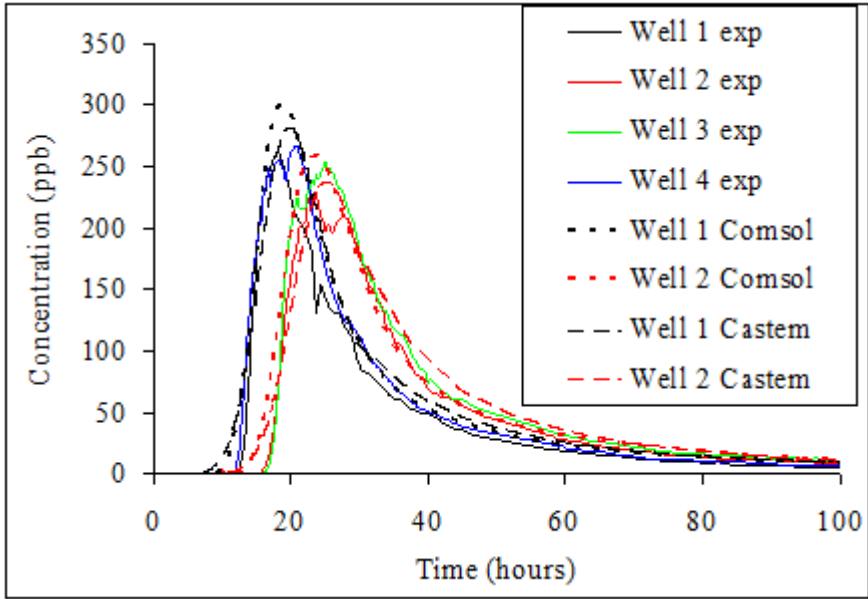
FIG. 120. Comparison between CFD code simulations using Castem and Comsol and experimental data.
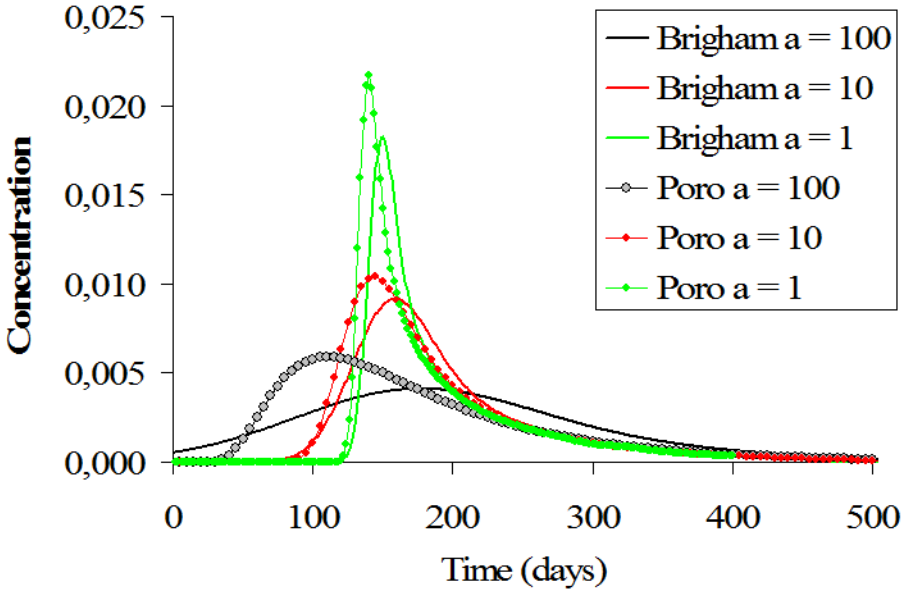


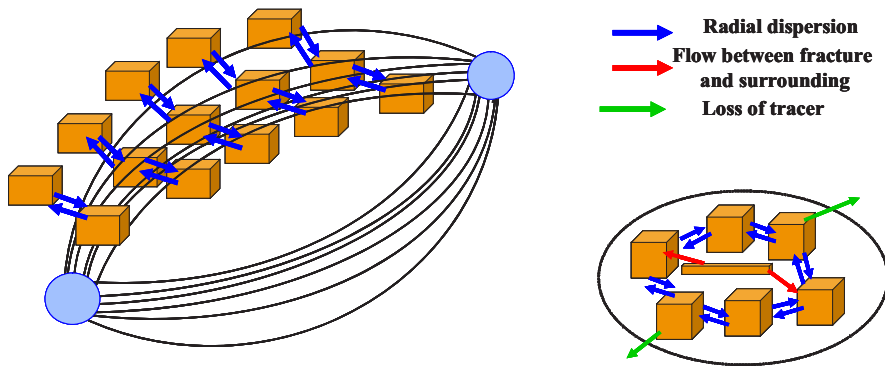FIG. 121. Comparison between the Brigham model and PORO simulations.

FIG. 122. Theoretical example of a 'compartmental model' in the case of a fracture surrounded by porous media zones with different characteristics.

*Classical chemical engineering approach applied to oilfield*

The residence time distribution method is used largely for modelling classical chemical engineering vessels and reactors. The classical chemical engineering approach may be adapted for oil field tracer experiment interpretations. Some attempts have been made using the residence time distribution software (DTSpro) to verify how it can be used for non-boundary systems and low tracer recovery. In practice, the software package may be used but it is not well adapted to the problem. The elementary bricks available are representative of simple flow: dispersive flow and dispersive flow exchanging with the porous zone of lower velocity, but the parameters are not directly correlated with the usual parameters used by oilfield engineers. Moreover, the artifact used to take into account the loss of tracer is complex; it is not recommended for such an application. On the other hand, the recent approach of the compartmental model derived from both CFD and residence time distribution is promising. It consists of structural and functional descriptions of the studied structure (CFD is only a structural description with a mesh and DTSpro is used as a functional description of the structure with a network of elementary behaviours).

Figure 122 shows an academic example of such a model. The advantage of such a model is that it is derived from results from several models (PORO for the streamline network, CFD, information about fracture). In a first step, the user should define an elementary 'slice' based on the internal structure of the oilfield, the exchange flow of major importance (radial dispersion, convection) and the boundary layer continuity rules. It is then necessary to calculate the flows

between the different parts and the number of slices simultaneously by an iterative process and by fitting the tracer response.

*Conclusions*

Owing to the complexity of oilfields, experimental measurements of tracers have been carried out on the laboratory scale to test different models and/or software packages. It has been found that all software packages allow a reasonable representation of the experimental data. The CFD software required excessive knowledge of the internal structure of the oil field to be applied in actual situations. Moreover, most of the codes are commercial and expensive. The Brigham model is valid only for the simple configuration which required basic information (e.g. breakthrough time). The PORO software seems to be the most adapted tool at this time. It offers a good trade off between the necessity to take into account the complexity of the reality and the assumptions required by a lack of knowledge. The new approach of the compartmental models based on both structural and functional descriptions of the oilfield with a limited number of compartments seems to be promising and very well adapted to the fractured oilfields found in Vietnam.

# REFERENCES

[1]   WATKINS, J.W., MARDOCK, E.S., Use of radioactive iodine as a tracer in water-flooding operations, J. Petrol. Technol. **6** 9 (1954) 117.

[2]   FLAGG, A.H., et al., Radioactive tracers in oil production problems, J. Petrol. Technol. **7** (1955) 1.

[3]   BIRD, J.M., DEMSEY, J.C., How you can follow your flood?, World Oil **143** (1956) 152.

[4]   FEARON, R.E., Tritium — Newest tool for tracing reservoir flow, World Oil **145** (1957) 114.

[5]   BJORNSTAD, T., Selection of Tracers for Oil and Gas Reservoir Evaluation, Res. Rep. IFE/KR/E-91/009, Inst. Energy Technol., Kjeller (1991) 43.

[6]   BJORNSTAD, T., DUGSTAD, O., GALDIGA, C., SAGEN, J., "Interwell tracer technology in oil reservoirs: State-of-the-art", paper presented at TRACER 2 Conference on Tracers and Tracing Methods, Nancy, 2001.

[7]   BJORNSTAD, T., Recent and Current Oil Field Tracer Development for Interwell Application, Res. Rep. IFE/KR/E-95/002, Inst. Energy Technol., Kjeller, Norway (1995) 101.

[8]   BJORNSTAD, T., New Development in Tracer Technology for Reservoir Description, Res. Rep. IFE/KR/E-98/006, Inst. Energy Technol., Kjeller, Norway (1998) 24.

[9]   ZEMEL, B., Tracers in the Oil Field, Developments in Petroleum Science, Vol. 43, Elsevier Science, Amsterdam (1995).

[10]  BJORNSTAD, T., HAUGEN, O.B., HUNDERE, I.A., Dynamic Behavior of Radio-labelled Water Tracer Candidates for Chalk Reservoirs, J. Petrol. Sci. Eng. **10** (1994) 223.

[11]  WOOD, K.N., LAI, F.S., HEACOCK, D.W., "Water tracing enhances miscible pilot", paper presented at 65th Annual SPE Technical Conference, San Antonio, Tx (1989).

[12]  ROSE, P.E., BENOIT, W.R., KILBOURN, P.M., The application of the polyaromatic sulphonates as tracers in geothermal reservoirs, Geothermics **30** (2001) 617.

[13]  ROSE, P., CAPUNO, V., PEH, A., KILBOURN, P., KASTELER, C., "The use of the naphtalene sulfonates as tracers in high temperature geothermal systems", paper presented at 23rd PNOC-EDC Geothermal Conference, Makati City, Philippines (2002) 53.

[14]  ADAMS, M.C., et al., Hydrofluorocarbons as geothermal vapor-phase tracers, Geothermics **30** (2001) 747.

[15]  ADAMS, M.C. et al., Stability of Methanol, Propanol and $SF_6$ as High-Temperature Tracers, in Proc. of the World Geothermal Congress 2000, May 28 – June 10, Kyushu-Tohoku, Japan.

[16]  ADAMS, M.C., "Vapor, liquid and two-phase tracers for geothermal systems", paper presented at 1995 World Geothermal Congress, Florence, 1995.

[17]  LOVELOCK, B.G., Steam flow measurements using alcohol tracers, Geothermics **30** (2001) 641.

[18]    FOOD AND AGRICULTURE ORGANIZATION OF THE UNITED NATIONS, INTERNATIONAL ATOMIC ENERGY AGENCY, INTERNATIONAL LABOUR ORGANISATION, OECD NUCLEAR ENERGY AGENCY, PAN AMERICAN HEALTH ORGANIZATION, WORLD HEALTH ORGANIZATION, International Basic Safety Standards for Protection against Ionizing Radiation and for the Safety of Radiation Sources, Safety Series No. 115, IAEA, Vienna (1996).

[19]    FOOD AND AGRICULTURE ORGANIZATION OF THE UNITED NATIONS, INTERNATIONAL ATOMIC ENERGY AGENCY, INTERNATIONAL LABOUR ORGANISATION, OECD NUCLEAR ENERGY AGENCY, PAN AMERICAN HEALTH ORGANIZATION, WORLD HEALTH ORGANIZATION, Radiation Protection and the Safety of Radiation Sources, Safety Series No. 120, IAEA, Vienna (1996).

[20]    INTERNATIONAL ATOMIC ENERGY AGENCY, INTERNATIONAL LABOUR OFFICE, Occupational Radiation Protection, IAEA Safety Standards Series No. RS-G-1.1, IAEA, Vienna (1999).

[21]    INTERNATIONAL ATOMIC ENERGY AGENCY, Regulations for the Safe Transport of Radioactive Material, IAEA Safety Standards Series No. TS-R-1 (ST-1, Rev.), IAEA Vienna (2000).

[22]    FOOD AND AGRICULTURE ORGANIZATION OF THE UNITED NATIONS, INTERNATIONAL ATOMIC ENERGY AGENCY, INTERNATIONAL LABOUR ORGANIZATION, OECD NUCLEAR ENERGY AGENCY, PAN AMERICAN HEALTH ORGANIZATION, UNITED NATIONS OFFICE FOR THE CO-ORDINATION OF HUMANITARIAN AFFAIRS, WORLD HEALTH ORGANIZATION, Preparedness and Response for a Nuclear or Radiological Emergency, Safety Requirements, Safety Standards Series No. GS-R-2. IAEA, Vienna (2002).

[23]    HUBBELL, J.H., SELTZER, S.M., Tables of X Ray Mass Attenuation Coefficients and Mass Energy-Absorption Coefficients from 1 keV to 20 MeV for Element $Z = 1$ to 92 and 48 Additional Substances of Dosimetric Interest, NISTIR 5632, July 2004, http://www.nist.gov/pml/data/xraycoef/index.cfm

[24]    INTERNATIONAL ATOMIC ENERGY AGENCY, Dangerous quantities of radioactive material (D-values), EPR-D-VALUES 2006, IAEA (2006) 154.

[25]    DANCKWERTS, P.V., Continuous flow systems, distribution of residence times, Chem. Eng. Sci. **2** 1 (1953) 1.

[26]    LEVENSPIEL, O., Chemical Reaction Engineering, 2nd ed., John Wiley and Sons, New York, Chapter 9 (1972).

[27]    POPE, G.A., et al., "Partitioning tracer tests to characterize organic contaminants", paper presented at Second Tracer Workshop, Center for Petroleum and Geosystems Engineering, University of Texas, Austin, 1994.

[28]    ROBINSON, B.A., TESTER, J.W., Dispersed fluid flow in fractured reservoirs: An analysis of tracer-determined residence time distributions, J. Geophys. Res. **89** B12 (1984) 10374.

[29]    ROBINSON, B.A., TESTER, J.W., Reservoir sizing using inert and chemically reacting tracers, SPE Formation Evaluation (1988) 227.

[30]    SHOOK, G.M., A simple, fast method of estimating fractured reservoir geometry from tracer tests, Trans. Geoth. Res. Council **27** (2003).

[31] SHOOK, G.M., FORSMANN, J.H., Tracer Interpretation Using Temporal Moments on a Spreadsheet, USDOE Contract-AC07-05ID14517, Idaho Natl Laboratory, ID (2005).

[32] DYKSTRA, H., PARSONS, R.L., The Prediction of Oil Recovery by Waterflood: Secondary Recovery of Oil in the United States, Principles and Practice, 2nd ed., American Petroleum Institute (1950) 160.

[33] BRIGHAM, W., SMITH, D., "Prediction of tracer behavior in five-spot flow", paper presented at Soc. Petrol. Eng. Prod. Res. Symp., Tulsa, 1965.

[34] BRIGHAM, W., "Mixing equations in various geometries", paper presented at 48th Annual Fall Meeting of AIME, Las Vegas, 1973.

[35] ABBASZADEH-DEHGHANI, M., BRIGHAM, W., Analysis of Unit Mobility Ratio Well-to-Well Tracer Flow to Determine Reservoir Heterogeneity, Rep. SUPRI TR-36, Stanford University Petroleum Institute, Stanford, CA (1982).

[36] ABBASZADEH-DEHGHANI, M., BRIGHAM, W., Tracer testing for reservoirs description, J. Pet. Technol. **5** (1987) 519.

[37] ABBASZADEH-DEHGHANI, M., Analytical flow model for design and analysis of tracer pulse tests, Dev. Petrol. Sci. **43** (1995) 429–473.

[38] TANG, J.S., Extended Brigham Model for Residual Oil Saturation Measurement by Partitioning Tracer Tests, SPE J. **10** 2 (2005) 175–183.

[39] MASINI, G., SOMARUGA, C., "Interwell tracer interpretation in oil secondary recovery projects employing the software Mathematica", paper presented at TRACER IV, Fourth Int. Conf. on Tracers and Tracing Methods, Autrans, France (2006).

[40] CORONADO, M., RAMIREZ, S.J., VALDIVIEZO, O., SOMARUGA, C., A New Scheme to Describe Multi-well Compressible Gas Flow in Reservoirs, Transport in Porous Media, Springer, Netherlands (2008).

[41] TROCCHIO, T., Investigation of Fateh Mishrif fluid conductive faults, J. Pet. Technol., 42 8 (1990) 1038–1045.

[42] NITZBERG, K.E., BROMAN, W.H., Improved reservoir characterization from waterflood tracer movement, northwest fault block, Prudhoe Bay, Alaska, SPE Form. Eval. **7** 3 (1992) 228.

[43] KLEVEN, R., et al., "Non-radioactive tracing of injection gas in reservoirs", paper presented at Gas Technology Conf., Calgary, 1996.

[44] DUGSTAD, O., et al., "Application of tracers to monitor fluid flow in the Snorre field: A field study", paper presented at SPE Ann. Tech. Conf., Houston, 1999.

[45] LANGE, A., BOUZIAN, J., BOURBIAUX, B., "Tracer-test simulation on discrete fracture network models for the characterization of fractured reservoirs", paper presented at SPE Europec/EAGE Annual Conf., Madrid, 2005.

[46] McDIARMID, A., ALEXANDER, I., ION, A., THOMPSON, J., "Experience of a reservoir waterflood failure and remediation treatment in the Stag Reservoir, Australia", SPE Asia Pacific Improved Oil Recovery Conf., Kuala Lumpur, 2001.

[47] PERALTA, M.B., PROCAK, C., DE LA FUENTE, M.V., SOMARUGA, C., "Tracers for characterization and gel treatment design and evaluation in oil secondary recovery", paper presented at TRACER V, Fifth Int. Conf. on Tracers and Tracing Methods, Tiradentes, Brazil, 2008.

# CONTRIBUTORS TO DRAFTING AND REVIEW

| | |
|---|---|
| Abidin, Z. | National Nuclear Energy Agency, Indonesia |
| Berne, P. | Commissariat à l'énergie atomique, France |
| Bjørnstad, T. | Institute for Energy Technology, Norway |
| Jin, Joon-Ha | International Atomic Energy Agency |
| Khan, I.H. | Pakistan Institute of Nuclear Science and Technology, Pakistan |
| Leclerc, J.-P. | Laboratory of Chemical Engineering Sciences of Nancy, France |
| Maggio, E.G. | NOLDOR S.R.L., Argentina |
| Moreira, M.R. | Comissão Nacional de Energia Nuclear, Brazil |
| Olivar, M.V. | Philippine National Oil Co., Philippines |
| Quang, N.H. | Vietnam Atomic Energy Commission, Vietnam |
| Somaruga, C. | Universidad Nacional del Comahue, Argentina |
| Tang, S.H.J. | JT Petroleum Consulting, Canada |
| Zhang, Peixin | China Institute of Atomic Energy, China |

# IAEA
**International Atomic Energy Agency**

# Where to order IAEA publications

**In the following countries** IAEA publications may be purchased from the sources listed below, or from major local booksellers. Payment may be made in local currency or with UNESCO coupons.

**AUSTRALIA**
DA Information Services, 648 Whitehorse Road, MITCHAM 3132
Telephone: +61 3 9210 7777 • Fax: +61 3 9210 7788
Email: service@dadirect.com.au • Web site: http://www.dadirect.com.au

**BELGIUM**
Jean de Lannoy, avenue du Roi 202, B-1190 Brussels
Telephone: +32 2 538 43 08 • Fax: +32 2 538 08 41
Email: jean.de.lannoy@infoboard.be • Web site: http://www.jean-de-lannoy.be

**CANADA**
Bernan Associates, 4501 Forbes Blvd, Suite 200, Lanham, MD 20706-4346, USA
Telephone: 1-800-865-3457 • Fax: 1-800-865-3450
Email: customercare@bernan.com • Web site: http://www.bernan.com

Renouf Publishing Company Ltd., 1-5369 Canotek Rd., Ottawa, Ontario, K1J 9J3
Telephone: +613 745 2665 • Fax: +613 745 7660
Email: order.dept@renoufbooks.com • Web site: http://www.renoufbooks.com

**CHINA**
IAEA Publications in Chinese: China Nuclear Energy Industry Corporation, Translation Section, P.O. Box 2103, Beijing

**CZECH REPUBLIC**
Suweco CZ, S.R.O., Klecakova 347, 180 21 Praha 9
Telephone: +420 26603 5364 • Fax: +420 28482 1646
Email: nakup@suweco.cz • Web site: http://www.suweco.cz

**FINLAND**
Akateeminen Kirjakauppa, PO BOX 128 (Keskuskatu 1), FIN-00101 Helsinki
Telephone: +358 9 121 41 • Fax: +358 9 121 4450
Email: akatilaus@akateeminen.com • Web site: http://www.akateeminen.com

**FRANCE**
Form-Edit, 5, rue Janssen, P.O. Box 25, F-75921 Paris Cedex 19
Telephone: +33 1 42 01 49 49 • Fax: +33 1 42 01 90 90
Email: formedit@formedit.fr • Web site: http://www. formedit.fr

Lavoisier SAS, 145 rue de Provigny, 94236 Cachan Cedex
Telephone: + 33 1 47 40 67 02 • Fax +33 1 47 40 67 02
Email: romuald.verrier@lavoisier.fr • Web site: http://www.lavoisier.fr

**GERMANY**
UNO-Verlag, Vertriebs- und Verlags GmbH, Am Hofgarten 10, D-53113 Bonn
Telephone: + 49 228 94 90 20 • Fax: +49 228 94 90 20 or +49 228 94 90 222
Email: bestellung@uno-verlag.de • Web site: http://www.uno-verlag.de

**HUNGARY**
Librotrade Ltd., Book Import, P.O. Box 126, H-1656 Budapest
Telephone: +36 1 257 7777 • Fax: +36 1 257 7472 • Email: books@librotrade.hu

**INDIA**
Allied Publishers Group, 1st Floor, Dubash House, 15, J. N. Heredia Marg, Ballard Estate, Mumbai 400 001,
Telephone: +91 22 22617926/27 • Fax: +91 22 22617928
Email: alliedpl@vsnl.com • Web site: http://www.alliedpublishers.com

Bookwell, 2/72, Nirankari Colony, Delhi 110009
Telephone: +91 11 23268786, +91 11 23257264 • Fax: +91 11 23281315
Email: bookwell@vsnl.net

**ITALY**
Libreria Scientifica Dott. Lucio di Biasio "AEIOU", Via Coronelli 6, I-20146 Milan
Telephone: +39 02 48 95 45 52 or 48 95 45 62 • Fax: +39 02 48 95 45 48
Email: info@libreriaaeiou.eu • Website: www.libreriaaeiou.eu

## JAPAN
Maruzen Company, Ltd., 13-6 Nihonbashi, 3 chome, Chuo-ku, Tokyo 103-0027
Telephone: +81 3 3275 8582 • Fax: +81 3 3275 9072
Email: journal@maruzen.co.jp • Web site: http://www.maruzen.co.jp

## REPUBLIC OF KOREA
KINS Inc., Information Business Dept. Samho Bldg. 2nd Floor, 275-1 Yang Jae-dong SeoCho-G, Seoul 137-130
Telephone: +02 589 1740 • Fax: +02 589 1746 • Web site: http://www.kins.re.kr

## NETHERLANDS
De Lindeboom Internationale Publicaties B.V., M.A. de Ruyterstraat 20A, NL-7482 BZ Haaksbergen
Telephone: +31 (0) 53 5740004 • Fax: +31 (0) 53 5729296
Email: books@delindeboom.com • Web site: http://www.delindeboom.com

Martinus Nijhoff International, Koraalrood 50, P.O. Box 1853, 2700 CZ Zoetermeer
Telephone: +31 793 684 400 • Fax: +31 793 615 698
Email: info@nijhoff.nl • Web site: http://www.nijhoff.nl

Swets and Zeitlinger b.v., P.O. Box 830, 2160 SZ Lisse
Telephone: +31 252 435 111 • Fax: +31 252 415 888
Email: infoho@swets.nl • Web site: http://www.swets.nl

## NEW ZEALAND
DA Information Services, 648 Whitehorse Road, MITCHAM 3132, Australia
Telephone: +61 3 9210 7777 • Fax: +61 3 9210 7788
Email: service@dadirect.com.au • Web site: http://www.dadirect.com.au

## SLOVENIA
Cankarjeva Zalozba d.d., Kopitarjeva 2, SI-1512 Ljubljana
Telephone: +386 1 432 31 44 • Fax: +386 1 230 14 35
Email: import.books@cankarjeva-z.si • Web site: http://www.cankarjeva-z.si/uvoz

## SPAIN
Díaz de Santos, S.A., c/ Juan Bravo, 3A, E-28006 Madrid
Telephone: +34 91 781 94 80 • Fax: +34 91 575 55 63
Email: compras@diazdesantos.es, carmela@diazdesantos.es, barcelona@diazdesantos.es, julio@diazdesantos.es
Web site: http://www.diazdesantos.es

## UNITED KINGDOM
The Stationery Office Ltd, International Sales Agency, PO Box 29, Norwich, NR3 1 GN
Telephone (orders): +44 870 600 5552 • (enquiries): +44 207 873 8372 • Fax: +44 207 873 8203
Email (orders): book.orders@tso.co.uk • (enquiries): book.enquiries@tso.co.uk • Web site: http://www.tso.co.uk

On-line orders
DELTA Int. Book Wholesalers Ltd., 39 Alexandra Road, Addlestone, Surrey, KT15 2PQ
Email: info@profbooks.com • Web site: http://www.profbooks.com

Books on the Environment
Earthprint Ltd., P.O. Box 119, Stevenage SG1 4TP
Telephone: +44 1438748111 • Fax: +44 1438748844
Email: orders@earthprint.com • Web site: http://www.earthprint.com

## UNITED NATIONS
Dept. I004, Room DC2-0853, First Avenue at 46th Street, New York, N.Y. 10017, USA
(UN) Telephone: +800 253-9646 or +212 963-8302 • Fax: +212 963-3489
Email: publications@un.org • Web site: http://www.un.org

## UNITED STATES OF AMERICA
Bernan Associates, 4501 Forbes Blvd., Suite 200, Lanham, MD 20706-4346
Telephone: 1-800-865-3457 • Fax: 1-800-865-3450
Email: customercare@bernan.com · Web site: http://www.bernan.com

Renouf Publishing Company Ltd., 812 Proctor Ave., Ogdensburg, NY, 13669
Telephone: +888 551 7470 (toll-free) • Fax: +888 568 8546 (toll-free)
Email: order.dept@renoufbooks.com • Web site: http://www.renoufbooks.com

**Orders and requests for information** may also be addressed directly to:

**Marketing and Sales Unit, International Atomic Energy Agency**
Vienna International Centre, PO Box 100, 1400 Vienna, Austria
Telephone: +43 1 2600 22529 (or 22530) • Fax: +43 1 2600 29302
Email: sales.publications@iaea.org • Web site: http://www.iaea.org/books

The main purpose of interwell tracer tests in oil and geothermal reservoirs is to monitor qualitatively and quantitatively the injected fluid connections between injection and production wells and to provide important data for better understanding the reservoir geology in order to optimize the production strategy and thereby maximize the oil recovery or thermal energy production. Most of the information provided by the radiotracer tests cannot be obtained by other techniques. This publication describes the principles and the state of the art of radiotracer techniques for interwell investigations. It provides practical guidance on the design, implementation of tracer experiments and interpretation of the results.